ARO 17158.1-A-EL

FINAL REPORT

Atmospheric Optical Communication Systems

U.S. Army Research Office
Contract DAAG 29-80-C-0010

covering the period

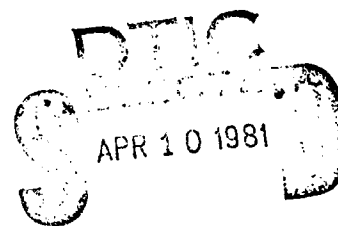22 October 1979 - 21 January 1981

Submitted by

R. S. Kennedy

APR 1 0 1981

A

February 1981

MASSACHUSETTS INSTITUTE OF TECHNOLOGY
Research Laboratory of Electronics
Cambridge, Massachusetts 02139

81 4 10 020

AD-A097 673

ARO-17158.1-A-EL

Pages 2-45 thru 2-49, 2-67; 2-68,3-22 thru 3-24
were deleted because of security reasons per the
author per ARO.

DTIC-DDA-2
12 May 81

REPORT DOCUMENTATION PAGE

READ INSTRUCTIONS
BEFORE COMPLETING FORM

1. REPORT NUMBER	2. GOVT ACCESSION NO.	3. RECIPIENT'S CATALOG NUMBER
	AD-A097673	

4. TITLE (and Subtitle)

ATMOSPHERIC OPTICAL COMMUNICATION SYSTEMS.

5. TYPE OF REPORT & PERIOD COVERED

Final Report.
22 Oct 79 - Jan 81.

6. PERFORMING ORG. REPORT NUMBER

7. AUTHOR(s)

R. S. Kennedy

8. CONTRACT OR GRANT NUMBER(s)

DAAG 29-80-C-0010

9. PERFORMING ORGANIZATION NAME AND ADDRESS

Research Laboratory of Electronics
Massachusetts Institute of Technology
Cambridge, Massachusetts 02139

10. PROGRAM ELEMENT, PROJECT, TASK AREA & WORK UNIT NUMBERS

11. CONTROLLING OFFICE NAME AND ADDRESS

U. S. Army Research Office
P. O. Box 12211
Research Triangle Park, N.C. 27709

12. REPORT DATE

February 81

13. NUMBER OF PAGES

307

14. MONITORING AGENCY NAME & ADDRESS(if different from Controlling Office)

15. SECURITY CLASS. (of this report)

Unclassified

15a. DECLASSIFICATION/DOWNGRADING SCHEDULE

16. DISTRIBUTION STATEMENT (of this Report)

Approved for public release; distribution unlimited

17. DISTRIBUTION STATEMENT (of the abstract entered in Block 20, if different from Report)

19. KEY WORDS (Continue on reverse side if necessary and identify by block number)

Optical communication
Optical scattering
Atmospheric optics
Secure communications

20. ABSTRACT (Continue on reverse side if necessary and identify by block number) The performance of off-axis optical communication receivers is considered. A statistical model of the photodetection process is presented and the influence of the received field statistics on the photodetection process is discussed. Upper and lower bounds on the probability of bit error for binary, one-shot, digital communication systems utilizing direct detection are developed. These bounds are based on the Bhattacharyya distance measure. A computer program is developed, which when interfaced with existing programs that model the propagation of optical radiation through the atmosphere, predicts the probability of bit error performance for off-axis optical communication systems.

DD FORM 1473 EDITION OF 1 NOV 65 IS OBSOLETE
1 JAN 73

July 30, 1980

Dear OFF-AXIS Program Users:

The OFF-AXIS program is a coded model of laser beam
propagation through single scatter atmospheres. The pro-
gram was developed at Hughes Aircraft for the National
Security Agency. At MIT the program was modified and
expanded to include performance analysis of off-axis
digital communication receivers.

The performance analysis added at MIT takes the form
of upper and lower bounds on the probability of bit error.
These calculations occur in a Mode 6, parallel to Modes
1-5 in the terrestrial link analysis. The modifications
to the original program are mainly the inclusion of
additional input parameters necessary for performance
analysis and the transfer of control to the new Mode 6.
The major work of the study is contained in two sub-
routines, ERROR and APERTR.

Section I of this document contains the original pro-
gram documentation written at Hughes. Modifications and
additions made at MIT are noted. Section II contains a
sample run of the program. Section III is a listing of
the modified program as run on MIT's Multics system.
Changes from the original Hughes code are highlighted with
comments.

Section IV is a user's manual for the subroutine
ERROR. This is the subroutine that calculates the bounds
on the probability of error. The background for these
calculations is presented in my thesis, "Performance of
Off-axis Optical Communication Receivers in Scattering

Atmospheres" (MIT MS thesis 1980).

Section V contains documentation for the subroutine APERTR. This subroutine calculates if there is enough aperature averaging to ignore the effects of turbulence induced fading in the clear atmosphere betweeen the scattering volume and the off-axis receiver. Such fading would degrade the performance of an off-axis receiver.

If at a later date there are questions, feel free to contact me at my new location:

> Bell Laboratories, Blg WB
> Crawford Corners Road
> Holmdel, N.J. 07733

> Sincerely,

> William Jaeger

WJ:nl

SECTION I

ORIGINAL DOCUMENTATION

Though it does not effect program operation, ████████████████████████

████████████████████████████ The noise (variance) of the output voltage
due to dark current events is

$$N_d = \frac{2\eta\lambda}{hc}\ P_d(qG)^2 FBR_L$$

The dark power, P_d, is the average power that if applied to an ideal
detector would give rise to the average (DC) dark current, i_d.

$$i_d = \frac{\eta\lambda}{hc}\ P_d(qG) \qquad \text{and} \qquad P_d = \frac{i_d hc}{\eta\lambda(qG)}$$

Thus the correct expression for N_d (equation 2-9) is

$$N_d = 2i_d qGFBR_L$$

and the correct expression of NEP (equation 2-12) is

$$NEP = (hc/\eta\lambda q)[2qi_d F + 4kT/G^2 R_L]^{1/2}$$

Due to fundamental differences in the underlying statistics, ████████
████████████████████████ The input parameter NEP is replaced by two
input noise parameters; the dark current, i_d, and the noise equivalent
power due to thermal noise alone, P_{therm}.

$$P_{therm} = \frac{hc}{\eta\lambda(Gq)}\left(\frac{4kT}{R_L}\right)^{1/2}$$

$$P_{therm} = [NEP^2 - (hc/\lambda q)^2(2qi_d F/G)]^{1/2}$$

The noise equivalent power due to thermal noise is related to the spectral density of the thermal noise, $N_0/2$,

$$N_0/2 = 2kT/R_L$$

$$P_{therm} = \frac{hc}{\eta \lambda Gq} \left(2\frac{N_0}{2} \right)^{1/2}$$

$$N_0/2 = 1/2 \left(\frac{\eta \lambda Gq}{hc} P_{therm} \right)^2$$

$$\frac{S}{N} = \frac{P^2}{(2hc/\eta \lambda) FB(P_s + P_b + P_d) + (NEP)^2 B}$$

where P_d is again a fictitous power that gives rise to the dark current

$$P_d = \frac{hci_d}{\eta \lambda qG}$$

COMPUTER SOFTWARE FLOWCHART STANDARDS
INTERCEPTIBILITY ANALYSIS PROGRAM –
ECKSTROM, LACM 2. 0
CONTRACT NO. MDA904-77-C-0566

CDRL A006

```
                                    ┌──────────────┐
                                    │   COMPUTE    │
                                    │   ANGLES &   │
                                    │   RANGES     │
                                    └──────┬───────┘
                                           │
                                    ╱──────┴───────╲
                                   ╱  PRINT  SR     ╲
                                   ╲  LOCATION      ╱
                                    ╲──────┬───────╱
                                           │                                    ┌──────────────┐
                                           │                                    │  CALCULATE   │
                                    ┌──────┴───────┐                            │  CHANNEL     │
                                    ║    CALL      ║─── SIGNAL                   │  IMPULSE     │
                                    ║    COMTOT    ║    POWER                    │  RESPONSE    │
                                    └──────┬───────┘                            └──────┬───────┘
                                           │                                           │
                                           │                                           │
                                    ┌──────┴───────┐         FUTURE             ┌──────┴───────┐
                                    │ RECEIVED POWER =         TIME             │ CONVOLUTION  │
                                    │ SIGNAL  POWER │         DISPERSION        │ OF IMPULSE   │
                                    │ • WAVEFORM    │         ANALYSIS          │ RESPONSE     │
                                    └──────┬───────┘                            │ AND          │
                                           │                                    │ WAVEFORM     │
                                           │                                    └──────┬───────┘
                                           │                                           │
                                    ┌──────┴───────┐                            ┌──────┴───────┐
                                    ║    CALL      ║─── BACKGROUND              │ CHECK FOR    │
                                    ║    BACK      ║    POWER                   │ INTERSYMBOL  │
                                    └──────┬───────┘                            │ INTERFERENCE │
                                           │                                    └──────────────┘
                                           │              CHECK IF THERE
                                           │              IS ENOUGH APERTURE
                                    ┌──────┴───────┐      AVERAGING TO
                                    ║    CALL      ║──── IGNORE EFFECTS
                                    ║    APERTR    ║      OF FADING DUE
                                    └──────┬───────┘      TO TURBULENCE
                                           │
                                           │
                                        ╱──┴──╲
                                       │   A   │
                                        ╲─────╱
```

(U)   Attempts at establishing realistic error bounds on the data reviewed were aggravated by the fact that there was in many instances inadequate data to establish a meaningful standard deviation. A sensitivity analysis has instead been suggested wherein the computer program is used to establish the significance of extreme variations to parametric values in those cases where reasonable bounds are difficult to predict.

Section 2 — Data-Base Review and Model Formulation
Subsection B — Scenario Characterization

1. CHARACTERIZING AN OPTICAL COMMUNICATIONS LINK

The ECKSTROM computer program has been designed to model the vulnerability of specific optical links. This discussion outlines those parameters which must be considered to describe the overall system and site to be modeled.

(C). In order to establish the vulnerability of an open-beam, optical communications link to detection.   , the basic characteristics of the link design, of its geometry, and of its environment must be specified. These basic characteristics are illustrated in Figure 2-1 where a transmitter, receiver, and link surroundings are depicted in an arbitrary scenario.

(U) Basic transmitter parameters which must be specified are the operational optical wavelength λ, the peak optical output power P_0 at the transmitter exit aperture, the diameter of the exit aperture D_t, the angular spread of the optical beam ϕ_t, and the modulation format employed. If the system is diffraction limited, the beam spread can be specified in terms of the wavelength and exit aperture diameter, but this is not usually the case. However, the diffraction limit does set a lower limit to beamwidth. Receiver parameters of interest include the entrance aperture diameter D_r, the detector field of view ϕ_r, and whether direct or heterodyne detection is employed. These parameters, however, are of only secondary importance.

The system modulation format is quite significant when considered. The optical source may be either continuous wave (CW) or pulsed, and either analog, pulse, or digital modulation may be used. Moreover, the carrier may be modulated in amplitude (or intensity), frequency, phase, or polarization, or one of a number of pulse modulation formats (such as pulse position modulation) may be employed. Pratt [2-1] considers an extensive list of possible modulation formats.

(U) Because of the wide diversity of possible formats, we will initially restrict attention to three basic types. This number can be extended in the future as found necessary. The three types include CW intensity modulation, pulse-code intensity modulation, and CW frequency modulation (requiring heterodyne detection). For both CW and pulse systems the link's information bandwidth B and the depth of modulation M must be specified, and for pulse systems the pulse duration τ must be specified.

(U) Two important aspects of a system not to be found on vendor data sheets are the optical quality of the transmitter optics and the reflection characteristics of the receiver. These factors are considered in detail in subsequent discussions of the link scattering and reflection models.

(U) Geometrical aspects of the link include the range Z of the link and the respective heights above ground level of the transmitter and receiver, h_t and h_r. The heights are significant because of the variation in atmospheric scattering and absorption coefficients with altitude and the variation of turbulence effects with altitude. Atmospheric turbulence causes spreading of the transmitted beam.

Site characteristics include local meteorological conditions and physical characteristics of the link environment. Weather conditions will effect changes in atmospheric scattering, absorption, and turbulent beam spreading. Temperature, relative humidity, atmospheric pressure, and visibility are weather condition descriptors, but it has been found that such parameters are difficult to functionally relate to the significant effects. General meteorological descriptors as documented by the Air

2-4

Force Geophysics Laboratories (AFGL) have been found to be more appropriate. Important physical characteristics identified include the presence of window panes in front of either the transmitter or receiver, or both, the presence of trees or foliage along the beam path, and the nature and orientation of the backstop at the receiver. The backstop is a primary source of scattering, and window panes or foliage will act as secondary but perhaps significant sources of scatter. The ground itself may also be a significant source of reflection.

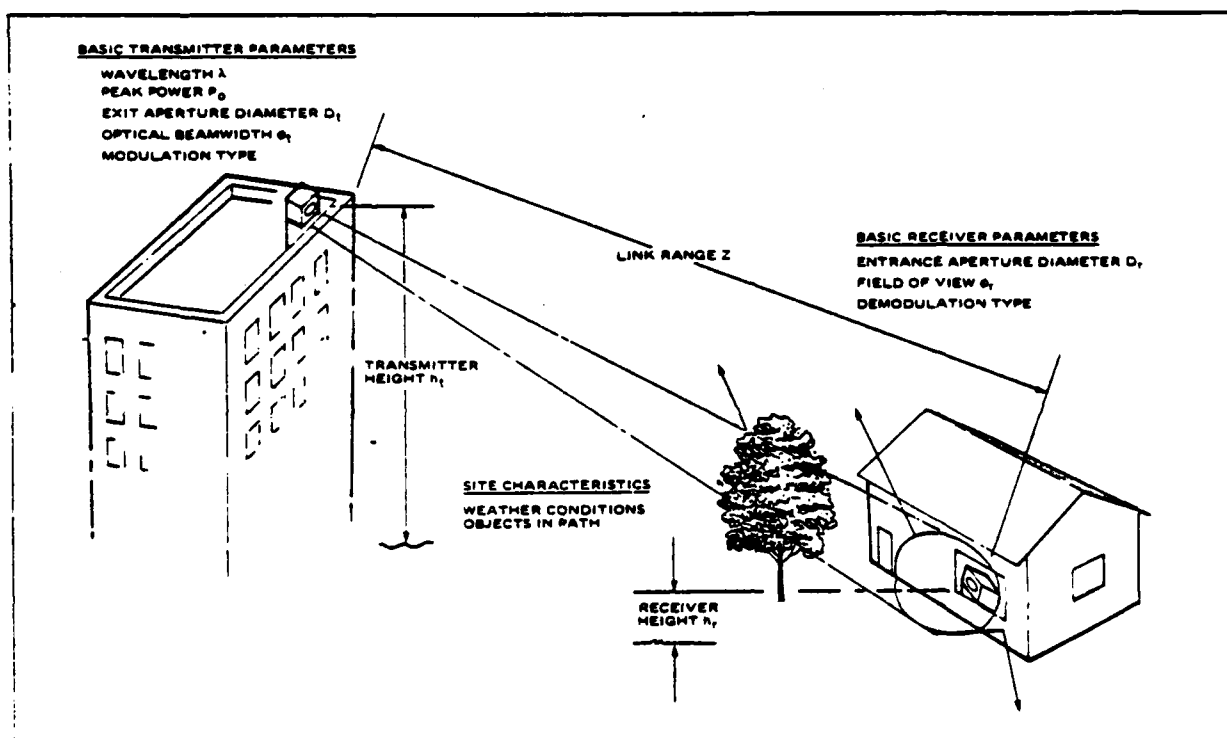(U) Models for each of these effects are considered in the scattering analyses to follow.

Figure 2-1. (U) A Depiction of the Basic Characteristics of an Open-Beam Optical Communications link (U)

This discussion provides a general overview of the basic parameters which must be specified in order to properly characterize a   ·er. A more extensive receiver investigation is presented in Section 5, including the fundamental consideration of detector sensitivity, not discussed here.

There are numerous tradeoffs necessary in determining an optimum receiver design. However, most of them are unimportant with regard to computer modeling except insofar as they may complicate the surveillance problem. For example, whether optical components are refractive or reflective is unimportant in this regard. For computer modeling, the receiver used for off-axis detection is therefore specified only in terms of its pertinent system design parameters and its geometrical relation with respect to the link. Significant parameters are diagrammed in Figure 2-2 assuming a simple refractive system.

The area A_s of the   : aperture, assumed circular, must be specified. From the   ·int of view this area should be maximized, but it is limited by practical considerations such as cost, weight, transportability, and   . Another design parameter of importance is the system solid angular field of view Ω_s. Ω_s is given by

$$\Omega_s = a_s/f^2 \tag{2-1}$$

where a_s is the area of the system's optical detector, assumed rectangular, of linear dimensions d_{sh} and d_{sv}, and f is the effective system focal length. The focal length is in turn related to the system aperture diameter D_s and focal ratio, or f-number (f#), by

$$f = D_s \, f\# \tag{2-2}$$

Since there are practical limitations on the size of detectors and system f-numbers, it is best to specify a_s and f#, and to then specify Ω_s in terms of them. Characteristic detector sizes are given in Section 5. A minimum f-number of unity is realistic. but values much lower than unity are very difficult to attain. Hence, from (2-2) and (2-3)

$$\Omega_s = a_s/(D_s f\#)^2. \tag{2-3}$$

Use of (2-3) will avoid the user's specifying an unrealistic threat in the model. The

heterodyne-detection system. For a general discussion of optical heterodyne
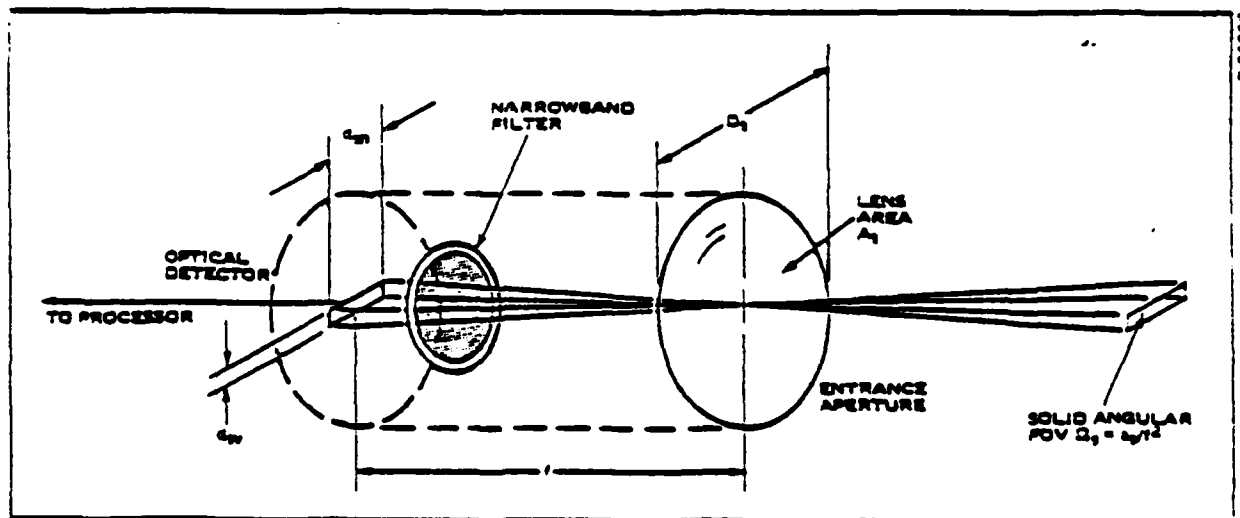
Figure 2-2. (U) Basic Characteristics of an Optical Receiver (U)

(U) Geometrical aspects of importance relating an optical link and a nearby receiver are shown in Figure 2-3. The location of the off-axis receiver is specified with respect to the transmitter and link axis in terms of z_s and x_s. Its location may alternatively be specified in terms of θ_t, θ_r, R_t, or R_r, defined as shown. The receiver is always assumed to be pointed in a direction which intercepts the link axis, the orientation being specified by either θ_i, the angle of intercept, or z_i. R_i is the distance from the axial point of intercept and the surveillance receiver.

(U) The linear receiver field of view shown, ϕ_{sh}, is given by

$$\phi_{sh} = d_{sh}/\ell \tag{2-4}$$

This is the field of view along the axis, usually horizontal (h). The linear field of view perpendicular to the link axis is

$$\phi_{sv} = d_{sv}/\ell \tag{2-5}$$

usually vertical (v). The field of view ϕ_{sh}, however, establishes what portion of the beam is under surveillance. By rotating the receiver, that is, varying θ_i, the transmitter, link path, and receiver may in turn be monitored. If ϕ_{sh} is sufficiently large, then all three sources of scattered radiation may simultaneously be monitored, a case which can be analyzed.

(U) Because of the variation of atmospheric effects with altitude, the receiver's altitude is also important. Such a variation is allowed in the program, the geometry of which is described in Section 3.

(U) Although the use of a large field of view ϕ_{sh} may allow more scattered energy to be collected, dispersion effects may lead to limitations if message intercept is attempted. The dispersion effects result because of the relative size of the receiver field of view. For example, two photons emitted simultaneously from the transmitter may be scattered from the two Points A and B of Figure 2-3 into the receiver. The difference in the two path lengths results in a difference in the time of arrival of the two photons. The response of the receiver will therefore be degraded. Pulses will be spread in time and CW modulated sources distorted. The amount of distortion is determined by convolving the resulting point spread function with the actual signal. It is not clear at what point the waveform is degraded beyond recognition, but distortion is clearly more severe for wider-band signals. It is particularly severe in the very wide-band, space-to-ground scenario, in which case the two points A and B may be very far apart. No provision is made in the computer program to highlight this limitation, and the user must consequently be aware that the limitation exists.
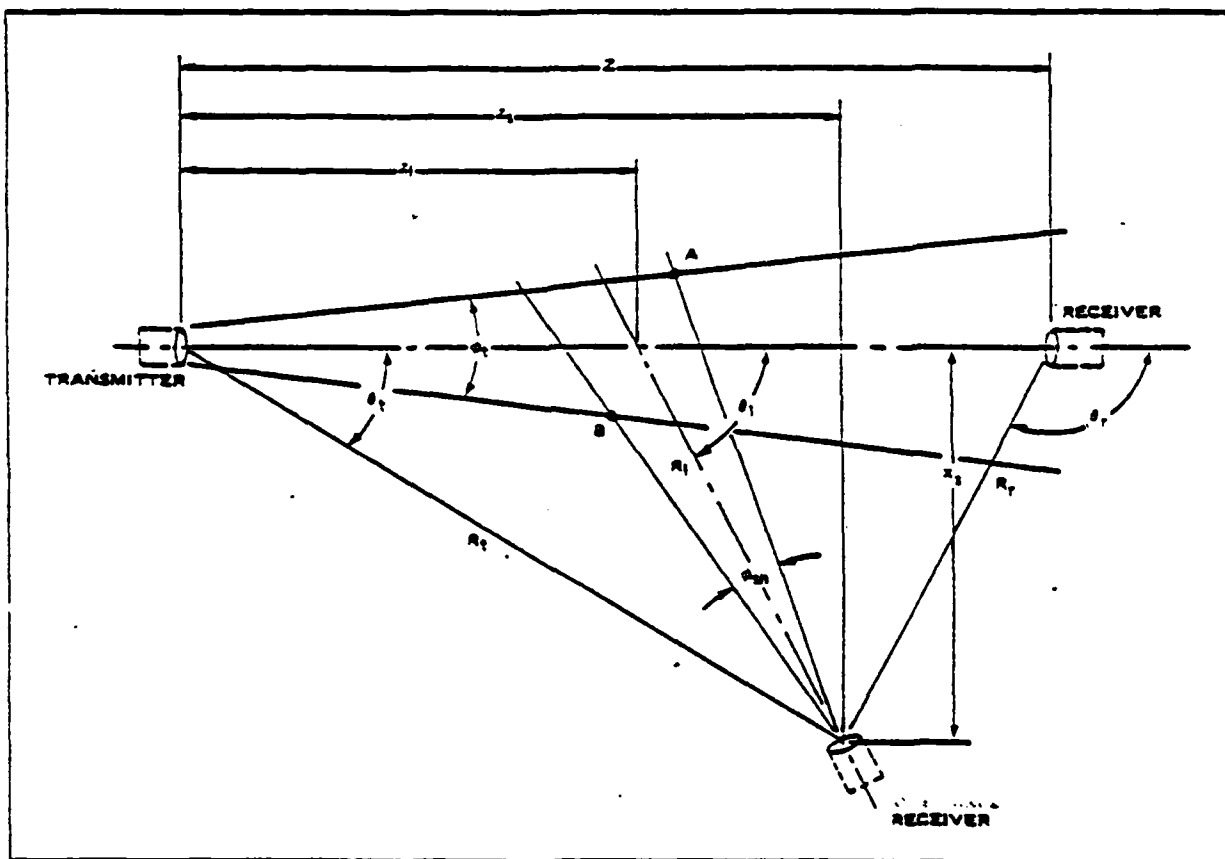
Figure 2-3   Basic Parameters Describing the Geometrical Interrelationships Between an Optical
Communications Link and a   Receiver

Section 2 — Data-Base Review and Model Formulation
Subsection C — Modeling the Detection Process

1. SIGNAL-TO-NOISE RATIO USING DIRECT DETECTION

(U) A signal-to-noise relationship is developed in terms of detection system NEP, with variables to account for the effects of modulation.

(U) Given an optical detector, its sensitivity must be established in terms of the signal power available and the noise power present. This discussion outlines the equations and associated parameters being used for calculating the ratio of signal plus noise to noise ((S + N)/N) for direct-detection receivers. The approach presented is in substantial agreement with those of Anderson and McMurtry [2-3], Pratt [2-1], and Melchior, Fisher, and Arams [2-4].

(U) The signal power generated across a load resistor R_L at the output of an optical detector subsystem due to incident optical power P is given by

$$S = (G \eta q \lambda / hc)^2 P^2 R_L \qquad (2-6)$$

where λ is the wavelength of the optical signal, q is the electronic charge, h is Planck's constant, c is the speed of light, η is the quantum efficiency of the photodetector at the specified wavelength, and G is its gain. The term in parenthesis is simply the detector responsivity, usually given in units of amperes per watt. The gain G is unity for many photodetectors of interest, but it is included to account for the use of avalanche photodiodes or photoemissive devices such as photomultipliers.

(U) The average noise power N associated with the photodetection process arises from four basic sources. That is,

$$N = N_s + N_b + N_d + N_t \qquad (2-7)$$

where N_s and N_b are signal-generated and background-generated shot (or generation-recombination) noise components respectively, N_d is detector dark-current shot noise, and N_t is thermal noise in the detector-preamplifier system. We emphasize inclusion of preamplifier noise since in some instances a detection system may be preamplifier-noise limited, and noise calculations must account for total system noise and not only those sources arising from the photodetector itself.

(U) The externally induced noise components N_s and N_b are given by

$$N_{s,b} = (2G^2 \eta q^2 \lambda / hc) P_{s,b} FBR_L \qquad (2-8)$$

where $P_{s,b}$ refers to either signal power P_s averaged over a period 1/B or background power P_b; F is an excess noise factor accounting for noise induced by the mechanism providing the gain G; and B is the electrical bandwidth of the detection system. The background power P_b may arise from reflected or scattered solar radiation from the terrain, sky, clouds, or other background within the detector field of view, or it may arise from blackbody emissions of the 300 K surroundings, depending on the optical wavelength. The excess-noise factor F is unity for photodetectors with unity gain.

(U) Internal system noise due to dark current i_d is given by

$$N_d = 2qi_d G^2 FBR_L. \tag{2-9}$$

Dark current is due to detector biasing in some instances, and in some instances it is caused by thermal radiation incident on the photodetector from detector enclosure surfaces (usually minimized by cryogenic cooling). Thermal (Johnson) noise is given by

$$N_t = 4kTB \tag{2-10}$$

where k is Boltzmann's constant and T the effective detection-system temperature.
(U) In lieu of specifying detection system dark current, load resistance, and effective temperature (preamplifier and load temperature may differ from detector temperature) it is more expedient to specify system internal noise characteristics in terms of noise-equivalent power (NEP), a measurable quantity frequently specified by vendors which lumps the noise characteristics of the detector-preamplifier combination into a single number. The NEP is the optical power necessary to provide a signal-to-internal-noise ratio of unity normalized to a 1 Hz bandwidth. That is,

$$\frac{S}{N_{int}} = 1 = \frac{(G\eta q \lambda/hc)^2 (NEP)^2 R_L}{2qi_d G^2 FR_L + 4kT} \tag{2-11}$$

Solving for NEP,

$$NEP = (hc/\eta q \lambda) [2qi_d F + 4kT/G^2 R_L]^{1/2}. \tag{2-12}$$

(U) NEP as it is sometimes specified may also account for background noise. However, since background noise at visible and near-infrared wavelengths is a variable depending on field of view, time of day, background type, and other highly varying conditions, such a parameter is impossible to generically specify. Consequently, the NEP values used in evaluating a system should be system parameters, assumed measured with the detector aperture covered; that is, without background. Such an assumption leads to no difficulty except with regard to photoconductive detectors, whose sensitivity is dependent upon the background level. However, these detectors are only used at infrared wavelengths where the highly varying solar component is negligible.
    Another important aspect of the system NEP of (2-12) is its dependence on load resistance, another variable subject to design variations. However, for the modes of interest consideration can be restricted to two cases: for link detection the load will be large, so that thermal noise is small and dark current dominates; and for signal demodulation and message   , small load is generally required because of RC time - constant limitations on bandwidth, so that thermal noise will be dominant, usually requiring a detector with high gain G to overcome it. These cases correspond to the narrow-band and wide-band cases respectively, discussed in Section 5.
 (U) Using (2-6) - (2-10) and (2-12), an overall signal-to-noise ratio (SNR) can be specified in the relatively simple form

(U)

$$\frac{S}{N} = \frac{P^2}{(2hc/\eta\lambda)\ FB\ (P_s + P_b) + (NEP)^2 B} \tag{2-13}$$

from which $(S + N)/N$ can be specified, i.e.,

$$\frac{S + N}{N} = \frac{S}{N} + 1. \tag{2-14}$$

The specification of the optical power P in (2-13) depends on whether link detection or message _____ is to be examined. For link detection of CW signals carrier-to-noise ratio is the signal quantity of interest, and P corresponds to the average optical power during the period $1/B$ regardless of the modulation type. Thus $P = P_s$, and a very narrow bandwidth can be assumed for the _____ e receiver. About 0.1 Hz is technically feasible, though requiring approximately 10 sec for integration. For pulsed systems P_s is given by the product of the peak power and the pulse duty factor.

When mes_____ is attempted, the bandwidth must be widened, and the type of modulation and the depth of modulation must be taken into account. To account for these variables a modulation factor M is introduced: letting $P = MP_s$,

$$\frac{S}{N} = \frac{M^2 P_s^2}{(2hc/\eta\lambda)\ FB\ (P_s + P_b) + (NEP)^2 B} \tag{2-15}$$

This is the general form used in the computer model for direction detection.
(U)   Numerical values for M are dependent on the specific modulation formats considered. They have not yet been determined for all cases of interest. However, Section 5 discusses several cases assuming quantum-limited detection performance (implying heterodyne detection, as discussed in the next topic).

Section 2 – Data-Base Review and Model Formulation
Subsection C – Modeling the Detection Process

2. SIGNAL-TO-NOISE RATIO USING HETERODYNE DETECTION

(U) Heterodyne detection of an optical signal can provide quantum-limited sensitivity.

(U)   Coherent optical detection, or heterodyne detection, differs from direct optical detection in that a coherent laser reference beam is provided at the receiver to illuminate the photodetector as shown in Figure 2-4, so that signal frequency and phase information is retained. Even if frequency or phase modulation is not employed, use of a heterodyne receiver can greatly reduce the effective system noise level.

(U)   Consider a signal to be incident on the detector of power $P_s = \langle A_s A_s^* \rangle$ where A_s is a coherent, complex waveform given by

$$A_s = U \exp(j\omega t + j\phi). \qquad (2-16)$$

Either the wave amplitude U, the optical frequency ω, or the phase ϕ may be the time-varying signal component depending on the modulation format of the transmitter. The time average indicated for P_s is over an optical period which is short in comparison to the reciprocal of the signal bandwidth B_0. If a reference signal, or local oscillator signal, P_{lo} of complex amplitude

$$A_0 = U_0 \exp(j\omega_0 t + j\phi_0) \qquad (2-17)$$

where $P_{lo} = \langle A_0 A_0^* \rangle$ is mixed with the signal beam so that the wavefronts are parallel, the resultant detector current is given by

$$(\eta q \lambda / hc) \langle (A_0 + A_s)(A_0 + A_s)^* \rangle =$$

$$(\eta q \lambda / hc) \, [P_{lo}^2 + P_s^2 + 2U_0 U \cos(\omega_0 t - \omega t + \phi_0 - \phi)] \qquad (2-18)$$

where we have assumed unity detector gain. If a narrow-band IF filter centered at the frequency $\Delta\omega = \omega_0 - \omega$ is inserted behind the detector to remove the unmodulated signal elements, the instantaneous signal current at the IF output will be

$$i_s = (\eta q \lambda / hc) \, 2U_0 U \cos(\Delta\omega t + \phi - \phi_0). \qquad (2-19)$$

The resulting IF signal power is

$$S = \langle i_s^2 \rangle R_L = 2 \, (\eta q \lambda / hc)^2 \, P_{lo} P_s R_L \qquad (2-20)$$

where the time average is now over the IF wave period.

(U)   The noise power is essentially the same as for direct detection, except that additional shot noise is generated by the local-oscillator signal. Thus

(U)
$$N = [(2\eta q^2 \lambda/hc)(P_s + P_b + P_{\ell o})R_L + 2qi_d R_L + 4kT]B_{IF} \quad (2\text{-}21)$$

where B_{IF} is the IF bandwidth.

The ratio of signal to noise in the IF channel is therefore

$$\left(\frac{S}{N}\right)_{IF} = \frac{2(\eta q\lambda/hc)^2 P_{\ell o}P_s R_L}{[(2\eta q^2\lambda/hc)(P_s + P_b + P_{\ell o})R_L + 2qi_d R_L + 4kT]\,B_{IF}}$$

$$= \frac{(\eta\lambda/hcB_{IF})P_s}{1 + P_{\ell o}^{-1}[P_s + P_b + (hc/\eta q^2\lambda)(qi_d + 2kT/R_L)]} . \quad (2\text{-}22)$$

As the local-oscillator power $P_{\ell o}$ is increased, the noise contributions in the second term of the denominator becomes negligible, and the SNR approaches the quantum limit,

$$\left(\frac{S}{N}\right)_{IF} = \frac{\eta\lambda}{hcB_{IF}}P_s . \quad (2\text{-}23)$$

The NEP for this case can be determined by setting the IF SNR equal to unity and solving for P_s.

(U) The ability to achieve such quantum-limited sensitivity is possible only if the local-oscillator power required does not cause detector damage or nonlinear operation. Such performance has been demonstrated in practical wideband systems operating at 10.6 μm with less than 1 mW of local-oscillator power. Quantum-limited sensitivity is therefore practical and will be assumed for the heterodyne-detection case.

(U) A limitation on heterodyne applicability results from the need for phase-matching of the reference beam to that of the signal beam, as discussed in Section 5. In practice matching can be achieved only over a detector area on the order of 0.7 d where

$$d = 1.22\lambda f/D_s \quad (2\text{-}24)$$

is the diameter of the Airy disc for a system with effective entrance aperture diameter D_s and focal length f. Even then a mismatch loss occurs, which under optimum conditions leads to a SNR reduction of $L_M \approx 0.7$, so that

$$\left(\frac{S}{N}\right)_{IF} = L_M \frac{\eta\lambda}{hcB_{IF}}P_s . \quad (2\text{-}25)$$

Moreover, since the detector's field of view is given by

$$\Omega_s = a_s/f^2 , \quad (2\text{-}26)$$

then

$$\Omega_s \approx (\lambda/D_s)^2 , \quad (2\text{-}27)$$

a substantial limitation on detector field of view.

(U)   A second detection is required to convert the IF signal to a usable video signal.
The final video output SNR depends on the type of modulation, the type of second
detection, and the magnitude of the input IF SNR. For demodulation, the best video
SNR can be obtained using linear video detection, in which case, assuming a reasonably
large IF SNR [2-1],

$$\frac{S}{N} = 2 \left(\frac{S}{N}\right)_{IF}.$$

(2-28)

If the IF bandwidth is twice the information bandwidth B_0 (the optimum condition) then

$$\frac{S}{N} = L_M \frac{\eta\lambda}{hcB_0} M^2 P_s$$

(2-29)

where we have reintroduced the modulation factor M to account for various modulation
types. This form is assumed in the computer model for heterodyne detection.
(U)   For detection only, square-law video detection and video integration of a chopped
optical input are appropriate when the IF input SNR is less than unity. This is the case
for the Dicke radiometer, which is discussed in Section 5. Because of the numerous
video detection schemes possible, however, it is unrealistic to consider all possible
cases.
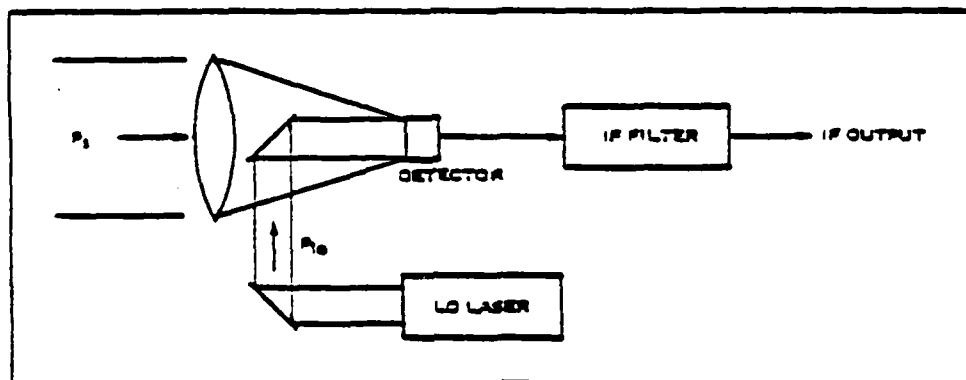
Figure 2-4. A Typical Receiver Configuration for Coherent Heterodyne Optical
Detection. The optical detector area is limited to less than a diffraction-limited
spot size.

3. BACKGROUND NOISE

(U) A background model is developed which accounts for both solar and blackbody background components and is adaptable to varying sky conditions.

(U) Contributions to detector background noise arise primarily from two sources: scattered or reflected solar radiation during daylight hours, and earth blackbody radiation at all times. Establishing blackbody background radiation is generally straightforward, whereas solar radiation is complicated by the selective absorption effects of the atmosphere and of reflecting surfaces.

(U) Natural radiation emitted from diffuse background objects in thermal equilibrium at a temperature T is specified in terms of the spectral radiance N_λ of the source, where [2-5]

$$N_\lambda = \epsilon(\lambda)(2hc^2/\lambda^5)\left[\exp(hc/\lambda kT)-1\right]^{-1}. \tag{2-30}$$

$\epsilon(\lambda)$ is the spectral emissivity of the source. If ϵ is unity for all wavelengths, then the source is termed a blackbody. A plot of N_λ versus wavelength is shown in Figure 2-5 for a 293° K blackbody. A comparison with measured values is made at the end of this discussion, showing that the values for N_λ given by Figure 2-5 provide an accurate model for most natural sources. This is true because most materials have emissivities near unity in the infrared region where the blackbody radiance peaks, as indicated by the data of Table 2-1 [2-6].

(U) The resulting background power P_{bb} incident on the receiver photodetector due to blackbody radiation is given by

$$P_{bb} = N_\lambda A_b \Omega_b \Delta\lambda \tag{2-31}$$

where A_b is the area of the blackbody source at a range R_b subtended by the surveillance receiver solid angular field of view Ω_s;

$$\Omega_b = A_s/R_b^2, \tag{2-32}$$

which is the solid angle into which the source radiation must propagate to be seen by the detector; and $\Delta\lambda$ is the optical filter bandwidth of the receiver. Since the blackbody source fills the receiver field of view,

$$A_b = R_b^2 \Omega_s, \tag{2-33}$$

so that

$$P_{bb} = N_\lambda A_s \Omega_s \Delta\lambda, \tag{2-34}$$

which is independent of source range.

The component of solar radiation contributing to background noise must be reflected or scattered into the detector field of view (barring the unlikely chance that the sun is directly in the field of view, a geometry to be avoided.
Assuming the   receiver is looking directly at the transmitter, or at the link receiver, the source area A_b which would be reflecting radiation would probably

be the side of a building, a backstop, or perhaps natural terrain. If the receiver were directed elsewhere along the path, it still would probably intercept the same features, or it might intercept the sky background.

(U)   Consider the case where the receiver field of view intercepts a building, as shown in Figure 2-6. The field of view defines the area A_b from which solar radiation, assumed to emanate at an angle θ_{sol}, is reflected. The total solar power incident on A_b in a wavelength range $\Delta\lambda$ is given by

$$P_{inc} = H_\lambda A_b \ \Delta\lambda \sin\theta_{sol} \qquad (2-35)$$

where H_λ is the spectral irradiance from the sun.

(U)   A plot of H_λ as a function of wavelength is shown in Figure 2-7 for the sun at zenith [2-7]. The solar spectral irradiance is closely approximated by a blackbody source at 5900° K. As seen in Figure 2-7, however, atmospheric attenuation effects further reduce H_λ, and it is highly structured due to strong molecular absorption bands. Gast [2-7] provides tabulated data for H_λ at sea level assuming a solar zenith angle θ_{sol} of 60° (air mass 2) a nominal condition.

(U)   The radiance N_{sol} within $\Delta\lambda$ from the area A_b due to the reflected sunlight, assuming a diffusely reflecting surface of reflectance ρ, is given by

$$N_{sol} = \rho P_{inc}/\pi A_b \qquad (2-36)$$

so that the total solar power on the surveillance receiver is

$$P_{sol} = N_{sol} A_s \Omega_s. \qquad (2-37)$$

Combining (2-35) - (2-37),

$$P_{sol} = \rho \sin\theta_{sol} \ H_\lambda \ A_s \ \Omega_s \ \Delta\lambda/\pi. \qquad (2-38)$$

(U)   With reference to Figures 2-5 and 2-7, the solar component is clearly dominant in the visible and near-infrared regions of the spectrum, whereas the blackbody radiation dominates in the far-infrared region. Some measured values [2-8] are presented in Figures 2-8 through 2-15, and comparison with Figure 2-5 shows consistently good agreement for the blackbody component. It is difficult to compare the measured reflected solar components of these figures with theory because the measurements are provided primarily in the region between 1.5 μm and 3.0 μm, where both material reflectances and atmospheric absorptance are both highly varying with wavelength. However, they are in reasonable agreement assuming a 5900° K blackbody model for the sun.

(U)   Figure 2-15 also indicates a comparable solar spectral radiance component from the sky to that from terrestrial sources, although a region around 10 μm can be significantly lower depending on temperature and cloud conditions [2-8, p. 99].

(U)   The total background power P_b is given by the sum of the blackbody and solar components,

$$P_b = P_{bb} + P_{sol}. \qquad (2-39)$$

However, as shown in Figure 2-10, the solar component is absent at night, as expected, whereas the blackbody component is always present. A background model should therefore have provisions for specifying daytime or nighttime conditions. Moreover,

(U) intermediate conditions such as an overcast sky may exist, but such a generalization requires that sky radiance be considered rather than direct solar irradiance. This requires an integration over that portion of the sky irradiating A_b, a rather complex way to determine the reflected radiance. However, little additional accuracy can be gained by using such an approach. Table 2-2 [2-9] provides the relative magnitudes of scene illuminance under different sky conditions. Scaling of H_λ by these factors should be adequate for a reasonable characterization of solar noise under various intermediate conditions.
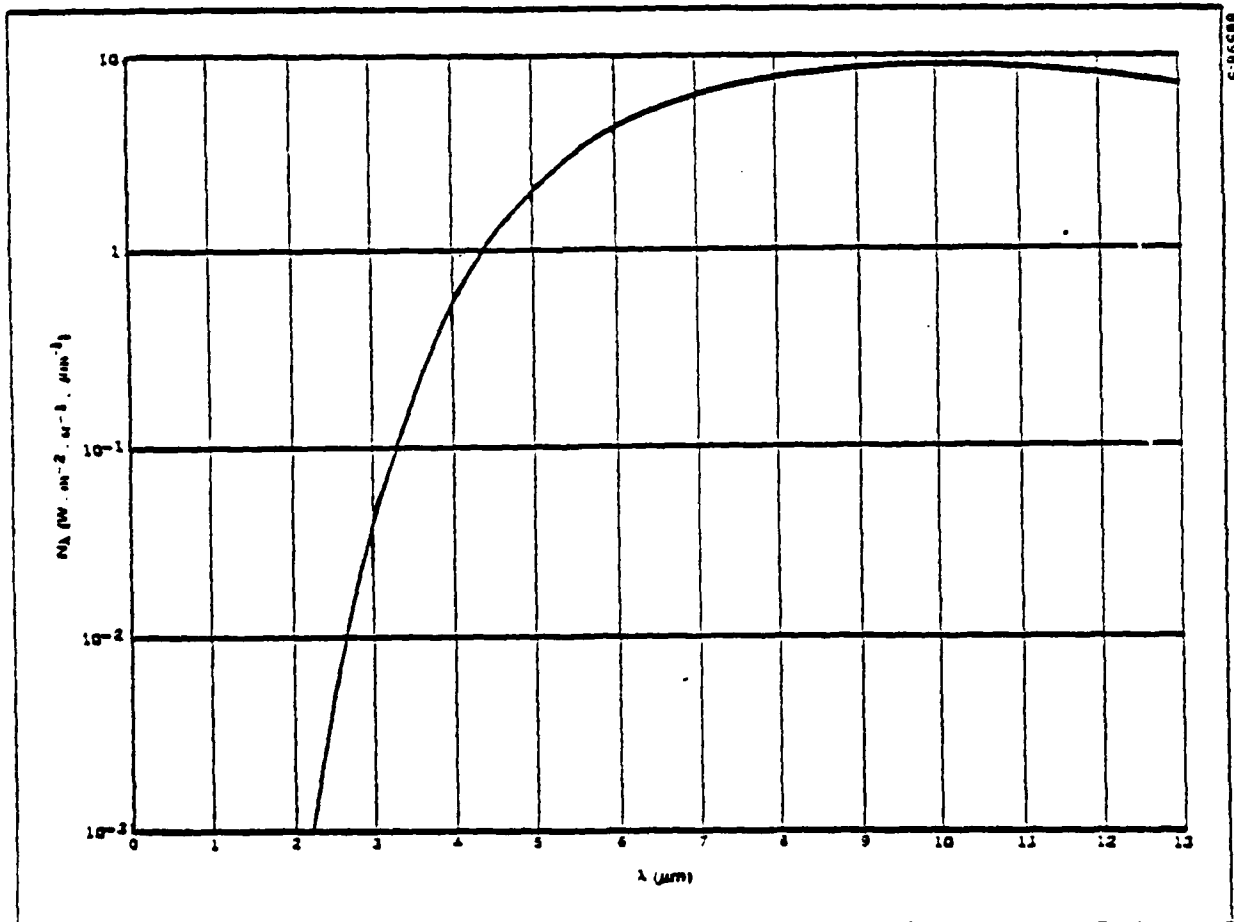
Figure 2-5. Spectral Radiance for a 293°K Blackbody

TABLE 2-1. (U) REFLECTANCE (ρ) AND EMISSIVITY (ε) OF COMMON
TERRAIN FEATURES FOR VARIOUS INFRARED BANDS [2-6] (U)

	0.7-1.0 μm	1.8-2.7 μm	3-5 μm	8-13 μm
Green Mountain Laurel	ρ = 0.44	ε = 0.84	ε = 0.90	ε = 0.92
Young Willow Leaf (dry, top)	0.46	0.82	0.94	0.96
Holly Leaf (dry, top)	0.44	0.72	0.90	0.90
Holly Leaf (dry, bottom)	0.42	0.64	0.86	0.94
Pressed Dormant Maple Leaf (dry, top)	0.53	0.58	0.87	0.92
Green Leaf Winter Color — Oak Leaf (dry, top)	0.43	0.67	0.90	0.92
Green Coniferous Twigs (Jack Pine)	0.30	0.86	0.96	0.97
Grass — Meadow Fescue (dry)	0.41	0.62	0.82	0.88
Sand — Hainamanu Silt Loam — Hawaii	0.15	0.82	0.84	0.94
Sand — Barnes Fine Silt Loam — So. Dakota	0.21	0.58	0.78	0.93
Sand — Gooah Fine Silt Loam — Oregon	0.39	0.54	0.80	0.98
Sand — Vereiniging — Africa	0.43	0.56	0.82	0.94
Sand — Maury Silt Loam — Tennessee	0.43	0.56	0.74	0.95
Sand — Dublin Clay Loam — California	0.42	0.54	0.88	0.97
Sand — Pullman Loam — New Mexico	0.37	0.62	0.78	0.93
Sand — Grady Silt Loam — Georgia	0.11	0.58	0.85	0.94
Sand — Colts Neck Loam — New Jersey	0.28	0.67	0.90	0.94
Sand — Mesita Negra — lower test site	0.38	0.70	0.75	0.92
Bark — Northern Red Oak	0.23	0.78	0.90	0.96
Bark — Northern American Jack Pine	0.18	0.69	0.88	0.97
Bark — Colorado Spruce	0.22	0.75	0.87	0.94
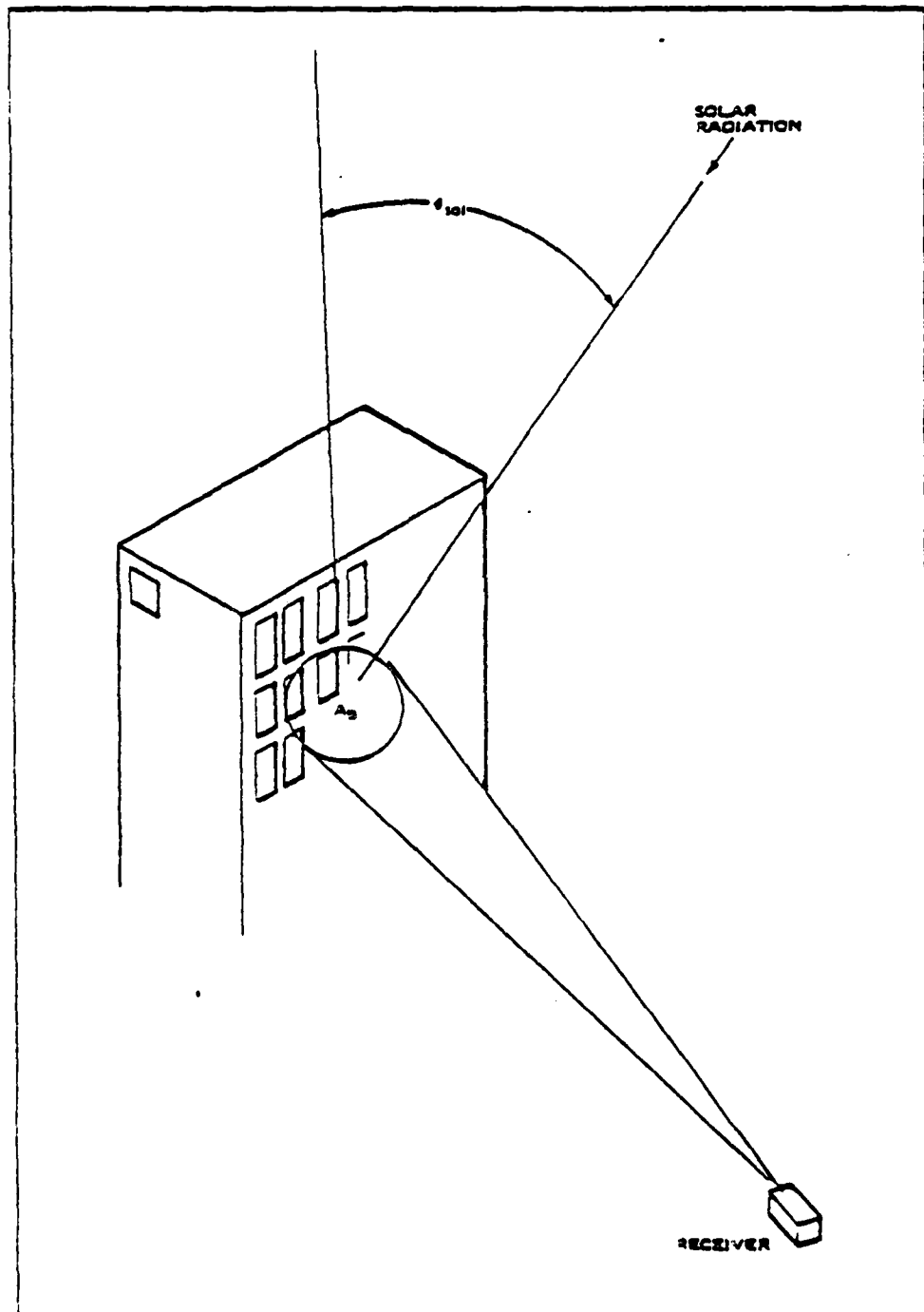
Figure 2-6. Characteristic Geometry for Establishing Solar Background
Radiation
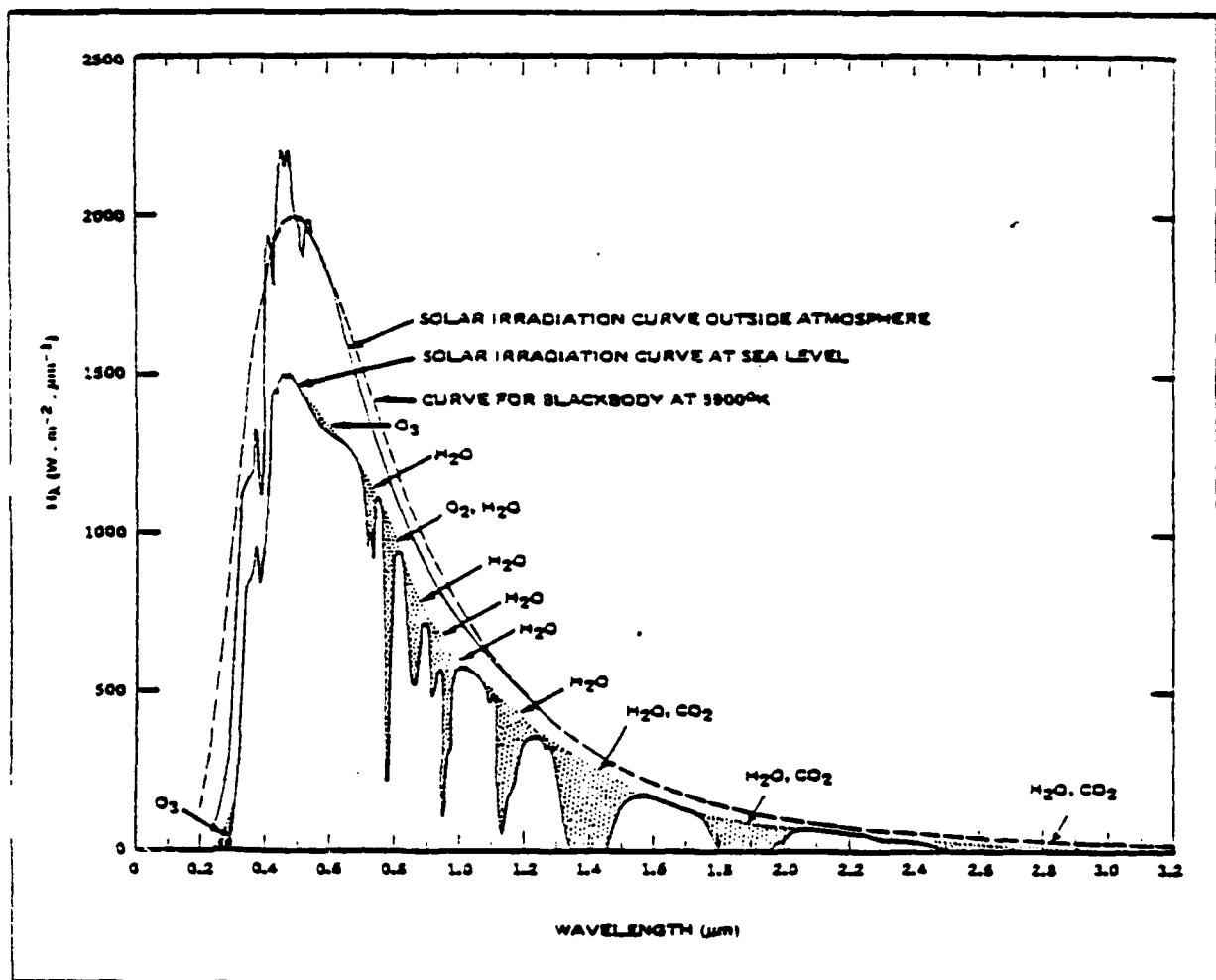
Figure 2-7. Solar Spectral Irradiance with Sun at Zenith. Shaded areas indicate absorption, at sea level, due to the atmospheric constituents shown [2-7].
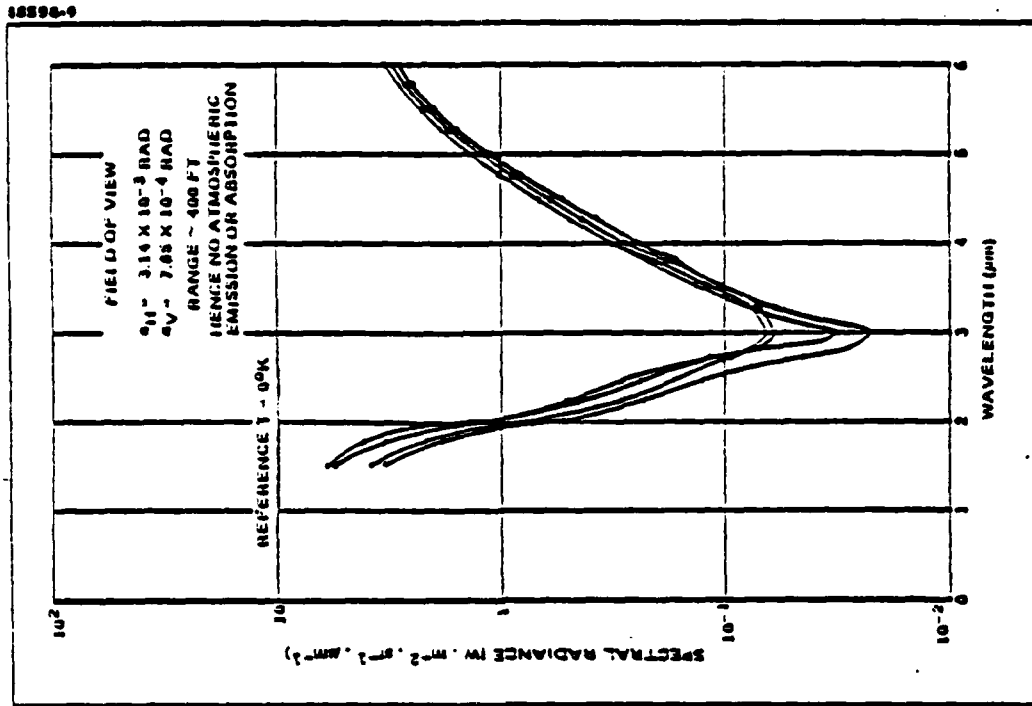
Figure 2-9. Spectral Radiance of Concrete, Winter Day, Clear [2-8]
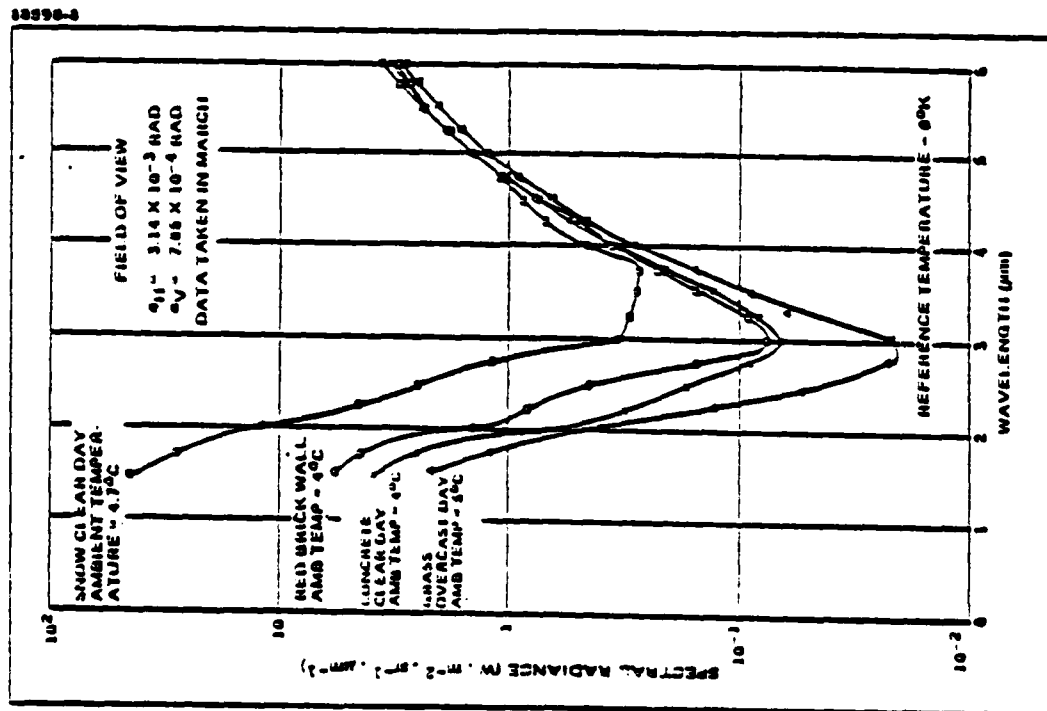
Figure 2-8. Daytime Spectral Radiance of Miscellaneous Targets [2-8]
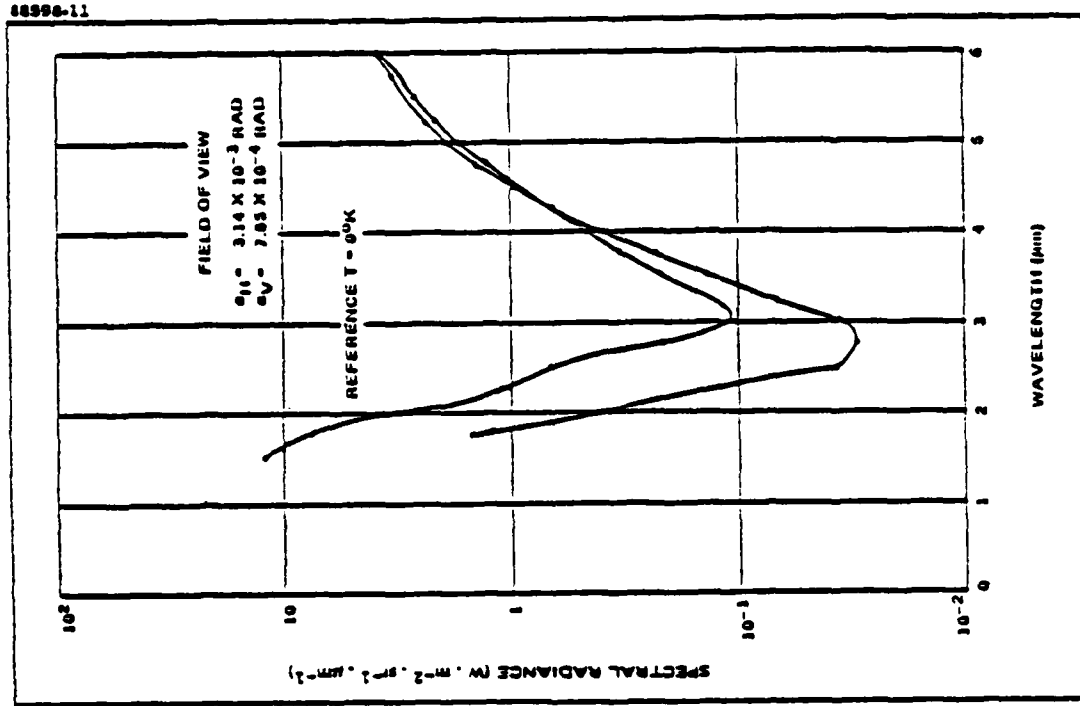
Figure 2-11. Spectral Radiance of Concrete, Summer Day. Overcast [2-8]
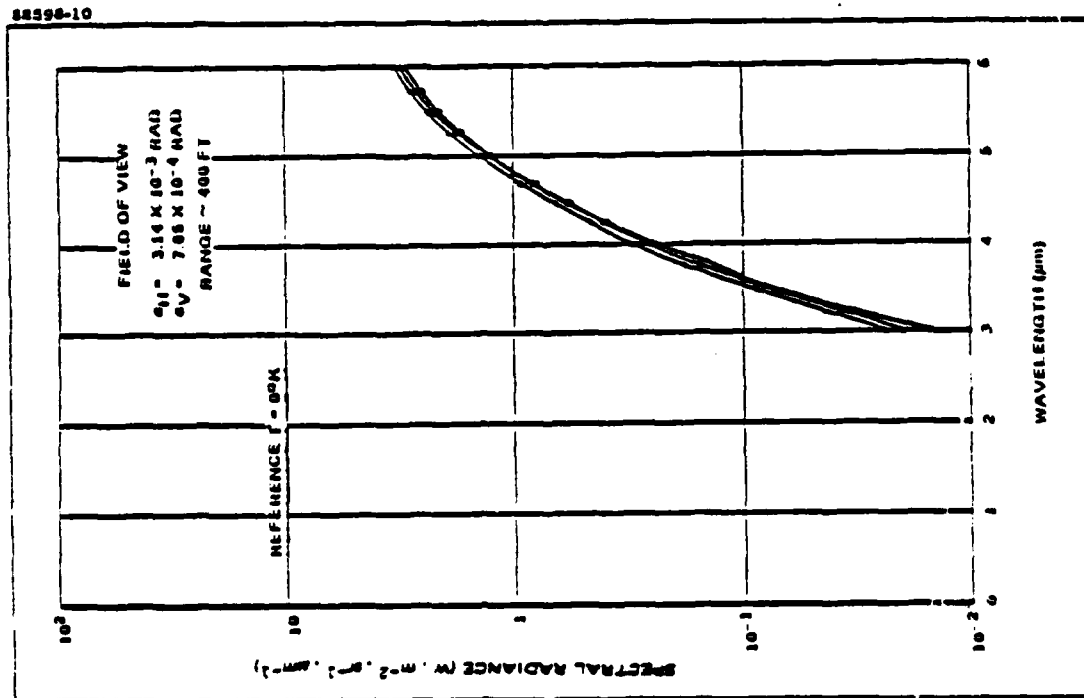
Figure 2-10. Spectral Radiance of Concrete, Summer Night, Clear [2-8]
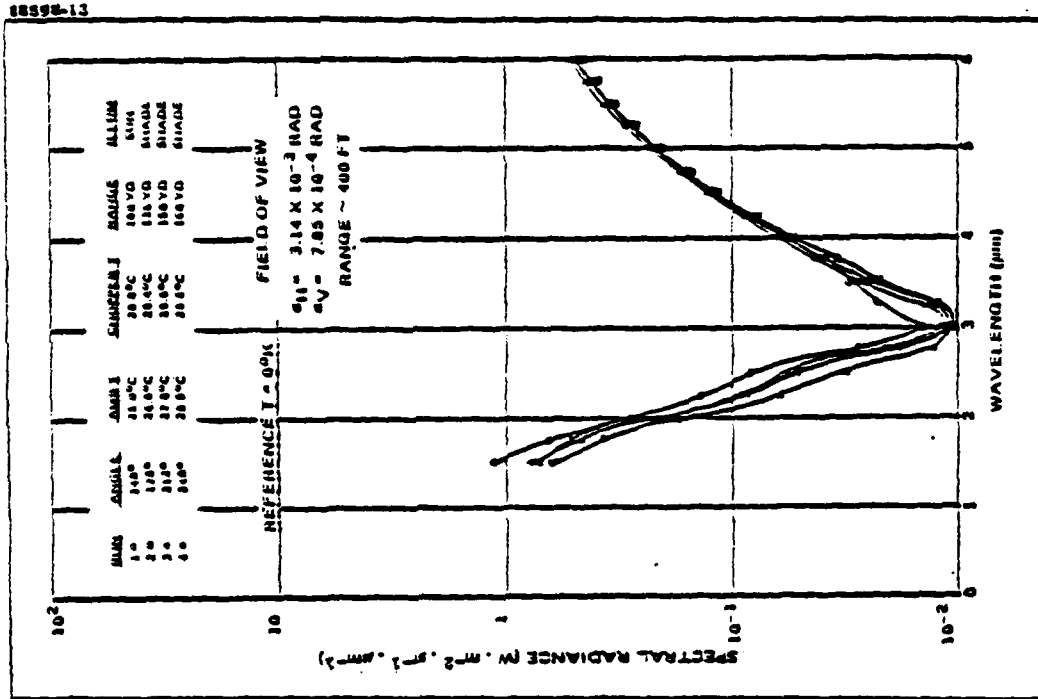
Figure 2-13. Spectral Radiance of Concrete Wall from Four Different Angles [2-8]
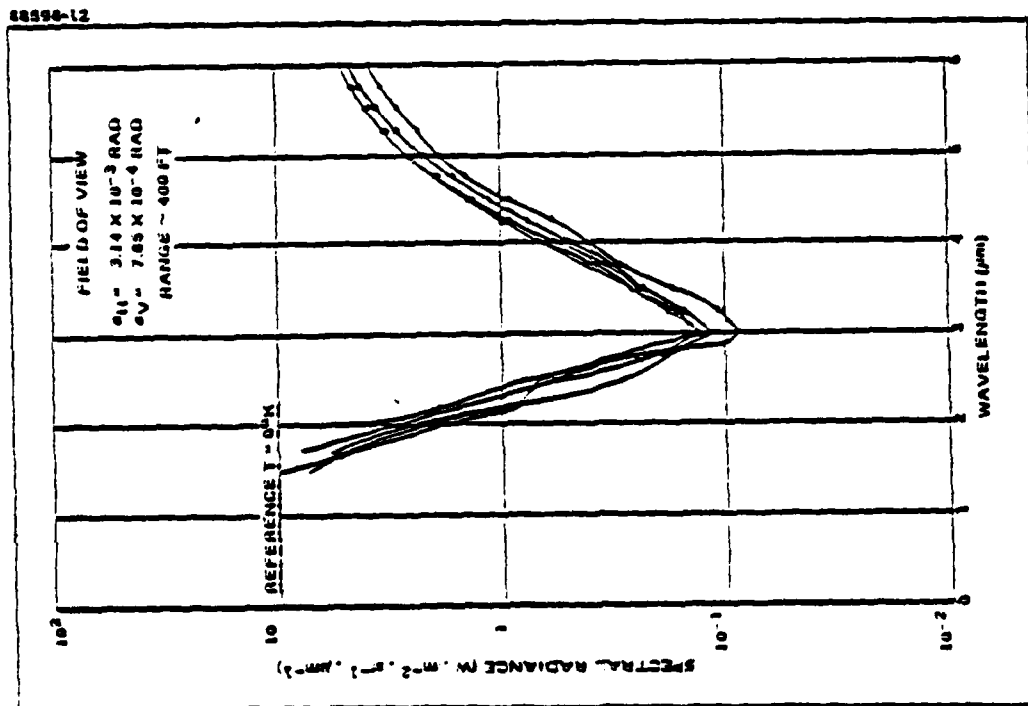
Figure 2-12. Spectral Radiance of Damp Concrete [2-8]
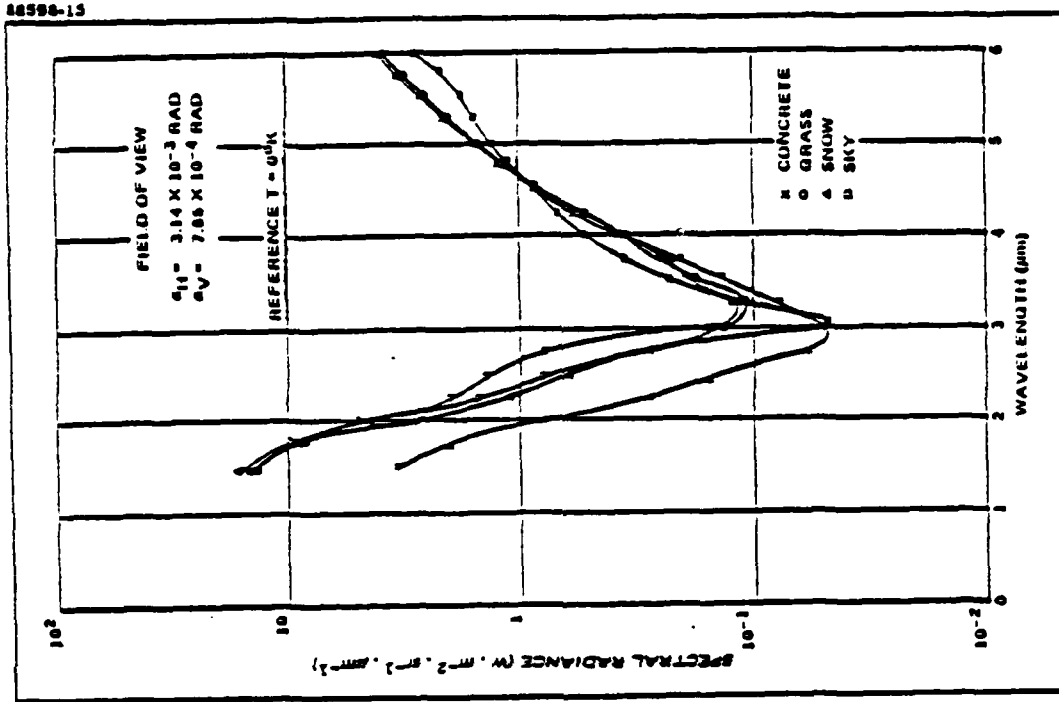
Figure 2-15. Spectral Radiance of Sky, Concrete, Snow, and Grass, Winter Day [2-8]
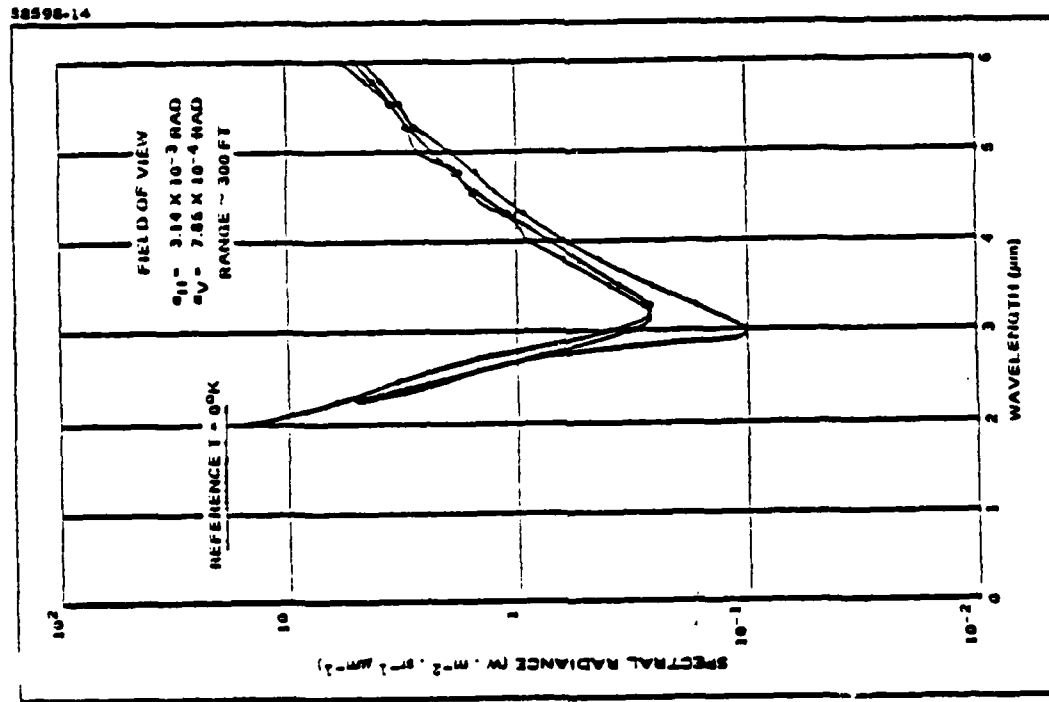
Figure 2-14. Spectral Radiance of Grass, Summer Day, Clear [2-8]

TABLE 2-2. APPROXIMATE NATURAL SCENE ILLUMINANCE FROM THE SKY UNDER VARIOUS CONDITIONS [2-9]

	lumens/m^2
Direct sunlight	1-1.3 x 10^5
Full daylight*	1-2 x 10^4
Overcast day	10^3
Very dark day	10^2
Twilight	10
Deep twilight	1
Full moon	10^{-1}
Quarter moon	10^{-2}
Starlight	10^{-3}
Overcast starlight	10^{-4}

* Not direct sunlight

Section 2 - Data-Base Review and Model Formulation
Subsection D - Scattering Mechanisms

1. OVERVIEW

(U) In this section the major mechanisms for scattering radiation are modeled, and data for
determining their significance is identified and discussed.

The total signal power P_s available to an off-axis receiver attempting to
radiation from an optical communications link may arise from four major sources.
They include transmitter sidelobes, transmitter window scatter, atmospheric scatter,
and backscatter from the receiver, backstop, or any foliage, structure, or other object
along the beam path, including the ground itself. Denoting the scattered power available
from the transmitter, atmosphere, and receiver as P_t, P_a, and P_r respectively then

$$P_s = P_t + P_a + P_r. \qquad (2\text{-}40)$$

Other, less obvious sources may also be present, but they are difficult to model in
general, and means for dealing with such extraneous sources must be developed as
they arise or are suspected. Some modeling techniques assuming virtual sources are
discussed.

Generally, all three major radiation sources cannot be collected simultaneously
because of the presumably limited field of view of the   receiver. A general
model should therefore specify the source power available as a function of
receiver field of view ϕ_{sh} and pointing direction. The three power sources have there-
fore been specified in terms of these parameters. To identify the most extreme case,
however, the total power available from all three sources at a given point can be cal-
culated by assuming the field of view ϕ_{sh} adequately wide to encompass the whole link.

Section 2 — Data-Base Review and Model Formulation
Subsection D — Scattering Mechanisms

2. TRANSMITTER SCATTER-SIDELOBES

(U) Aperture sidelobe radiation is completely specifiable in terms of exit aperture diameter
and optical wavelength for diffraction beyond one degree.

(U) If a coherent, uniform plane wave is transmitted through a transmitter aperture
of diameter D_t, the resulting radiant intensity distribution is given by the Airy pattern
[2-10],

$$I_s(\theta) = I_s(0) \left[2 \frac{J_1(\pi D_t \theta/\lambda)}{\pi D_t \theta/\lambda} \right]^2 , \tag{2-41}$$

where J_1 is the first-order Bessel function. A plot of the Airy pattern is shown in
Figure 2-16. This distribution also holds if the aperture is a lens or parabolic mirror
used to collimate a point source [2-11]. The radiant intensity on axis, $I_s(0)$, is given
by [2-10, p. 386]

$$I_s(0) = (\pi D_t^2/4\lambda^2)P_o, \tag{2-42}$$

based on the requirement that the total power P_o emitted from the transmitter be
conserved.

(U) The sidelobes of the Airy pattern shown in Figure 2-16 are noted to rapidly de-
crease in amplitude with increasing x, where $x = \pi D_t \theta/\lambda$. For the majority of cases
of interest we will be concerned only with large values of x. For example, with
$D_t = 10^{-2}$ m, $\lambda = 10^{-6}$ m, then for $\theta > 1^\circ$, $x > 500$. An asymptotic approximation to
$J_1(x)$ for large x is thus usually reasonable. From Olver [2-12],

$$J_1(x) \simeq (2/\pi x)^{1/2} \cos(x - 3\pi/4) \tag{2-43}$$

for large x. Since x is a rapidly varying function of θ, the sinusoidal variations will
average out, so that we may replace $[J_1(x)]^2$ by $\overline{[J_1(x)]^2}$, its average value, and

$$\overline{[J_1(x)]^2} = 1/\pi x. \tag{2-44}$$

Combining (2-41), (2-42), and (2-44)

$$I_s(\theta) = \frac{\lambda}{D_t} \frac{P_o}{(\pi\theta)^3} . \tag{2-45}$$

(U) The validity of (2-45) for practical systems must be questioned since uniform
plane waves are rarely achieved in practice, and various aperture shapes and obscura-
tions are often used. Also, gaussian rather than uniform beam profiles and extended
rather than point sources are commonly encountered. However, an analysis of calcu-
lations made by Rosen [2-13] indicates that variations due to gaussian beam profiles

(U) and central obscurations are only experienced by near-in sidelobes. Extreme sidelobes ($\theta > 1^\circ$) approach the same asymptotic limit. A similar result occurs if extended sources, either coherent or incoherent, are considered.

(U) The major shortcoming of (2-45) is experienced when very long link paths are considered, such as for a satellite-to-ground link, where values of θ less than one degree must be analyzed. The exact Airy solution may then be appropriate.

(U) Another minor problem with (2-45) is that it predicts sidelobes at 90° from the aperture. This results because of the neglect of the so-called obliquity factor [2-11] in the derivation of the Airy pattern. The rigorous equation from which (2-41 is derived contains a multiplicative factor $\cos \theta$, the obliquity factor, which is neglected. Reintroducing it into (2-45) in order to avoid the physically unrealizable condition of diffraction sidelobes at 90°,

$$I_s(\theta) = \frac{\lambda}{D_t} \frac{P_0}{(\pi\theta)^3} \cos \theta. \tag{2-46}$$

Whereas the variation is clearly negligible except at large angles, the resulting distribution is more plausible and intuitively satisfying.
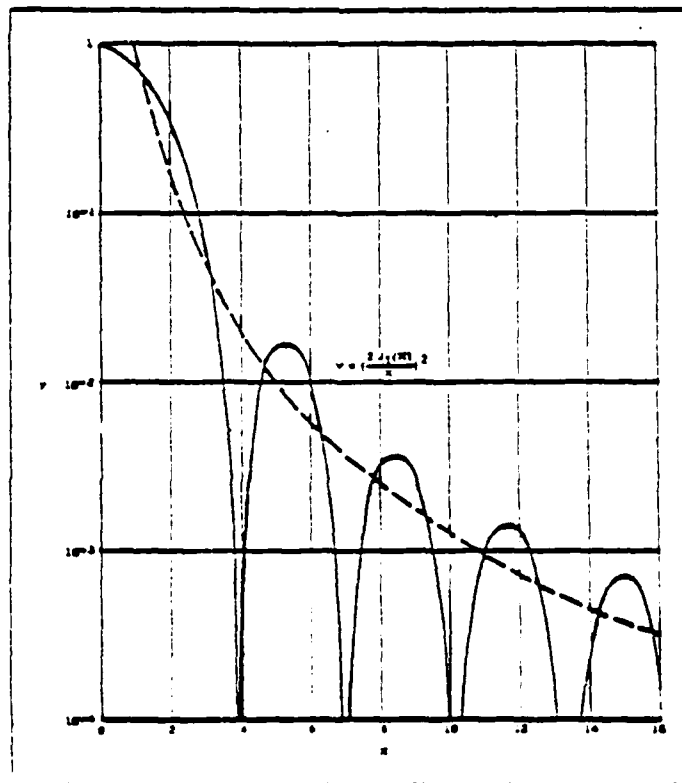
Figure 2-16. The Airy Pattern, or Fraunhofer Diffraction Pattern for a Circular Aperture. The asymptotic average for large x is shown dotted.

Section 2 – Data Base Review and Model Formulation
Subsection D – Scattering Mechanisms

3. TRANSMITTER SCATTER – PORT SCATTER

The complexity of port scattering mechanisms suggest that an empirical rather than an analytical approach be taken.

Port scatter results from microscopic surface irregularities, bulk optical material imperfections, and dust, moisture, and other contaminants on and within the optical system. A general analytical approach to establishing the amount of radiant intensity scattered from systems due to the various scattering sources is complicated by the fact that the scattered radiation may then be refracted or reflected by the following optics. Therefore, not only does the distribution of scattering centers have to be specified, but also complex off-axis ray tracing must be performed. Measured data on many systems and optical materials have been compiled, however, and an empirical rather than analytical approach appears to be more tractable.

Regardless of how the data are derived, the scattering profile will be expressed in terms of a normalized port scattering distribution function $\sigma_p(\theta)$, defined such that

$$\sigma_p(\theta) = I_p(\theta)/P_0 \cos\theta \qquad (2\text{-}47)$$

where $I_p(\theta)$ is the measured radiant intensity scattered at an angle θ from the transmitter exit aperture when it is transmitting power P_0. This is consistent with definitions used by Nicodemus* [2-14].

It is assumed here that scattering is radially symmetrical, depending only on θ, which may not always be a valid assumption. Real-world systems may also contain specular components. Variations can be introduced as necessary to represent specific cases by appropriately selecting the function $\sigma_p(\theta)$.

---

*Use of Nicodemus' definition, which includes the factor $\cos\theta$, is somewhat arbitrary for characterizing port scatter. The purpose of including the factor $\cos\theta$ is clearer in the context of surface reflections, as discussed ahead, in which case a reflectance distribution function is defined similarly to (2-47) so that its value will equal a constant if the surface is perfectly diffuse, or lambertian, a common assumption for natural features. σ_p is similarly defined here for the sake of consistency.

4. TRANSMITTER SCATTER - TOTAL POWER COLLECTABLE

) The total power available to a. ⋯ ⋯ ⋯ from the transmitter is the sum of the attenuated sidelobe and port-scatter components scattered within the ⋯ receiver field of view.

The contributions from sidelobes and window scatter comprise the total scattered power available from the transmitter. In order to detect it the ⋯ receiver field of view must intercept the transmitter window. We shall disregard the narrow transition region and assume that the whole window either can or cannot be seen. With reference to Figure 2-17 we shall assume that it can be seen if and only if $\theta_t - \sigma_{sh}/2 \leq \theta_i \leq \theta_t + \sigma_{sh}/2$. If this condition is met, then the total scattered transmitter power P_t incident on the detector will be

$$P_t(\theta_i) = [L_s(\theta_i) + L_p(\theta_i)] \exp(-\alpha R_t) \Omega'_s \tag{2-48}$$

where R_t is the range from the transmitter to the ⋯ receiver,

$$\alpha = \alpha_a + \alpha_s \tag{2-49}$$

is the atmospheric extinction coefficient at the operating wavelength due to absorption (α_a) and scattering (α_s) by atmospheric constituents, and

$$\Omega'_s = A_s / R_t^2, \tag{2-50}$$

which defines that solid angular portion of radiation scattered from the transmitter into the ⋯ receiver. Combining (2-46)-(2-48) and (2-50)

$$P_t(\theta_i) = \begin{cases} P_o \left[(\lambda/D_t)(\pi\theta_i)^{-3} + \sigma_p(\theta_i) \right] \cos\theta_i \exp(-\alpha R_t) A_s / R_t^2 \\ \quad \text{for } \theta_t - \phi_s/2 \leq \theta_i \leq \theta_t + \phi_s/2 \\ 0 \quad \text{otherwise.} \end{cases} \tag{2-51}$$

(U) We note that, in general, the net change dP in optical power due to atmospheric extinction over an elemental path length dr is

$$dP = -\alpha P dr. \tag{2-52}$$

If α is constant over the path length of interest, in this case R_t, then the simple exponential form for the extinction loss, as introduced in (2-48), holds. However, if α is not constant over the path length, then we must make the replacement

(U)

$$\exp(-\alpha R_t) \longrightarrow \exp\left[-\int_0^{R_t} \alpha(r)\,dr\right].$$

(2-53)

( )   The extinction coefficient is in general a function of both the atmospheric state and the link altitude. The change (2-53) must be invoked whenever the spatial variation is significant. The most obvious case where the substitution will be needed is for the satellite-to-ground geometry. All other parameters are dependent only on the transmitter or ̄ ̄ ̄ receiver characteristics or their relative positions and altitudes.
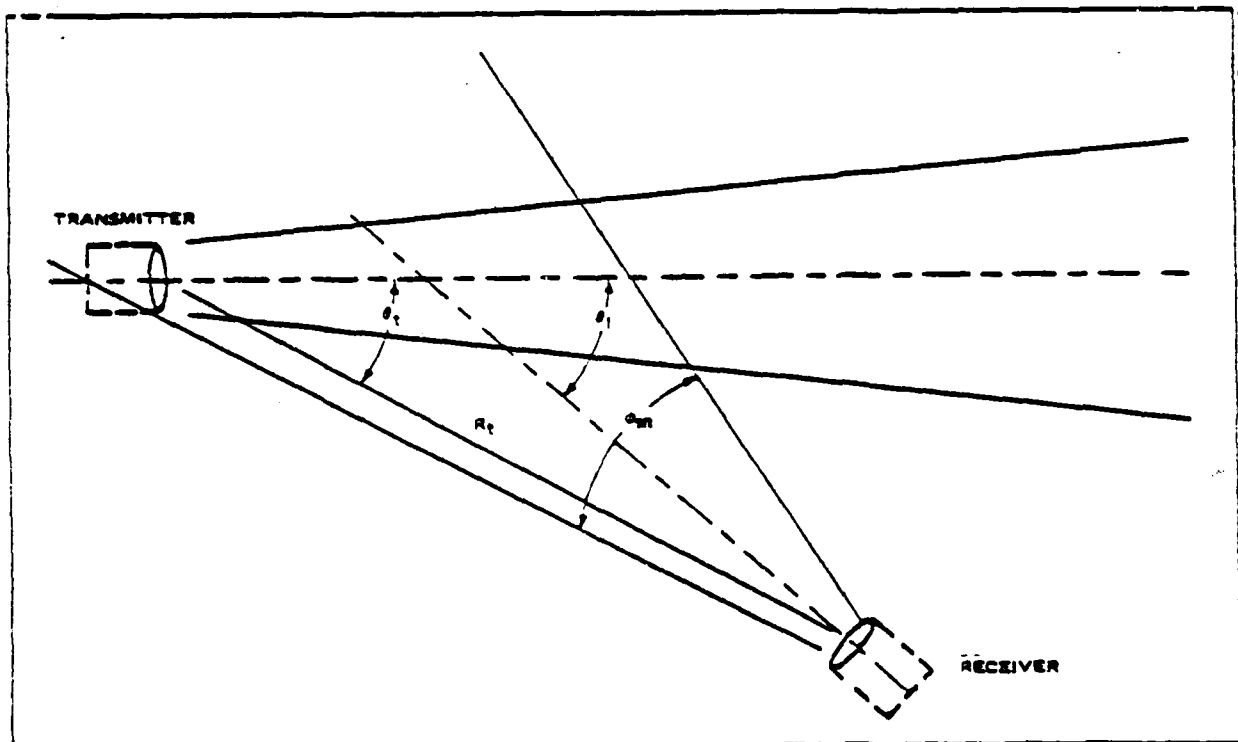
Figure 2-17. (C) Geometry Necessary for _____ of Transmitter Scatter. The transmitter must be within the _____ receiver's field of view. ′ ;

5. TRANSMITTER SCATTER – MEASUREMENT DATA

(U) Port scattering from practical optical systems generally varies exponentially with off-axis angle, with variations due to differences in design and degree of cleanliness. Internal-wall scattering can result in strong specular glints.

(U) As noted, it is very difficult to develop a generalized analytical approach for describing port scatter from an optical transmitter because of the wide variety of geometries and phenomena involved. Figure 2-18 illustrates the complexity of such an approach. Assuming, for example, a light-emitting diode or laser diode as a source in a refractive system, the radiation must be collected and focused by a lens, and the scattering profile will be dependent on the spatial pattern of light incident on the lens. The lens will scatter light at both surfaces and from bulk imperfections. Moreover, a nonnegligible amount of doubly reflected light will be refocused towards a short secondary focal point at a distance of about $(n-1)(2n)^{-1}f$, where f is the lens focal length and n its index of refraction. Light may also be scattered off internal walls of the system.

(U) A more sophisticated system might use a collimated laser and a beam expander, also shown in Figure 2-18 assuming reflective optics. Though such a design approach is inherently cleaner, structures such as the web required to hold the secondary mirror will introduce an additional scattering component which is nonsymmetrical and difficult to model predictively.

(U) Several investigations have examined the scattering properties of optical materials. Scheele [2-15] has performed scattering distribution measurements on numerous transparent optical materials (flats) useful at both visible and infrared wavelengths. A portion of his results which are representative are shown in Figures 2-19, 2-20, and 2-21 for various optical materials at 0.633 μm, 1.06 μm, and 10.6 μm. He also has made measurements at 3.39 μm. Leinert and Kluppelberg [2-16] have examined the scattering properties of mirrors at visible wavelengths. Some of their results are also shown in Figure 2-19. A / report provides measured data for a germanium anti-reflection coated optical flat irradiated at 10.6 μm, also shown in Figure 2-21. Carmer and Lindquist [2-18] also made scattering measurements at 1.06 μm for various materials, and their results fell within the envelopes shown in Figure 2-20. They also varied the source polarization in their measurements and observed only minor variations. For each of the programs cited, the optical beam was incident normal to the sample.

(U) All of these results show a basic θ^{-2} angular dependence. Also, Scheele notes that scattering generally decreases with increasing optical wavelength, showing approximately a λ^{-2} wavelength dependence. The bulk scattering properties of a transparent material can be ascertained by comparing the scattering properties of the same material but different thicknesses such as those shown in Figure 2-20 for IRTRAN.

(U) Leinert and Kluppelberg also made measurements on lenses at 0.633 μm, the results of which are shown in Figure 2-22. Again the curves are roughly proportional to θ^{-2} when double reflection is suppressed. The doubly reflected component tends to increase scattering at larger angles. It can be substantially suppressed using anti-reflection (AR) coatings, but some coatings tend to increase surface scattering, especially after cleaning [2-18].
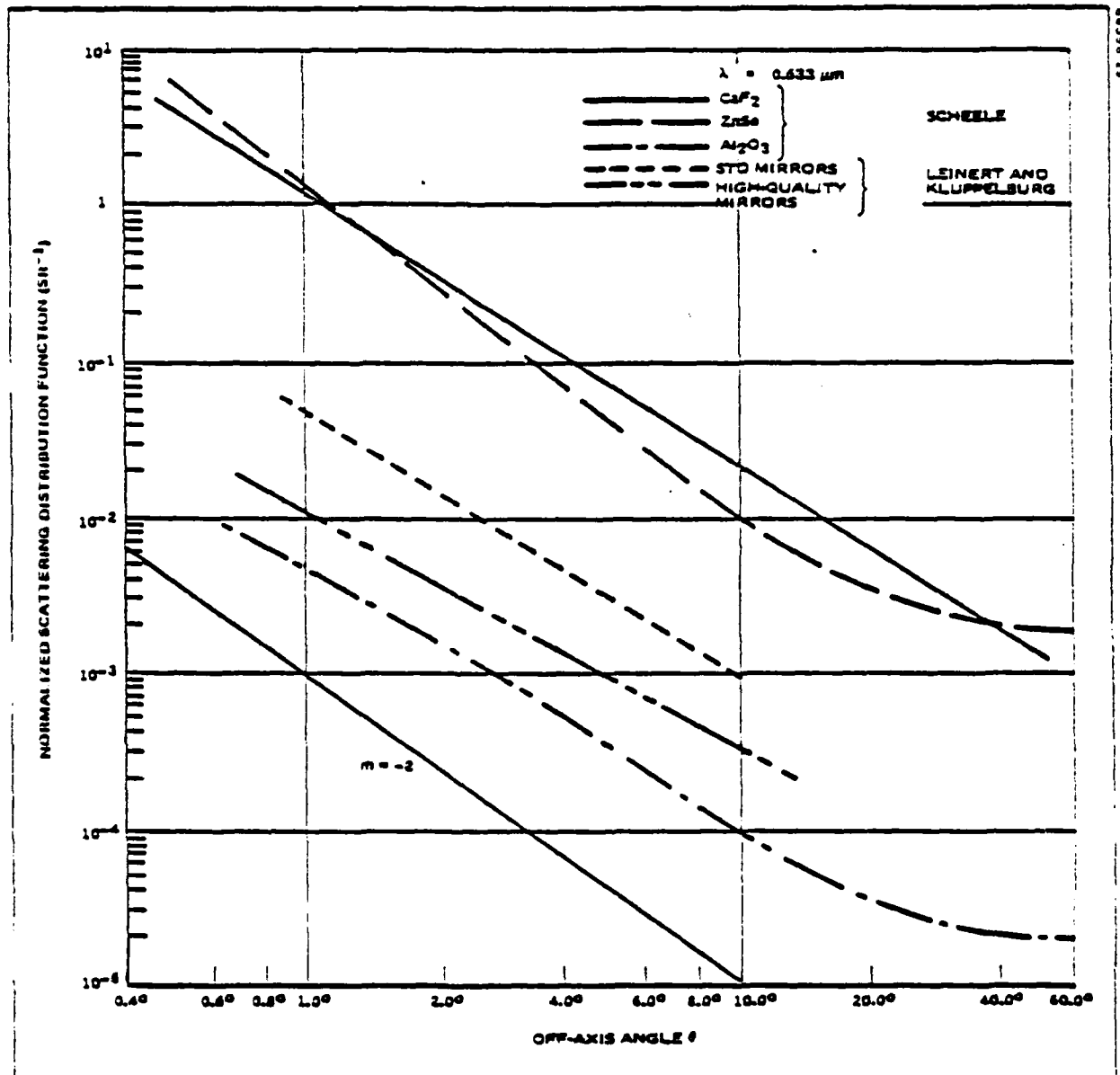
Figure 2-19. (U) Normalized Scattering Distribution Functions for Various Optical Materials irradiated Normally at 0.633 μm. Data were obtained from Scheele [2-15] and Leinert and Kluppelberg [2-16] (U)
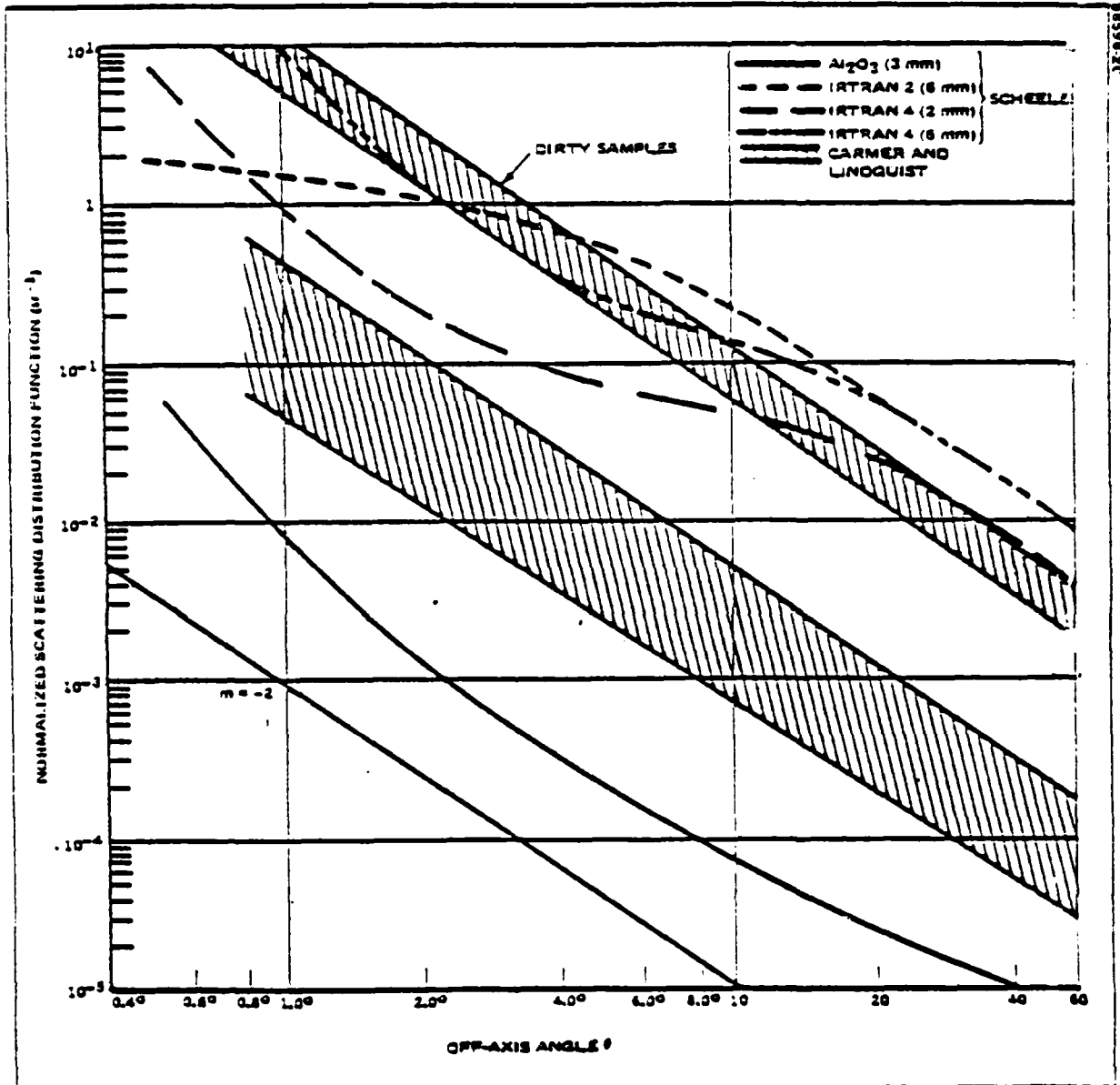
Figure 2-20. (U) Normalized Scattering Distribution Functions for Optical Materials of Various Thicknesses Irradiated Normally at 1.06 μm [2-15], [2-18] (U)
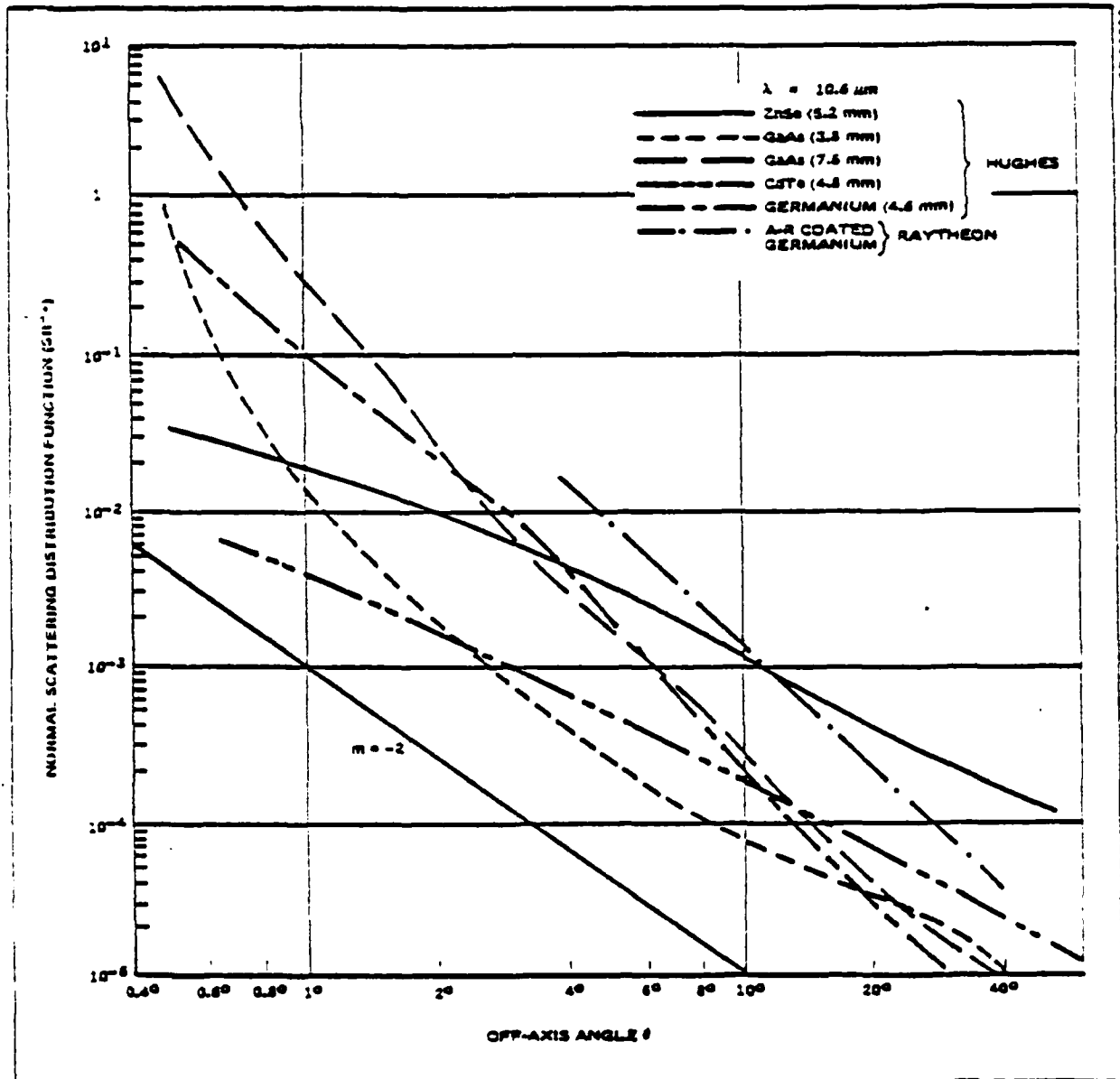
Figure 2-21. (U) Normalized Scattering Distribution Functions for Optical Materials of Various Thickness Irradiated Normally at 10.6 μm [2-15], [2-17] (U)
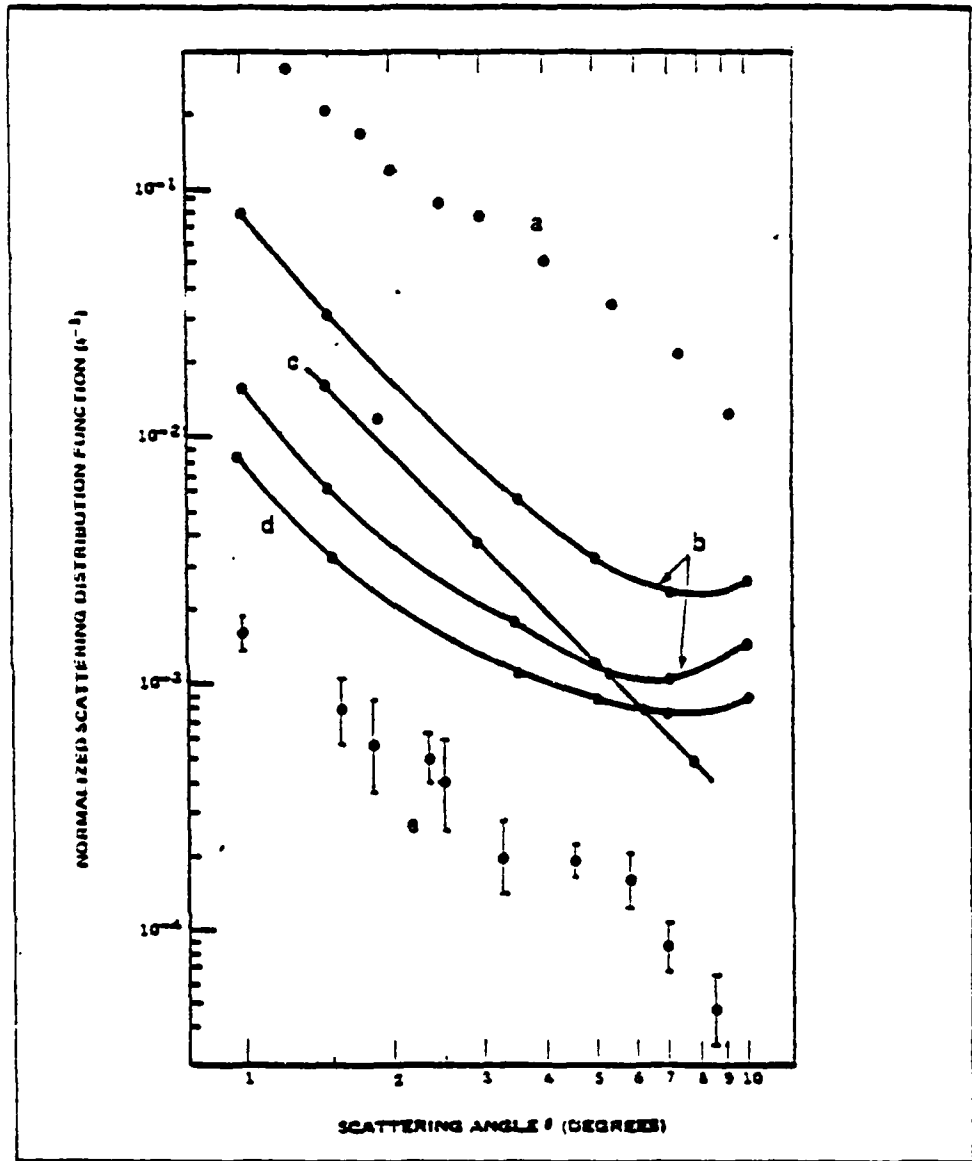
Figure 2-22. (U) Normalized Forward Scattering Distribution for Various Lenses
at 0.633 μm: (a) slightly dusty lens: (b) lens cleaned with collodium or ultrasonic
bath: (c) ultrasonically cleaned lens with doubly reflected component suppressed:(
(d) quartz lens with higher surface quality: (e) polished (λ/20) flat of Suprasil I
[2-16] (U)

Section 2 - Data-Base Review and Model Formulation
Subsection D - Scattering Mechanisms

6. ATMOSPHERIC SCATTERING - THEORETICAL MODELING

(U) The power available via atmospheric scattering must in general be calculated using numerical integration, but a closed-form approximation is usable in the majority of cases of interest.

(U) The major parameter used to characterize atmospheric scattering is the atmospheric scattering coefficient α_s. When an optical beam passes through a scattering media, the net power scattered out of the beam is proportional to the incident power P_i and to the path length. The elemental atmospheric scattering loss dP_{sc} in length dz is given by

$$dP_{sc} = \alpha_s P_i \, dz \tag{2-54}$$

(U) Atmospheric scattering is further characterized by the scattering distribution function $F(\theta)$, which describes the relative intensity of scattered radiation as a function of off-axis angle. If a total power P_{sc} is scattered from an arbitrary volume element, and $I_{sc}(\theta)$ is the resulting intensity scattered at the angle θ, then the scattering distribution function is defined as

$$F(\theta) = I_{sc}(\theta)/P_{sc} \tag{2-55}$$

Moreover, since

$$\int_{4\pi} I_{sc}(\theta) \, d\Omega = P_{sc} \tag{2-56}$$

where the integration is over a sphere, it follows that

$$\int_{4\pi} F(\theta) \, d\Omega = 1 \tag{2-57}$$

The scattering distribution function used here is therefore normalized.

Now consider the geometry of Figure 2-25. Using (2-54) and (2-55), the amount of radiation originating from the transmitter and scattered from the elemental volume $dV' = dx' \, dy' \, dz'$ into the receiver field of view is given by

$$dI_{sc}(\theta_i') = P_i(\underline{R}') \, F(\theta_i') \, \alpha_s(\underline{R}') \, dz' \tag{2-58}$$

where $P_i(\underline{R}')$ is the transmitter power incident on dV', $\underline{R}'$ is the vector from the transmitter to dV', and θ_i' is the scattering angle from dV' into the receiver. (Note that the volume element dV' of Figure 2-25, and consequently $\underline{R}'$, ϕ_i', $\underline{R}_i'$, and θ_i' are not necessarily in the plane of the diagram.) The power incident on dV' is given by
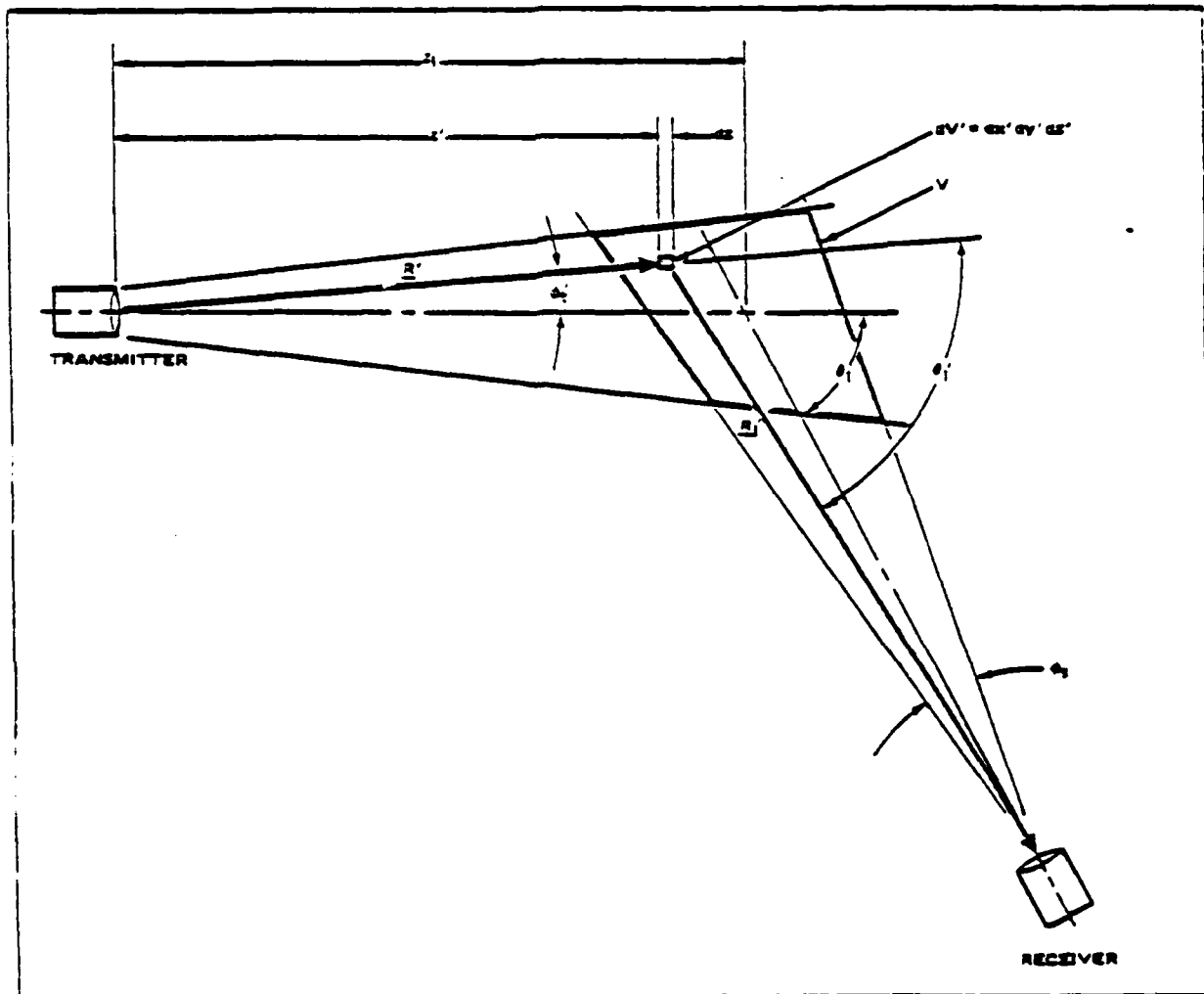
Figure 2-25.   Generalized Geometry Depicting Variables which Describe Atmospheric Scattering.
V is the volume of intersection of the beam, not necessarily assumed uniform, with the
receiver field of view. The vectors (indicated by underline) are not necessarily in the plane of the
diagram.

(C)

$$P_i(R') = I_0(\theta_t') \exp\left[-\int_0^{|R'|} \alpha(R)\, dR\right] d\Omega' \qquad (2\text{-}59)$$

where $d\Omega' = dx'\, dy'/(R')^2$. The atmospherically scattered power incident on the receiver detector from dV' is

$$dP_a = dI_{sc}(\theta_i') \exp\left[-\int_{R_i''}^{|R' + R_i''|} \alpha(R)\, dR\right] A_s/(R_i')^2 \qquad (2\text{-}60)$$

Combining (2-58), (2-59), and (2-60) and integrating,

$$P_a = A_s \int_V dV' I_0(\phi_t') F(\theta_i') \alpha_s(R')\exp\left[-\int_0^{|R'|} \alpha(R)dR - \int_{|R'|}^{|R' + R_i''|} \alpha(R)dR\right] /(R'R_i')^2 \qquad (2\text{-}61)$$

where V is the volume of intersection of the   receiver field of view and the transmitter beam.

(U) Aside from secondary scattering effects, (2-61) is essentially exact assuming $D_s/R_i' \ll \theta_i'$ so that θ_i' can be considered constant over the   receiver aperture, a condition which we assume is always met. For the general case, a solution requires numerical integration. Such an approach is necessary usually only for very long links where the beam diameter can become quite large, or for vertical links where large variations of α and α_s with altitude are experienced. Space-to-ground links, for example, fit both conditions and must be solved numerically. However, (2-61) may be expressed in closed form if several simplifying assumptions are made. These assumptions are applicable to the large majority of conventional laser communication links, as illustrated in Figure 2-26.

(U) The first simplifying condition is that α and α_s be reasonably uniform over the region so that the exponential extinction losses can be expressed in closed form. Secondly, if the beamspread and link range are sufficiently small, then $R' \approx z'$ and $R_i' \approx R_i$ throughout dV'. Finally, if the beam is fairly uniform and narrower than the receiver's field of view, then

$$I_0(\phi_t')\, dV'/(R')^2 \approx P_0\, dz_i. \qquad (2\text{-}62)$$

Using these three simplifying assumptions and the relationships

$$z_i = z_s - x_s/\tan \theta_i \qquad (2\text{-}63)$$

and

$$dz_i = x_s \csc^2 \theta_i\, d\theta_i = R_i\, d\theta_i/\sin \theta_i, \qquad (2\text{-}64)$$

Figure 2-26.   Basic Geometry for Which Equation 2-65 Holds. Also required is that α and α_s be uniform throughout the beam and scattering regions. (U)

(U)

then

$$P_a = (P_0 A_s \alpha_s / x_s) \int_{-\phi_s/2}^{+\phi_s/2} d\theta_i \; F(\theta_i) \; \exp\left[-\alpha z_s\right] \; \exp\left[\alpha x_s (\cos \theta_i - 1)/\sin \theta_i\right]. \qquad (2-65)$$

If the field of view ϕ_s is sufficiently small that terms in the integrand of (2-65), especially $F(\theta_i)$, does not vary appreciably, then

$$P_a(\theta_i) = [P_0 A_s \alpha_s \phi_s F(\theta_i)/x_s] \; \exp\left[-\alpha z_s\right] \; \exp\left[\alpha x_s (\cos\theta_i - 1)/\sin \theta_i\right]. \qquad (2-66)$$

For larger fields of view, ϕ_s may be subdivided into elements for which (2-66) holds and the power available from each element summed to obtain the total power available. (U)   Turbulence effects of the atmosphere have been considered and appear to be significant only when phase coherence is essential (the heterodyne case) or for the space-to-ground scenario. Typical beam spreading due to turbulence, even considering ground-level paths in very turbulent conditions, is of the order of 100 μrad. Since typical beam spreads for ground links are $\lesssim$ 10 mrad, the increase in spot size is insignificant. However, for satellite-to-ground links an incremental increase in beam spread may increase the central radiation spot size on the ground by as much as a kilometer. Such cases must clearly be considered.

Section 2 – Data-Base Review and Model Formulation
Subsection D – Scattering Mechanisms

7. ATMOSPHERIC SCATTERING - EXTINCTION AND SCATTERING DATA

(U) Atmospheric extinction characteristics vary both temporally and spatially, depending on global locale, with changing weather, seasonal, and diurnal conditions. Data collected by AFGL and NRL comprise the major source for atmospheric modeling.

(U)   Atmospheric absorption and scattering characteristics are dependent on the individual molecular and aerosol constituents which make up the atmosphere. Absorption is primarily associated with specific molecular species, especially H_2O and CO_2, and can be established in terms of the vibrational and rotational absorption-line characteristics of the specific molecules.. Scattering is dependent on the number density, size distribution, shape, and index of refraction of the constituent molecular and aerosol particles. These parameters are not only difficult to measure, but they are also highly variable both spatially and temporally at a given locale, and different locales will have different characteristic atmospheric profiles.

(U)   The majority of atmospheric data for ECKSTROM modeling has been obtained from the Air Force Geophysics Laboratories (AFGL, formerly Air Force Cambridge Research Laboratories) atmospheric data compilation. AFGL has had an extensive program concerned with the optical properties of the atmosphere for over a decade, and they continue to compile data from which they have established models for both low- and high-resolution atmospheric transmittance. Additional supportive data has been obtained from Naval Research Laboratory (NRL) publications.

(U)   Because of the wide diversity of atmospheres encountered globally, AFGL has defined five standard atmospheres as a representative cross section [2-22]. These include models referred to as Tropical, Midlatitude Summer and Winter, and Subarctic Summer and Winter. These models are defined in terms of the atmospheric pressure and density, temperature, and ozone and water vapor concentrations as a function of altitude. In addition, two aerosol models have been defined, referred to as continental clear and continental hazy, corresponding to visibilities of 23 km and 5 km respectively. A total of ten models can thus be specified.

(U)   Because of the extensiveness and ready availability of the AFGL data on atmospheric models [2-22] - [2-25] none of it will be reprinted here. The data available covers most nominal conditions and consists of a compilation of absorption and scattering coefficients for each atmospheric model as a function of wavelength and altitude. Most major laser lines are included.

(U)   An alternate approach to determining absorption and scattering coefficients is to calculate them using either of two computer models developed by AFGL. LOWTRAN [2-26] is a low-resolution code (20 cm^{-1}) useful for characterizing broad-band sources such as light-emitting diodes and diode lasers. The most recent version, LOWTRAN 3B, introduces four new aerosol models, the Maritime, Urban, Rural, and Tropospheric Models. This extends the modeling variations possible.

(U)   LOWTRAN, however, is inappropriate for characterizing narrow-band laser sources. A comparison of the spectral characteristic of a narrow-band (DF) laser source to that of the atmosphere is shown in Figure 2-27 [2-27]. The LOWTRAN code does not provide the fine structure exhibited here, and a higher-resolution code is required.

(U)   HITRAN, actually a line compilation, can be used to establish atmospheric
absorption characteristics for a particular laser line to the degree of resolution desired
[2-28], [2-29]. This code has been made possible because of an extensive compilation
of absorption line spectra due to all major molecular atmospheric constituents, includ-
ing H_2O, CO_2, O_3, N_2O, CO, CH_4, and O_2.

(U)   Ongoing measurements at NRL have confirmed with good agreement the general
band structure predicted by the HITRAN model. Measurements made at DF laser
wavelengths (3.6 - 4.1 μm) have shown excellent agreement [2-30]. However, the
HITRAN code has been found to substantially over-predict transmission in the region
from 4.7 μm to 5.1 μm [2-31]. In both regions the results have been found to be
strongly dependent on local water vapor pressure. Code updates at AFGL and measure-
ments at NRL continue, however, and differences in the theoretical models and mea-
sured data are rapidly converging. Moreover, extensive additional data will soon be
available from an AFGL atmospheric measurements program taking place in Europe
in cooperation with NATO [2-32].
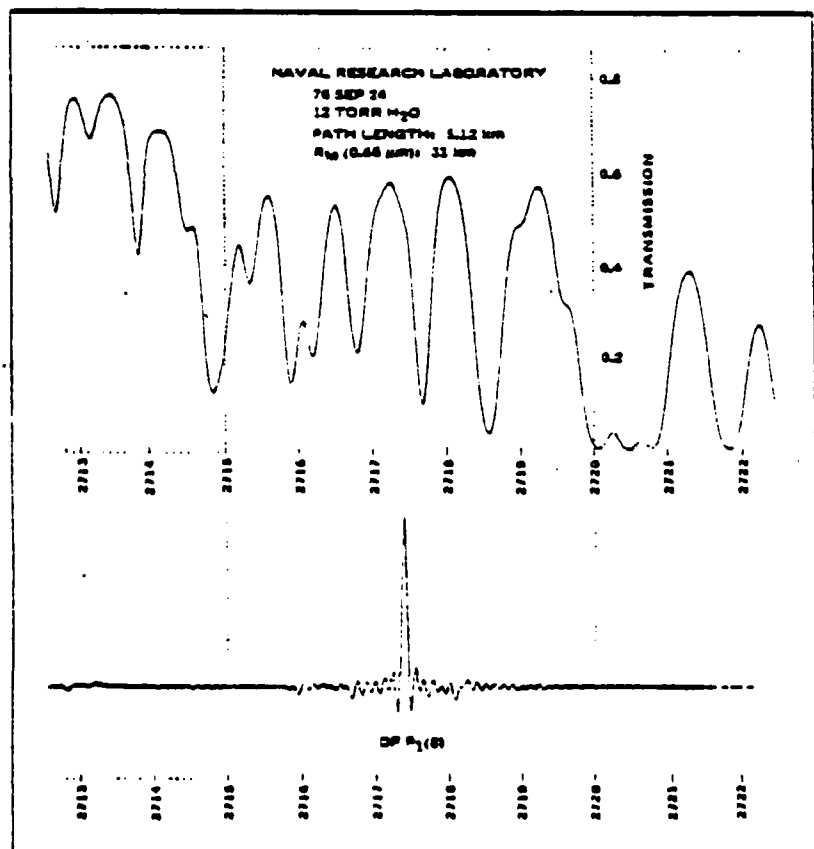
Figure 2-27. Comparison of the Atmospheric Transmission Spectrum and the
DF Laser Emission Spectrum. The transmittance is rapidly varying in the
vicinity of the laser line and requires a high-resolution mode. to maintain
accuracy [2-27].

Section 2 - Data-Base Review and Model Formulation
Subsection D - Scattering Mechanisms

3. ATMOSPHERIC SCATTERING - DISTRIBUTION FUNCTION DATA

(U) Atmospheric scattering profiles have been obtained from scattered measurement programs and from the general Mie scattering theory, with which the measured data are in fairly good agreement.

(U) If the atmosphere were composed only of molecules, whose diameters are much less than optical wavelengths, appropriate approximations would result in the Rayleigh scattering theory, which predicts an almost uniform scattering distribution. However, aerosol components of the atmosphere are almost always the dominant scattering mechanism. Such aerosol particles typically have diameters of the order of the optical and infrared wavelengths of interest, and the more general Mie theory must be used. Scattering distribution function measurements have not been as extensive as extinction measurements, and though predictions based on the Mie model are theoretically well-founded, they are strongly dependent on the size distribution of atmospheric constituents, a function which is difficult to measure.

(U) The theory developed by Mie [2-33] provides an exact solution for the scattering of a polarized plane wave from a single spherical particle of arbitrary size and index of refraction, which may be complex. The general theory specifies amplitude, phase, and polarization as a function of scattering angle. The Mie solution has been extended to describe the scattering by an array of particles simply by summing the scattering contributions from each individual particle in the array, and computer codes exist for performing such calculations. Such an approach tacitly neglects the effects of multiple scattering, and inaccuracies also arise from the difficulties in specifying the number and size distribution of the aerosol particle array and the effective indexes of refraction of the particles. Such measurements have been made, however [2-34], [2-35], and distribution models have been developed for general use [2-22], [2-36], though Nella notes that the models lead to discrepancies in atmospheric water content [2-35].

(U) Bullrich [2-37] and Nella [2-35] have both made extensive scattering profile measurements in actual atmospheres at ground level, and their results are generally consistent with Mie calculations. Results from Nella's measurements are shown in Figures 2-28 and 2-29 for wavelengths of 1.06 μm and 10.6 μm respectively. The graphs show the composite plots for numerous measurements.

(U) Nine of the eleven measured curves of Figure 2-28 fall in the cross-hatched region. Curve A reflects conditions of very low humidity (24%) and extremely good visibility (> 40 km). No unusual meteorological conditions were observed when curve B was measured. The curves of Figure 2-28 are consistent with Mie calculations made by McClatchey et al [2-22] as shown in Figure 2-30. A calculation at 1.06 μm would fall in between the two curves shown. Moreover, quasi-simultaneous measurements at six different laser wavelengths between 0.47 μm and 1.06 μm by Nella yielded scattering functions similar to Figure 2-28 and within a factor of two of each other.

(U) Fourteen different measurements were used to make the composite curve of Figure 2-29 for 10.6-μm, CO_2 laser radiation, and only one anomalous result was recorded. It is shown dotted. The major distinction between these curves and those at shorter wavelengths lies in the less pronounced forward scattering peak and the absence of an increased backscatter component beyond 120°, the so-called glory. This is a general behavior associated with scattering when the particle sizes are less than the wavelength. The ultimate limit is the Rayleigh scattering distribution due to molecular scattering, also shown in Figure 2-30.

2-58

(U) Generally speaking, as particle sizes increase, forward and back scattering at a given wavelength becomes more pronounced, and the distribution is generally more structured. For example, rainbows result from large-particle scattering [2-33].

(U) For clear weather conditions scattering functions like those of Figures 2-28 and 2-29 cover the majority of cases encountered. Because the scattering distribution function is normalized, an increase in forward scattering must be compensated by a decrease in backscattering. Scattering intensity is therefore much more sensitive to extinction coefficient than distribution function.

(U) Very little data has been compiled on scattering from fog or rain. A truly useful fog model must account for multiple scattering effects, which have not been considered here. However, Bullrich did make scattering distribution measurements in fog, which exhibit the pronounced forward and back scatter characteristics noted. No measured scattering profiles for rain were found though Gumprecht et al [2-38] provide calculations for such a case. Chu and Hogg [2-39] have examined rain particle size distributions and densities.
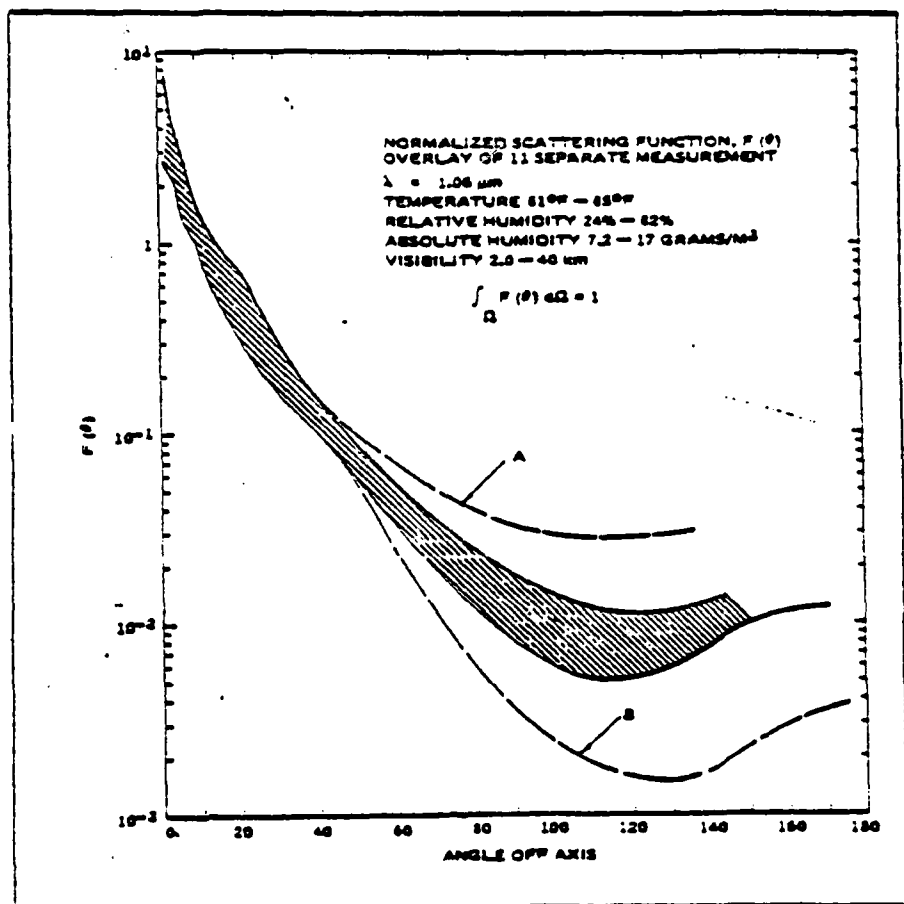
Figure 2-28. Composite of Normalized Scattering Functions at 1.06 μm Measured by Nella [2-35]
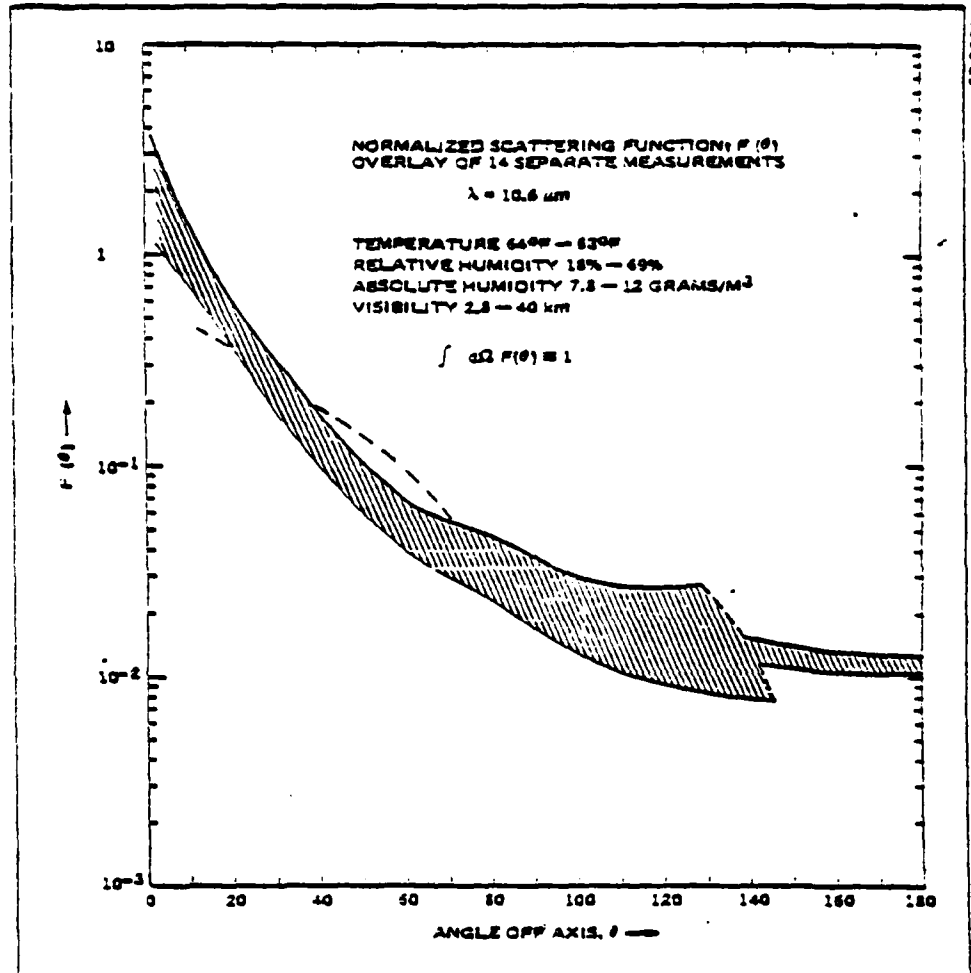
Figure 2-29. Composite Normalized Scattering Functions at 10.6 μm Measured by Neila [2-35]
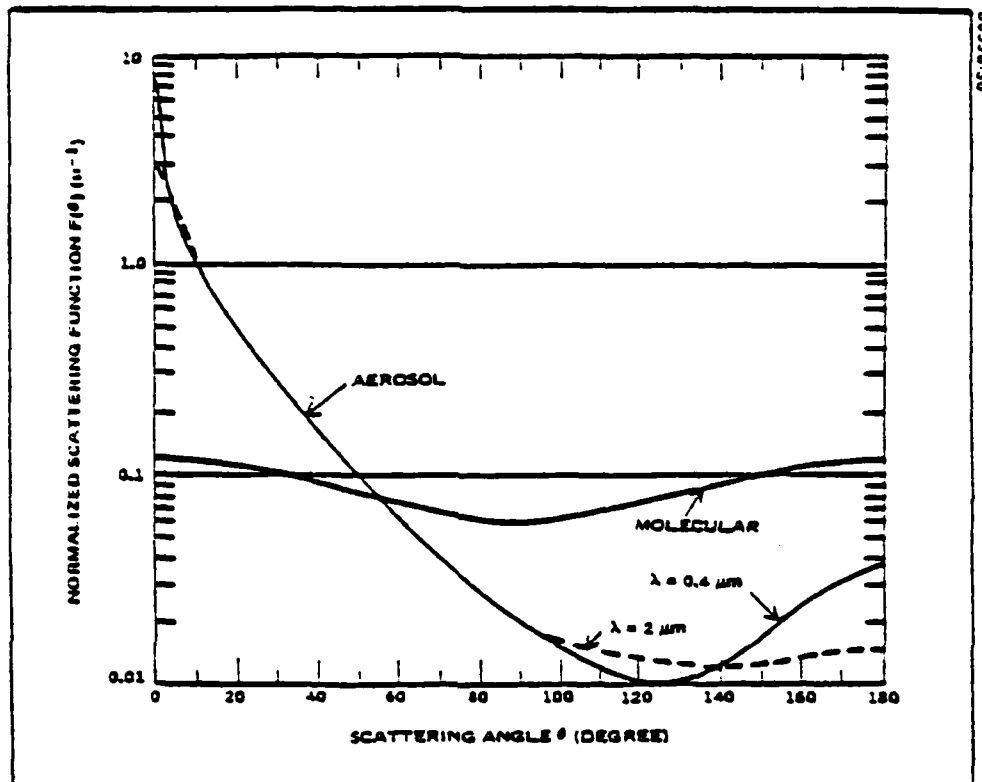
Figure 2-30. Normalized Scattering Distribution Functions Calculated Using Mie Theory for Aerosols with $\lambda = 0.4$ μm and $\lambda = 2$ μm. The Rayleigh molecular scattering distribution function which is independent of wavelength is also shown.

9. RECEIVER BACKSCATTER - THEORETICAL MODELING

(U) A complex distribution of backscattered radiation can result, consisting of both specular and diffuse components, arising from backstop or housing reflections, window reflections, and reflections from the receiver and its optical components.

(U) The basic approach to modeling backscattered radiation is very similar to that used for modeling port scatter except that we assume an angle ψ between the incoming beam and the normal to the structure housing or backstopping the receiver. The scenario which must be modeled is illustrated in Figure 2-31.

(U) Consideration must be given to a typical spot size of the received radiation. Commercial optical communication systems vary significantly in beamwidth and useful range, but, of the numerous such systems listed in Table 2-3, all appeared to project a spot size in excess of 10-m diameter at their nominal operating ranges, in some cases significantly larger. Consequently, the radiated area depicted in Figure 2-31 will usually be much larger than a typical window. It is also assumed that, for a proper ... radiation from the main lobe will not be allowed to pass behind the receiver in an uncontrolled manner.

(U) The major portion of backscatter will therefore be that reflected from the structure, or from a backstop if the receiver is not enclosed. Typical structural materials will reflect somewhat diffusely with a moderate specular component. With ξ the angular variable referenced to the building normal, we generally define this reflectance in terms of Nicodemus' bidirectional reflectance distribution function (BRDF)*

$$\rho_b(\xi) = L_b(\xi)/P_{inc}\cos\xi \qquad (2\text{-}67)$$

where $L_b(\xi)$ is the intensity of the backscattered radiation in the direction ξ due to P_{inc}, the total optical power on the building. For complete generality it is necessary to consider incident and reflected rays at angles ψ and ξ which are non-coplanar.

---

* (U) Much of the data available and presented in the following discussion is expressed in terms of the directional reflectivity $r_b(\xi)$, where

$$r_b(\xi) = \sigma_b(\xi) \cos\xi = L_b(\xi)/P_{inc}.$$

We prefer BRDF and use it here because, as mentioned earlier, it is a constant independent of scattering angle for a perfectly diffuse reflector and consequently convenient for programming.
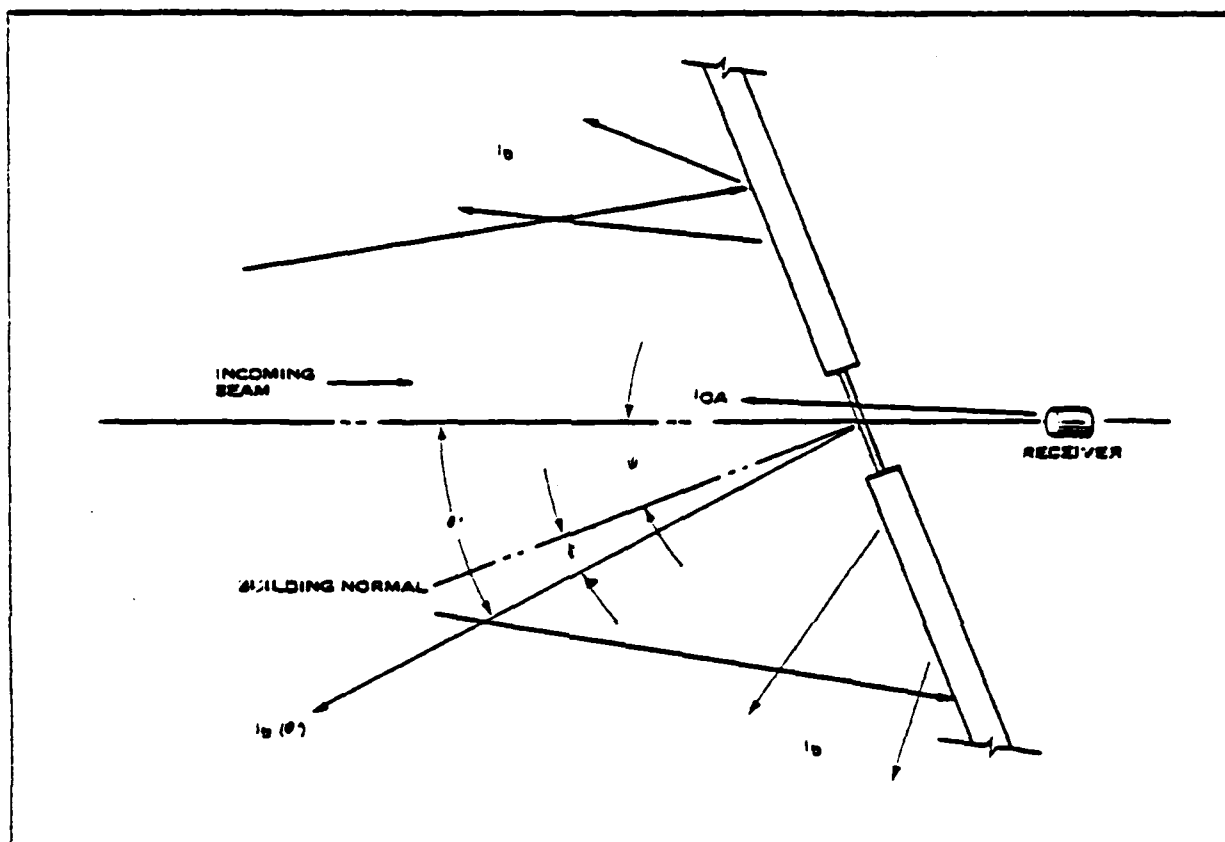
Figure 2-31. The Backscatter Scenario. The building or backstop will provide primarily diffuse reflection, the window a specular glint at $\theta' \approx 2\psi$, and the receiver a retro-reflected OA component, all of which must be considered.

(U) Expressing (2-67) in terms of θ', a variable angle referenced to the link axis, instead of ψ,

$$\rho_b = \rho_b(\theta', \psi) = I_b(\theta')/P_{inc} \cos(\theta' - \psi). \qquad (2-68)$$

With $P_{inc} = P_o \exp(-\alpha Z)$ for a link of length Z,

$$I_b(\theta') = \begin{cases} P_o \, \rho_b(\theta',\psi) \cos(\theta' - \psi) \exp(-\alpha Z) & \text{for } |\theta' - \psi| < 90^\circ \\ 0 & \text{otherwise.} \end{cases} \qquad (2-69)$$

Again, the exponential form of (2-63) must be used if α varies significantly along Z.

(U) We have neglected the minor difference in spot area and reflectance due to the presence of a window in (2-67) since its area would typically be much smaller than that of the spot. Specularly reflected components from the window can be considered separately by including them in the function ρ_b. This component of intensity should generally be much smaller than that from the building since the reflectance from glass is low compared to that from the structure surface, and the incident power on the window is scaled by the ratio of the window area to the beam spot size; but its specular nature requires that it be included. The common use of the Dirac delta function to describe specular components would be incompatible with a computer calculation. We shall use instead a continuous model which is highly peaked in a direction $\theta' = 2\psi$ with θ' in the same plane as ψ.

(U) Another specular component of interest is the so-called optically augmented (OA) return from the receiver aperture itself. The intensity of this reflection must be separately characterized as

$$I_{OA}(\theta') = P_{inc} \, \delta_{OA}(\theta') \cos\theta' \, A_r/\pi(\phi_t/2)^2 Z \qquad (2-70)$$

where A_r is the receiver aperture area and δ_{OA} is defined analogous to ρ_b in (2-68). The ψ - dependence is absent for the OA return since the receiver aperture is necessarily normal to the link path. The small value of A_r compared to the spot size, and the narrow, retroreflected nature of the OA beam indicate that this component will not be accessible to a   receiver at an appreciable off-axis angle. It should, however, be considered as an additional source which may be scattered from the atmosphere.

(U) Analogous to (2-51) and with reference to Figure 2-3 the total power scattered from the receiver into the   receiver may be expressed as

$$P_r(\theta_i, \psi) = \begin{cases} \left[I_b(\theta_i, \psi) + I_{OA}(\theta_i) \right] \exp(-\alpha R_r) A_s/R_r^2 \\ \qquad \text{for } \theta_r + \phi_{sh}/2 \geq \theta_i \geq \theta_r - \phi_{sh}/2 \\ 0 \qquad \text{otherwise} \end{cases} \qquad (2-71)$$

where R_r is the range from the link receiver to the off-axis receiver.

Section 2 — Data-Base Review and Model Formulation
Subsection D — Scattering Mechanism

10. RECEIVER BACKSCATTER – MEASUREMENT DATA

(U) A review of reflectance data for a variety of wavelengths indicates that most real-world cases can be modeled by assuming the combination of a simple lambertian diffuse element and a gaussian specular element.

(U) In specifying the reflection characteristics of a backstop material in terms of its bidirectional reflectance distribution function (BRDF) ρ_b, three different aspects must be considered: the wavelength dependence of the material's reflectance, surface roughness characteristics of the material, and the BRDF's dependence on the direction of the incident radiation.

(U) The wavelength dependence of the reflectance depends on the detailed absorption-band structure of the material, and because of the wide variety of materials which must be considered and the fact that most are chemically inhomogeneous (e.g., concrete) any attempt at modeling their absorption-band properties is unrealistic. We therefore rely instead on measured reflectance data.

(U) The complexity of the BRDF's dependence on surface roughness and incident beam direction is best illustrated by an example. Shown in Figure 2-32 is a series of reflected-radiation profiles (isointensity contours) for aluminum polished with 600-grit silicon carbide illuminated at various angles by a HeNe laser [2-40]. The profiles exhibit a pronounced but rather broad specular peak, a smaller diffuse component, a moderate backscatter lobe, and an anomalous array of smaller lobes. Other materials will exhibit these same characteristics but in varying degrees.

(U) Modeling these geometric attributes of a material to theoretically establish its reflection profile is reasonable for most homogeneous materials, and several models have been proposed. However, there is a wide disparity in the nature of the theoretical approaches taken (though a careful comparison might show that the seemingly diverging approaches are in fact identical). Shack and DeBell [2-41] and Shack and Harvey [2-42] use the techniques of linear systems theory to treat the reflection profile from a surface with a given statistical height distribution and autocovariance function as an angular spectrum of plane waves. Using a ray-optics model Trowbridge and Reitz [2-43] treat the surface as an ensemble of randomly oriented, randomly curved microareas and show that an optically smooth curved surface of revolution can be chosen which will give the same distribution of reflected light as the actual surface. Sauermann and Waterman [2-44] do a Fourier decomposition of the surface and consider the reflection (diffraction) properties of each sinusoidally corrugated surface component separately, and they in addition include the effects of shadowing of the corrugated surface on non-normally incident rays, as illustrated in Figure 2-33.

(U) All of these approaches assume single-valued surface profiles and homogeneous material characteristics. However, disregarding these minor limitations the difficulty with any of the approaches is that they all must eventually rely on measured data, that is, the surface roughness properties. Nevertheless, they do provide a means for determining reflection profiles if surface roughness and material properties can be estimated reasonably.

(U) Actual BRDF measured data are rather scarce. The wide range of background materials which must be considered, and the inconsistency of results for a given material (e.g., wood) leads experimentalists to consider laboratory environments over which they have more control rather than real-world environments. Natural materials are frequently treated as perfectly diffuse reflectors, in which case the BRDF ρ_b is a

p. 2-67 – 2-68 deleted

UNCLASSIFIED
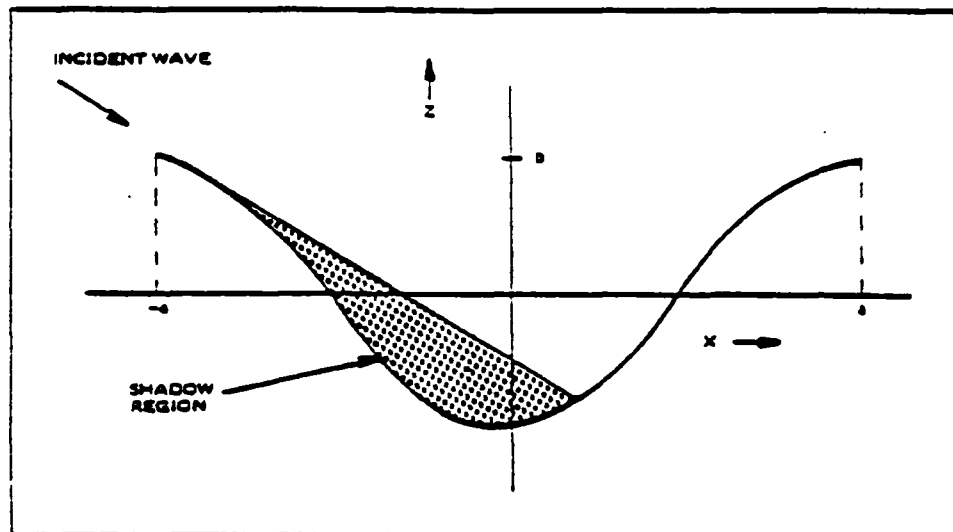
Figure 2-33. (U) Location of the Shadow Region Accounted for in the Reflection Model of Sauermann and Waterman [2-44] (U)
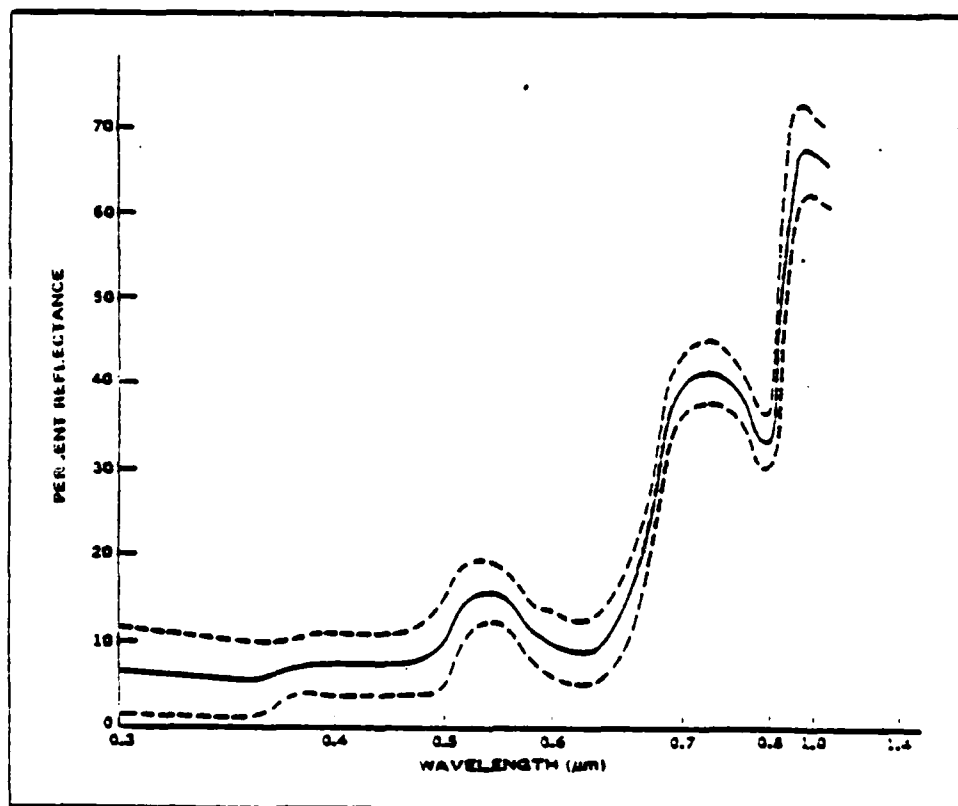
Figure 2-34. (U) Mean and Standard Deviation Reflectance for Miscellaneous Leaves [2-46] (U)

UNCLASSIFIED

2-69
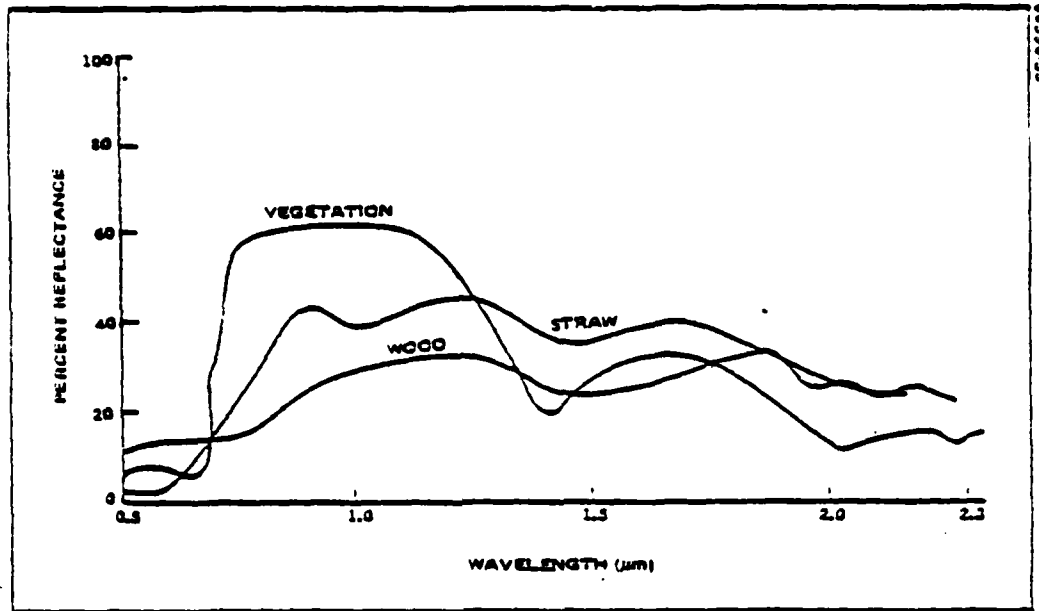
Figure 2-35. (U) Typical Reflectances of Vegetation, Wood and Straw [2-46] (U)
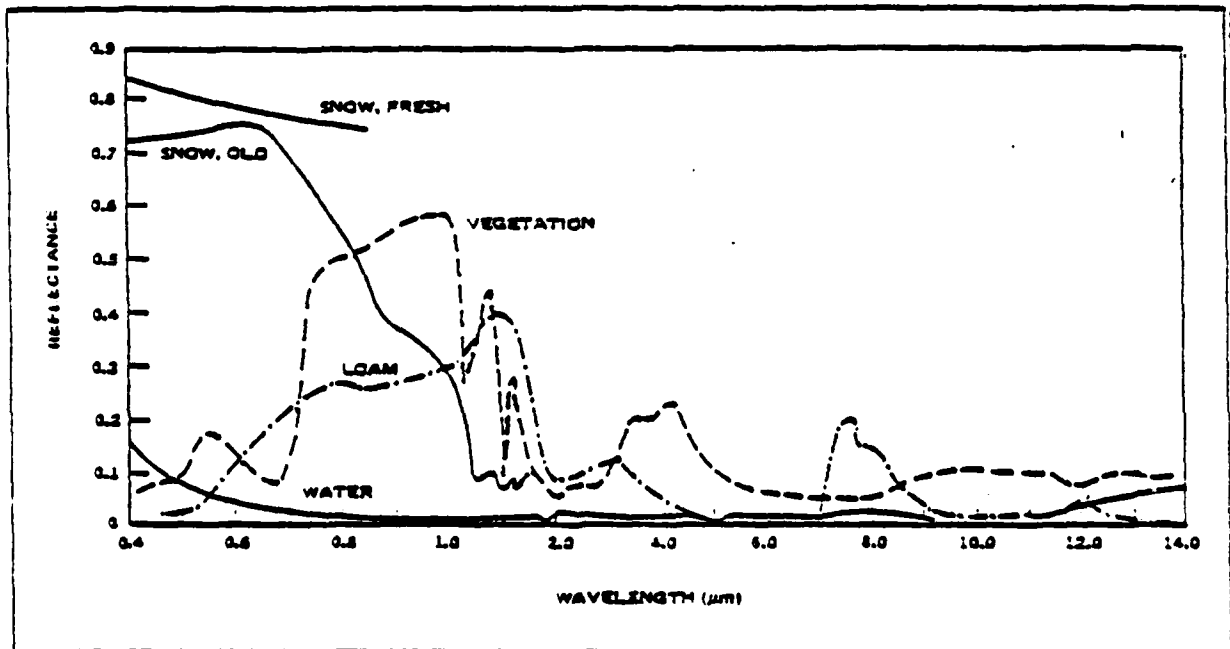
Figure 2-36. (U) Typical Reflectances of Water Surface, Snow, Dry Soil and Vegetation [2-46] (U)
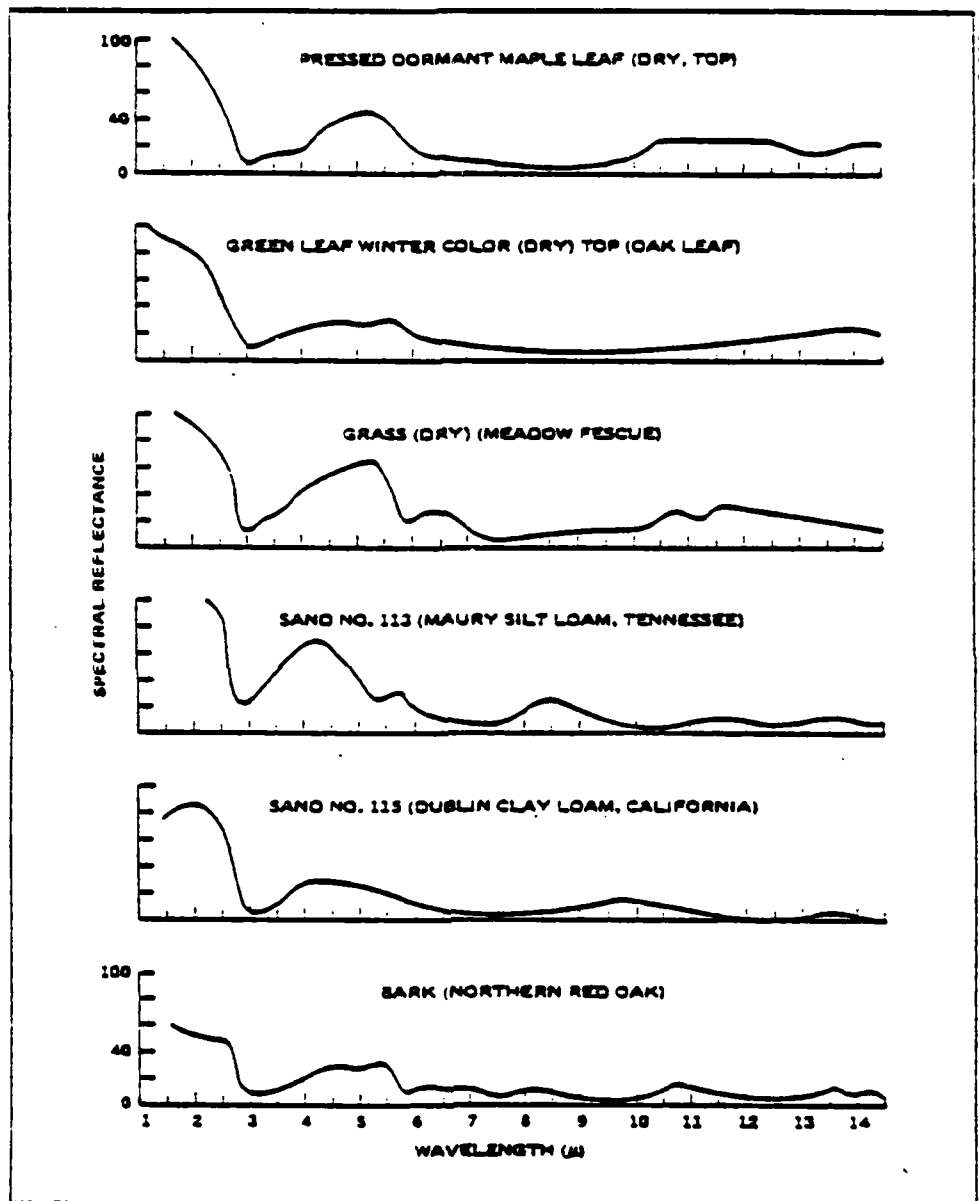
Figure 2-37. (U) Spectral Reflectance of Six Terrain Features in the 1-15 μm Region [2-6] (U)
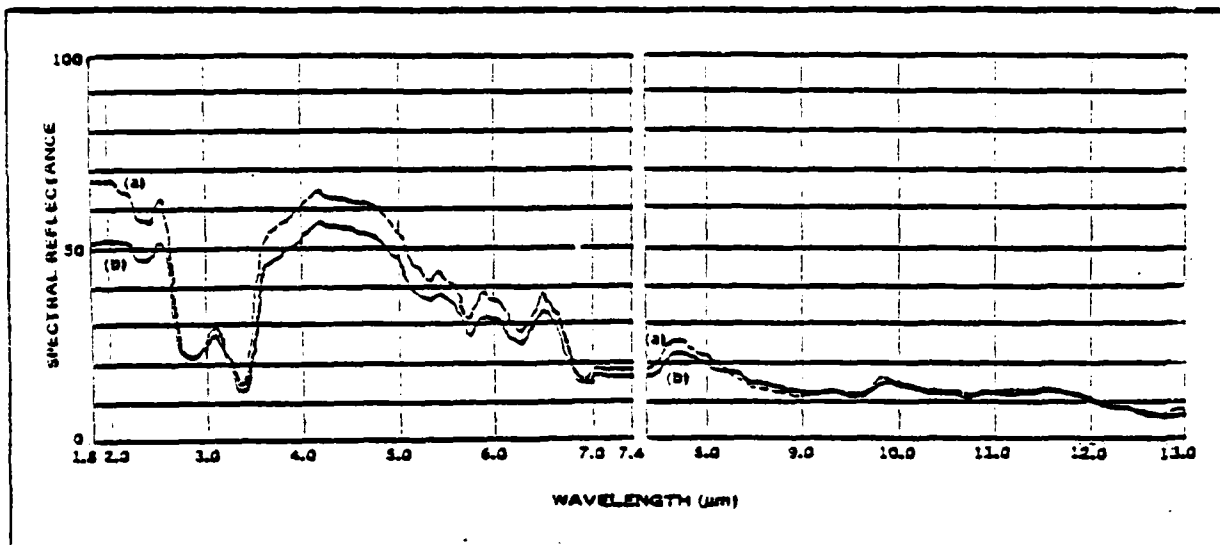
Figure 2-38. (U) Spectral Reflectance of (a) ideal masonry, No. 150 (red), (b) ideal masonry, No. 170 (green), exterior masonry paint (Ideal Chemical Products Inc) [2-6] (U)
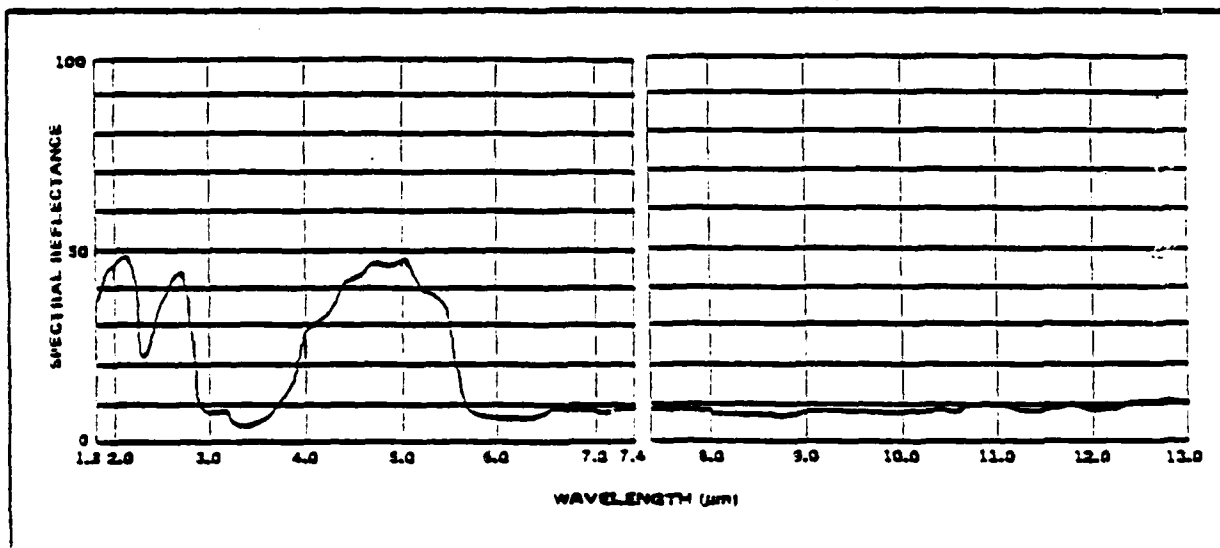
Figure 2-39. (U) Spectral Reflectance of Asphaltic Road Material, SC-4 (Standard Oil Company of California) [2-6] (U)

baseline profile. It was shown that classical error analysis techniques could not be applied at this point in time, due to the lack of an adequate amount of data and the complexity of the problem, so the sensitivity analysis represents a reasonable means to quantize the effects of possible uncertainty. A space-to-ground model was developed which, although limited in capability, is an important first step in developing a generalized model. Lastly, a detailed solar background model was included which takes into account the line structure of the solar spectrum and its modification by the atmospheric transmission characteristics.

In reviewing the capabilities of the program several improvements would appear to be helpful in future analyses. These include:

- Development of a performance evaluation code to determine the impact of security measures on link performance.
- Development of an atmospheric program from existing codes to generate tables of coefficients for any wavelength and atmospheric absorption line shape, and to also generate the scattering distribution function using a Mie calculation.
- Development of a separate, comprehensive space-to-ground model. The space-to-ground case is a more complex problem to treat than 'narrow-beam' links.
- Expansion of LACM 2.0 to allow more detailed modeling of scenario characteristics. This will require a thorough analysis of data and will likely produce a very large program, considering the data requirements and preliminary schemes developed.
- Development of a classification system for classifying link type and scenario combination to produce 'rules of thumb' in estimating link security. This would be accomplished by parametric analysis using the program.

TABLE 3-1. FEATURES OF THE ECKSTROM
COMPUTER MODEL, LACM 2.0

General Features	• Interactive • Modular • Flexible
Specific Features	• Pseudo 3-D curved earth • Improved atmospheric model • Flexible port scatter model • Flexible receiver/backstop model • Improved beamscatter algorithm • SNR or power computational capability • Detailed solar background model • Modes to simplify geometry • Contour generation capability • Sensitivity analysis • Space to ground capability

1. NARROW-BEAM ANALYSIS GEOMETRY

(U) The analysis of link beam scatter where the link beam diameter is negligible in comparison to the off-axis distance, termed narrow-beam analysis, is based upon power considerations, with beam-shape (power versus off-axis distance) effects neglected.

(U) The narrow-beam link is a point-to-point link over a curved earth as presented in Figure 3-1. The altitudes above sea level can range upward from -1000 meters to exo-atmospheric altitudes. The distance between the link transmitter and link receiver is the link range, RL. The off axis receiver (SR) location is defined in terms of a cylindrical coordinate system, with the transmitter at the origin and the link beam coincident with the axis of symmetry. The off-axis receiver location is specified by the coordinator RPX (axis of symmetry coordinate), X (range orthogonal to axis of symmetry), and GAMINT (angular coordinate). GAMINT (γ_{int}) is defined such that 0° defines a horizontal half plane, $\pm 180^{o}$ the opposite half plane, with 90° being the upper vertical half plane of a horizontal link. (Note that the radial distance X is parallel to a tangent of the earth's surface at its intersection with the link beam for GAMINT = 0° or 180°.)

(U) The concept of the intercept plane is very important to grasp in order to fully appreciate the definition and description in this report. The intercept half-plane is defined as that half-plane whose edge coincides with the link axis and contains the SR. Thus there is a half-plane at $\gamma_{int} = 0^{o}$ and $\gamma_{int} = 180^{o}$ which may have different interceptibility profiles (i.e., they may not be mirror images) in each half-plane.

(U) Figure 3-2 shows the intercept half-plane geometry, including the orientation of the SR in the plane. The SR is assumed to be looking at a portion of the beam specified by THETA, the off-axis angle. Note that THETA is not necessarily the angle subtended by the SR and link axes at the transmitter, but the angle subtended at the scattering volume. In order to simplify and minimize the amount of geometry required of the user, several modes were designed which obtain a profile of the link scatter using only one or two geometric parameters for the whole set. These are described in the User's Guide later in this section.

(U) The computer model uses a curved earth, and the equations for calculation of ranges and altitude of points are cumbersome. They are derived using the geometry in Figure 3-3. Using the law of cosines and solving for each of the required variable leads to

$$HP = \left[(RE+HT)^2 + R^2 + 2(RE+HT) R \cos(DP) \right]^{1/2} - RE$$

$$DP = \cos^{-1} \left\{ \frac{(RE+HP)^2 - (RE+HT)^2 - R^2}{2(RE+HT)R} \right\}$$

$$R = \left[(RE+HT)^2 \cos^2(DP) - (RE+HT)^2 + (RE+HP)^2 \right]^{1/2}$$

$$- (RE+HT) \cos(DP)$$

These expressions are used in the routines TSHARE and SETUP. If the geometry specified by the user is such that the bottom of the link beam touches the earth between the transmitter and receiver, a warning is printed out.

3-2
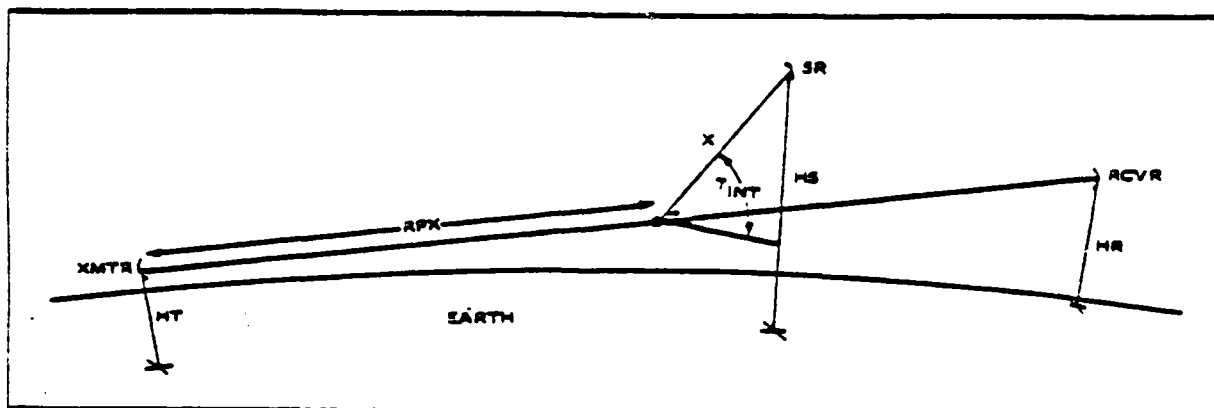
Figure 3-1. Illustration of Narrow-Beam Link Geometry. The intercept half plane has the link axis as its edge, and contains the SR. At the intersection of the link axis and the γ_{INT} (GAMINT) reference axis, the reference axis is tangent to the earth's surface.
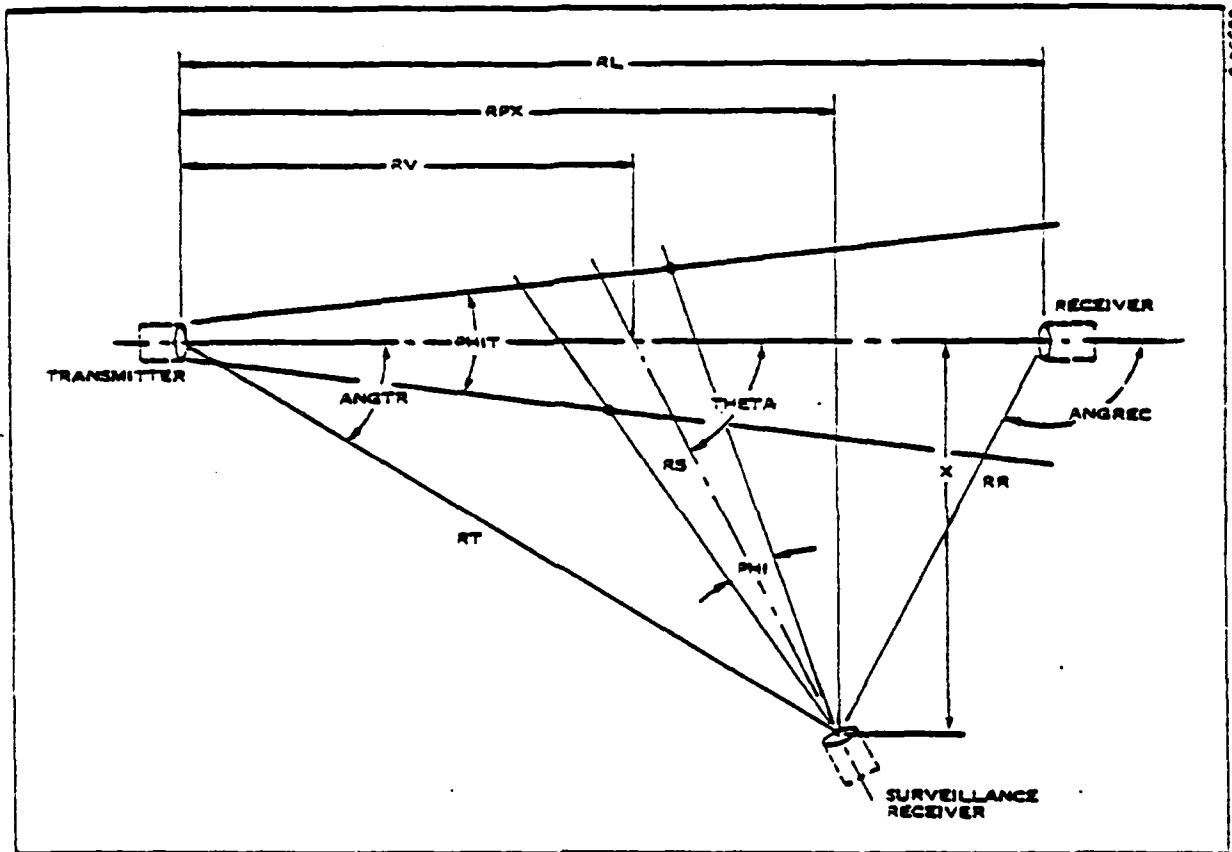
Figure 3-2. Intercept Half-Plane Geometry. Note that this half-plane may be rotated about the link axis. The scattering volume is defined by the SR field of view PHI and orientation THETA.
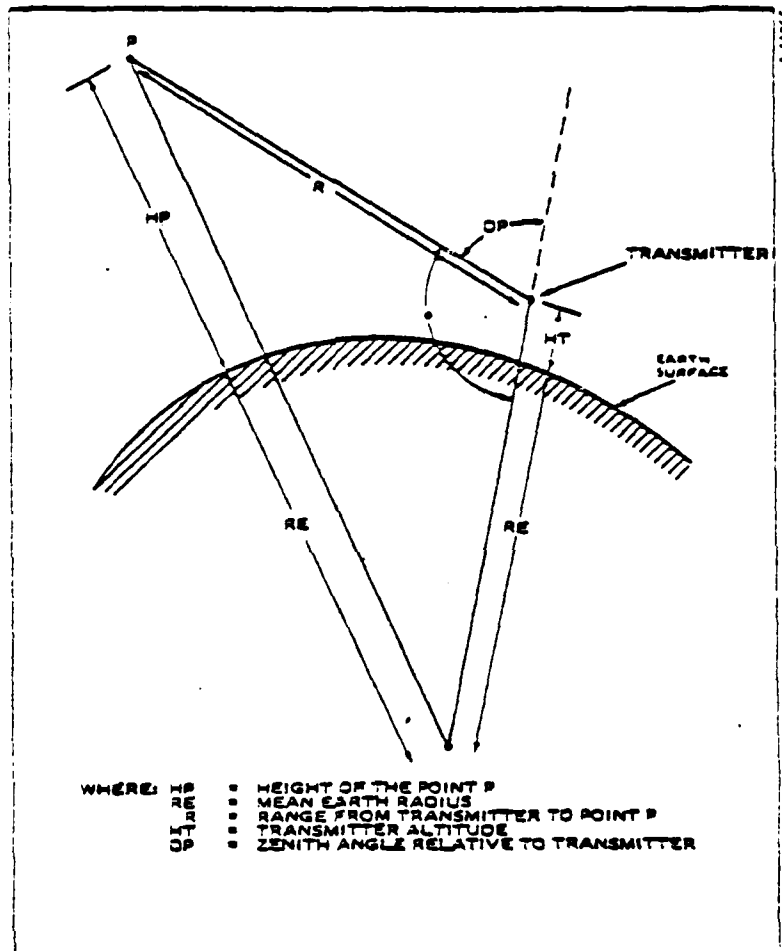
Figure 3-3. Geometrical Model Used to Derive Earth Curvature Effects.

Section 3 – The Computer Model
Subsection B – Description of Mathematical Models

2. LINK TRANSMITTER

(U) A simple model based on empirical data was developed to account for port scatter and the effects of baffles.

(U) The link transmitter is a significant source of off-axis radiation. Due to differences in transmitter designs and quality of optics a variety of scattering profiles can be postulated for a link transmitter, presenting a problem in modeling the off-axis scatter.

(U) The transmitter model assumes a beam divergence angle PHIT (ϕ_t), supplied by the user. If the user-supplied ϕ_t violates the diffraction limit, a warning is printed. Also required are the optical power out the lens PT, and the lens diameter DT. For cases involving hooding, the hood diameter and length are required. The optics are assumed circular. Figure 3-4 illustrates the link transmitter.

(U) Lens hooding is simulated by a simple model that assumes a hood arbitrarily larger than the beam diameter, neglects diffraction by the hood (which is reasonable when the hood only touches the sidelobes) and assumes a totally absorbing hood interior. Thus the scatter at a given angle is reduced by the percentage of the aperture that is hidden by the hood. Figure 3-4 illustrates the behavior of this function for several different aperture size to hood diameter ratios. The case of equal hood diameter and aperture size is the same as the optical transfer function of an ideal circular aperture [3-1].

(U) The components of transmitter off-axis radiation can be separated into a diffracted portion (sidelobes) and a portion scattered from the optical materials, which includes surfaces and bulk scattering of the lenses. At optical wavelengths with typical apertures the sidelobe structure is extremely fine, so an expression for the sidelobe envelope as shown in Section 2 is used instead:

$$I_s(\theta) = \frac{\lambda}{DT} \frac{PT}{(\pi\theta)^3} \cos\theta.$$

(U) The bulk and surface scatter is treated using a bidirectional scattering distribution function (BSDF), as is developed in the literature and discussed in Section 2. Empirical relationships for the BSDF obtained from experimentation with various optical flats and lenses show that the function is roughly linear in log space. Figure 3-5 illustrates a typical curve for an optical flat. As can be seen the slope is approximately −2.0, and the value at one degree is 2×10^{-3}. Also shown on the figure is a system BSDF which, although not representing a particular system, is typical in form of the experimental data available on existing transmitters. As can be seen, the function is roughly a straight line, with the exception of several 'glitches' which could be due to internal reflections peculiar to a particular design. Thus, apart from the glitches, the BSDF can be expressed as

$$BSDF(\theta) = A\theta^B$$

where A is the value of the BSDF at one degree, θ the off-axis angle in degrees, and B the slope of the curve.

(U) The 'glitches' can be accounted for by using a fixed value for the BSDF at the glitch. Thus the user of the program must define (for each glitch) the starting angle,

3-6
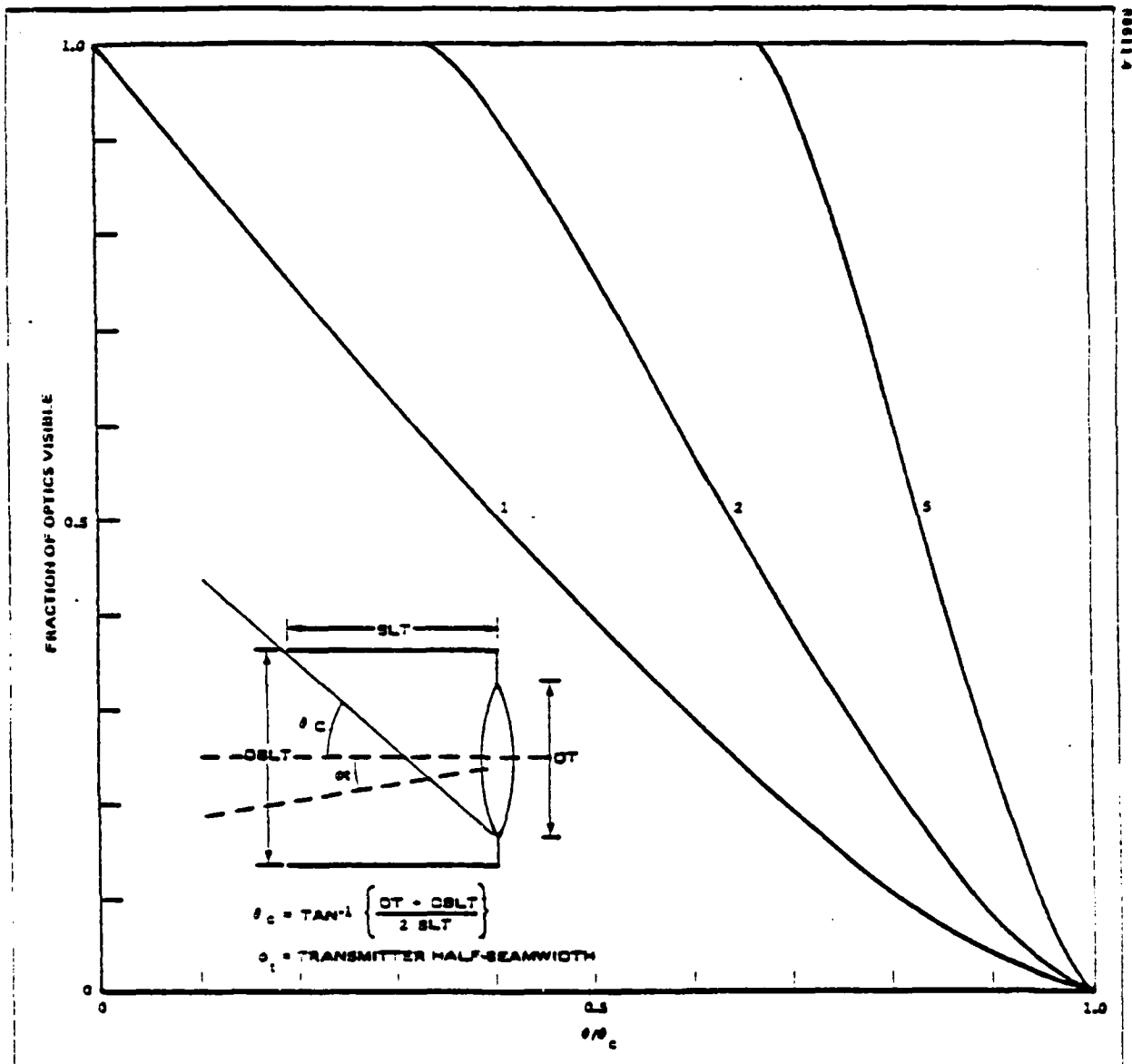
Figure 3-4. Fraction of Exit Aperture Visible as a Function of Normalized Off-Axis Angle θ/θ_c for Three Ratios of Hood to Optics Diameter. Past θ_c no scatter from optics is visible.

(U) amplitude, and ending angle of the glitch. Up to three glitches can be input. The sample BSDF curve shown in the figure is what the program would use if the user specified a glitch from 1.7 to 2.7 degrees with an amplitude of 2×10^{-1} sr^{-1}.

(U) If the BSDF to a system is known, the BSDF subroutine can be easily replaced by a user-supplied function interpolating the experimental data. However, a good estimate of the transmitter scatter can be obtained for many BSDF curves using the built-in model.
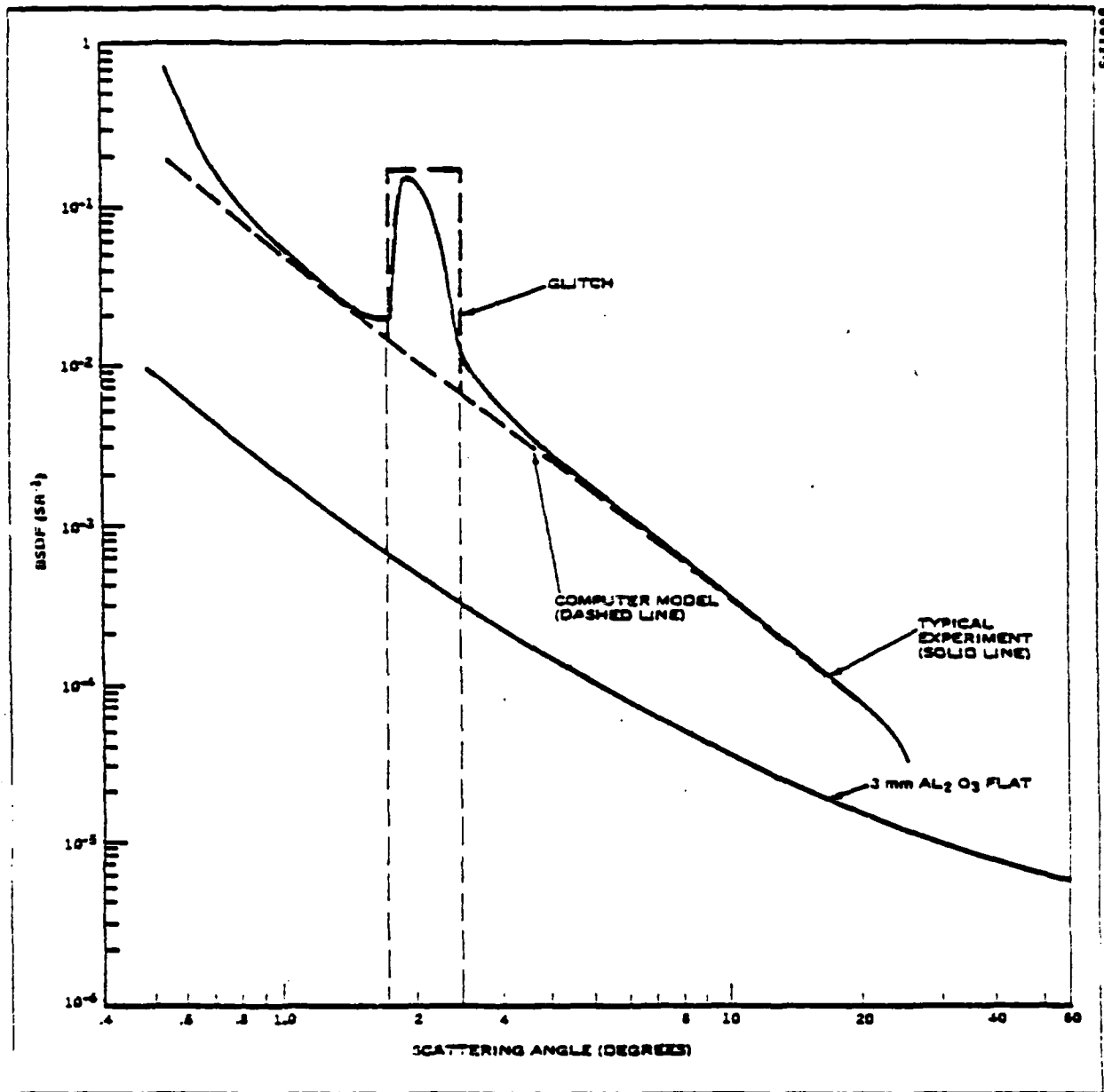
Figure 3-5. BSDF Curves for an Optical Flat and a Hypothetical System, Showing the Computer Model's Approximate Fit.

Section 3 — The Computer Model
Subsection B — Description of Mathematical Models

3. LINK RECEIVER AND BACKSTOP

(U) The reflection from the link receiver and backstop are of significance due to their location in the main beam. A model is described which accounts for diffuse and specular reflections from the receiver/backstop combination.

(U)   The link receiver is assumed to be collocated with a backstop (which can be positioned in any orientation). Figure 3-6 illustrates the arrangement along with the angular conventions used in the program.

(U)   The diameter of the optics and hood diameter and lengths are input to the program, and the scheme is identical to that of the transmitter model, i.e., the scatter off the receiver aperture is assumed to be proportional to the visible area. The backstop is assumed to be large enough to block the main beam, and may be oriented in elevation angle by specifying PSIEL (ψ_{EL}) which is the elevation orientation of the normal relative to the 0° or 180° intercept plane. Azimuth orientation is accomplished by specification of PSIAZ (ψ_{AZ}), which is the angle of the projection of the normal of the backstop onto the 0° (positive ψ_{AZ}) or 180° (negative ψ_{AZ}) intercept plane with the link optical axis. Figure 3-7 illustrates these angles, along with the specularly reflected component's ray. For an arbitrary orientation of the backstop, the direction of the specular component is given by specifying which intercept plane it lies in. The intercept plane angle γ_{int} is given by

$$\gamma_{int} = \tan^{-1}\left\{\frac{\sin\psi_{EL}}{\sin\psi_{AZ} \cdot \cos\psi_{EL}}\right\}$$

The above expression will not give values from -180° to $+180^\circ$, but only from -90° to $+90^\circ$, so the FORTRAN function ATAN2 is used in the program to yield the correct half-plane orientation. This angle is printed out for the user in the input summary so he may be informed of which intercept plane to run to get the specular component 'worst case'.

(U)   Two expressions are used to model the directional reflection distribution of the backstop, as discussed in Section 2. The simplest of these is a lambertian reflection model which corresponds to a diffuse reflector, containing no specular component. The expression for the backstop directional reflectance (BRDF) ρ_b in this case is a constant independent of angle given by

$$\rho_b = \pi^{-1} \rho_d$$

where ρ_d (BDIFF) is the total diffuse reflectance of the backstop. The more complicated model allows a gaussian-shaped specular component along with a diffuse (lambertian) component. In this case the full width of the specular component at half maximum $\delta\Theta$ (BFWHMS) is input in degrees, along with the peak value of the specular and diffuse components. The expression for BRDF is then

$$\rho_3(\Theta) = \pi^{-1} \rho_d + A_{sp} \exp\left\{-4\ln2 \ (\Theta-2\psi)^2/(\delta\Theta)^2\right\}.$$
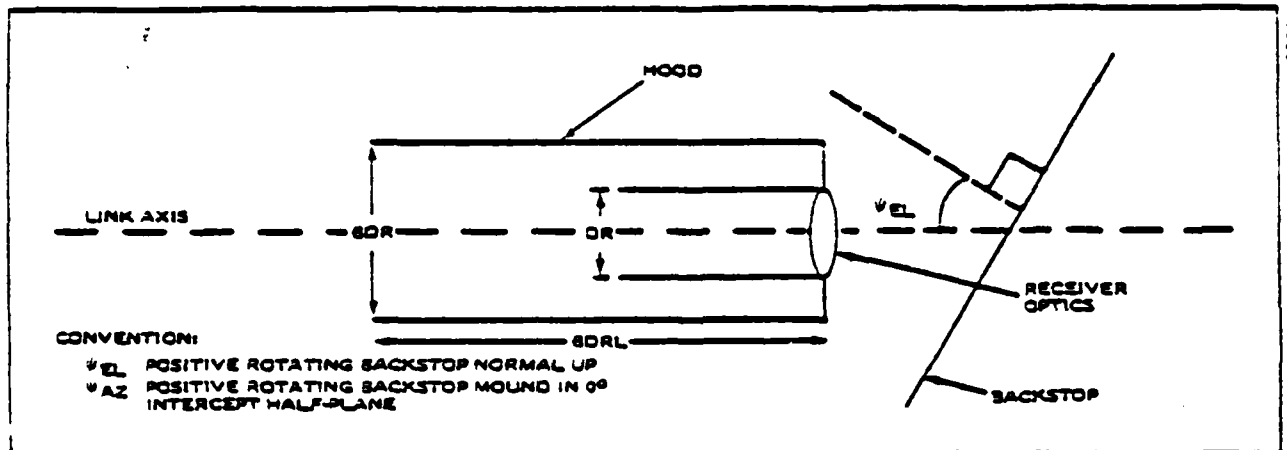
Figure 3-6. Illustration of Major Features of Backstop/Receiver Geometry. The backstop is tilted up at an angle ψ_{EL}.

(U) where

ρ_d (BDIFF) = total diffuse directional reflectance of backstop ($0 \leq \rho_d \leq 1$)

A_{sp} (BMAXS) = peak specular reflectance of backstop ($0 \leq A_{sp} < \infty$)

ψ (PSIEFF) = angle between incoming beam and backstop normal

$\delta\Theta$ (BFWHMS) = FWHM of specular component.

(U)   Thus the power at the SR due to the reflection is given by

$$P_s = \frac{P_{inc} \, T \, A_r \, \rho_b \, (\Theta_r) \, \cos \Theta_r}{R_r^2}$$

where

P_{inc} is the power incident on the backstop

T   is the transmittance from the receiver to the SR

A_r is the SR entrance aperture area

$\rho_b(\Theta_r)$ is the BRDF at the angle Θ_r

Θ_r is the off-axis angle from the receiver to the SR

R_r is the range from the receiver to the SR.

(U)   The reflection off the receiver optics uses an identical model to the specular/diffuse combination model of the backstop. However, in this case the specular component is narrow and the diffuse component is small. The smaller amount of power incident on the optics (as compared to the backstop) and the fact that its reflections are retroreflected primarily down the link axis make the receiver optics scatter much smaller than that of the backstop, so the program defaults are set to ignore receiver scatter. However, the user has the option of introducing the components.
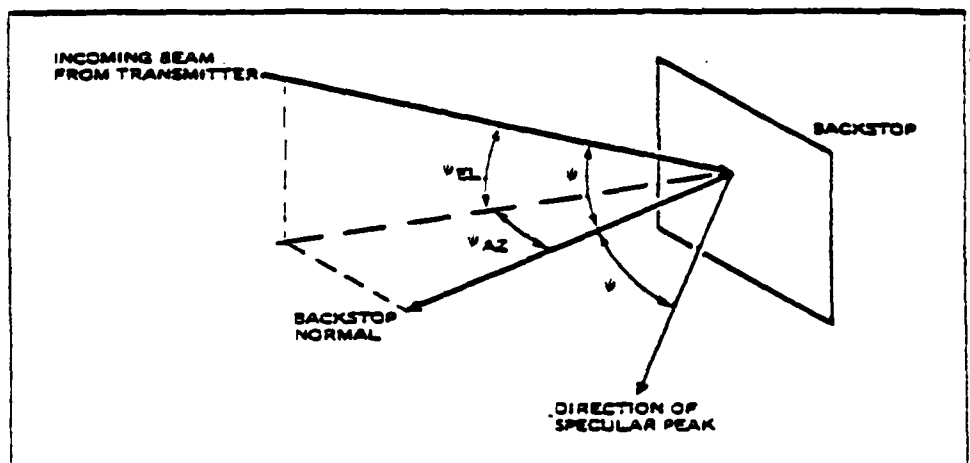
Figure 3-7. Basic Geometry Relating Angle of Backstop Normal to Incoming Beam Angle. The vector representing the specular reflection peak is in the plane common to the beam axis and the backstop normal. In this case ψ_{EL} is negative and ψ_{AZ} is positive.

4. ⁻OFF-AXIS   RECEIVER AND BACKGROUND

(U) The off-axis e receiver model includes specifications of detection type and sensiti·ity.
The model is discussed in light of expressions used in the program and the background model
is described.

(U) The   receiver (SR) is only characterized sufficiently to obtain the
desired output. For example, a power computation only requires the aperture area
(ASR) and the field of view (FOV) in the intercept half plane, as the background power
is not required, and the FOV in the cross-beam direction is assumed large enough to
intercept the entire width of the link beam.
(U) In contrast, the expression for direct-detection signal-to-noise ratio, developed
in Section 2, is

$$\frac{S}{N} = \frac{M^2 P_S^2}{(2hc/\eta\lambda)\, FB\, (P_S + P_b) + (NEP)^2 B}$$

where

P_S	(PS)	= signal power
M	(XM)	= modulation depth of signal
B	(BWR)	= SR electrical bandwidth
~~NEP~~	~~(PNEP)~~	= SR system noise-equivalent power
F	(F)	= ███████████████
η	(ETA)	= quantum efficiency of the detector
λ	(ALAM)	= wavelength
h	(H)	= Planck's constant
c	(C)	= speed of light
P_b	(PB)	= background power

(U) Several parameters deserve special consideration, in particular the NEP and
background power. The NEP is described here as the noise power "with the lid on".
Thus this figure characterizes the entire SR detection system, including gain from a
device such as a photomultiplier tube, but it does not include background noise effects.
The background power is calculated based on the wavelength, and day/night and meteor-
ological conditions have a very strong influence on the SNR observed.
(U) The background model used in the program is composed of an earth blackbody
curve and a solar irradiance table. The blackbody curve is only significant in the mid-
to far-IR and uses the classical blackbody radiation expression discussed in Section 2.
The solar background is a line model taken from Gast [3-2]. The program interpolates
to get the solar irradiance assuming an optical air mass of 2, and the table includes
the solar line structure and atmosphere transmission characteristics. A sunny day,
cloudy day or night condition are the options available to the program user.

(U)   In the case of heterodyne detection the signal-to-noise ratio is given by

$$\frac{S}{N} = L_M \frac{\eta \lambda}{hcB} \; M^2 P_S$$

where

L_M	(EM)	=	local oscillator mixing efficiency
η	(ETA)	=	detector quantum efficiency
λ	(ALAM)	=	wavelength
B	(BWR)	=	SR electrical bandwidth
h	(H)	=	Planck's constant
c	(C)	=	speed of light
M	(XM)	=	modulation factor
P_S	(PS)	=	signal power.

In general this expression only represents the IF SNR, though in some cases it may also represent the video SNR. It should therefore be used with care, especially when radiometric detection is being evaluated. The mixing efficiency, which can have a maximum value of 0.7, may also be lower in a practical system. Moreover, coherence requirements may be only partially met in a random geometry. The calculated heterodyne SNR is thus felt to be of only marginal validity.

Section 3 – The Computer Model
Subsection B – Description of Mathematical Models

5. ATMOSPHERIC MODELS

(U) Atmospheric effects play a major role in the interceptibility profiles of narrow-beam links. The scattering and transmission models are discussed in this topic.

(U) Equation 2-66, the expression derived for atmospherically scattered power in Section 2, is developed for use in the computer model in an equivalent differential form as

$$dP_a(\theta_1) = \frac{P_o A_s \alpha_s d\varphi_s \, T_1 T_2 \, F(\theta_1)}{R_1 \sin \theta_1}$$

where

P_o	(PT)	=	link transmit power
A_s	(ASR)	=	SR aperture area
α_s	(ALFSCT)	=	atmospheric scattering coefficient
$d\varphi_s$	(DPHI)	=	element of SR FOV along beam
T_1	(T1)	=	atmospheric transmittance from transmitter to scattering volume element
T_2	(T2)	=	atmospheric transmittance from scattering volume element to SR
$F(\theta_1)$	(FTHETA)	=	atmospheric scattering distribution function
R_1	(RS)	=	range from scattering volume to SR
θ_1	(THETA)	=	angle of intercept of $d\varphi_s$ and the link beam.

This expression is then numerically integrated across the SR FOV in the program. It can be seen that the atmospheric parameters are critical in the calculation of atmospheric scatter.

(U) The transmittance from point to point in the atmosphere is given by

$$T = \exp\left[\int_0^R \sigma(h)\, dz\right]$$

where the integration is carried out along the propagation path, and

$$R = \text{length of propagation path}$$
$$\sigma(h) = \text{altitude-dependent extinction coefficient}$$
$$h(z) = \text{altitude of propagation point at a distance } z \text{ along the path}$$

The routine used in the computer program uses a stepwise integration to provide all-altitude capability given a function $\sigma(h)$.

(U)   The absorption and scattering of the atmosphere is due to the molecular and aerosol constituents of the atmosphere. The scattering properties (coefficients) are dependent on particle size and wavelength, but vary in a relatively well-behaved manner with wavelength for a given set of atmospheric conditions. The molecular absorption however, has a very fine structure, due to its dependence on the quantum structure of the atoms and molecules in the atmosphere. The many lines which make up the absorption spectrum vary in intensity (resonance strength) and width, and are not predictable using simple theory. Instead, a line compilation computer program (such as HITRAN) must be used, particularly in the case of laser propagation, where the linewidth is so narrow that a detailed knowledge of the atmospheric structure in the neighborhood of the laser line is required. For this reason a set of tables [3-3] is used in the computer model, and for each wavelength option a subset of five atmospheric types are available, each with the choice of clear or hazy condition. The tables from the reference also contain the altitude dependence of the parameters, giving the model an all-altitude modeling capability. Table 3-2 is a sample of such a table. The computer program has five built-in choices of these tables at wavelengths of .5145, .6326, .860, 1.06, and 10.591 μm. The user also has the option of inputting a table for an optional wavelength and using it in the program. If such a table is not available, the user may select to use a fixed-coefficient system where the coefficients are supplied by the user. This method has the advantage that experimental results may be compared with the program when the coefficients were determined experimentally; but on the other hand the results are only good for near co-altitude geometries where variation of atmospheric properties over the altitude differences in the scenario are negligible, since only one coefficient can be input.

(U)   The normalized scattering function is dependent on many atmospheric parameters, including relative humidity and particle size distribution. The computation of such a function for a specific set of conditions requires a Mie scattering calculation. After examining the experimental and calculated curves available, two curvefit approximations were chosen for the program. The first of these, given in Figure 3-8, is shown superposed on measurements reported by Neila [3-4] for a wavelength of 1.06 μm. The second, at 10.6 μm, appears in Figure 3-9, where the data is taken from the same source. In the program the first curve is used to approximate $F(\theta)$ for wavelengths smaller than 2 μm and the 10.6 μm curvefit is used for wavelengths greater than 2 μm. The normalization of the curves allows their use at any altitude with errors only in the particle size distribution.

TABLE 3-2. VALUES OF ATTENUATION COEFFICIENT/KM AS A FUNCTION OF ALTITUDE FOR EACH LASER WAVELENGTH AND EACH ATMOSPHERIC MODEL IN SECTION 2 (k_m = MOLECULAR ABSORPTION, $_m$ = MOSECULAR SCATTERING, k_a = AEROSOL ABSORPTION, $_a$ = AEROSOL SCATTERING) [3-3]

λ=0.337µm														
	TROPICAL		MIDLATITUDE SUMMER		MIDLATITUDE WINTER		SUBARCTIC SUMMER		SUBARCTIC WINTER		AEROSOL			
											CLEAR		HAZY	
Ht(km)	k_m (km^{-1})	σ_m (km^{-1})	k_m (km^{-1})	σ_m (km^{-1})	k_m (km^{-1})	σ_m (km^{-1})	k_m (km^{-1})	σ_m (km^{-1})	k_m (km^{-1})	σ_m (km^{-1})	k_a (km^{-1})	σ_a (km^{-1})	k_a (km^{-1})	σ_a (km^{-1})
0	3.34E-04	8.40E-02	3.52E-04	8.64E-02	3.52E-04	9.30E-02	3.07E-04	8.83E-02	1.71E-04	9.80E-02	<E-06	1.35E-01	<E-06	1.11E-00
0-1	3.32E-04	8.07E-02	3.52E-04	8.23E-02	3.30E-04	8.73E-02	3.16E-04	8.00E-02	1.71E-04	8.84E-02		1.30E-01		6.02E-01
1-2	3.27E-04	7.36E-02	3.53E-04	7.47E-02	3.16E-04	7.91E-02	3.30E-04	7.59E-02	1.71E-04	8.24E-02		4.36E-02		2.52E-01
2-3	2.10E-04	6.60E-02	3.57E-04	6.76E-02	3.01E-04	7.23E-02	3.36E-04	6.65E-02	1.74E-04	8.11E-02		2.80E-02		8.23E-02
3-4	1.93E-04	6.03E-02	3.63E-04	6.12E-02	3.01E-04	6.32E-02	2.40E-04	6.13E-02	1.85E-04	7.10E-02		1.36E-02		3.31E-02
4-5	1.84E-04	5.40E-02	3.74E-04	5.53E-02	3.23E-04	5.50E-02	2.61E-04	5.53E-02	1.96E-04	6.30E-02		6.40E-03		1.23E-02
5-6	1.78E-04	4.86E-02	3.83E-04	4.99E-02	3.56E-04	5.06E-02	3.04E-04	4.86E-02	2.03E-04	5.80E-02		4.37E-03		4.27E-03
6-7	1.68E-04	4.47E-02	3.80E-04	4.47E-02	3.91E-04	4.81E-02	3.06E-04	4.43E-02	2.32E-04	4.83E-02		3.07E-03		5.07E-03
7-8	1.62E-04	4.02E-02	3.32E-04	4.01E-02	3.51E-04	4.01E-02	3.24E-04	3.88E-02	3.30E-04	4.01E-02		4.81E-03		4.07E-03
8-9	1.62E-04	3.61E-02	3.44E-04	3.59E-02	4.50E-04	3.53E-02	3.87E-04	3.17E-02	5.23E-04	3.53E-02		4.06E-03		4.04E-03
9-10	1.62E-04	3.23E-02	3.47E-04	3.21E-02	5.80E-04	3.14E-02	4.05E-04	3.11E-02	8.10E-04	3.03E-02		4.73E-03		4.73E-03
10-11	1.46E-04	2.88E-02	4.10E-04	2.85E-02	7.83E-04	2.73E-02	5.44E-04	2.78E-02	1.11E-03	2.50E-02		4.64E-03		4.54E-03
11-12	1.74E-04	2.56E-02	6.06E-04	2.53E-02	9.86E-04	2.36E-02	8.33E-04	2.30E-02	1.32E-03	2.21E-02		4.33E-03		4.53E-03
12-13	1.82E-04	2.26E-02	6.76E-04	2.24E-02	1.16E-03	2.01E-02	8.83E-04	2.03E-02	1.84E-03	1.89E-02		4.44E-03		4.44E-03
13-14	1.87E-04	2.00E-02	6.84E-04	1.84E-02	1.21E-03	1.72E-02	1.12E-03	1.76E-02	1.93E-03	1.63E-02		4.31E-03		4.34E-03
14-15	1.91E-04	1.76E-02	7.74E-04	1.60E-02	1.27E-03	1.40E-02	1.23E-03	1.61E-02	2.32E-03	1.30E-02		4.06E-03		4.06E-03
15-16	1.96E-04	1.56E-02	8.46E-04	1.42E-02	1.35E-03	1.26E-02	1.37E-03	1.30E-02	2.45E-03	1.10E-02		3.84E-03		3.84E-03
16-17	2.63E-04	1.31E-02	9.84E-04	1.22E-02	1.64E-03	1.08E-02	1.51E-03	1.13E-02	2.56E-03	1.01E-02		3.73E-03		3.73E-03
17-18	3.33E-04	1.11E-02	1.10E-03	1.04E-02	1.73E-03	9.20E-03	1.46E-03	9.61E-03	2.60E-03	8.60E-03		3.66E-03		3.44E-03
18-19	4.84E-04	9.12E-03	1.25E-03	8.78E-03	1.66E-03	7.87E-03	1.71E-03	8.37E-03	2.55E-03	7.41E-03		3.20E-03		3.20E-03
19-20	6.86E-04	7.87E-03	1.40E-03	7.44E-03	1.61E-03	6.83E-03	1.66E-03	7.11E-03	1.93E-03	6.33E-03		2.59E-03		2.50E-03
20-21	8.80E-04	6.72E-03	1.40E-03	6.36E-03	1.66E-03	5.81E-03	1.36E-03	6.11E-03	2.27E-03	5.43E-03		1.89E-03		1.89E-03
21-22	1.04E-03	5.76E-03	1.50E-03	5.42E-03	1.60E-03	4.96E-03	1.45E-03	5.26E-03	2.04E-03	4.66E-03		1.33E-03		1.30E-03
22-23	1.23E-03	4.44E-03	1.47E-03	4.63E-03	1.71E-03	4.26E-03	1.36E-03	4.53E-03	1.81E-03	3.99E-03		1.04E-03		1.04E-03
23-24	1.40E-03	3.76E-03	1.40E-03	3.95E-03	1.61E-03	3.62E-03	1.33E-03	3.88E-03	1.66E-03	3.41E-03		8.23E-04		8.23E-04
24-25	1.68E-03	3.10E-03	1.33E-03	3.38E-03	1.40E-03	3.00E-03	1.32E-03	3.33E-03	1.44E-03	2.91E-03		6.73E-04		6.73E-04
25-30	1.34E-03	2.12E-03	1.06E-03	2.28E-03	1.10E-03	2.15E-03	5.30E-04	2.25E-03	6.75E-04	1.93E-03		3.38E-04		3.38E-04
30-35	6.90E-04	9.72E-04	6.13E-04	1.03E-03	5.04E-04	1.04E-03	4.66E-04	1.03E-03	3.00E-04	8.38E-04		8.63E-05		8.63E-05
35-40	3.70E-04	4.62E-04	3.70E-04	5.00E-04	2.70E-04	4.66E-04	2.70E-04	4.08E-04	2.70E-04	3.83E-04		3.81E-05		3.81E-05
40-45	1.33E-04	2.20E-04	1.33E-04	2.44E-04	1.13E-04	1.95E-04	1.13E-04	2.66E-04	1.13E-04	1.76E-04		6.41E-06		6.41E-06
45-50	3.60E-05	1.16E-04	3.60E-05	1.24E-04	3.60E-05	8.33E-05	3.60E-05	1.28E-04	3.60E-05	7.67E-05		1.74E-06		1.74E-06
50-70	8.00E-06	4.31E-05	8.00E-06	4.73E-05	8.00E-06	3.48E-05	8.00E-06	4.88E-05	8.00E-06	2.91E-05		<E-06		<E-06
70-100	<E-06	3.35E-06	<E-06	3.90E-06	<E-06	3.30E-06	<E-06	4.12E-06	1.00E-06	3.01E-06		<E-06		<E-06

Figure 3-8. Normalized Atmospheric Scattering Distribution Function Used in LACM 2.0 for Wavelengths greater than 2 μm. The fitted curve is compared to composite measurement data at 10.6 μm [3-4].

Figure 3-9. Normalized Atmospheric Scattering Distribution Function Used in LACM 2.0 for Wavelengths less than 2 μm. The fitted curve is compared to composite measurement data at 1.06 μm [3-4].

p. 3-22 - 3-24
deleted

Figure 3-12. The Refractive Index Structure Function, Comparing the Computer Fit to Theoretical Models [3-6].

Section 3 — The Computer Model
Subsection C — User's Guide to LACM 2.0 Computer Program

1. COMPUTER PROGRAM OVERVIEW

(U) LACM 2.0, written in ANSI Fortran, is designed to be user oriented, in that it is interactive and the user is guided through his calculation by the program, freeing him from the need to laboriously prepare input data. In addition, he can monitor results and investigate in more detail those results that may interest him. Thus, a user may sit down at the terminal and in one session investigate a link, first determining the critical parameters and then investigating them in detail.

(U) A simplified functional flow diagram is presented in Figure 3-13 and illustrates the general flow of the program. Appendix B contains flow diagrams for each module. The main routine initially calls the interactive input routine which prompts the user for data on the link and the type of output he requires. The interactive routine, TSHARE, is programmed so that only the parameters required to do what the user wants are asked for. For example, if the user requires a power computation, the routine will not prompt him for the background type, as it is not used. Additionally, default values are provided and displayed to the user so he can see what sort of input is expected of him. (After executing a run the user has the option of changing a few inputs without having to go through the whole process, unless he makes a change that requires more inputs than he previously had specified.) Once the link parameters and run type flags have been set, the computational routines are called and execute the run. The user has the option to receive an input summary and to write the output on any file he chooses, or skip the output if all he desires is a plot.

(U) As can be seen in the figure, two different principal computational routines are available, one for a space-to-ground scenario called STOG and the other for narrow-beam analysis, called SETUP because it sets up the mode geometries, which will be described in more detail later on. In the former case, the user will have determined if he desires to compute the radius of the link beam at the ground or desires to input it; if it is to be computed, subroutine STBEAM is called to do the computation. The power at the off-axis receiver is computed, and printed. In the case of a narrow-beam link, SETUP calls computational routines as needed to generate a SNR or power profile of the link. Control then returns to the main program where the graphics routines are called, if available. Graphics are highly installation dependent, and are not required to run the program. Taking into account the installation's equipment a user can write a graphics routine best suited to his use.

(U) After a run is complete, the user can run a sensitivity analysis in which he may vary the atmospheric, port scatter, and reflectance parameters to determine how uncertainties in them may affect his conclusions about a link. The user can then begin a new run, or he may stop execution if he is done.
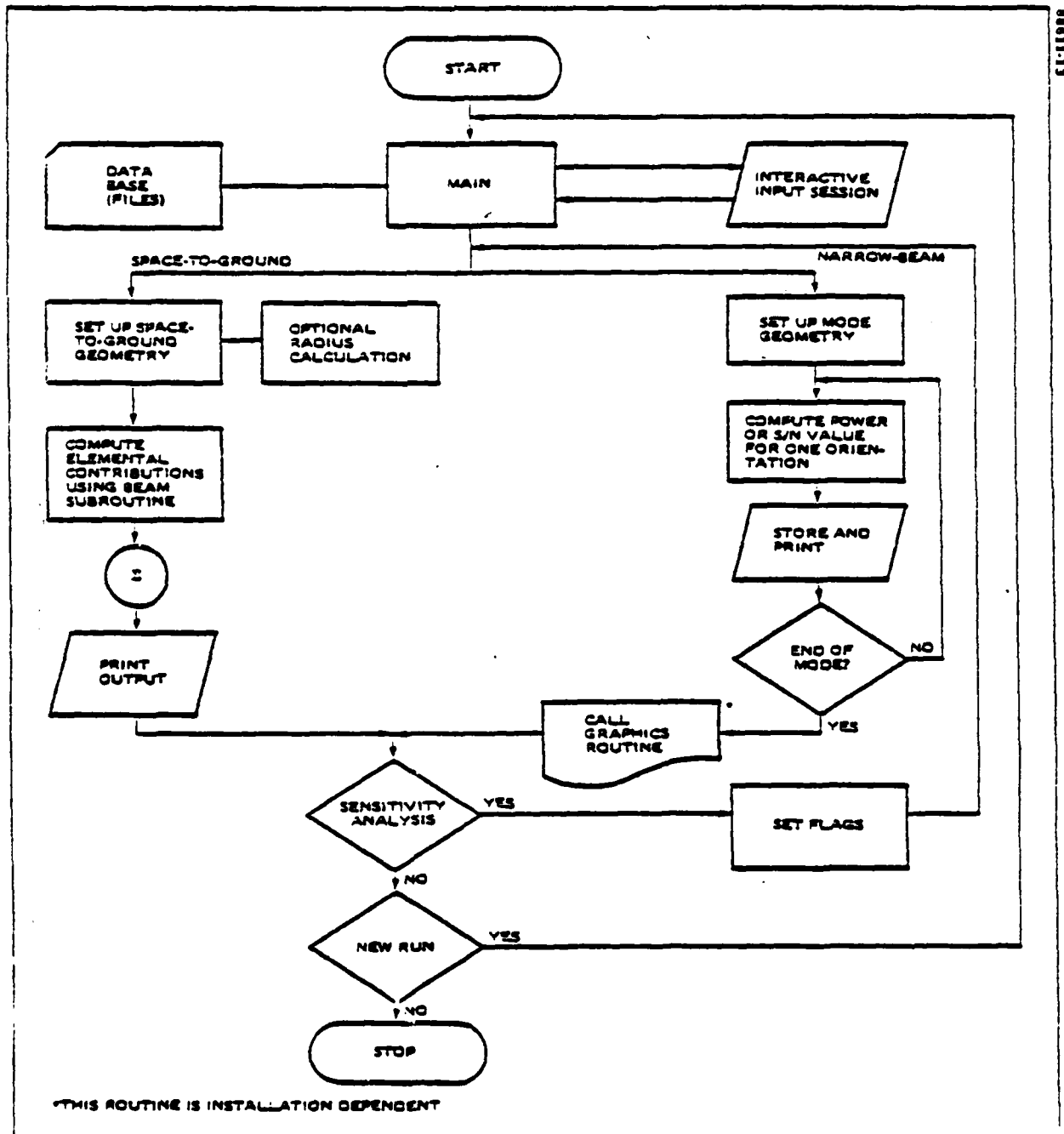
Figure 3-13. Simplified Flow Diagram of LACM 2.0

UNCLASSIFIED

Section 3 — The Computer Model
Subsection C — User's Guide to LACM 2.0 Computer Program

2. INPUT DESCRIPTION

(U) In this topic the inputs to LACM 2.0 are defined and the procedure for using the interactive routine is described.

(U)   The ECKSTROM Computer Model is interactive and has a very flexible input routine that is designed to allow an analyst to use the computer without extensive programming experience. Although the model is designed to be interactive, slight modifications will enable running of the program in a batch (background) processing environment, as described in Appendix B.

(U)   Figure 3-14 illustrates the input procedure. The user calls the program, and the program begins executing. The first parameter he is asked for is the link wavelength. Five choices are pre-set, and a sixth choice allows any other wavelength as a selection. (The sample input in the figure is somewhat system dependent. The question mark under the prompt statement is system generated, and the IBM TSO system allows defaulting to the present value in core by simply putting in a comma.) The selection of 4 then sets the wavelength to 1.06 μm. (However, all inputs except optical bandwidth are in MKS units). The standard prompt message has an input code followed by the variable name, description, and default value. A set of partial prompt messages can be used instead by typing in an end-of-file marker (/* on IBM) as an input. Details of this are described in Appendix B.

(U)   The user is prompted for the atmospheric model he wants. He has two options: to enter his own absorption and scattering coefficients (USER), or to use the AFGL data which provides an all-altitude capability. If AFGL data is selected and the user has selected a non-default wavelength (i.e., OTHER) a complete set of data for that wavelength will be expected by the program, and the user will be asked which unit the data will be read off of. This data is to be formatted in a 6X, 7E9.2 format with two cards per row of data from the table of AFGL data, shown in Table 3-2. In the case that a defaulted wavelength is selected, the data is in core and the program proceeds to the next prompt messages, requesting the atmospheric model type and visibility. Reference 3-3 contains a detailed description of these models and should be readily available to the user, so they will not be described further.

(U)   The next inputs are more straightforward; the transmitter optics diameter and beamwidth are input. If the beamwidth is less than the diffraction limit, a message with the diffraction limited beamwidth is printed and the beamwidth is requested again, which must be greater than the diffraction limited beamwidth. The BSDF model (port scatter) is required, with a default available; or, if USER is selected, the slope, intercept, and 'glitches' of the BSDF are requested, as described in the previous subsection.

(U)   The next group of inputs specify the backstop characteristics and orientation. The user can select either a lambertian backstop or one with a specular component. The default has a 3° specular component, but the user should try to find what model best suits his backstop. The lambertian model requires a reflection coefficient, and the specular model requires the diffuse reflection and the specular amplitude and width. The next inputs, PSLAZ and PSIEL, allow the backstop to be tilted back and forth or up and down relative to the default position normal to the link beam. The receiver scattering is the next input and is specified in the same manner as the backstop, having a specular and diffuse component.

3-28

UNCLASSIFIED

(U) The power transmitted, PT, is required in watts, followed by the link range and the altitudes of the link transmitter and link receiver. Note that the SR altitude is specified by the parameters X, RPX, and GAMINT, as described in the geometry description and illustrated in Figure 3-1.

(U) Two flags are set next, MCOMP, and MP. The program can be instructed to compute the power, or signal-to-noise ratio, and it can isolate the sources of scattered radiation to the atmosphere, transmitter, or receiver/backstop combination, or it can provide the total from all sources. As described later, the output tables will break these components out so the user can see the significance of each.

(U) The next parameters describe the off-axis ϕ receiver, its detection characteristics, and select the background type. The user is allowed to default the characteristics but this is not recommended in general. Two detection types are allowed, direct detection and heterodyne detection. The SNR expressions for the different detection types require different parameters, as shown in the previous subsection. The parameters common to both are the electronic bandwidth of the SR (BW), the quantum efficiency ETA, and the modulation depth XM. In the case of direct detection a noise factor F is specified, along with the system NEP, and the optical bandwidth BWOPT of the predetection background filter. If heterodyne detection is selected the mixing efficiency EM is required. Note that in the sample input session in Figure 3-14 a wavelength of less than 2 μm was selected, so that the choice of direct detection was assumed automatically.

(U) The area of the off-axis ϕ receiver, ASR, is required for all cases, as is the FOV in the intercept plane, PHI. For cases where the background power is computed a second input PHIAZ is required. This is the FOV is the plane orthogonal to the intercept plane, intersecting the intercept plane along the SR optical axis.

(U) The last few inputs are the hood lengths of the transmitter and link receiver. If the lengths are greater than zero their diameters are also requested by the program, as illustrated for the receiver hood. The final input we describe here is the intercept plane orientation angle, GAMINT. Figure 3-1 shows how this angle defines the intercept half-plane.

(U) The last few inputs select the modes and their related parameters and will be discussed in detail in the next topic.

(U) Figure 3-15 is a listing of the input summary that the user can request. The input summary contains the input variables and presents them in an orderly fashion. One parameter appears which merits special attention, and that is the angle of the intercept half-plane containing the specularly reflected component of the backstop, described in detail in Subsection B. The rest of the summary is self explanatory.

(U) The space-to-ground input is invoked by specifying a transmitter altitude of more than 100,000 meters. The SR distance to the beam is required, and the user either can input the beam radius and peak intensity at ground level, or have those parameters calculated. If they are to be calculated several other parameters are required. The platform jitter, specified in radians, will broaden the beamshape. Platform jitter quantifies the stability of the transmitter platform, as described in Subsection B.

(U) Table 3-3 summarizes the hierarchy of the inputs and will be useful to the user during a session in making changes between runs.

(U) Table 3-2 in Appendix B lists the input variables, their type, and any limitations or comments that are not obvious.

```
INPUT
CODE      VARIABLE          DESCRIPTION          DEFAULT

call eck(main)——CALL PROGRAM
         INTERCEPTIBILITY ANALYSIS PROGRAM — ENTER 1 TO START
1
   1     LAM     — WAVELENGTH INDEX                      4
         (1-.5145   2-.6328   3-.85   4-1.06   5-10.591   6-OTHER)
?
4 ——SELECT 1.06 μm
   29    IA      — ATMOSPHERICS (1-USER 2-AFGL)          1
?
2 ——SELECTED AFGL DATA
         MAT     — ATMOSPHERIC MODEL                     2
                   1 - TROPICAL
                   2 - MIDLATITUDE SUMMER
                   3 - MIDLATITUDE WINTER
                   4 - SUBARCTIC SUMMER
                   5 - SUBARCTIC WINTER
? ——COMMA TO USE DEFAULT VALUE OF 2
.
         MVIS    — VISIBILITY (1-CLEAR 2-HAZY)           1
?
2
   2     DT      — TRANSMITTER OPTICS DIAMETER, M        0.100
?
.1
   3     PHIT    — TRANSMITTER BEAMWIDTH, RADIANS        1.000E-04
? .
.
   31    IBSDF   — BSDF (1-DEFAULT, 2-USER)              1
?
2
         YBSDF   — BSDF Y-INTERCEPT AT 1 DEGREE          2.000E+02
?
.
         SBSDF   — BSDF SLOPE (LOG-LOG)                  -2.500E+00
?
.
         NG      — NUMBER OF GLITCHES   (0 - 3)          0
?
0
   4     DR      — LINK RECEIVER OPTICS DIAMETER, M      0.100
?
.
   32    NBAK    — BACKSTOP  (1-DEFAULT, 2-USER, 3-LAMBERTIAN)     1
?
3
         BDIFF   — REFLECTION COEFFICIENT
                   (LAMBERTIAN MODEL, EG. .1)
?
.15
   44    PSIAZ   — AZ. ORIENTATION OF BACKSTOP (DEG)     0.0
                   0 - NORMAL TO BEAM
?
0.0
```

Figure 3-14. Illustration of Interactive Session (1 of 3)

INPUT CODE	VARIABLE	DESCRIPTION	DEFAULT
	PSIEL	— EL. ORIENTATION OF BACKSTOP (DEG) 0 — NORMAL TO BEAM	0.0
33	NOA	— RCVR SCATTER (1-DEFAULT, 2-USER)	1
6	PT	— TRANSMIT POWER, WATTS	1.000E+00
8	RL	— LINK RANGE, METERS	5.000E+03
9	HT	— ALTITUDE OF TRANSMITTER, METERS	1.000E+01
10	HR	— ALTITUDE OF LINK RECEIVER, M	1.000E+01
25	MCOMP	— COMPUTE 1-POWER 2-S/N RATIO	1
5	MP	— SOURCE? 1-SUM, 2-ATM, 3-TR, 4-RC	1
13	IRTYPE	— SR TYPE (1-DEFAULT, 2-USER INPUT)	2
14	XM	— MODULATION DEPTH	1.000
16	ETA	— QUANTUM EFFICIENCY OF DETECTOR	0.700
17	F	— EXCESS NOISE FACTOR	1.000E+00
18	BWR	— BANDWIDTH OF SR, HZ	1.000E+06
19	PNEP	— NOISE EQUIVALENT POWER OF SR	1.000E-12
29	BWOPT	— SR OPTICAL BANDWIDTH, MICRONS	5.000E-02
30	NFLG	— 1-SUNNY 2-CLOUDY 3-NIGHTTIME	1

Figure 3-14. Illustration of Interactive Session (2 of 3)

INPUT CODE	VARIABLE	DESCRIPTION	DEFAULT
7	BW	— LINK BANDWIDTH, HZ	1.000E+06
12	ASR	— AREA OF SR APERTURE, SQ. METERS	5.000E−02
11	PHI	— SR FIELD OF VIEW, RADIANS	1.000E−02
40	PHIAZ	— SR FIELD OF VIEW (AZIMUTH), RAD	1.000E−02
20	BLT	— HOOD LENGTH OF TRANSMITTER, M	0.0
21	BLR	— HOOD LENGTH OF RECEIVER, M	0.0
43	BDLR	— RECEIVER HOOD DIAMETER, M	0.100
41	GAMINT	— ANGLE OF INTERCEPT PLANE, DEG 0 FOR HORIZONTAL PLANE	0.0
26	MODE	— SELECT OUTPUT MODE (7 FOR INFO)	4
23	RPX	— DISTANCE FROM XMTR TO BISECTOR, M	2.500E+03
24	X	— PERPENDICULAR DIST TO BEAM AXIS, M	1.000E+03

?
.05
?
5.e-3
?
5.e-3
?
0.
?
.01
?
?
?
1
?
?

```
END OF INPUTS
DO YOU WISH TO CHANGE ANYTHING? 1-YES  2-NO   3-ALL
? 
2 ——————— NO, PROCEED        (ALLOWS TO CORRECT ERRORS)
DO YOU WANT AN INPUT SUMMARY?      0-NO  1-YES
1 ——————— YES               (SHOWN IN NEXT FIGURE)
```

Figure 3-14. Illustration of Interactive Session (3 of 3)

SCENARIO GEOMETRY

LINK RANGE, M ———	5.000E+03	TR ALT, M ———	2.000E+01
RC ALT, M ———	2.000E+01	SR ALT, M ———	1.000E+01
BACKGROUND TYPE —	SUNNY		

LINK PARAMETERS

WAVELENGTH, M ———	1.060E-06	TR POWER, W ———	1.000E+00
RC APERTURE, M —	0.10000	TR APERTURE, M —	0.10000
RC HOOD LENGTH, M-	0.01	TR HOOD LENGTH, M	0.0
RC HOOD DIA., M —	0.10	TR HOOD DIA., M —	0.10
		TR BEAM WIDTH, RAD	1.000E-04

SR PARAMETERS

LINEAR FOV, RAD -	5.000E-03	APERTURE, SQ.M. -	0.0500
FOV ACROSS BEAM, R	5.000E-03	DETECTION TYPE, -	DIR
OPT BW, MICRONS —	5.000E-02	NEP, W/RT.HZ. ———	1.000E-12
MOD. DEPTH, ———	1.00	EXCESS NOISE ———	1.000E+00
BANDWIDTH, HZ ———	1.000E+06	QUANTUM EFF. ———	0.70

INTERCEPT MODE PARAMETERS

MODE TYPE ———	1	OUTPUT TYPE ———	S/N, DB
RPX, METERS ———	2.500E+03	X, METERS ———	1.000E+03
SR PLANE, DEG ———	0.0	SPECULAR GAMINT -	0.0

ATMOSPHERIC PARAMETERS

DATA SOURCE ———	AFGL		
MIDLATITUDE SUMMER		VISIBILITY IS	HAZY
	COEFFICIENTS FOR 0 TO 1000 METERS ALTITUDE		
SCAT COEF 1/M ———	2.008E-04	ABS COEF, 1/M ———	5.820E-05

SCATTERING DATA FOR TRANSMITTER, RECEIVER, AND BACKSTOP

BSDF MODEL TYPE —	AVERAGE	BSDF SLOPE DB/DB	-2.500
NONLINEARITIES —	0	BSDF INTERCEPT	200.000
BACKSTOP TYPE ———	LAMBERTIAN	REFLECTION COEF -	0.1500
BACKSTOP AZ, DEG	0.0	BACKSTOP EL, DEG	0.0
OA TYPE ———	UNKNOWN	DIFFUSE LEVEL —	0.0
SPECULAR MAX —	0.0	SPECULAR WIDTH, D	0.300

Figure 3-15. Sample Input Summary

TABLE 3-3. INPUT HIERARCHY OF TSHARE ROUTINE. EACH INPUT CODE HAS ONE OR MORE VARIABLES IT ACCESSES.

INPUT HIERARCHY

Input Code	Input Variables
1	Wavelength
28	Atmospherics
	Optional – Input absorption & scattering coefficients
	– Read in new AFGL tables
2	Transmitter Optics
3	Transmitter Beamwidth
31	BSDF Model
	Optional – BSDF Slope
	– BSDF Intercept
	– Glitches
4	Link Receiver Optics
32	Backstop Type
	– Diffuse Reflectance
	– Specular Width & Maximum
44	Backstop Orientation
	– Azimuth
	– Elevation
6	Link Transmit Power
8	Link Range
9	Transmitter Altitude
10	Link Receiver Altitude
34	Space-to-Ground Flag
	—If Space-to-Ground—
35	– Off-Axis Distance
36	– SR Elevation Angle
39	– Ground-Level Altitude
46	– Beam Computation Flag
47	– Jitter
48	– Turbulence Flag
37	– Beam Radius
38	– Intensity on Axis

TABLE 3-3. INPUT HIERARCHY OF TSHARE ROUTINE. EACH INPUT
CODE HAS ONE OR MORE VARIABLES IT ACCESSES. (Continued)

Input Code	Input Variables
25	Computation Flag (Power or SNR)
5	Source of Scatter Flag —For SNR Cases—
14	— Modulation Depth
45	— Detection Type (Direct or Heterodyne)
15	— Heterodyne Mixing Efficiency
16	— Quantum Efficiency
17	— Noise Figure (Direct Detection)
18	— SR Bandwidth
19	— SR NEP (Direct Detection)
29	— SR Optical Bandwidth (Direct Detection)
30	— Background Type (Direct Detection)
7	— Link Bandwidth
12	SR Aperture
11	SR FOV (In Intercept Plane)
40	SR AZ FOV (Out of Plane)
20	Transmitter Hood Length
42	Transmitter Hood Diameter
21	Receiver Hood Length
43	Receiver Hood Diameter
22	SR Altitude (Space-to-Ground Case)
41	Intercept Half-Plane Orientation
26	Mode Type — RPX (Modes 1-3) — X (Modes 1-3) — Contour Level

Section 3 — The Computer Model
Subsection C — User's Guide to LACM 2.0 Computer Program

3. DESCRIPTION OF MODES AND OUTPUT

(U) The intercept modes are designed to free the program user from setting up a significant amount of the geometry needed to do a calculation. Each mode goes through a sequence, moving or orienting the SR like a probe to produce a power or SNR profile of the link.

(U)   The calculation of power at an off-axis point requires five coordinates, three to define the SR position in three-dimensional space, and two to define its orientation. In the geometry established and discussed previously, the SR and its optical axis are confined to the intercept half-plane and thus only three coordinates remain to be specified once the intercept half plane has been specified. The position of the SR in the intercept half-plane can be specified by its off-axis distance X and its downrange distance RPX. Note that RPX may be negative (in the transmitter's rear hemisphere) or positive, while X must always be positive. The first three modes go through a set of standard points, while Modes 4 and 5 produce contours of power or SNR about the link axis in the intercept half-plane.

(C)   In Mode 1 the SR position is fixed by the input values of X and RPX. The optical axis of the SR is slewed from the transmitter to the receiver, incrementing the orientation angle θ by one degree near to the transmitter and receiver, and by no more than ten degrees in between, to yield a total of about 37 points. As illustrated in Figure 3-16, Mode 1 is ideal for evaluation of the point (RPX,X) as a potential SR location.

(U)   Figure 3-17 is a sample output table for a typical Mode 1 case. The signal-to-noise ratio in dB is listed, along with the power contributed by each source considered. As would be expected, the transmitter is seen first, and when θ is incremented it is no longer in the SR field of view. When the receiver falls into the field of view, the mode is complete. In Mode 1 the edge of the FOV is on the transmitter to maximize the atmospheric scatter visible, and on the opposite edge for the receiver/backstop. When the data is plotted (Figure 3-18) the transmitter and receiver contribution show up clearly. It may seem odd that the receiver contribution in this case is almost equal to the transmitter contribution; however, the transmitter scatter is very strong at small angles while the backstop is a lambertian reflector, and at 22 degrees off normal the transmitter scatter has dropped down significantly, while the backstop has only dropped by 7% from its maximum value.

(U)   In Mode 2 the SR views a fixed point along the beam, and   is incremented to effectively move the SR about the point with the center of the FOV oriented toward the point. Note that atmospheric transmission losses are (for a narrow FOV) constant for Mode 2, while in the Mode-1 geometry the path length from transmitter to scattering volume to SR increases with increasing θ. Another geometric factor is that the scattering volume, defined by the intersection of the link axis and SR FOV, is changing with θ, and is minimized at 90 degrees. The output of Mode 2 will show the scattering distribution function $F(\theta)$ very strongly, multiplied by the geometric scaling of the scattering volume. A sample output table has not been included, as it is identical in form to the table for Mode 1. The data is plotted in Figure 3-18 for comparison with Modes 1 and 3. In this sample case the fixed point is located halfway down the link axis.

(C)   Mode 2 has great utility in looking at the port or receiver/backstop scatter. By positioning the fixed point at the transmitter (RPX=0.) or at the receiver (RPX = RL, the link range) the angular scattering profile can be generated. Since the SR orientation
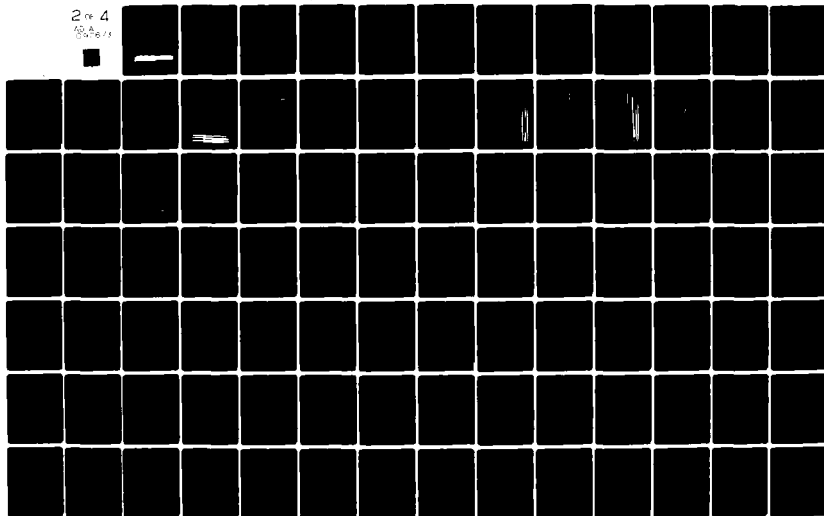
goes from 1 to 179 degrees, the transmitter profile will have no transmitter contribution for angles greater than 90 degrees, and the receiver will not have any from 1 to 90 degrees, unless the backstop is oriented away from the perpendicular to face the intercept half-plane. It should also be noted that in Mode 2 the X and RPX inputs define the distance from the scattering volume to SR and transmitter to scattering volume respectively rather than the SR location.

(U) Mode 3 is similar to Mode 2 in that a fixed point in the link beam is observed. However, the SR is moved along a parallel to the link beam in the intercept half-plane and thus at angles approaching 0 or 180 degrees the range from the SR to the fixed point becomes large. This causes the intensity to drop down due to attenuation, as illustrated by the Mode 3 curve in Figure 3-18. One interesting feature of this particular sample curve is that it reaches a maximum at about 10 degrees. It therefore predicts that minimizing the intercept angle does not necessarily maximize the available power if one is confined to a certain off-axis distance. This results because of tradeoffs between scattering distribution $F(\theta)$, transmission, and transmitter scatter characteristics.

(U) Modes 4 and 5 generate contours about the link using an iterative method. In Mode 4, the SR is assumed to always look at the transmitter and that portion of the beam immediately in front of it, within the SR FOV. As shown in Figure 3-19, beginning at an angle θ of one degree the SR position is adjusted until a desired contour level is found on the off-axis ray. The SR coordinates at that point are then stored, θ is incremented, and the next point is searched for. The increment used is smaller for the small angles, and gets larger with θ until it reaches a maximum of 2.5°, so that the points are spaced more evenly in X and RPX.

(U) Mode 5 uses the same procedure as Mode 4 (Figure 3-19) but the contours represent the total collectible power at the SR from the entire link, if a FOV encompassing the transmitter, receiver, and beam were used. It is recommended Mode 5 be used for power contours rather than SNR because the SR FOV is used only as a probe, and the background noise will not be computed for the entire composite FOV, but only for the probe FOV. (The program will not compute SNR for Mode 5 but the user can remove the restriction in the input routine).

(U) Figure 3-21 compares plots for Modes 4 and 5 at the same contour level. The Mode 5 plots were run with the backstop and receiver at 5 and 10 km. (The ragged effect is due to the convergence criteria, indicating here that the power is changing slowly with distance because the 2% convergence criterion is satisfied by many points just off the actual curve). Note the receiver reflections at 5 and 10 km for the respective cases. Note also that the scales are not identical, i.e., the average (X) scale goes out to 500 meters, but the downrange (RPX) scale goes out to 12 km. The first point to the right is at one degree off the link axis at the transmitter, since the models are limited to one degree off the axis.
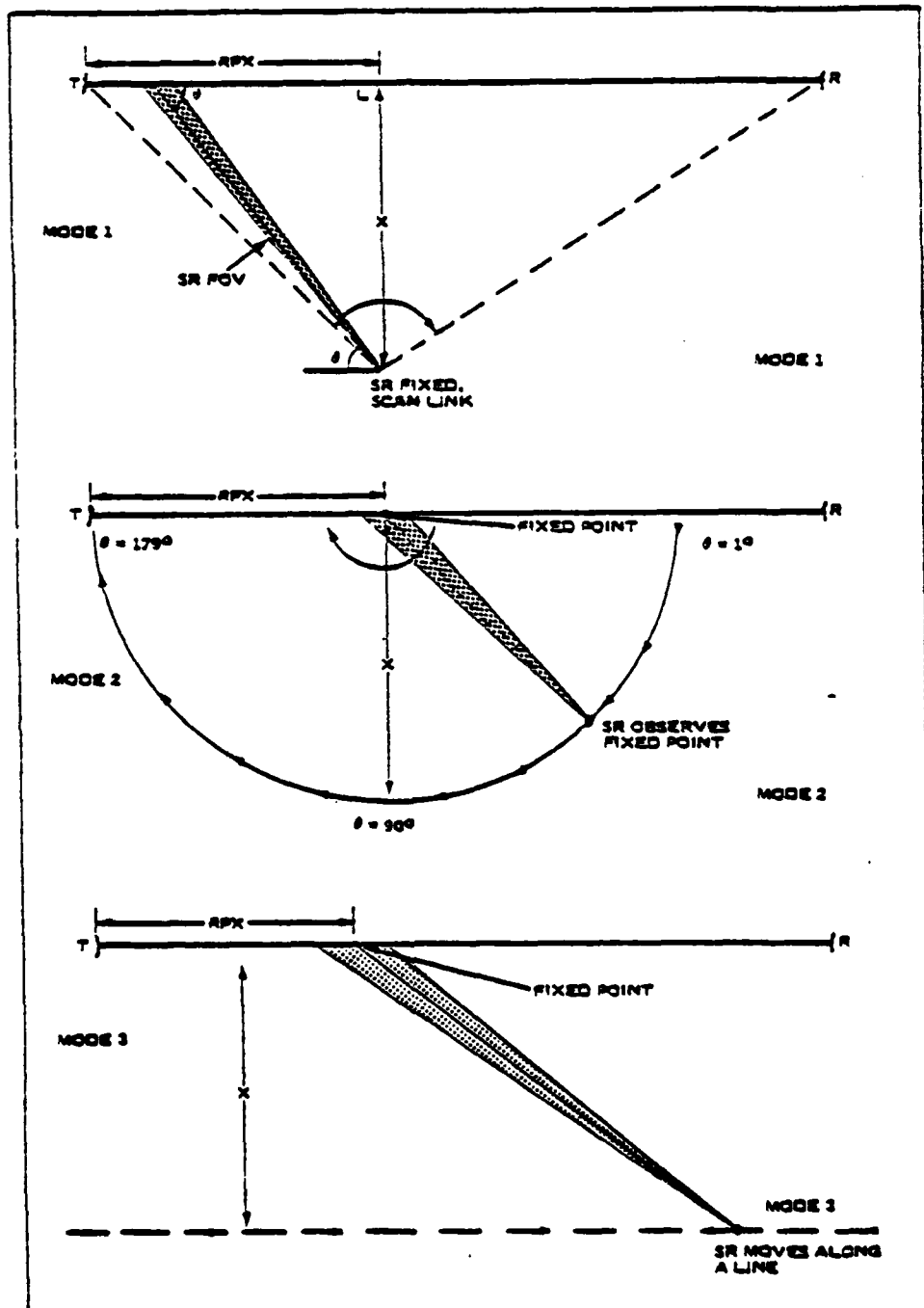
Figure 3-16. Geometry for Modes 1-3, as Described in the Text. Note that link transmitter and receiver/backstop are treated as points (i.e., vignetting is neglected).

INTERCEPTIBILITY MODE 1

| | | POWER CONTRIBUTED BY EACH SOURCE, WATTS | | |
THETA, D	S/N, DB	TRANSMITTER	RECEIVER	ATMOSPHERE
2.1945E+01	-2.0195E+01	2.8738E-10	0.0	1.2459E-11
2.2945E+01	-4.8591E+01	0.0	0.0	1.1405E-11
2.3945E+01	-4.9351E+01	0.0	0.0	1.0449E-11
2.4945E+01	-5.0104E+01	0.0	0.0	9.5821E-12
2.5945E+01	-5.0849E+01	0.0	0.0	8.7946E-12
2.6945E+01	-5.1586E+01	0.0	0.0	8.0791E-12
2.7945E+01	-5.2315E+01	0.0	0.0	7.4288E-12
2.8945E+01	-5.3035E+01	0.0	0.0	6.8373E-12
2.9945E+01	-5.3748E+01	0.0	0.0	6.2989E-12
3.0945E+01	-5.4451E+01	0.0	0.0	5.8087E-12
3.8202E+01	-5.9292E+01	0.0	0.0	3.3269E-12
4.5458E+01	-6.3650E+01	0.0	0.0	2.0143E-12
5.2715E+01	-6.7535E+01	0.0	0.0	1.2880E-12
5.9972E+01	-7.0990E+01	0.0	0.0	8.6531E-13
6.7229E+01	-7.4070E+01	0.0	0.0	6.0696E-13
7.4486E+01	-7.6824E+01	0.0	0.0	4.4201E-13
8.1743E+01	-7.9285E+01	0.0	0.0	3.3296E-13
8.9000E+01	-8.1463E+01	0.0	0.0	2.5911E-13
9.6257E+01	-8.3351E+01	0.0	0.0	2.0849E-13
1.0351E+02	-8.4930E+01	0.0	0.0	1.7384E-13
1.1077E+02	-8.6180E+01	0.0	0.0	1.5055E-13
1.1803E+02	-8.7095E+01	0.0	0.0	1.3549E-13
1.2528E+02	-8.7704E+01	0.0	0.0	1.2631E-13
1.3254E+02	-8.8083E+01	0.0	0.0	1.2092E-13
1.3980E+02	-8.8375E+01	0.0	0.0	1.1693E-13
1.4705E+02	-8.8825E+01	0.0	0.0	1.1102E-13
1.4805E+02	-8.8921E+01	0.0	0.0	1.0980E-13
1.4905E+02	-8.9029E+01	0.0	0.0	1.0844E-13
1.5005E+02	-8.9152E+01	0.0	0.0	1.0692E-13
1.5105E+02	-8.9291E+01	0.0	0.0	1.0522E-13
1.5205E+02	-8.9449E+01	0.0	0.0	1.0332E-13
1.5305E+02	-8.9629E+01	0.0	0.0	1.0121E-13
1.5405E+02	-8.9833E+01	0.0	0.0	9.8857E-14
1.5505E+02	-9.0065E+01	0.0	0.0	9.6253E-14
1.5605E+02	-9.0328E+01	0.0	0.0	9.3374E-14
1.5705E+02	-9.0629E+01	0.0	0.0	9.0201E-14
1.5805E+02	-2.5275E+01	0.0	1.6699E-10	8.6715E-14

Figure 3-17. Sample Mode-1 Output Table
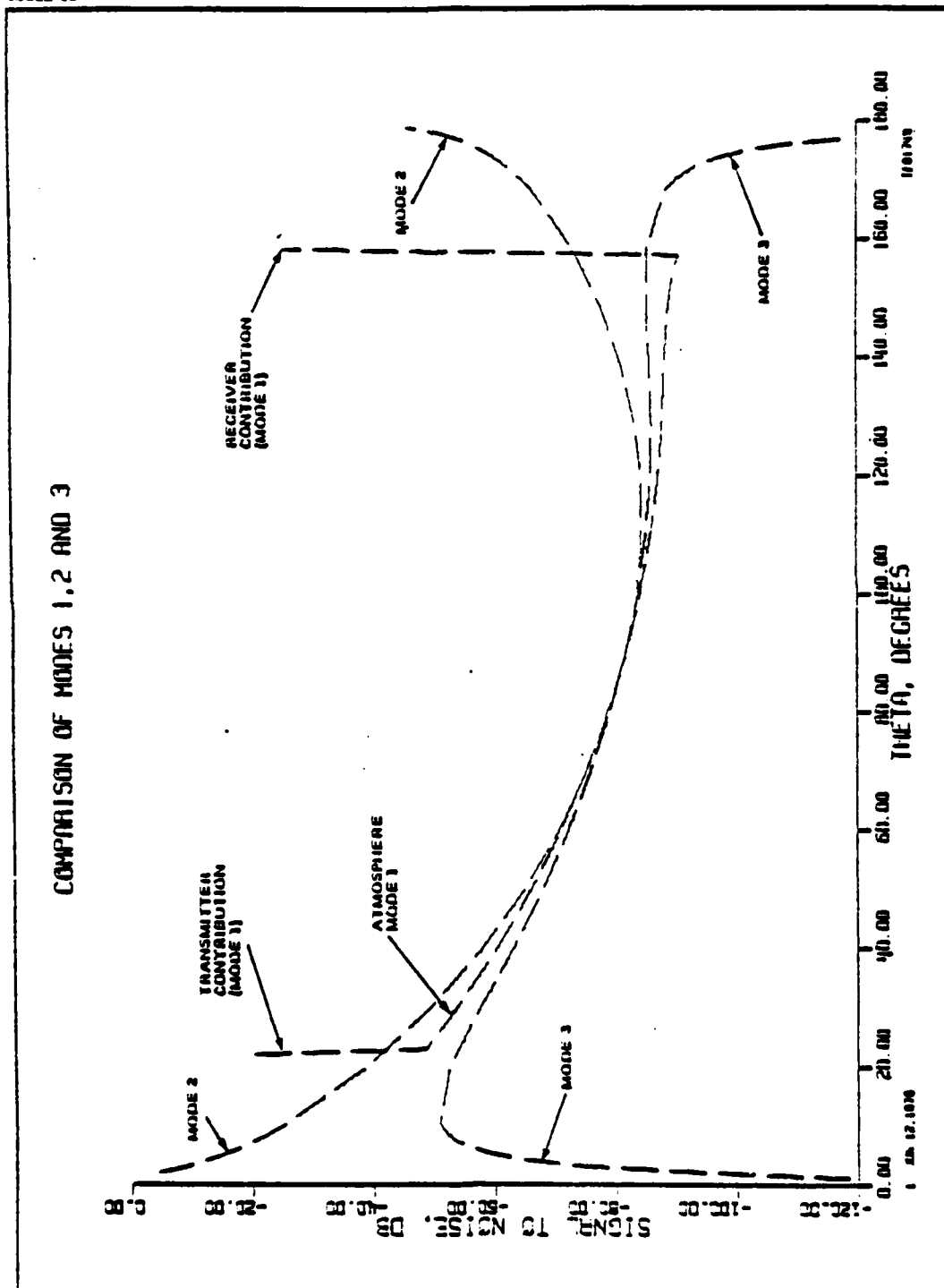
Figure 3-18. Computer Generated Plot Comparing Output of Modes 1, 2 and 3
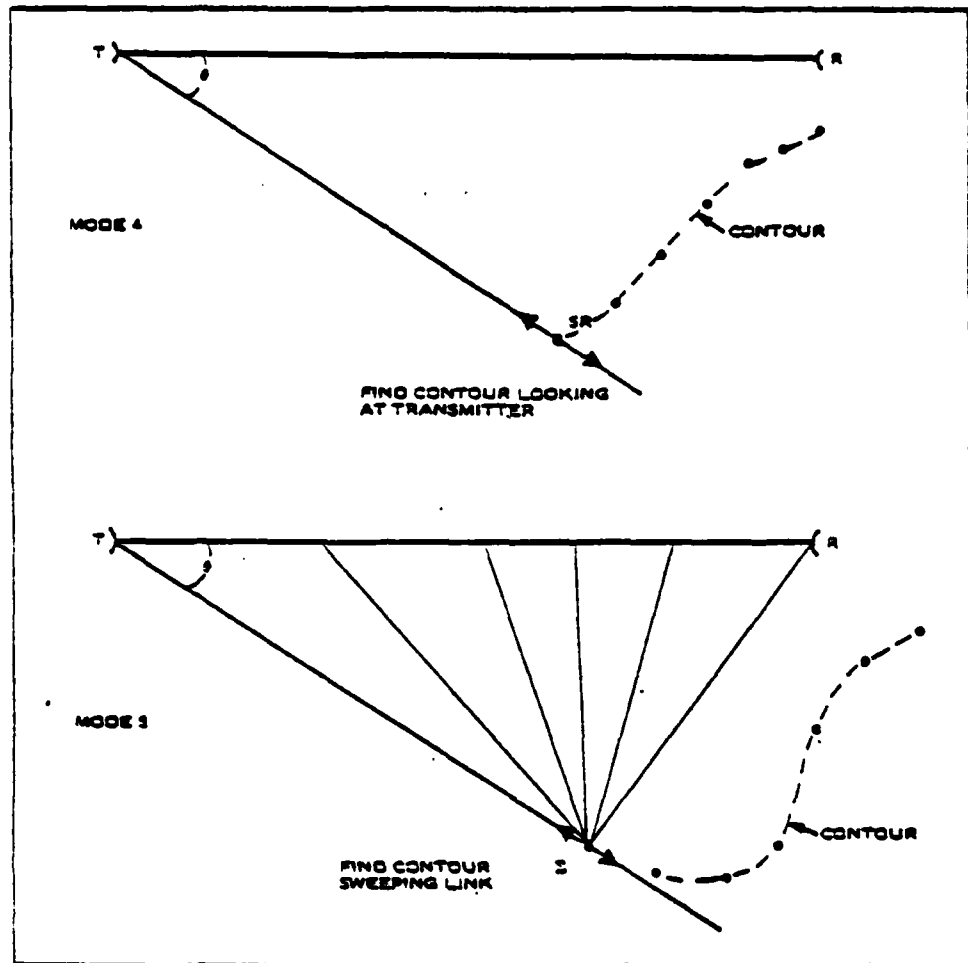
Figure 3-19. Geometry for Modes 4 and 5

UNCLASSIFIED

```
INTERCEPTIBILITY MODE  5
                                  POWER CONTRIBUTED BY EACH SOURCE, WATTS
  X,METERS        RPX ,M          TRANSMITTER        RECEIVER        ATMOSPHERE
1.6419E+02      9.4064E+03    3.    9.3879E-09      0.0             2.8486E-10
1.7156E+02      8.9351E+03    3.    9.7543E-09      0.0             3.7176E-10
1.7891E+02      8.4911E+03    3.    9.6046E-09      0.0             4.8312E-10
1.8626E+02      8.0746E+03    3.    9.4317E-09      0.0             6.2493E-10
1.9368E+02      7.6859E+03    3.    9.2285E-09      0.0             8.0409E-10
1.9944E+02      7.2602E+03    2.    9.3053E-09      0.0             1.0813E-09
2.0812E+02      6.9635E+03    2.    8.8457E-09      0.0             1.3365E-09
2.1697E+02      6.6856E+03    2.    8.3913E-09      0.0             1.6441E-09
2.2602E+02      6.4256E+03    2.    7.9426E-09      0.0             2.0114E-09
2.3529E+02      6.1821E+03    2.    7.5022E-09      0.0             2.4444E-09
2.4477E+02      5.9538E+03    2.    7.0740E-09      0.0             2.9449E-09
2.5445E+02      5.7389E+03    2.    6.6617E-09      0.0             3.5024E-09
2.6429E+02      5.5357E+03    2.    6.2697E-09      0.0             4.0796E-09
2.7763E+02      5.4081E+03    3.    5.6606E-09      0.0             4.3121E-09
2.8794E+02      5.2239E+03    3.    5.3241E-09      0.0             4.6822E-09
2.9773E+02      5.0374E+03    3.    5.0447E-09      0.0             4.9593E-09
3.1554E+02      4.9854E+03   12.    4.3960E-09      8.9564E-10      4.7180E-09
3.3590E+02      4.9621E+03   10.    3.7707E-09      1.9570E-09      4.3840E-09
3.5703E+02      4.9373E+03    7.    3.2473E-09      2.7006E-09      4.0757E-09
3.7816E+02      4.9011E+03   13.    2.8260E-09      3.5258E-09      3.8190E-09
3.9970E+02      4.8603E+03    8.    2.4738E-09      4.0486E-09      3.5864E-09
3.9742E+02      4.5390E+03   20.    2.6333E-09      5.3339E-09      4.0956E-09
3.8732E+02      4.1592E+03    4.    2.9636E-09      2.7395E-09      4.7103E-09
3.6817E+02      3.7208E+03    3.    3.5617E-09      1.2941E-09      5.5266E-09
                   ---PORTION OF TABLE OMITTED---
1.5016E+02      1.1353E+02    5.    7.9611E-09      4.0433E-11      1.7132E-09
1.4246E+02      1.0117E+02    8.    8.2230E-09      4.0109E-11      1.7098E-09
1.3730E+02      9.1339E+01    8.    8.1823E-09      3.9853E-11      1.6791E-09
1.3250E+02      8.2297E+01    8.    8.0764E-09      3.9619E-11      1.6436E-09
1.2530E+02      7.2387E+01    9.    8.2578E-09      3.9366E-11      1.6562E-09
1.1981E+02      6.4094E+01    9.    8.1980E-09      3.9155E-11      1.6460E-09
1.1467E+02      5.6906E+01    9.    8.0802E-09      3.8963E-11      1.6361E-09
1.0667E+02      4.8117E+01   10.    8.3209E-09      3.8754E-11      1.6785E-09
9.9928E+01      4.0949E+01   10.    8.3794E-09      3.8575E-11      1.7110E-09
9.2003E+01      3.3930E+01   10.    8.6329E-09      3.8402E-11      1.7766E-09
8.9329E+01      2.9301E+01   11.    7.8684E-09      3.8287E-11      1.7490E-09
8.2496E+01      2.3706E+01    7.    7.7920E-09      3.8150E-11      1.8175E-09
7.4214E+01      1.8311E+01    9.    7.9462E-09      3.8019E-11      1.9429E-09
6.7923E+01      1.3995E+01    9.    7.8819E-09      3.7914E-11      2.0416E-09
5.9614E+01      9.8450E+00   10.    7.5290E-09      3.7814E-11      2.2444E-09
5.0420E+01      6.2504E+00   11.    7.5105E-09      3.7728E-11      2.5660E-09
4.2284E+01      3.4829E+00    9.    6.7143E-09      3.7662E-11      2.9613E-09
3.0502E+01      1.2308E+00   11.    5.9019E-09      3.7609E-11      3.9779E-09
1.2512E+01     -3.2966E-02   12.    0.0             3.7581E-11      9.5271E-09
1.1316E+01     -5.3320E-01   13.    0.0             3.7568E-11      1.0009E-08
1.1139E+01     -1.0041E+00   13.    0.0             3.7557E-11      1.0019E-08
1.0794E+01     -1.4499E+00   13.    0.0             3.7546E-11      1.0025E-08
1.0478E+01     -1.8761E+00   13.    0.0             3.7535E-11      1.0030E-08
1.0190E+01     -2.2371E+00   13.    0.0             3.7525E-11      1.0028E-08
9.9232E+00     -2.6869E+00   13.    0.0             3.7513E-11      1.0023E-08
   ** ITERATION DID NOT CONVERGE AT   1 POINTS
```

Figure 3-20. Sample Mode-5 Output Table

UNCLASSIFIED
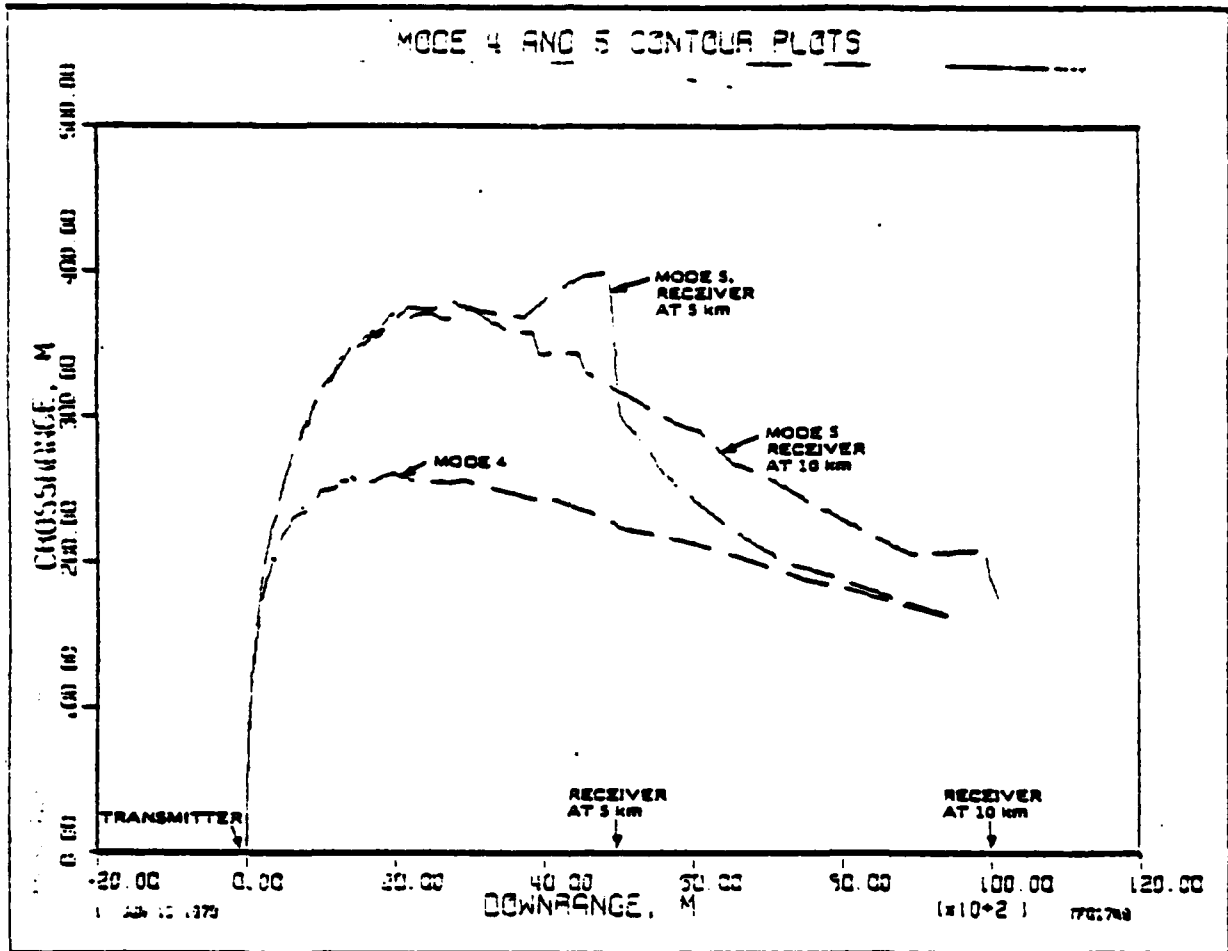
Figure 3-21. Contour Plots for Mode 4 and 5. Note that scales of axes are different, distorting the contour shape.

Section 3 — The Computer Model
Subsection C — User's Guide to LACM 2.0 Computer Program

4. GRAPHICS USAGE

(U) Computer generated graphics are highly device dependent, so the basic LACM 2.0 Computer model allows the user to supply his own. This topic describes some options that may be available to the user even when he has no plotting devices.

(U)   As can be seen by examining the previous topics and the computer runs presented in Section 4, graphics are very useful in presenting a large amount of data in a meaningful manner. In particular, the contour plots should prove much more useful in practice than the raw data points. For this reason the main routine calls subroutine GRAFIX after it finishes computing a set of points generated for the chosen mode. The HUGHES IBM TSO (time sharing option) on which this program was developed did not have on-line (at the terminal) graphics, so the plot file was generated, stored on disc, and later plotted.

(U)   Several options are possible in the selection of a graphics procedure, and the most general in order of increasing remote-terminal complexity are:
- printer plot/store data
- printer plot/store plot files
- on-screen graphics/hard copy

The first two options are possibilities for terminals that do not provide graphics capability, such as a simple teletype, while the third option would require a much more advanced terminal.

(U)   The printer plot is a useful aid to the analyst because it provides crude on-the-spot graphics capability. The poor resolution limits its utility, as shown by the example in Figure 3-22, since details are easy to overlook or may not appear. However, it is quick and, in the case where the terminal printing speed is not too slow, is of use when other graphics are not readily available. The first option is to use a printer plot, write the output on a file, and either plot by hand or use another plotting program.

(U)   The second option (used at Hughes in developing the program) is to generate a printer plot (if desired) and interactively create the plot file on disc. The Hughes system allows the user to create a plot frame and plot one or more curves. The advantages to this are that he can select "nice" bounds for his plots, input titles, and preview the plots via the printer plot to select the curves he wants plotted. After the program is executed, the plots are routed to an on-line plotter at an output center. Samples of these plots appear in this report. As an example, Figure 3-22 is the printer plot generated before the Mode-1 curve of Figure 3-19 was plotted out.

(U)   The on-screen graphics option is of course the most attractive to an analyst or programmer, but such terminals are still costly and not readily available to many users.

(U)   Due to the widely varying types and capabilities of systems in use in scientific computing, Hughes has chosen to write a routine to suit its own system and let the LACM 2.0 user write his own. However, the user should be reminded that graphics are not essential to the operation of the program and the call to GRAFIX can be deleted while the program is being used, until a suitable graphics package can be obtained or written by the user.

UNCLASSIFIED
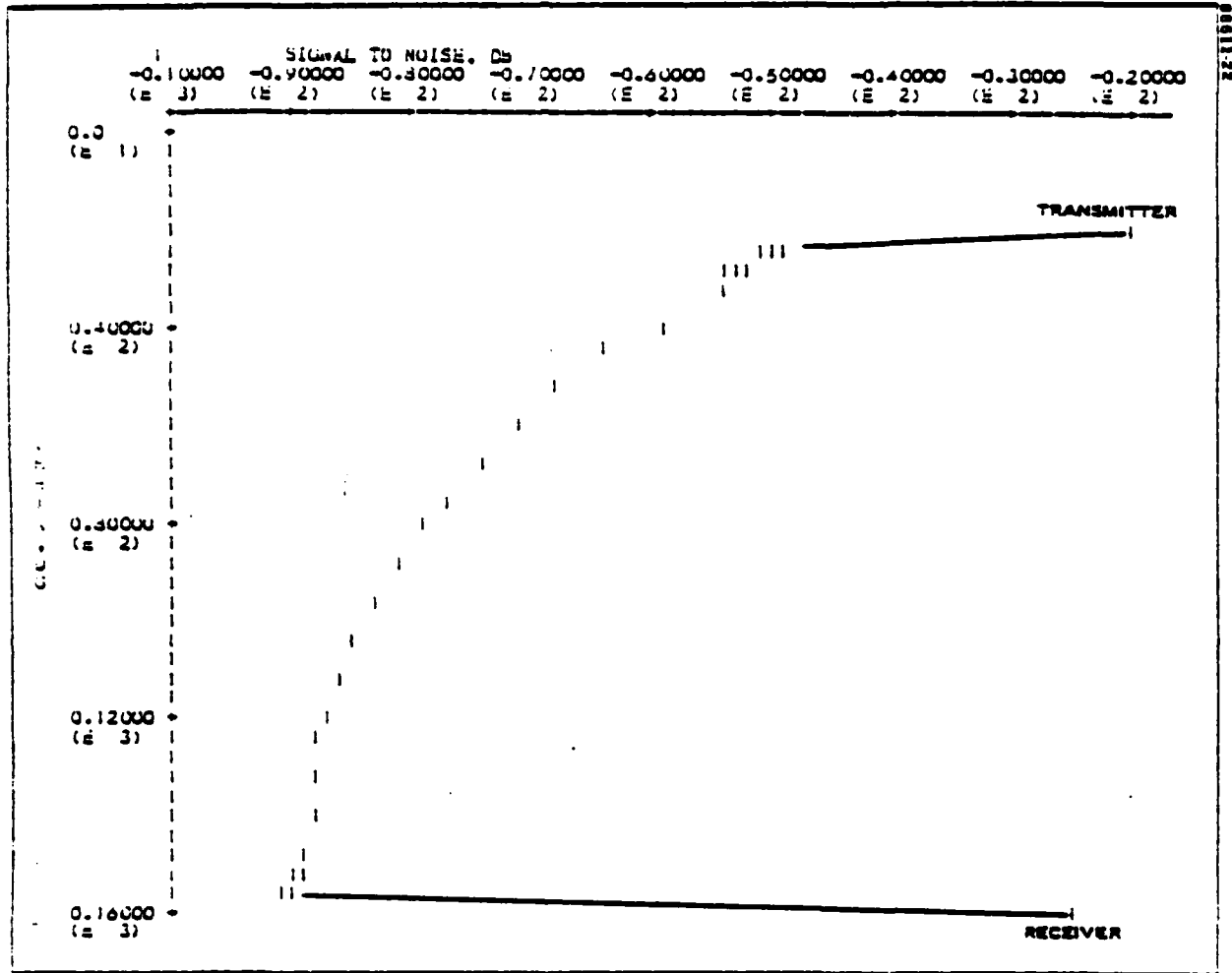
Figure 3-22. Printer Plot Output from Hughes LACM 2.0 Graphics

Section 3 – The Computer Model
Subsection C – User's Guide to LACM 2.0 Computer Program

5. PROGRAM LIMITATIONS

(U) The LACM 2.0 program uses methods, data, and assumptions that impose limitations on its use or the validity of its output. Improper use of the program will be less likely if the limitations are understood by the user.

(U) Due to the complexity of LACM 2.0 it is impossible to foresee every situation that a user will want to analyze, so the limitations will be stated in the most general form possible. Most of the limitations result directly from the models used by the program. It is assumed that a user/analyst will have a good working understanding of the models as described in this report, so that he can properly input data and correctly interpret the result. However, the program structure and operation is simple enough to be run by someone with a cursory knowledge of the models to check the program to see that it executes properly on a given system.

(U) The previous limitations of the LACM 1.0 interceptibility program are largely solved in the present program, as illustrated in Table 3-3. The current limitations are of a more specific nature, as the basic model has proven to perform adequately under pathological testing. (Pathological testing involves running the program with extremes in data, for example, using a link range of one meter.) Table B-2 Appendix B contains comments about the input variables, but the restrictions are of a "common sense" type, such as making the transmitter hood diameter at least as large as the optics it hoods. The limitations described here summarize the limitations of the models, and are presented in Table 3-4. It should be noted that many of these limitations could be overcome to a significant extent by more extensive modeling, as suggested in the summary to this section.

TABLE 3-3. (U) LACM 1.0 INTERCEPTIBILITY RESTRICTIONS (U)

Previous Limitation	Present Improvement
● Flat Earth Model	Curved earth included
● Low Altitude Atmosphere Models	More detailed models for all altitudes
● First Order Beamscatter Function	Expanded, more detailed function based on experiment
● First Order Geometry	Exact analytical forms
● No Error Limits	Determined major sources of uncertainty; provided means of sensitivity analysis
● Requirement for Weather Data Set	Defaulted sets provided
● Untested Model	Point comparison with experiment
● No Provision for Intercept S/N	Added computation to routines

TABLE 3-4. (U) SUMMARY LIMITATIONS AND ASSUMPTIONS OF THE
LACM 2.0 MODEL (U)

Model	Limitation/Assumption
General	• SR orientation $\theta \geq 1^{\circ}$ • SR does not have access to main beam • Operator manipulation is required for scenario interaction other than backstop & atmospheric variations
Transmitter	• Modeled as a point source • Sidelobes are smoothed • Baffle assumed 100% absorptive • Axial scattering symmetry assumed
Link Receiver/Backstop	• Modeled as a point source • Has only one specular component • Backstop always collocated on link axis
Signal-to-Noise Model	• Heterodyne expression yields IF value • Does not account for modulation type
Atmospherics	• Horizontally homogeneous (no local variations) • $F(\theta)$ is fixed • Single scattering only • Atmospheric multipath neglected • Data tables required for optional wavelengths
Background	• Assumes fixed solar geometry independent of SR orientation • Assumes 20 dB cloudy day to sunny day difference
Space-to-Ground Case	• Vertical link assumed • Gaussian profile assumed (no sidelobe structure) • Power calculation only • Approximate method

REFERENCES

3-1 Joseph W. Goodman, Introduction to Fourier Optics, McGraw-Hill, New York, 1968.

3-2 P.R. Gast, "Solar Electromagnetic Radiation", Chapter 16, Handbook of Geophysics and Space Environments, Shea L. Valley, Ed., McGraw-Hill, New York, 1965.

3-3 R.A. McClatchey, R.W. Fenn, J.E.A. Selby, F.E. Volz, and J.S. Garing, "Optical Properties of the Atmosphere (Third Edition)", Air Force Cambridge Research Laboratories (AFGL) Report No. AFCRL-72-0497, 1972 (U).

3-4 John Nella, "Vulnerability Study-Aerosol Scattering Measurements Task", Volume 1, Hughes Aircraft Company Report No. P75-99 (DARPA Order No. 2274) March, 1974 (U).

3-5 L.N. Peckham, "A Simplified Equation for Calculating Far-Field Intensity", Air Force Weapons Laboratory, AFWL-TR-70-146, April, 1971 (U).

3-6 L.N. Peckham and R.W. David, "A Simplified Propagation Model for Laser System Studies", Air Force Weapons Laboratory, Report No. AFWL-TR-72-95 (REV), April, 1973 (U).

APPENDIX B - LACM 2.0 FLOW DIAGRAMS, MODULE DESCRIPTIONS,
AND JCL

The purpose of this appendix is to provide a programmer/analyst a starting point in modifying LACM 2.0. It contains descriptions of the source modules, a detailed listing of the program inputs, and module flow diagrams. The appendix begins with a brief discussion of the Job Control Language (JCL) used at Hughes.

JOB CONTROL LANGUAGE (JCL)

The JCL used at Hughes to run LACM 2.0 consists of TSO (Time Sharing Options) command procedures (CLISTS). The CLISTS used are listed in Figure B-1.

The first CLIST, named GETSET.CLISTS is used prior to running the program. Execution of GETSET allocates the datasets to be used in the program to the appropriate logical units. The user's terminal is represented by dataset (*) and is allocated to logical unit 5. Logical unit 5 is used to read the data, which the user must input from his keyboard (prompt messages are written on unit 6, but the TSO system automatically allocates the terminal to unit 6 so it doesn't appear in GETSET). If an end-of-file marker (/* on IBM system) is encountered on unit 5, the next file on unit 5 will be read from in subsequent read instructions unless no other file numbers have been allocated. For example, the first read will be made on the first file of unit 5, designated FT05F001. The first end-of-file marker read in from the terminal will cause it to branch if an END= (end-of-file mark) is encountered, and it will read next from file 2 of unit 5, FT05F002. However, the terminal is also allocated to this file so the user will not notice any difference; and all he has done is to make the program branch to a preset portion of code up to ten times; the eleventh file is not allocated. This is not a problem in actuality, since this feature is only used to switch prompt mode and should not be needed more than a few times in a session. The last instruction in the CLIST allocates a dataset named PLOT.DATA for plotter output. The raw plot data for the plotter generated in the plotting routines will be written on the dataset to be kept until plotted out using the CLIST named GETPLT.CLIST, also in the figure.

To compile the FORTRAN source and resolve external references, two CLISTs are used. The CLIST named FORTPL.CLIST compiles the graphics routines in data set GRAFIX.FORT and loads the object module into a data set named LINKEM.CLIST. The CLIST named LINKEM.CLIST compiles the rest of the source (located in data set ECK1.FORT), links it with the plotting routines, and resolves external references from the FORTLIB, SCIN.PGMLIB, and SCIN.SCILIB libraries. The load module is placed in data set ECK.LOAD and a message is printed on the terminal telling the user the program may be executed by typing 'CALL ECK(MAIN)'.

The libraries referenced contain the plotting routines and the interpolative routine used in subroutine BACK.

Usually the program is ready to execute, so the user only needs to execute the CLIST GETSET.CLIST and call the program without having to compile and linkedit, unless he has modified the source code. Note that if the user wants to write the

```
GETSET.CLIST
00010 ALLOC FI(FT05F001) DA(*)
00020 ALLOC FI(FT05F002) DA(*)
00030 ALLOC FI(FT05F003) DA(*)
00040 ALLOC FI(FT05F004) DA(*)
00050 ALLOC FI(FT05F005) DA(*)     }  ALLOCATE FIRST 10 FILES OF LOGICAL
00060 ALLOC FI(FT05F006) DA(*)        UNIT 5 TO TERMINAL
00070 ALLOC FI(FT05F007) DA(*)
00080 ALLOC FI(FT05F008) DA(*)
00090 ALLOC FI(FT05F009) DA(*)
00100 ALLOC FI(FT05F010) DA(*)
00110 ALLOC FI(PLOTTER) DA(PLOT.DATA) ─── ALLOCATE THE PLOTTER OUTPUT TO
                                          DATA SET PLOT.DATA

LINKEM.CLIST
00001 FORT ECK1.FORT ─────────────────── COMPILE
00002 DELETE ECK.LOAD ────────────────── DELETE OLD LOAD MODULE TO MAKE ROOM
00030 LINK ((ECK1.OBJ GRAFIX.OBJ(MAIN)) FORTLIB PRINT(*) LIB('SCIN.PGMLIB' 'SCIN.SCILIB')-
00031     LOAD(ECK.LOAD(MAIN)) ───────── CREATE NEW LOAD MODULE
00050 TPRINT 'CALL ECK(MAIN)' ────────── PROMPT MESSAGE TO USER

FORTPL.CLIST
00010 FORT GRAFIX.FORT LOAD(GRAFIX.OBJ(MAIN)) ─── COMPILE GRAFIX

GETPLT.CLIST
00010 PLOTDS PLOT.DATA ORG(RN014) ─────── SEND OUT PLOTS
00020 TPRINT 'PLOT SUBMITTED' ─────────── PROMPT MESSAGE TO USER
```

Figure B-1. TSO Command Procedures Used to Run LACM 2.0 at Hughes. Each procedure is involved by typing "ex name" where name is the procedure to be involved.

output on a unit other than unit 6, he must have allocated the unit prior to running the program, since the program will ask him for the logical unit number.

MODULE DESCRIPTIONS

The module descriptions that follow are not intended to fully describe the entire module in detail. The modules are commented and thus the source code contains a great deal of information, so the material presented here describes the general features of the modules and explains unusual portions of code. Table B-1 presents a summary of the modules, their function in the program, and flow diagrams for the modules appear in the following pages.

MAIN

This is the routine that directs the flow of the program, reading the input, calling the routines to compute the output and generate graphics. The first read statement reads a flag which is 1 for time-sharing. The write statement immediately proceding it prompts the interactive user to start by entering a 1. Note that the interactive input routine TSHARE is called or the program skips to read the inputs in formatted form in the case of batch (background) processing. The rest of the program flow is straight-forward, as illustrated in Figure B-2. Note that a few interactive write/read combinations are in the code but are skipped in the batch mode. In all cases the interactive user is prompted for his input.

BLOCK DATA

The input variables and constants are initialized (defaulted) in this portion of code. Most of the data is for the atmospheric model and consists of scattering and absorption coefficients for the aerosol and molecular atmospheric constituents.

Subroutine TSHARE

This subroutine, shown in Figure B-3, does the bulk of the interactive inputs. It prompts the user for information, taking into account what choices he already has made about his system, scenario, or desired output. Two characteristics make this routine a bit unusual: they are the availability of two levels of prompting, and the capability to input one or more variables after a run for the next run without going through the entire list.

The prompt level is controlled by a logical flag PROMPT which is true for full prompt and false for partial prompt. The full prompt message prints out the input code (if it exists for the input), the variable name, description, and default value if there is one. The partial prompt mode only prints the input code and variable name. The prompt flag may be switched by the user by typing in an end of file (/* on IBM). The READ statement has an end-of-file check which branches to statement 650 where the prompt switch is negated (PROMPT = .NOT.PROMPT), the file is incremented, and the program resumes at the input code it was at when the end of file was encountered. Two methods are available in the program to accomplish this; the choice of methods is dependent on the installation the user has (See the JCL notes in this appendix). If the user can use a logical unit with several files, as is done at Hughes, the first file will be on logical unit 5 (variable LUNIT) and is denoted FT05F001. When an end-of-file on the terminal is encountered the system automatically will read off of FT05F002 in subsequent read instructions. Thus FT05F001, FT05F002, etc. are

TABLE B-1 LACM 2.0 MODULE NAMES AND FUNCTIONAL DESCRIPTIONS

Module	Function
MAIN	Controls program flow; writes output
BLOCK DATA	Initialization of default data values
TSHARE	Interactive inputs
SETUP	Sets up mode geometry
MODE5	Calculates total power at a point
COMTOT	Computes power or SNR for a single SR orientation
BEAM	Computes atmospheric scatter into SR FOV
TRANS	Computes transmission from point to point
FTHETA	Returns value for scattering distribution $F(\theta)$
DELPHI	Returns FOV integration stepsize required to maintain 1% accuracy
ALFAEX	Returns extinction coefficient
ALFAAB	Returns absorption coefficient
ALFASC	Returns scattering coefficient
TSCAT	Computes transmitter scatter power at SR
BSDF	Returns value for BSDF of transmitter
RSCAT	Computes receiver/backstop scatter power at SR
RHOBAK	Computes backstop directional reflectance
RHOOA	Computes receiver optics directional reflectance
BAFRAT	Computes hood effectiveness
STON	Computes SNR
BACK	Computes background power in SR
GRAFIX	Produces graphics (user supplied)
STOG	Computes power for space-to-ground case
STBEAM	Computes space-to-ground link beam radius and on-axis irradiance
SIGMAT	Computes atmospheric turbulence beamspread
QG10	Gaussian quadrature integrator
CNSQ	Returns atmospheric structure constant

B-4
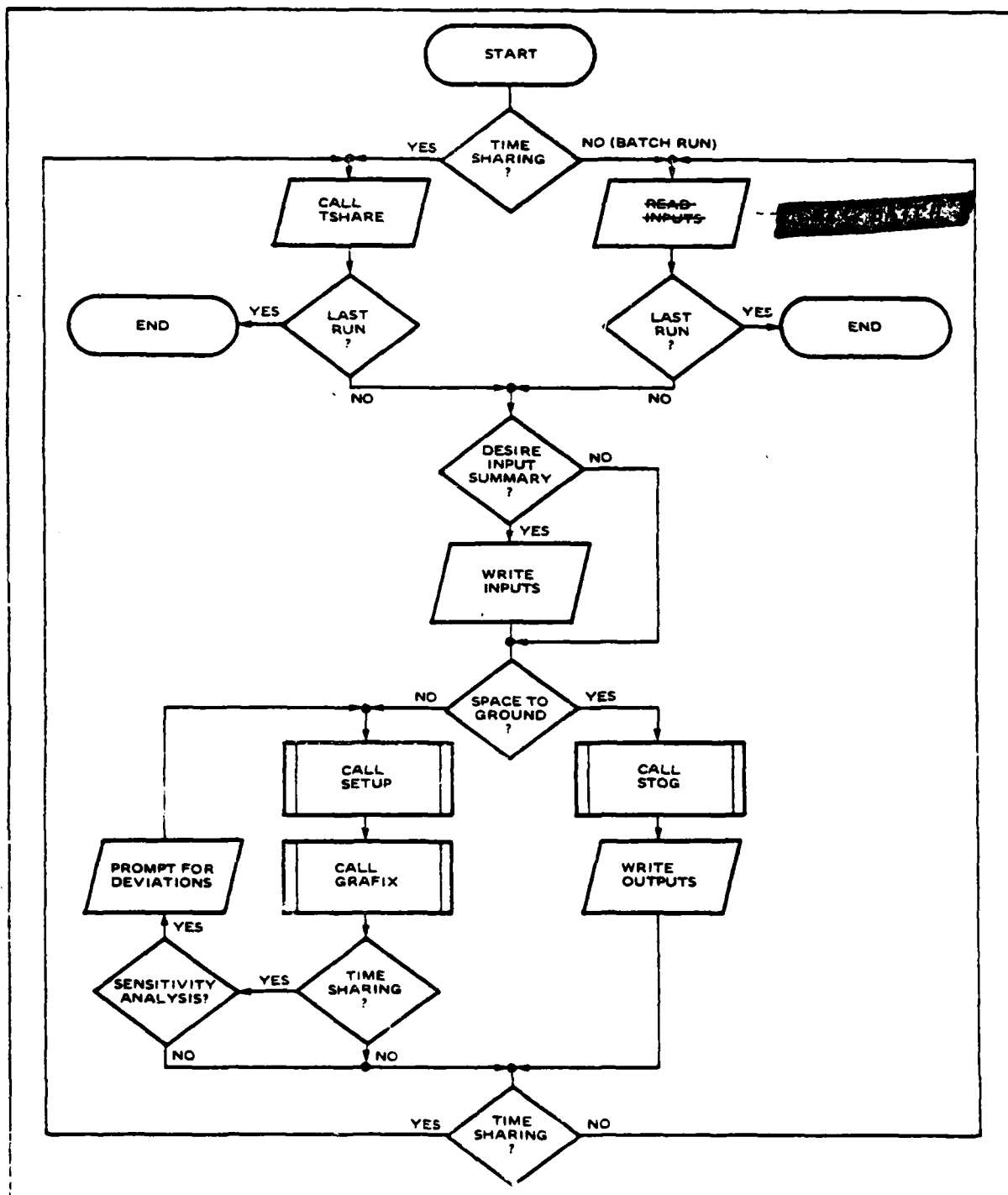
Figure B-2. Flow Diagram for LACM 2.0 MAIN

Figure B-3. Subroutine TSHARE. The major flow is shown, and the input list is described in the text.

allocated to the terminal and the end of file will simply cause branching to statement number 650 to reset the prompt flag. The alternative way is to start reading on unit N and increment the unit. For example, allocate logical unit 20 to the terminal, and an end of file will cause branching to statement number 650 where the logical unit would be incremented (LUNIT = 21). The variable MODESW controls which method is used, and the programmer should default the value in BLOCK DATA to 1 or 2 to select the desired method. Note that the program will assume input is coming from logical unit 5 and unless the proper files are allocated the prompt switching will not work. However, the program will work in the full prompt mode with no special preparation other than the usual allocation of unit 5 to the terminal.

The capability of selecting only those inputs that the user wants changed is accomplished by assigning an input code to each key variable. As shown in Figure B-4, the transmitter hood length has an input code of 20. At the proper time the program will request the input code. In certain cases changing one parameter will affect others. In many of those cases the program will prompt the user for other variables. Referring to the figure, it can be seen that if the hood length is changed on a one-at-a time basis (i.e., the logical variable CHANGE is true) the program will also ask for the hood diameter before returning to ask for the next input code. If no other inputs are to be changed a response of zero will end the input session. Table B-2 lists the variables, their descriptions, input codes, and default values.

Subroutine SETUP

The geometry for each mode is set up and a sequence of data points is computed. A flow chart is shown in Figure B-5. The first computation performed checks to see if the bottom edge of the link beam hits the earth between the transmitter and receiver. If this is the case, a warning is printed. The program flow then goes to a portion of code for the mode selected. Flow charts for each mode are shown in Figures B-6 through B-10.

- In Mode 1 the SR location is fixed so that the SR altitude is computed before entering the loop. The initial SR orientation is set such that the edge of the SR FOV is on the transmitter. The orientation angle THETA is then incremented until the edge of the SR FOV is on the receiver. The transmitter and receiver are treated as point sources, and placing them at the edge of the FOV enables maximum collection of atmospheric scatter at the same time. The power or SNR is returned from subroutine COMTOT and the output table is written on logical unit NOUT if NOUT is greater than zero. The values of power or SNR and THETA are stored in the arrays XINT and YINT and the number of data points computed NP is also kept.

Modes 2 and 3 are functionally very similar to Mode 1 except the SR position is changing, and the position variables X and RPX must be computed for each value of THETA. The SR altitude HS must also be recomputed at each location. Note that the smallest orientation angle THETA allowed is one degree. The call to subroutine COMTOT and output table WRITE statement are done in the same way as in Mode 1.

Modes 4 and 5 iterate to find contours about the link. The root finder in the program uses a secant method of approximation. A simple expression supplies the

```
C
C       TRANSMITTER HOOD LENGTH, BLT
        NIM=20
520     IF (.NOT.PROMPT) WRITE (6,1100) NIM  ———— PARTIAL PROMPT MESSAGE
        IF (PROMPT) WRITE (6,1770) NIM,BLT   ———— FULL PROMPT MESSAGE
        READ (LUNIT,*,END=650) BLT           ———— READ IN VALUE FOR HOOD LENGTH
C
C       TRANSMITTER HOOD DIAMETER, BDRT
530     NIM=42
C       SET DEFAULT VALUE = TO OPTICS DIAMETER
        BDRT=DT
        IF (BLT.EQ.0.) GO TO 540
        IF (.NOT.PROMPT) WRITE (6,1110) NIM
        IF (PROMPT) WRITE (6,1780) NIM,BDRT
        READ (LUNIT,*,END=650) BDRT
        IF (CHANGE) GO TO 670
C
```

Figure B-4. Sample Input Code From Subroutine TSHARE, Illustrating the Input Scheme Discussed in Text.

TABLE B-2.

Variable	Description	Units	Defaults	Input Code	Comments
ALAMDA	Optional Wavelength	Mete s	-	1	Required when LAM = 6
ALFAB	Absorption Coefficient	1/Meter	5.E-5	28	For user input atmospherics, note units
ALFSCT	Scattering Coefficient	1/Meter	5.E-3	28	For user input atmospherics, note units
A.3R	SR Aperture Area	Meter^2	.05	12	Note units
BDFF	Backstop Diffuse Reflectance	-	.3	32	$0 \leq BDFF < 1$
BDLR	Diameter of Receiver Hood	Meters	DR	43	BDLR > DR
BDRT	Diameter of Transmitter Hood	Meters	DT	42	BDRT ≥ DT
BFWHMS	FWHM of Backstop Specular	Degrees	3°	32	
BLR	Receiver Hood Length	Meters	0.	21	
BLT	Transmitter Hood Length	Meters	0.	20	
BMAXS	Backstop Specular Peak	-	0.	32	0. for no specular component
BW	Link Information Bandwidth	Hz	1.E6	7	
BWR	SR Electrical Bandwidth	Hz	1.E6	18	
BWOPT	SR Optical Bandpass	Micrometers	.05	29	Note units are micrometers
DCOMP	Value of Contour (Array)	S/N dB/TWR, dBW	0/-80.	27	Modes 4 and 5 only
DEVAB	Fractional Absorption Deviation	-	+.1	-	Use negative value
DEVSC	Fractional Scattering Deviation	-	+.1	-	# to reduce scattering
DEVBR	Fractional BSDF Deviation	-	+.1	-	
DIFFOA	Diffuse Receiver Optics Reflectance	-	0	33	DIFFOA < 1
DR	Receiver Optics Diameter	Meters	.1	4	
DT	Transmitter Optics Diameter	Meters	.1	2	
EM	L.O. Mixing Efficiency	-	.7	15	Heterodyne detection
ETA	Quantum Efficiency	-	.7	16	0 < ETA < 1
F	Excess Noise Factor	-	1	17	Unity for no excess noise from gain
GAMINT	Intercept Plane Orientation	Degrees	0.	3	0 = horizontal; 90° vertical
GAMPL(3)	Amplitude of BSDF Glitches	-	0.	31	Only for 0 < NG ≤ 3 (see BSDF documentation)
GEND(3)	Ending Point of BSDF Glitches	Degrees	0.	31	Only for 0 < NG ≤ 3 (see BSDF documentation)
GSTART(3)	Beginning Point of BSDF Glitches	Degrees	0.	31	Only for 0 < NG ≤ 3 (see BSDF documentation)
GL	Altitude of Ground Level	Meters	0.	39	Only for 0 < NG ≤ 3 (see BSDF documentation)

TABLE B-2. (cont)

Variable	Description	Units	Defaults	Input Code, Comments
HR	Link RCVR Altitude	Meters	10.	10
HS	SR Altitude	Meters	10.	22 In narrowbeam analysis GAMINT,X,RPX define HS
HT	Transmitter Altitude	Meters	10.	9
IA	Atmospherics Flag	-	2	28 1 - User's Data 2 - AFGL Data
IBFLAG	Beam Computation Flag	-	2	46 1 - Calculate link beam parameters / 2 - Input beam parameters
IBSDF	BSDF Flag	-	1	31 1 - Default 2 - user BSDF
IER	Sensitivity Analysis Flag	-	0	
IERAB	Sensitivity Analysis Flag	-	0	0 - skip sensitivity analysis
IERBR	Sensitivity Analysis Flag	-	0	1 - do sensitivity analysis
IERSC	Sensitivity Analysis Flag	-	0	
IHET	Detection Type Flag	-	1	45 1 - Direct 2 - Heterodyne (only for λ > 2N)
INPSUM	Input Summary Flag	-	1	- 0 - No 1 - Yes
IOTYPE	I/O Flag	-	1	- 0 - Batch, 1 - Interactive
IRTYPE	SR Parameters Flag	-	1	13 1 - Default 2 - User input SR parameters
ISTOG	Space to Ground Flag	-	0	34 0 - Narrowbeam 1 - Space to ground
IW	Turbulence Flag	-	2	48 1 - Mild 2 - Moderate 3 - Severe
LAM	Wavelength Index	-	4	1 1 - .5145, 2 - .6328, 3 - .85, 4 - 1.06, 5 - 10.591 6 - Other
MAT	Atmosphere Model	-	2	28 1 - Tropical 2 - Midlatitude Summer 3 - Midlatitude Winter 4 - Subarctic summer 5 - Subarctic winter
MCOMP	Output Type	-	1	25 1 - Power, DBW 2 - S/N, DB
MODE	Geometry Flag	-	4	26 See documentation of modes
MP	Scatter Sources Included	-	1	5 1 - All, 2 - Atmosphere, 3 - XMTR, 4 - RCVR
MVIS	Visibility Flag	-	1	28 1 - Clear, 2 - Hazy
NATFIL	Logical Unit for AFGL Data	-	-	28 Must be allocated prior to execution
NBAK	Backdrop Model Flag	-	1	32 1 - Default, 2 - User, 3 - Lambertian
NFLG	Background Flag	-	1	30 1 - Sunny, 2 - Cloudy, 3 - Night time
NG	Number of Glitches	-	0	31 BSDF Glitches 0 - 3

TABLE B-2. (cont)

Variable	Description	Units	Defaults	Input Code	Comments
NIM	Input Code	-	0	-	Used in Input scheme
NOA	RCVR Scatter Flag	-	1	33	1 - Default 2 - User Input
NSTOP	End of Run Flag	-	1	-	1 - Continue 2 - End Run
OAFWHM	FWHM of RCVR Specular	Degrees	$3°$	33	
OASMAX	Maximum of RCVR Specular	-	0.	33	
PHI	SR FOV in Intercept Plane	Radians	.001	11	
PHIAZ	SR FOV Out of Plane	Radians	.001	40	
PHIT	Transmitter Beamwidth	Radians	.0001	3	
PSIAZ	Backstop Azimuth Tilt	Degrees	0	44	Normal to link beam at $0°$
PSIEL	Backstop Elevation Tilt	Degrees	0	44	Normal to link beam at $0°$
PT	Link Transmit Power	Watts	1.0	6	
RB	Beam Radius at Ground	Meters	100	37	Space to ground only
RL	Link Range	Meters	5000.	8	
RPX	SR Position Coordinate	Meters	2500.	23	See documentation of modes
SBSDF	BSDF Slope	-	-2.5	31	See BSDF documentation
BGJ	Jitter Beamspread Term	Radians	5.E-6	47	Space to Ground Only
THETA	SR Elevation Angle	Degrees	-	36	Space to ground case
X	SR Off Axis Distance	Meters	1000.	24	See documentation of modes
XM	Modulation Depth	-	1.0	14	
YBSDF	1° Intercept of BSDF	-	200.	31	See BSDF documentation
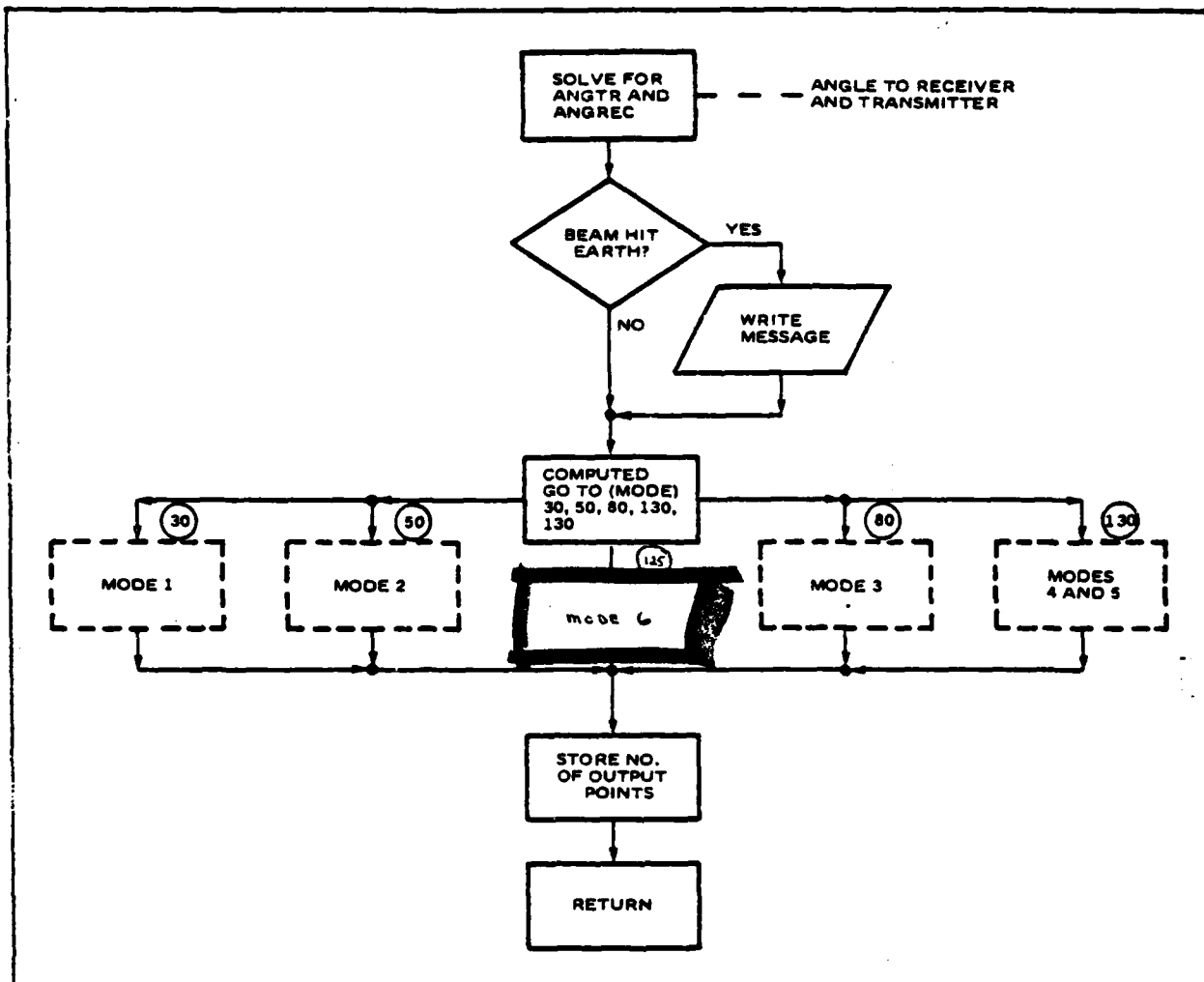
Figure B-5. Subroutine SETUP. This routine generates the sequence of geometry for the five modes.
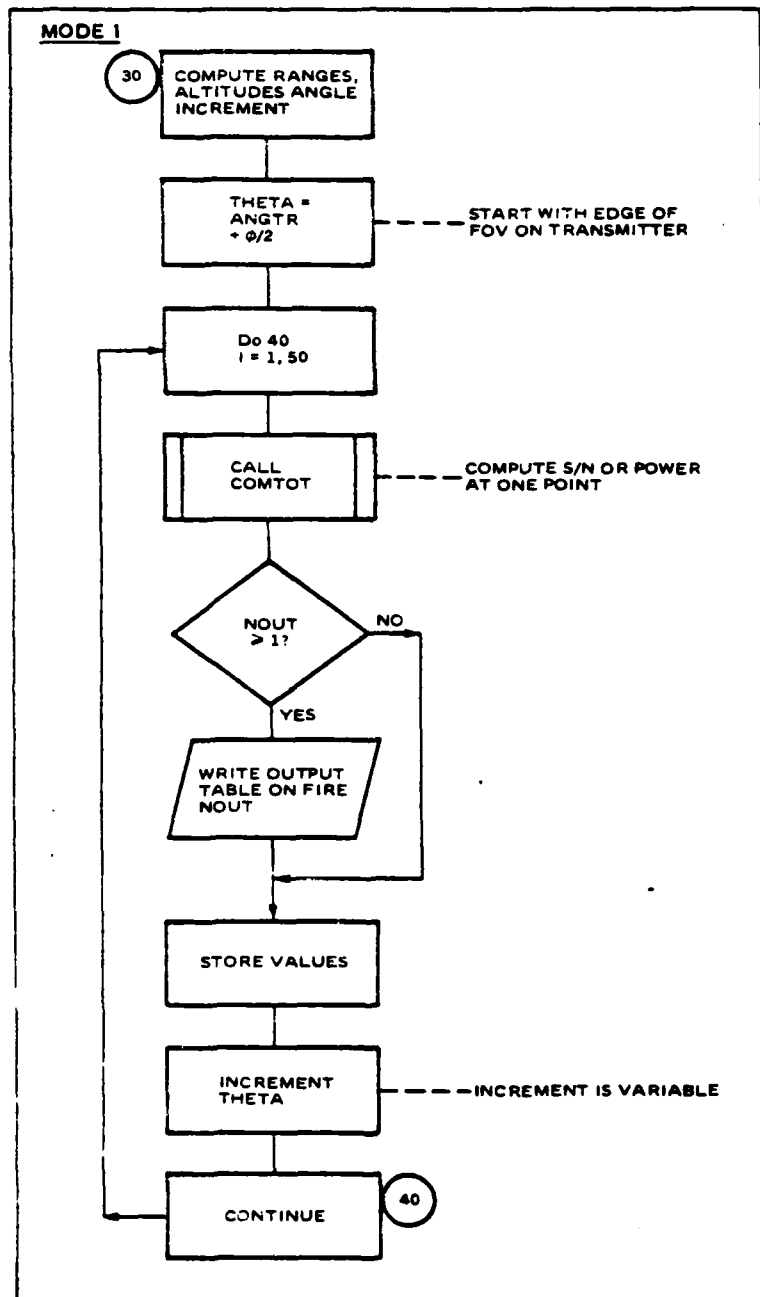
Figure B-6. Detail of Mode 1. Mode 1 scans the link from a fixed SR position.
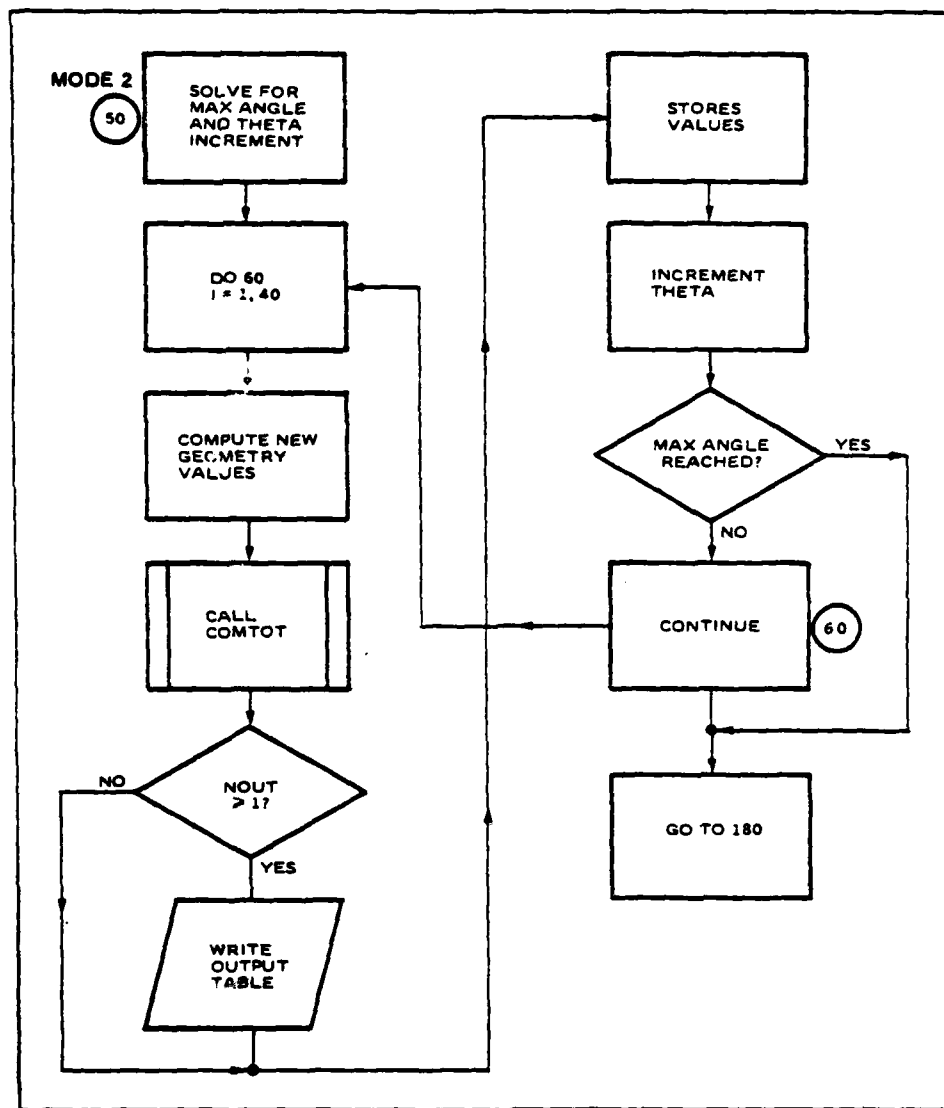
Figure B-7. Mode 2 Flow Detail. Mode 2 looks at a point from different angles from a fixed range.
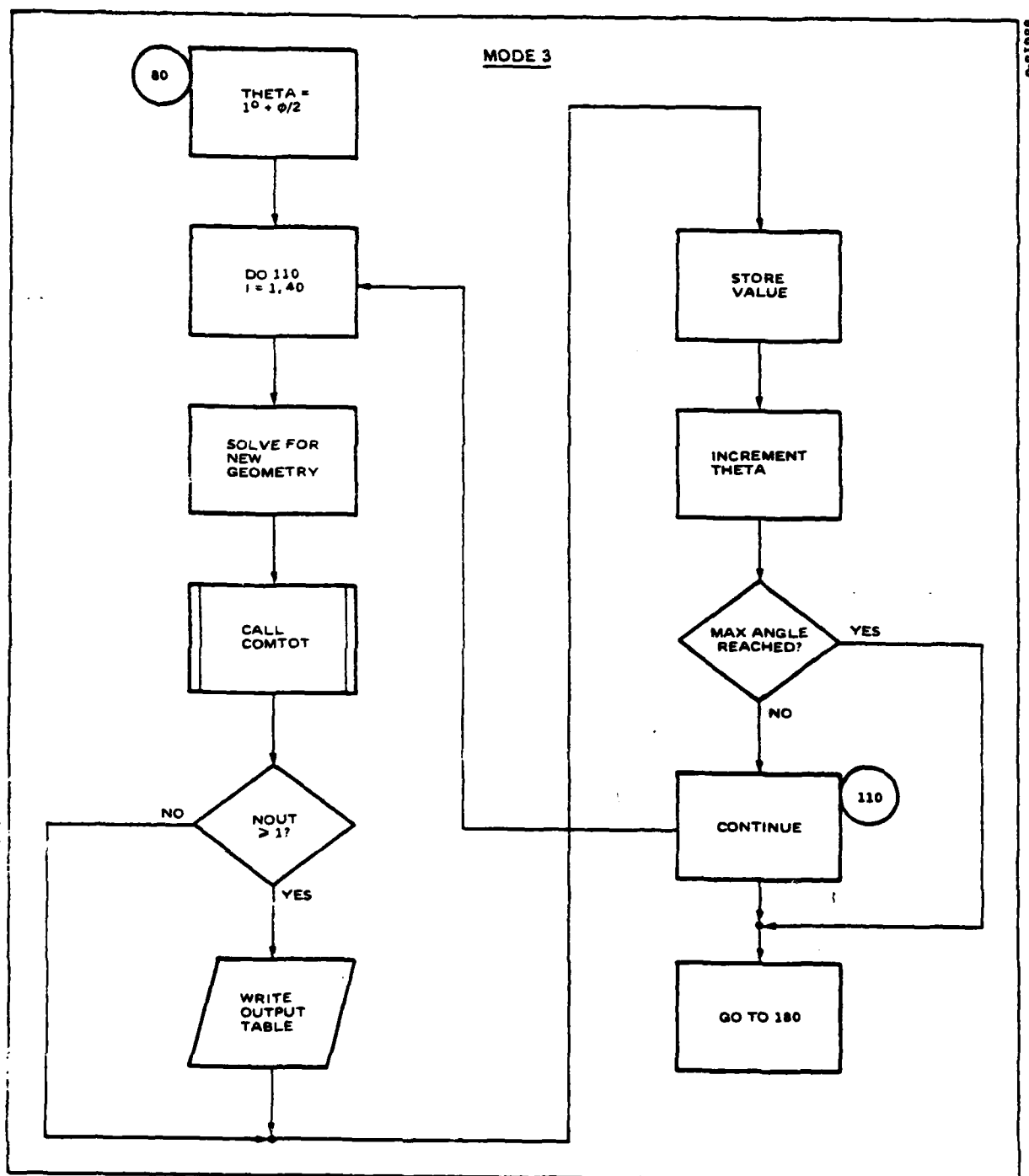
Figure B-8. Mode 3 Flow Detail. Mode 3 views the link from a fixed off-axis distance.
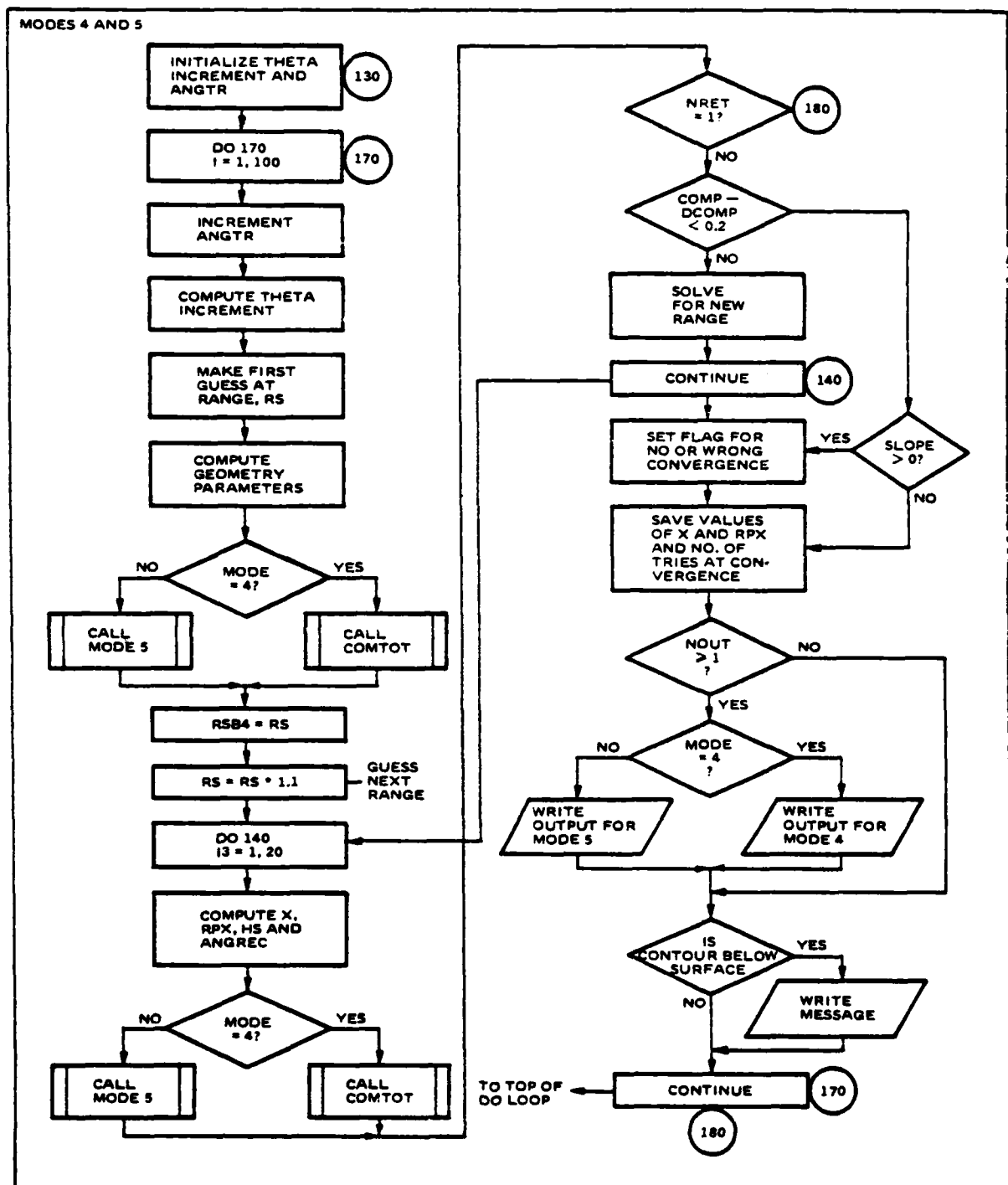
Figure B-9. Mode 4 and 5 Flow. These modes generate contours.

A

CALL
ERROR

COMBINATION
OF SHOT AND
THERMAL NOISE ?

Y

PRINT:
"BOUNDS NOT
ABSOLUTE"

N

PRINT $Pr(e)$
BOUNDS

SUBROUTINE MODE 5

COMPUTE
TOTAL ANGLE
SUBTENDED
BY LINK

COMPUTE NO.
OF STEPS IN
INTEGRATION
(NTHETA)

DO 10
N = 1, THETA

CALL
COMTOT

SUM
ATMOSPHERIC
POWER
CONTRIBUTION

INCREMENT
THETA

CONTINUE (10)

CALL
COMTOT   — OBTAIN
                  TRANSMITTER
                  CONTRIBUTION
                  ONLY

ADD
TRANSMITTER
CONTRIBUTION
TO SUM

CALL
COMTOT   — RECEIVER
                  CONTRIBUTION
                  ONLY

ADD
RECEIVER
CONTRIBUTION
TO SUM

CONVERT
TO dB

RETURN

Figure B-10. Subroutine MODE 5. This routine calculates the total power at a point off-axis.

initial guess of the root. Based on this guess, it will attempt to make better and better approximations of the root by the following formula:

$$RS_{i+1} = RS_i \ f(RS_i) \left[\frac{RS_i - RS_{i-1}}{f(RS_i) - f(RS_{i-1})} \right]$$

where RS = radial distance to transmitter

f(RS) = POWER or S/N at RS

       Iteration along radials from the transmitter was selected because other coordinates may have severe discontinuities and convergence may be impossible to attain. In Mode 4 f(RS) is provided by a call to COMTOT which provides power or S/N from the transmitter and the portion of the beam in the SR FOV, while for Mode 5 the subroutine MODE5 is called, which returns power from the entire link. In the case a guess for RS is negative, the previous guess for RS is divided in half and used instead. (Many contours are very rapidly varying functions of RS. To allow easier convergence the values are in dBW for power, dB for SNR, which vary less rapidly since they are in log space.) If convergence is not attained in 20 tries, the program goes to the next point, and will print a message warning the user of the number of points that did not converge. A sample output in Section 3 illustrates this. (Figure 3-20).

Subroutine COMTOT

       This routine, shown in Figure B-11, calls the routines that calculate the power at the SR from the transmitter, receiver, or atmosphere. It decides to call the routines based on the flag MP which is 1 for all sources of scatter to be included, 2 for atmospheric scatter only, 3 for transmitter scatter only, and 4 for receiver/backstop scatter only. In addition it calls STON to compute signal-to-noise ratio if MCOMP has been set to a value other than 1.

Subroutine BEAM

       The power scattered off the atmosphere to the SR is calculated in this routine as shown in Figure B-12. If the SR FOV is large enough, it is broken up into a number of smaller segments and these are treated separately. The transmittance from transmitter to SR is computed only once if it will not vary more than 2.5% for any of the small elemental fields of view. Subroutine DELPHI computes the number of FOV steps needed to maintain accuracy in $F(\theta)$, as $F(\theta)$ (Atmospheric Scattering Distribution) varies rapidly in places and a large FOV would intercept a range of values that differed by more than 1%.

Subroutine TRANS

       The transmittance from a point at an altitude H1 to a point at an altitude H2 at a range R is computed by this subroutine shown in Figure B-13. Function ALFAEX is used to get the extinction coefficient as a function of path altitude, as the integration
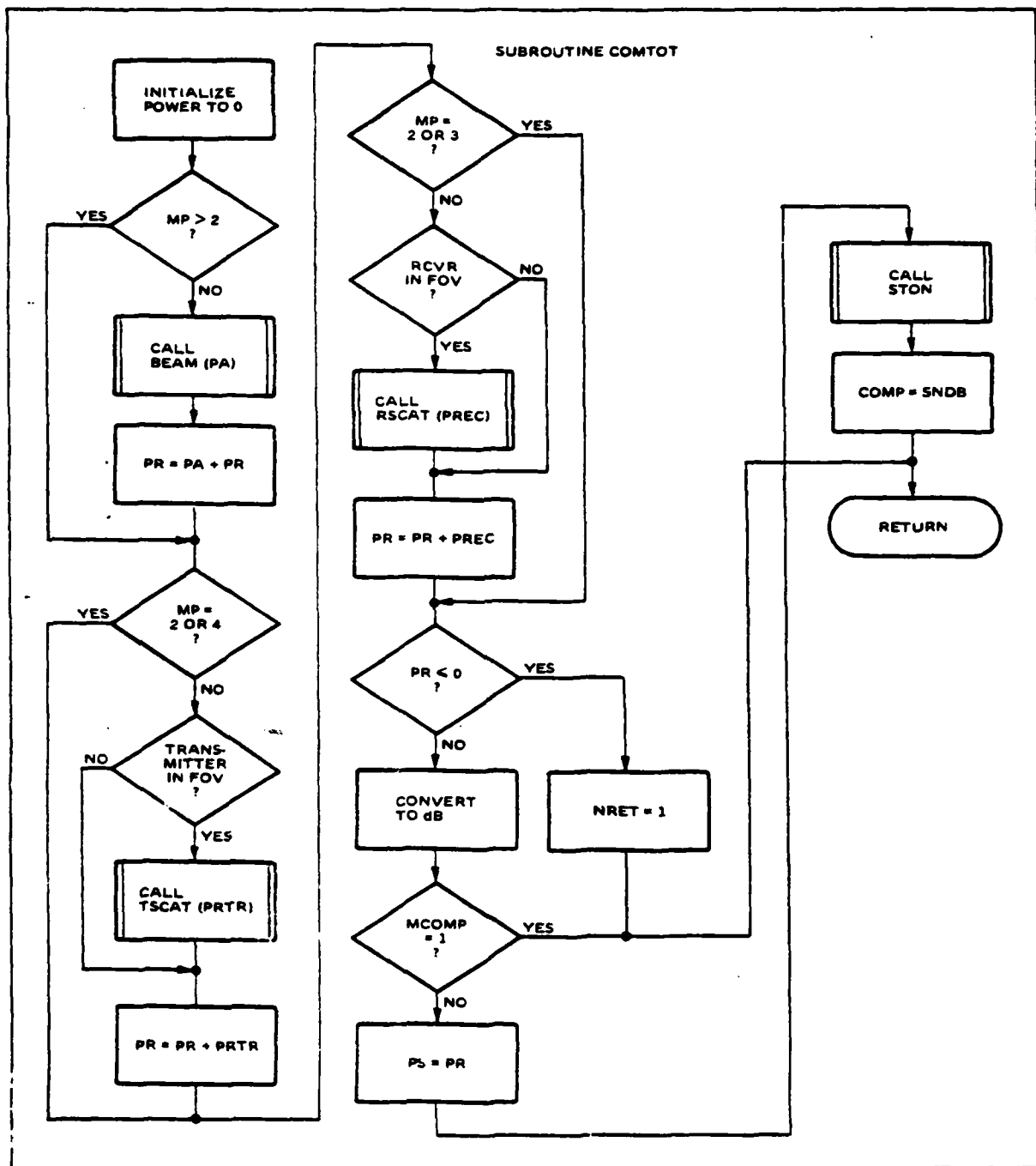
Figure B-11. Subroutine COMTOT. This routine computes power at a point for a fixed SR orientation.
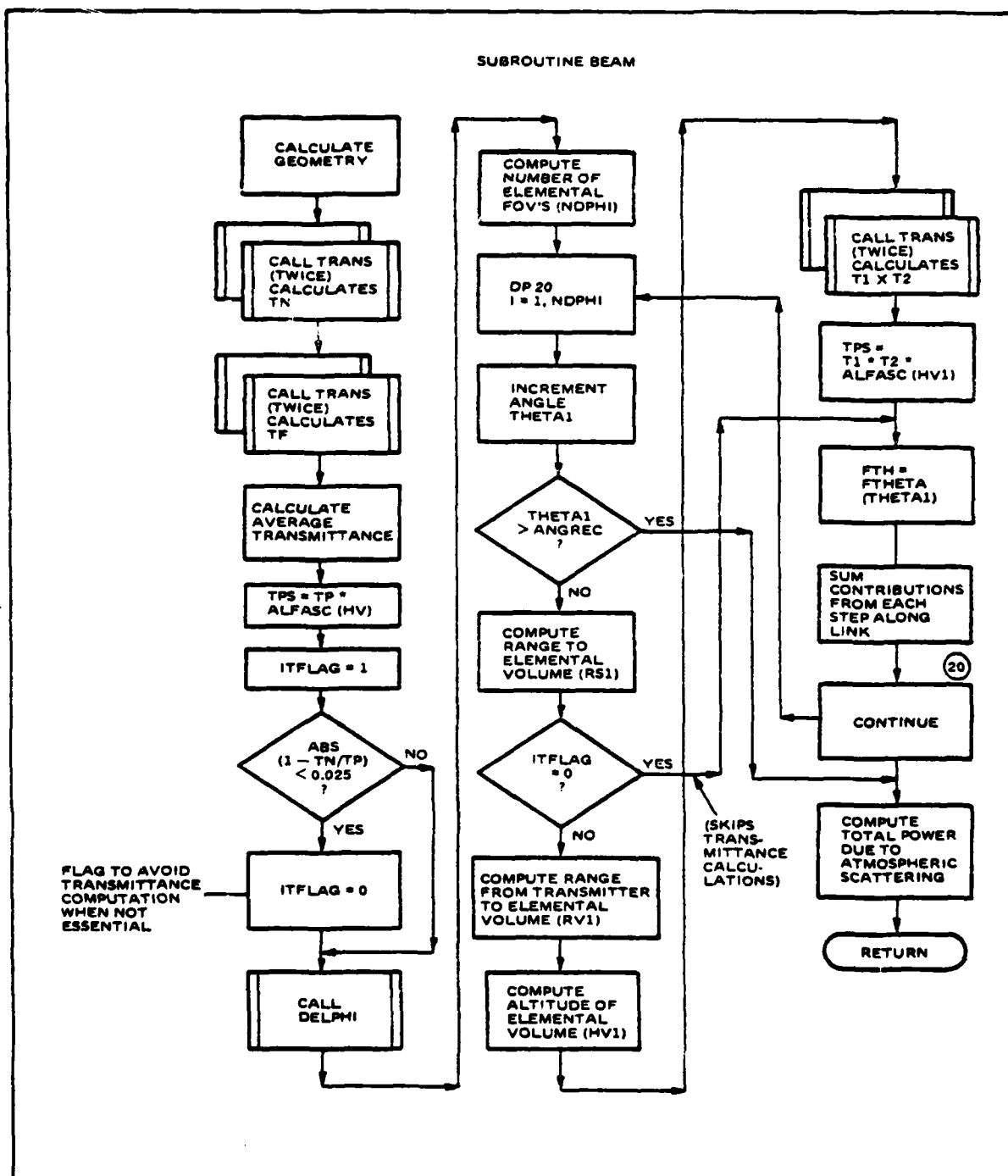
SUBROUTINE BEAM

Figure B-12. Subroutine BEAM. This routine computes scattered power from the beam.

B-20

SUBROUTINE TRANS (H1, H2, R, T)

```
                    ┌─────────────┐
                    │ COMPUTE     │
                    │ NUMBER OF   │
                    │ STEPS (NSTEP)│
                    │ ALONG PATH  │
                    └─────────────┘
```

COMPUTE NUMBER OF STEPS (NSTEP) ALONG PATH

RANGE < 200 OR CO-ALTITUDE ?

YES → TRANSMITTANCE $= e^{-\alpha R}$

NO

COMPUTE LENGTH OF STEP

COMPUTE COSINE OF ZENITH ANGLE

SET UPPER LIMIT ALT = H1

DO 10 K = 1, NSTEP

SET LOWER ALTITUDE LIMIT = TO UPPER ALTITUDE LIMIT

SOLVE FOR UPPER ALT LIMIT

FIND AVERAGE EXTINCTION COEFFICIENT BETWEEN UPPER AND LOWER LIMITS

MULTIPLY EXTINCTION COEFFICIENT BY THE LENGTH OF THE STEP

SUM CONTRIBUTIONS FROM EACH STEP ALONG PATH

CONTINUE (10)

COMPUTE TRANSMITTANCE OF PATH

RETURN

Figure B-13. Subroutine TRANS. This routine computes transmittance from point to point over a curved earth.

is carried out along the propagation path. In the case the range is less than 200 meters or the atmospheric model is only good for co-altitude (i.e., fixed coefficients) the transmission is computed without integration.

Function FTHETA

The atmospheric scattering distribution function $F(\theta)$ is difficult to calculate efficiently, since it involves application of the Mie theory and iterative techniques are usually used. For this reason, two curves were selected to be used in the program and the curve fit expression are used instead. The FTHETA flow chart is shown in Figure B-14. Note that one is used for wavelengths less than 5 μm while the other for wavelengths greater than 5 μm. It should also be noted that the form of these equations is of no physical significance, i.e., they were not derived, but curvefit by trial and error to fit experimental data.

Function DELPHI

This function, shown in Figure B-15, computes the number of elemental SR FOV needed to achieve a set accuracy. An approximate expression for $\partial F(\theta)/\partial \theta$ is used.

Functions ALFAEX, ALFASC, ALFAAB

These functions return the extinction, scattering, and absorption coefficients, respectively, as a function of altitude. ALFAEX does nothing more than add the absorption and scattering coefficients. ALFAAB and ALFASC, shown in Figures B-16 and B-17 respectively, are identical in form and have two modes of operation. The first of these returns a fixed coefficient that has been input by the user. The second uses the tables of AFGL data. The index of the proper coefficient is calculated from the altitude and the coefficient is returned. (Note that the choice of wavelength, climatic model, and visibility have already been made and the arrays AS and AB were loaded from the master array AT with the coefficients for the selected combination of parameters.) In the case an altitude greater than 100 km is specified, the coefficient is zero, and in the case an altitude is negative the coefficient for sea level is returned so that contours may be generated for the case of slant path links where part of the contour is under the earth. A message is printed to inform the user of this occurrence.

Subroutine TSCAT

This routine uses a straightforward application of the models described in Section 2 and 3 to compute power scattered from the transmitter. A flow chart is shown in Figure B-18. Functions BAFRAT and BSDF are used to evaluate the hood effectiveness and help compute the lens scatter. The transmittance from the SR to the transmitter is computed differently for the space to ground case, as only the distance inside the earth's atmosphere will affect the transmittance.
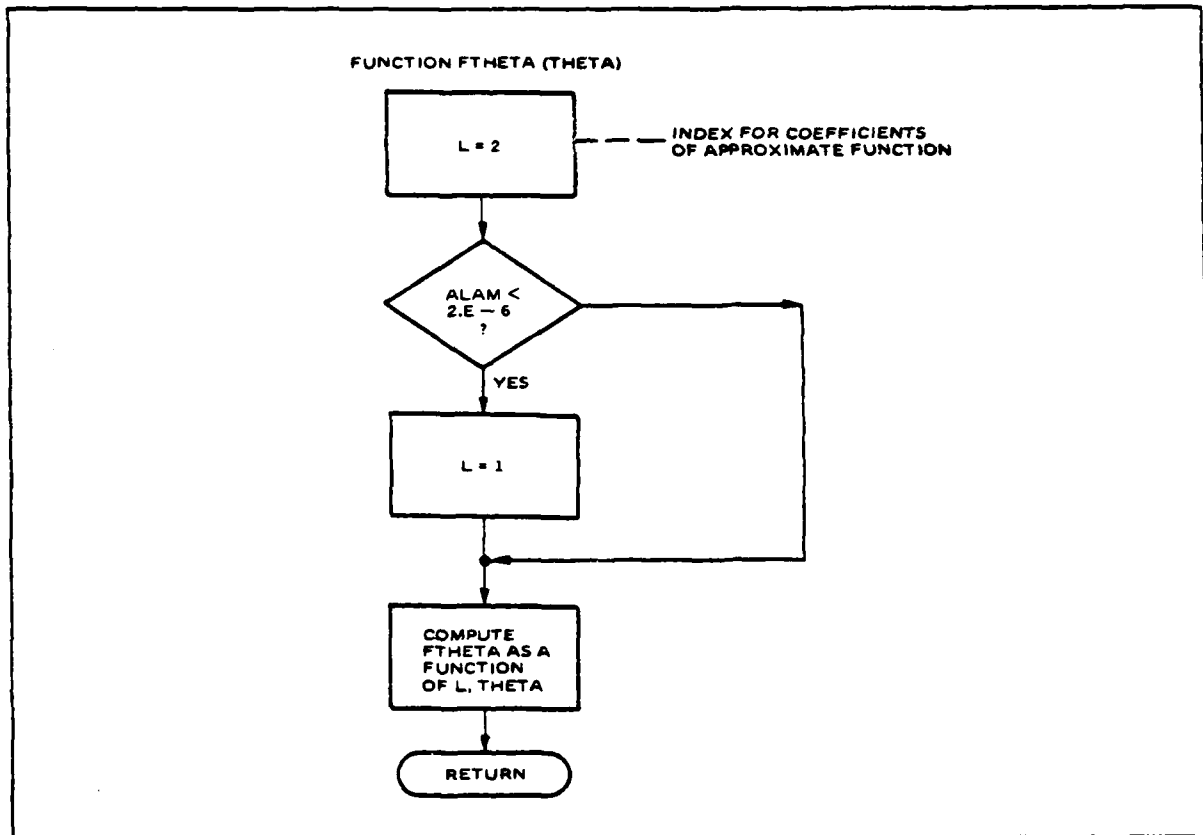
Figure B-14. Function FTHETA This routine computes an approximate atmospheric scattering distribution function. L is a flag delineating wavelength regimes.

FUNCTION DELPHI (THETA, PHI, DPHI)

```
┌──────────────┐
│ DPHIX        │
│ APPROXIMATE  │ ─ ─ ─ ─ STMT FUNCTION ∂F(θ)/∂θ
│ DERIVATIVE   │
│ OF FTHETA    │
└──────────────┘

┌──────────────┐
│ 1%           │
│ ACCURACY     │
└──────────────┘

┌──────────────┐
│ COMPUTE MAX  │
│ AND MIN THETA│
│ IN SR FOV    │
└──────────────┘

┌──────────────┐
│ FIND DPHI    │
│ NEEDED AT    │
│ MAXIMUM      │
│ THETA        │
└──────────────┘

┌──────────────┐
│ FIND DPHI    │
│ NEEDED AT    │
│ MINIMUM      │
│ THETA        │
└──────────────┘

┌──────────────┐
│ LET DPHI =   │
│ MIN OF TWO   │
│ VALUES ABOVE,│
│ PHI AND 1°   │
└──────────────┘

( RETURN )
```
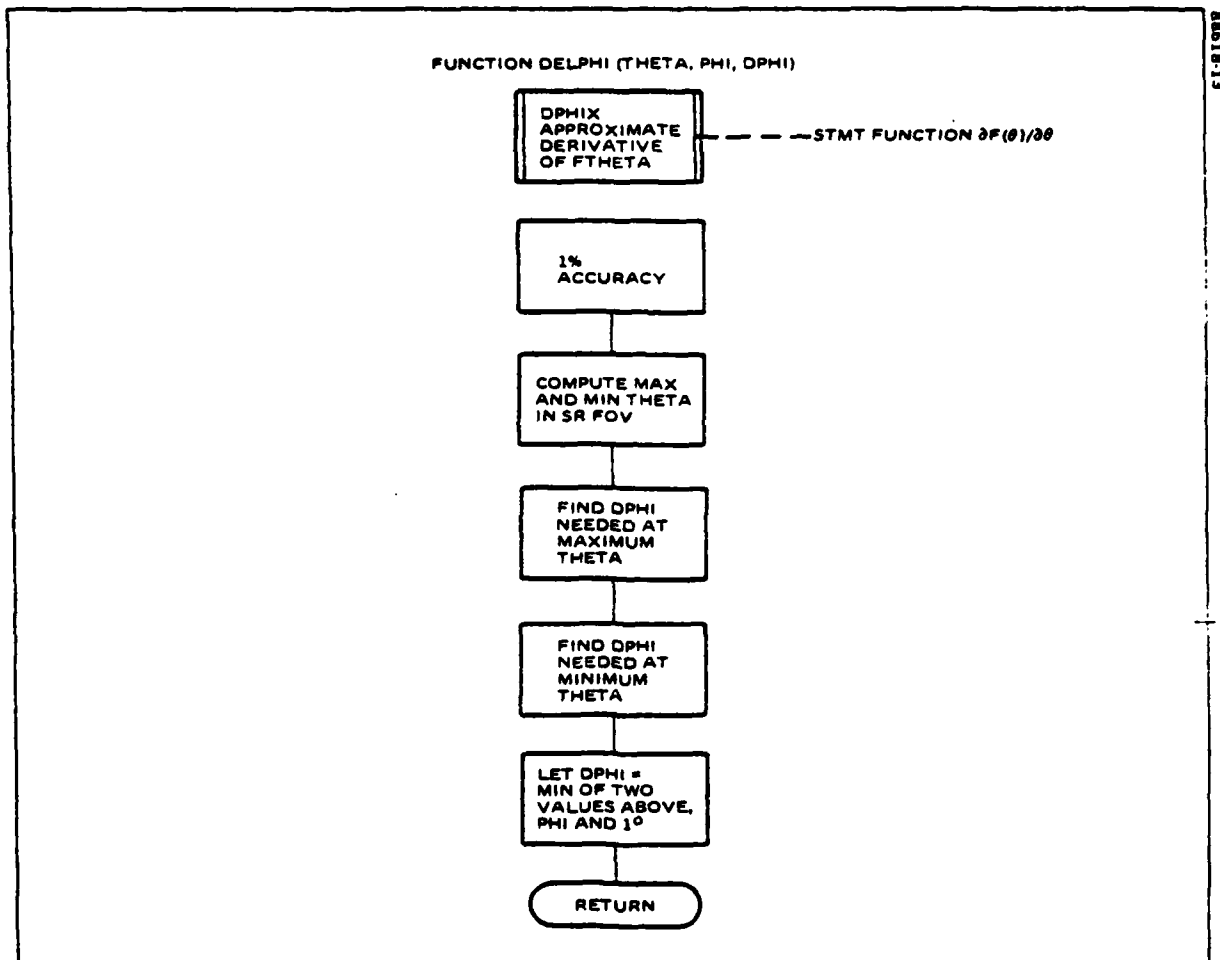
Figure B-15. Function DELPHI. This routine calculates the maximum size of the elemental field of view to maintain 1 percent accuracy.
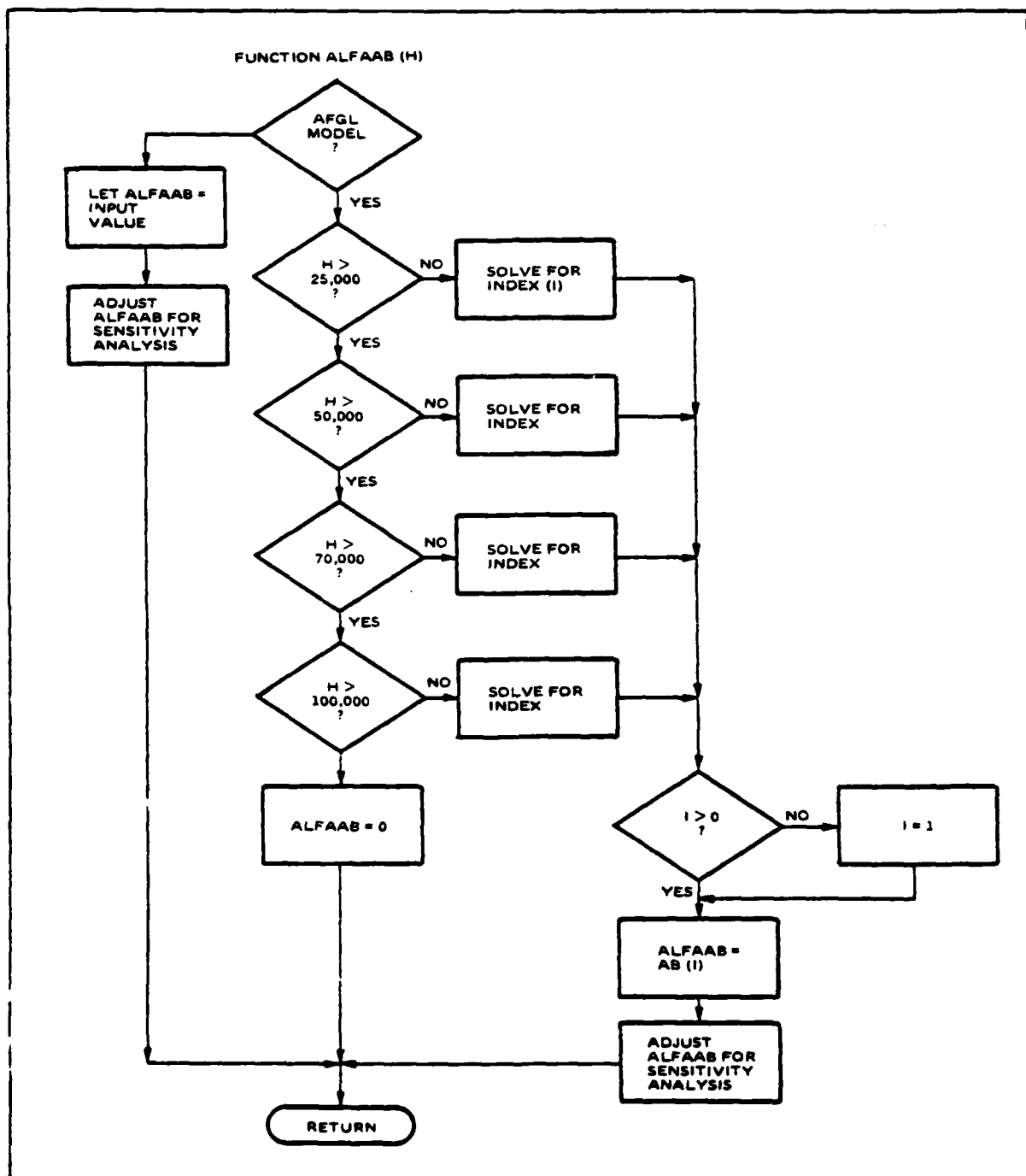
Figure B-16. Function ALFAAB. This function returns the absorption coefficient as a function of altitude using AFGL tables.

FUNCTION ALFASC(H)

```
                          ┌─────────────┐
                          │  AFGL       │
                   NO     │  MODEL      │
        ┌────────────────◄│    ?        │
        │                 └─────────────┘
        │                        │ YES
        ▼                        ▼
  ┌──────────┐            ┌─────────────┐         ┌──────────┐
  │LET ALFASC=│           │   H >       │  ────►  │SOLVE FOR │
  │INPUT     │            │  25,000     │         │INDEX (I) │
  │VALUE     │            │    ?        │         └──────────┘
  └──────────┘            └─────────────┘
        │                        │
        ▼                        ▼
  ┌──────────┐            ┌─────────────┐         ┌──────────┐
  │ADJUST    │            │   H >       │  ────►  │SOLVE FOR │
  │ALFASC FOR│            │  50,000     │         │INDEX     │
  │SENSITIVITY│           │    ?        │         └──────────┘
  │ANALYSIS  │            └─────────────┘
  └──────────┘                   │
        │                        ▼
        │                 ┌─────────────┐         ┌──────────┐
        │                 │   H >       │  ────►  │SOLVE FOR │
        │                 │  70,000     │         │INDEX     │
        │                 │    ?        │         └──────────┘
        │                 └─────────────┘
        │                        │
        │                        ▼
        │                 ┌─────────────┐         ┌──────────┐
        │                 │   H >       │  ────►  │SOLVE FOR │
        │                 │  10,000     │         │INDEX     │
        │                 │    ?        │         └──────────┘
        │                 └─────────────┘
        │                        │
        │                        ▼
        │                 ┌──────────┐      ┌─────────┐  NO  ┌────────┐
        │                 │ ALFASC = 0│      │  I > 0  │ ───► │I = 1 FOR│
        │                 └──────────┘      │    ?    │      │ H = 0  │
        │                        │          └─────────┘      └────────┘
        │                        │               │ YES
        │                        │               ▼
        │                        │          ┌──────────┐
        │                        │          │ ALFASC = │
        │                        │          │  AS (I)  │
        │                        │          └──────────┘
        │                        │               │
        │                        │               ▼
        │                        │          ┌──────────┐
        │                        │          │ADJUST    │
        │                        │          │ALFASC FOR│
        │                        │          │SENSITIVITY│
        │                        │          │ANALYSIS  │
        │                        │          └──────────┘
        └────────────────────────┤               │
                                  ▼◄──────────────┘
                            ╭──────────╮
                            │  RETURN  │
                            ╰──────────╯
```
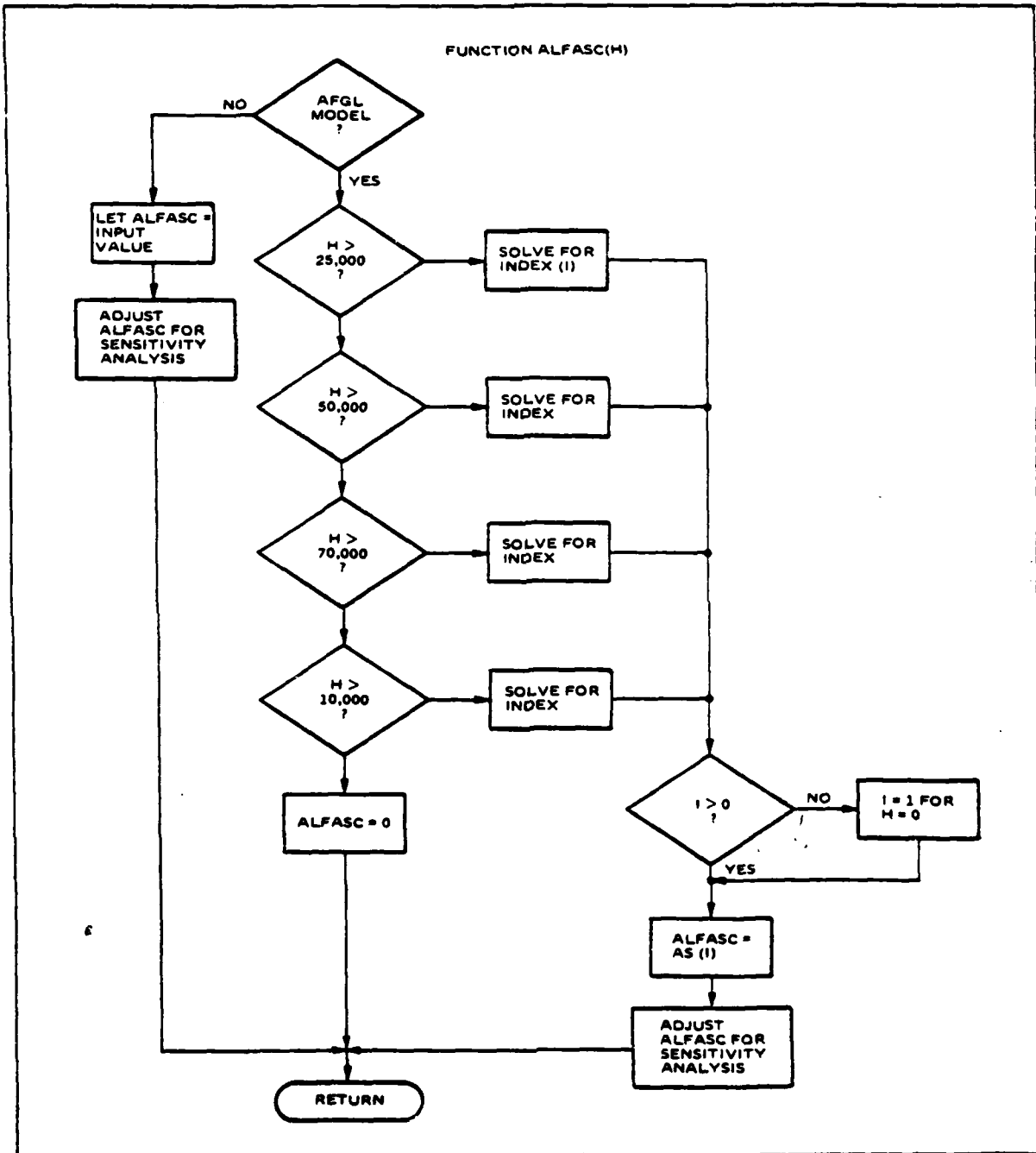
Figure B-17. Function ALFASC. This routine returns the scattering coefficient as a function of altitude.

B-26

SUBROUTINE TSCAT (PRTR)

```
              ┌──────────┐
              │ ANG >    │ ───YES──→  (NO PORT SCATTER)
              │ 1.57?    │
              └──────────┘
                   │
                  NO
                   │
            ┌──────────────┐          CALCULATE
            │   BAFRAT      │ ─ ─ ─ ─  EFFECTIVENESS
            │              │          OF BAFFLE
            └──────────────┘
                   │
            ┌──────────────┐
            │  CALCULATE   │
            │   RANGE      │
            └──────────────┘
                   │
              ┌──────────┐
       YES    │  SPACE   │   NO
     ┌────────│TO GROUND │────────┐
     │        │    ?     │        │
     │        └──────────┘        │
 ┌───────────────┐          ┌───────────────┐
 │  CALCULATE    │          │  CALCULATE    │
 │ TRANSMITTANCE │          │ TRANSMITTANCE │
 │  TO EDGE OF   │          │ TO TRANSMITTER│
 │  ATMOSPHERE   │          │               │
 └───────────────┘          └───────────────┘
     │                          │
     └────────────┬─────────────┘
                  │
          ┌───────────────┐
          │  COMPUTE      │
          │  TOTAL POWER  │
          │  DUE TO WINDOW│
          │  SCATTER      │
          └───────────────┘
                  │
          ┌───────────────┐
          │  COMPUTE      │
          │  POWER FROM   │
          │  SIDELOBES    │
          └───────────────┘
                  │
          ┌───────────────┐
          │  ADD POWER    │
          │  FROM WINDOW  │
          │  SCATTER AND  │
          │  SIDELOBES    │
          └───────────────┘
                  │
                  │
          ┌───────────────┐
          │   RETURN      │
          └───────────────┘
```
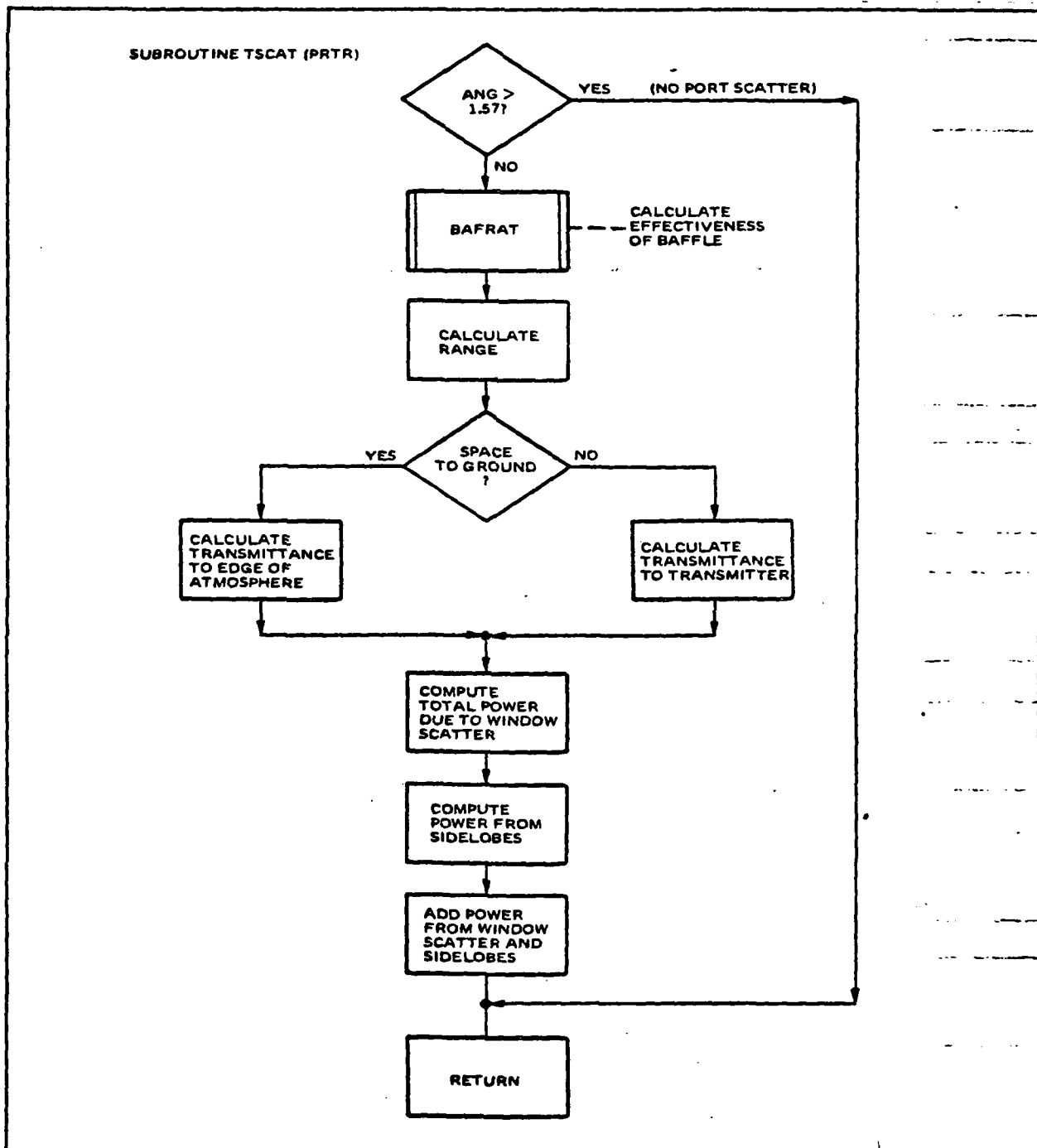
Figure B-18. Subroutine TSCAT. This routine computes total power at SR due to transmitter scatter.

Function BSDF

The bidirectional scattering distribution function (BSDF) is approximated by a straight line in log space and is computed in this function, shown in Figure B-19. After the straight line value is obtained the glitches are added in if applicable.

Subroutine RSCAT

The power reflected from the receiver/backstop is computed in this routine using the equation presented in Section 3. The backstop is assumed to intercept the entire main lobe of the beam. A flow chart is shown in Figure B-20.

Functions RHOBAK and RHOOA

The directional reflectance of the backstop and receiver optics are computed in these routines using the diffuse and specular component models. Flow diagrams appear in Figure B-21 and B-22. The backstop can be oriented in an arbitrary manner and can have a lambertian scattering profile, while the receiver optics are always assumed to be pointing at the link transmitter.

Function BAFRAT

Off-axis lens scatter may be blocked by using a hood. BAFRAT, shown in Figure B-23, calculates the effectiveness of such a hood assuming it is cylindrical and perfectly absorbing. The effectiveness of the baffle is the fraction of the area of the optics that can be seen at a given off-axis angle; so, for example, when this effectiveness is zero the baffle is blocking all transmitter off-axis radiation at that angle.

Subroutines STON and BACK

Subroutine STON, shown in Figure B-24, is a straightforward code of the signal-to-noise expressions discussed in Section 2. The SNR is returned in decibels. The background power PBACK is calculated in subroutine BACK of Figure B-25. Three choices are available, night, cloudy, or sunny. The earth background is computed using a blackbody curve, and the solar background is interpolated from tables. A multiplicative factor of .01 is used to obtain the cloudy day solar background from the sunny day figure. The solar background is broken into two tables of equally spaced points, one in the UV and the other from the visible into the near-IR, and IF statements prevent their use out of the tables' ranges.

Subroutines STOG and STBEAM

The space-to-ground beam power calculation is done in subroutine STOG shown in Figure B-26, by breaking up the vertical beam into many vertical elements. Each vertical element is treated by using the narrowbeam analysis routine BEAM. The vertical elements are arranged in an evenly spaced grid with a row down the SR optical axis and rows to either side. The center row is accounted for first, and the outer rows are done by multiplying the result for one side by two. Each element is checked to see if it is within the azimuth FOV of the SR and within the $1/e^2$ power points of the beam before its power contribution is accounted for, and the power weighting statement function WEIGHT is used to model the gaussian power density profile. Subroutine STBEAM, presented in Figure B-27 is a straightforward application of the equations

FUNCTION BSDF (AN6)

```
          ┌─────────────────┐
          │  STRAIGHT-LINE   │
          │  APPROXIMATION   │
          │  OF BSDF         │
          └─────────────────┘
                   │
                   ▼
              ╱─────────╲
             ╱   NO.     ╲        YES
            ╱    OF       ╲──────────────────────┐
            ╲  GLITCHES   ╱                        │
             ╲   = 0      ╱                        │
              ╲    ?     ╱                         │
               ╲───────╱                          │
                   │ NO                            │
                   ▼                               │
          ┌─────────────────┐                      │
      ┌──▶│  DO 10 I = 1, N6 │                      │
      │   └─────────────────┘                      │
      │            │                               │
      │            ▼                               │
      │       ╱─────────╲                          │
      │      ╱ GETSTART(I)╲        NO               │
      │     ╱   < ANG <    ╲──────────────┐        │
      │     ╲   GEND(I)?    ╱              │        │
      │      ╲─────────────╱               │        │
      │            │ YES                   │        │
      │            ▼                       │        │
      │   ┌─────────────────┐              │        │
      │   │  BSDF = GAMP(I)  │              │        │
      │   └─────────────────┘              │        │
      │            │                       │        │
      │            ◄───────────────────────┘        │
      │            ▼                                │
      │   ┌─────────────────┐   ⎛  ⎞                │
      └───│    CONTINUE      │   ⎝10⎠                │
          └─────────────────┘                      │
                   │                               │
                   ◄───────────────────────────────┘
                   ▼
          ┌─────────────────┐
          │  ADJUST          │
          │  BSDF FOR        │
          │  SENSITIVITY     │
          │  ANALYSIS        │
          └─────────────────┘
                   │
                   ▼
             (  RETURN  )
```
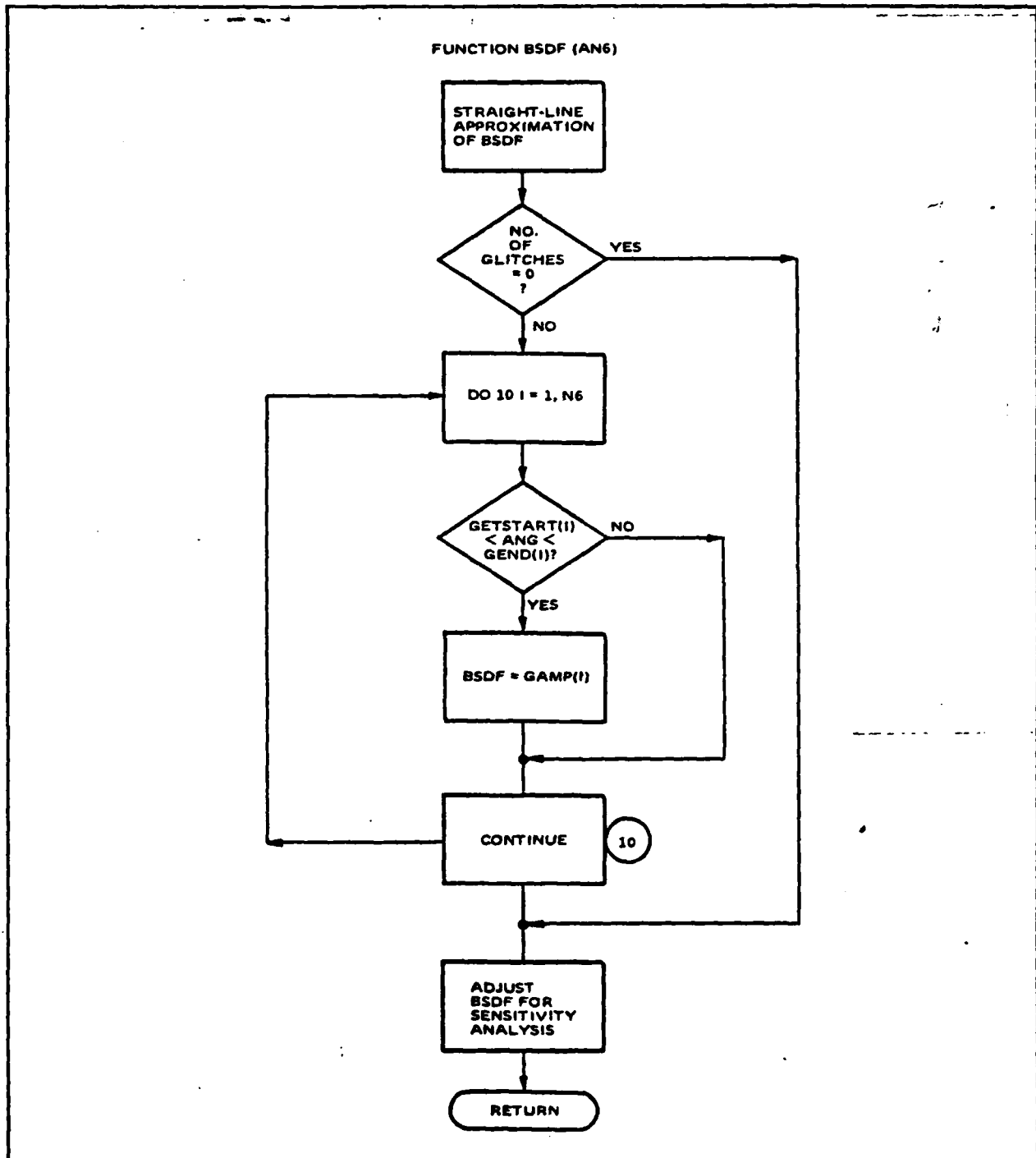
Figure B-19. Function BSDF. This routine returns the bidirectional scattering distribution function for the transmitter optics.
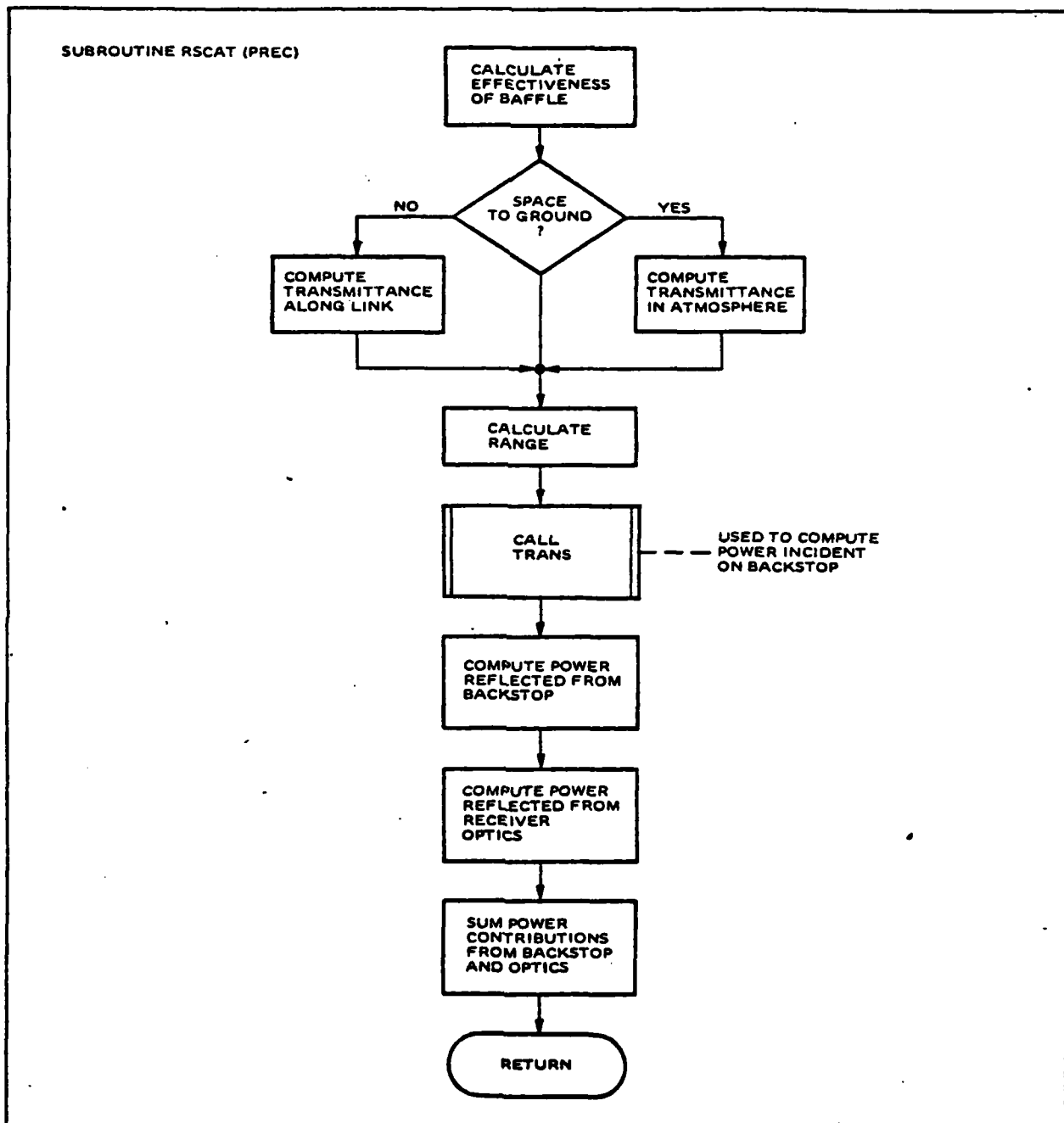
Figure B-20. Subroutine RSCAT. This subroutine returns the power at the SR that is scattered from the receiver and backstop.

FUNCTION RHOBAK (THETAP)

```
        ┌─────────────────┐
        │ COMPUTE         │
        │ BACKSTOP        │
        │ ORIENTATION     │
        │ FACTORS         │
        └─────────────────┘
                │
                ▼
        ┌─────────────────┐
        │ COMPUTE ANGLE   │
        │ BETWEEN BACK-   │
        │ STOP NORMAL     │
        │ AND SR          │
        └─────────────────┘
                │
                ▼
             ╱╲
            ╱  ╲     SR
           ╱    ╲  BEHIND        YES
           ╲    ╱  BACKSTOP ?  ──────┐
            ╲  ╱                     │
             ╲╱                      │
              │ NO                   │
              ▼                      │
        ┌─────────────────┐         │
        │ COMPUTE         │         │
        │ SPECULAR        │         │
        │ COMPONENT       │         │
        │ OF BACKSTOP     │         │
        │ REFLECTANCE     │         │
        └─────────────────┘         │
                │                    │
                ▼                    │
        ┌─────────────────┐         │
        │ COMPUTE         │         │
        │ DIFFUSE LEVEL   │         │
        │ AND ADD TO      │         │
        │ SPECULAR        │         │
        │ COMPONENT       │         │
        └─────────────────┘         │
                │                    │
                ▼                    │
                ●◄──────────────────┘
                │
                ▼
         (   RETURN   )
```
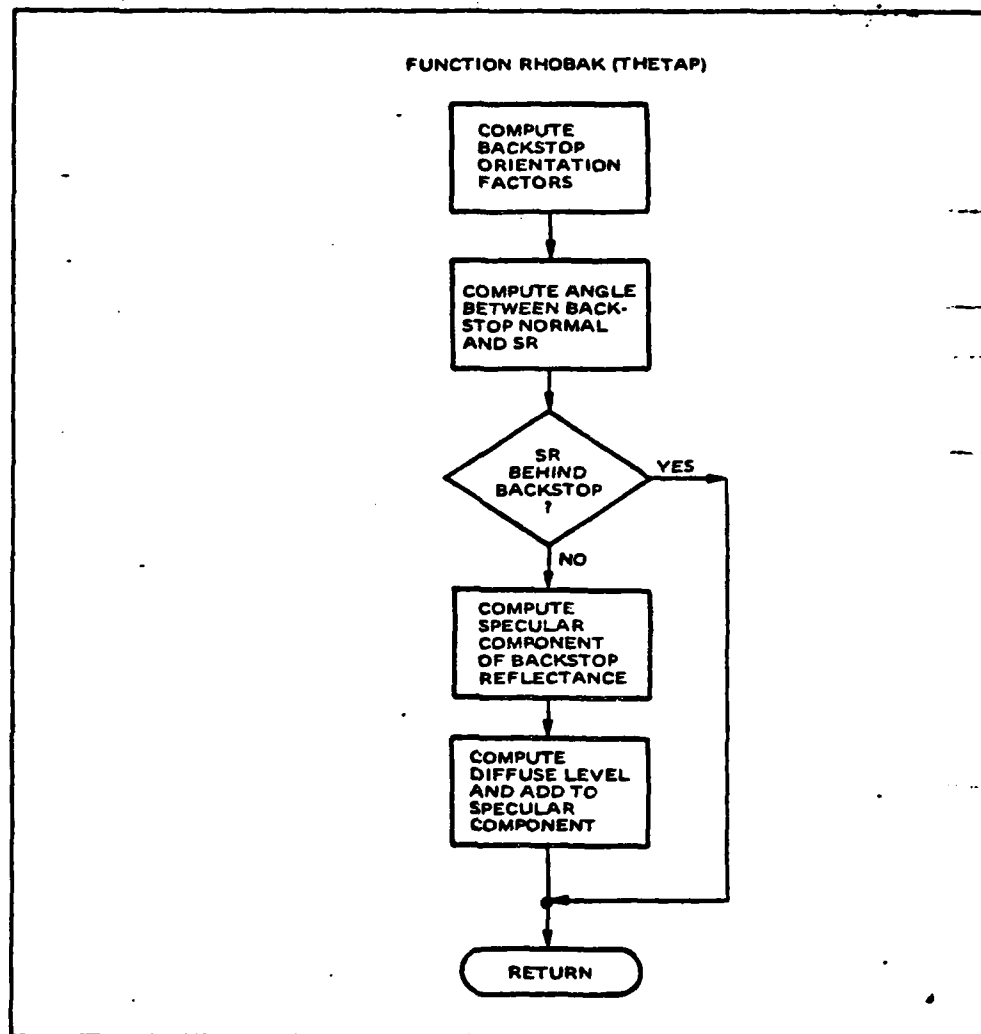
Figure B-21. Function RHOBAK. This function calculates the reflection of the backstop in the direction of the SR.

FUNCTION RHOOA (THETAP)

COMPUTE
SPECULAR
COMPONENT
OF RECEIVER
REFLECTANCE

ADD DIFFUSE
LEVEL TO
SPECULAR
COMPONENT

RETURN
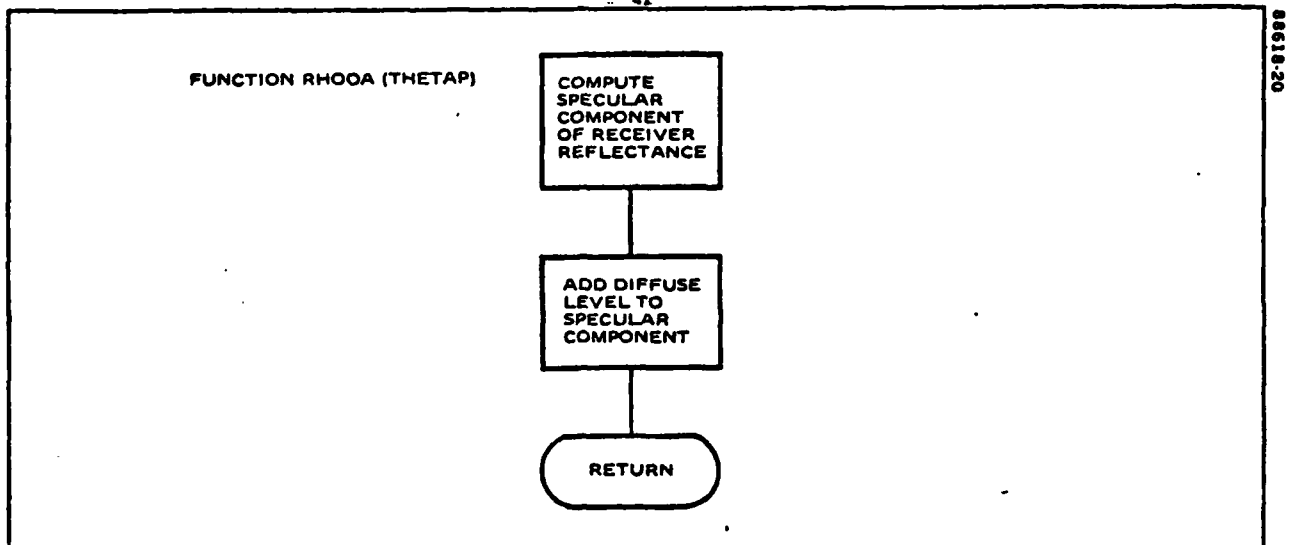
Figure B-22. Function RHOOA. This function calculates the directional reflectance of the receiver optics for a given off-axis angle.

FUNCTION BAFRAT (D1, D2, THETA, BL)

```
                    ┌─────────────┐
                    │   BAFFLE    │  YES
                    │   LENGTH    │────────────────────────────┐
                    │     < 0     │                            │
                    │      ?      │                            │
                    └──────┬──────┘                            │
                           │                                   │
                    ┌──────┴──────┐                            │
                    │   THETAP    │  NO                        │
                    │    > 90     │──────────┐                 │
                    │      ?      │          │                 │
                    └──────┬──────┘          │                 │
                      YES  │                 │                 │
                    ┌──────┴──────┐          │                 │
                    │  THETAP =   │          │                 │
                    │ π − THETA   │          │                 │
                    └──────┬──────┘          │                 │
                           │←────────────────┘                 │
                    ┌──────┴──────┐                            │
        YES         │   CIRCLES   │                            │
    ┌───────────────│  SEPARATED  │                            │
    │               │      ?      │                            │
    │               └──────┬──────┘                            │
    │                  NO  │                                   │
    │               ┌──────┴──────┐                            │
    │               │   CIRCLES   │  YES                       │
    │               │ CONCENTRIC  │───────────────┐            │
    │               │      ?      │               │            │
    │               └──────┬──────┘               │            │
    │                  NO  │                       │            │
    │               ┌──────┴──────┐                │            │
    │               │  SOLVE FOR  │                │            │
    │               │ COORDINATES │                │            │
    │               │ OF          │                │            │
    │               │INTERSECTION │                │            │
    │               └──────┬──────┘                │            │
┌───┴────┐       ┌─────────┴──────┐         ┌──────┴─────┐
│BAFRAT  │       │   SOLVE FOR    │         │  BAFRAT    │
│  = 0   │       │  OVERLAPPING   │         │   = 1      │
│        │       │  AREA OF       │         │            │
│        │       │  CIRCLES       │         │            │
└───┬────┘       └─────────┬──────┘         └──────┬─────┘
    │               ┌──────┴──────┐                │
    │               │  BAFRAT =   │                │
    │               │  RATIO OF   │                │
    │               │   AREAS     │                │
    │               └──────┬──────┘                │
    └──────────────────────┼───────────────────────┘
                    ┌───────┴───────┐
                    │    RETURN     │
                    └───────────────┘
```
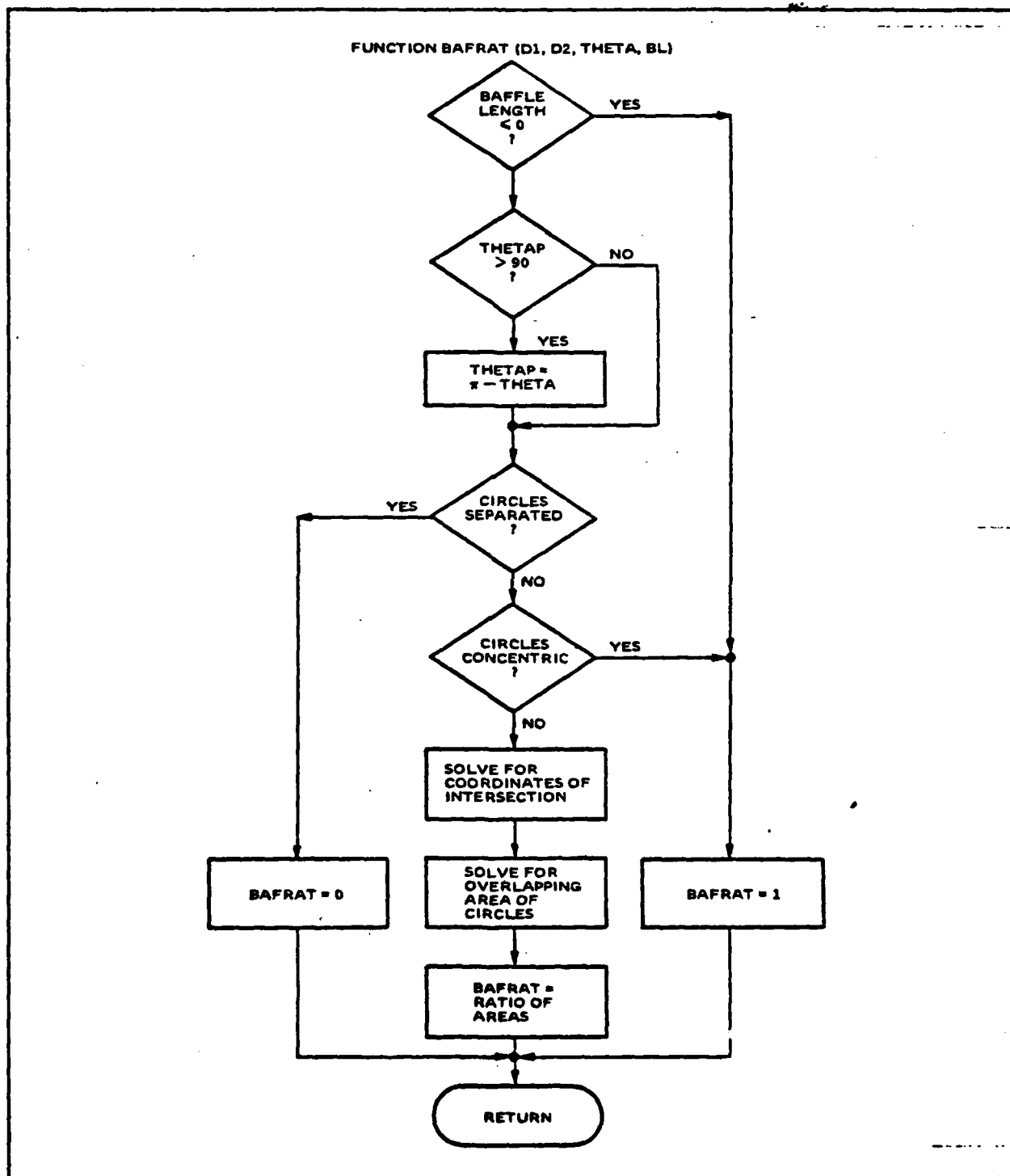
Figure B-23. Function BAFRAT. This routine calculates the fractional area of the transmitter optics visible at an off-axis angle θ.

SUBROUTINE STON

```
                    ┌─────────┐
                    │HETERO-  │  YES
                    │ DYNE    ├────────────────────┐
                    │RECEIVER │                     │
                    │    ?    │                     │
                    └────┬────┘              ┌──────┴──────┐
                         │ NO                │ HETERODYNE  │
                         │                   │  S/N EQN    │
                         │                   └──────┬──────┘
                         │                          │
                   ┌─────┴─────┐                    │
                   ║  CALL     ║ ── ── BACKGROUND    │
                   ║ BACK (PB) ║        POWER        │
                   ╚═══════════╝                     │
                         │                           │
                   ┌─────┴─────┐                     │
                   │ DIRECT    │                     │
                   │ S/N EQN   │                     │
                   └─────┬─────┘                     │
                         │←────────────────────────┘
                   ┌─────┴─────┐
                   │ CONVERT   │
                   │  TO dB    │
                   └─────┬─────┘
                         │
                   ╭─────┴─────╮
                   │  RETURN   │
                   ╰───────────╯
```
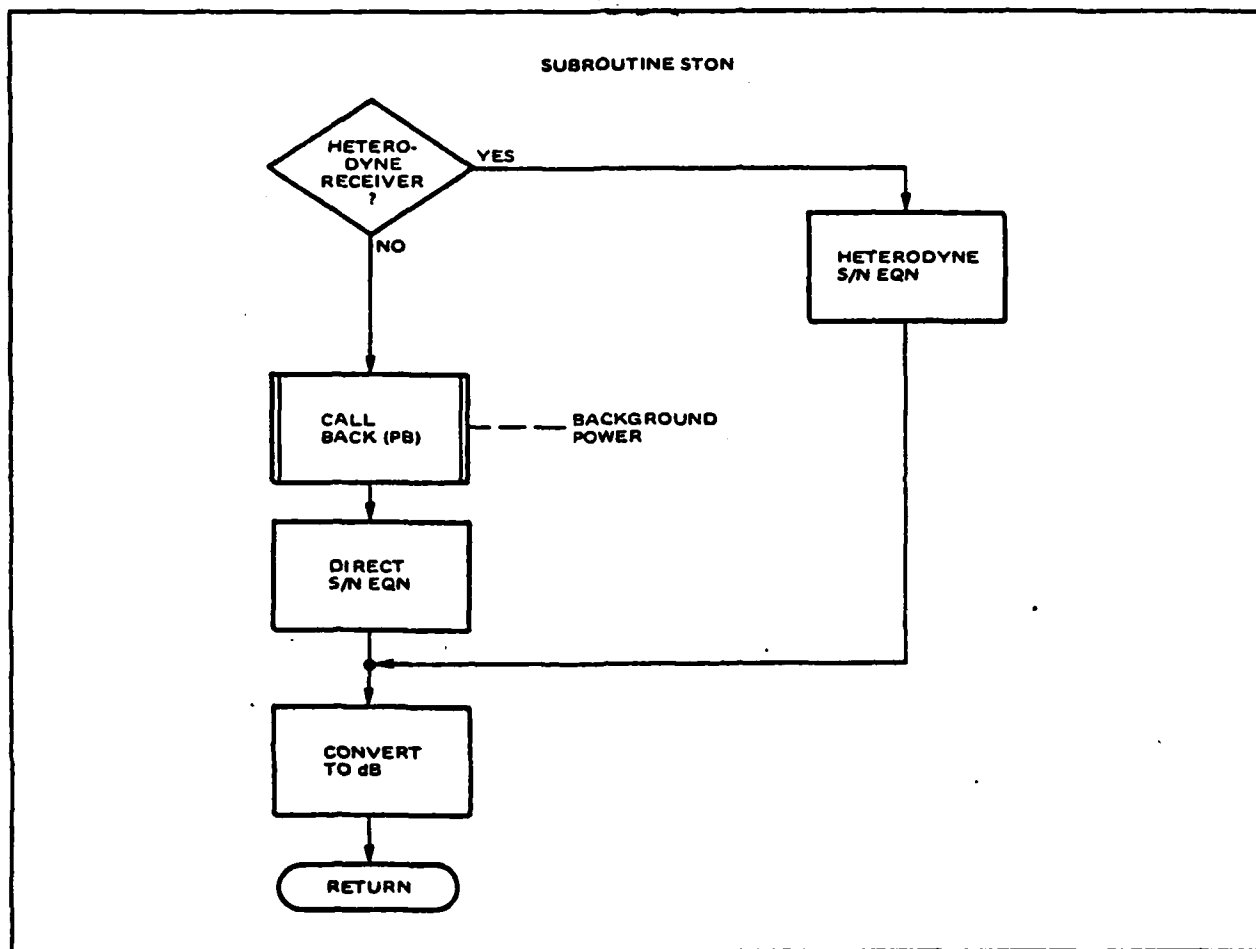
Figure B-24. Subroutine STON. This routine calculates the SNR for either direct or heterodyne receivers.
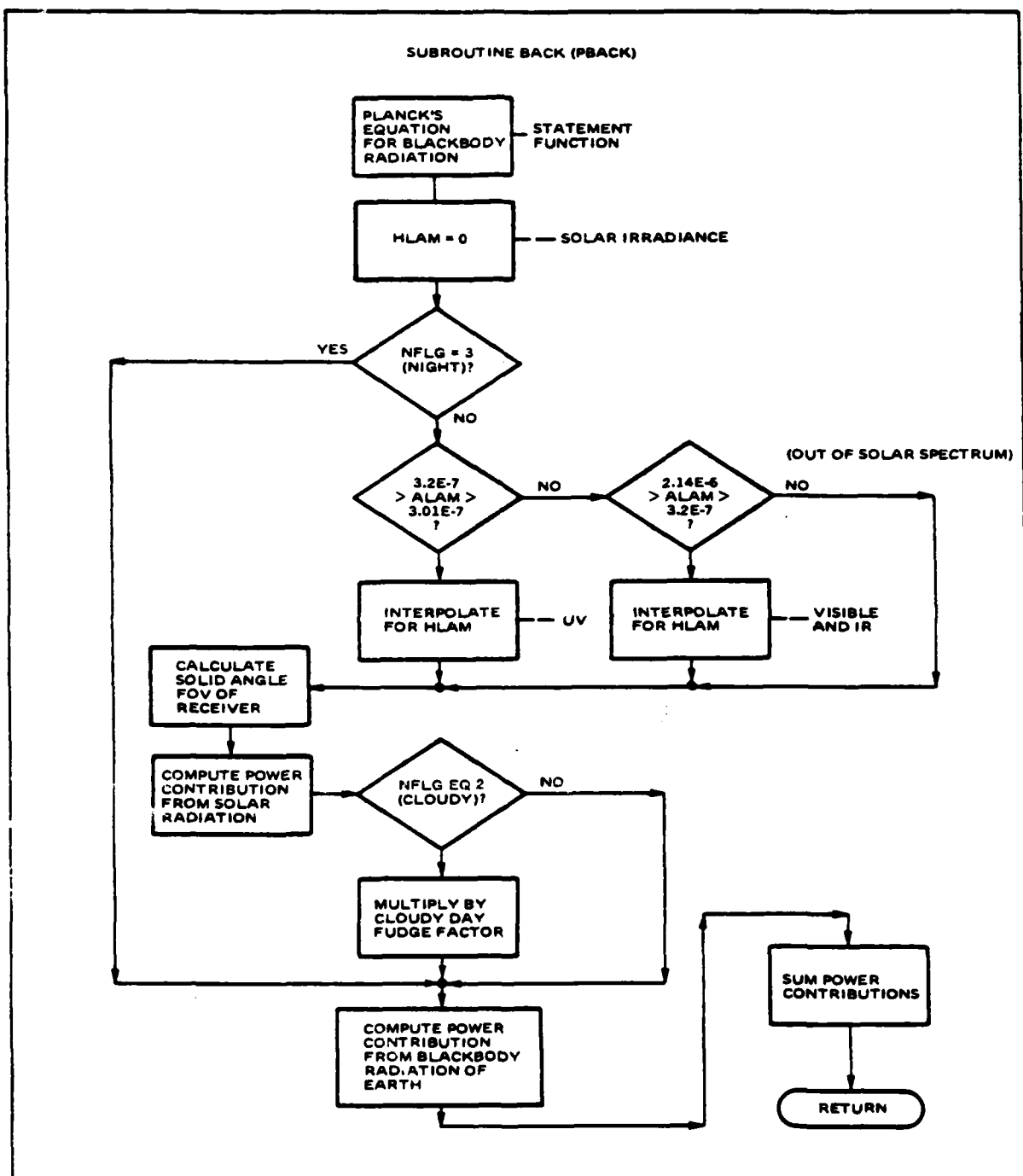
Figure B-25. Subroutine BACK. This routine computes the background noise power for a sunny day, cloudy day or nighttime scenario.
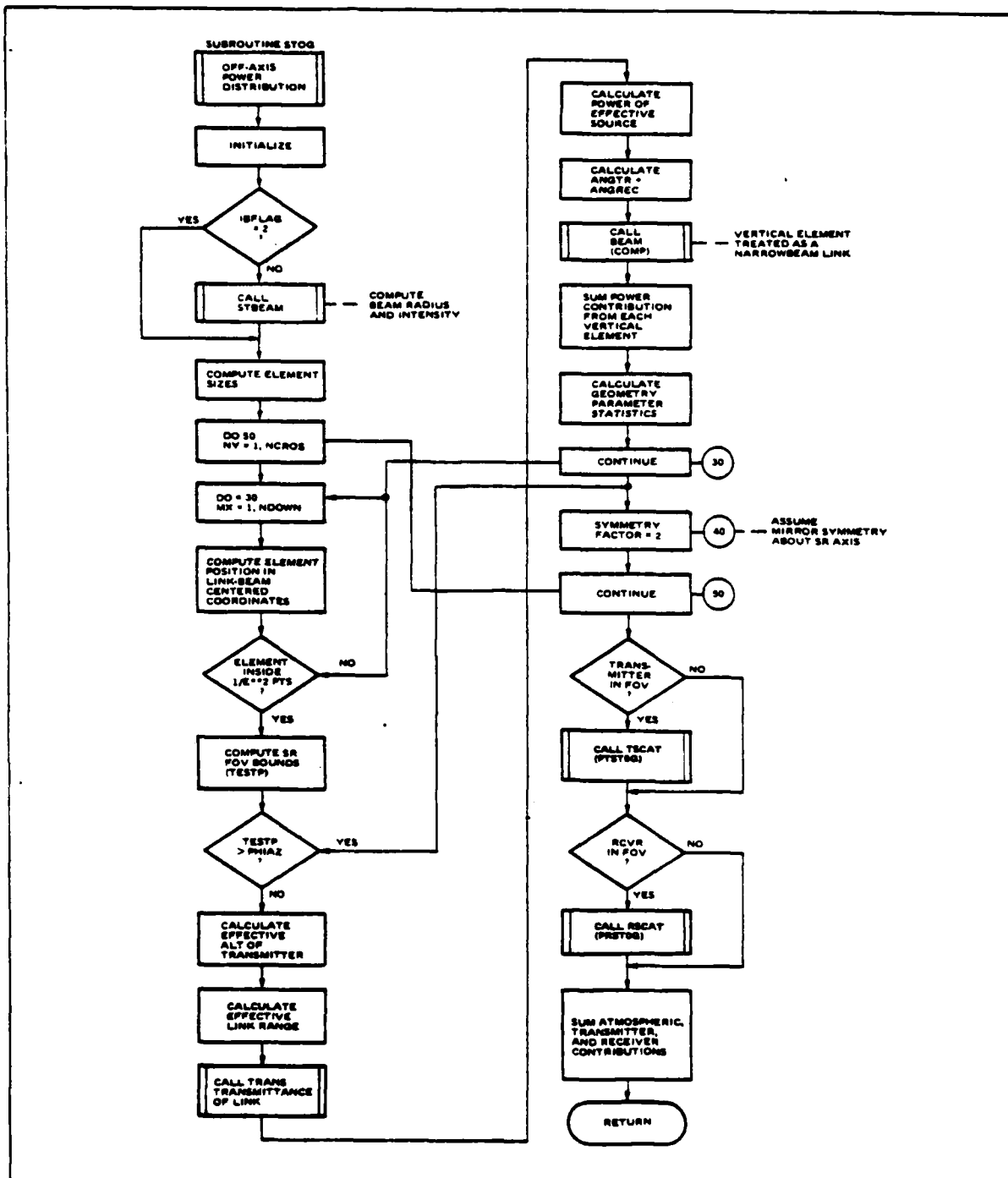
Figure B-26. Subroutine STOG. The space to ground case is set up in this routine, making use of the narrowbeam routine to compute the power.

SUBROUTINE STBEAM (RBEAM, GRNDIR)

CALL
SIGMAT — — — CALCULATE TURBULENCE JITTER

CALCULATE
RADIUS OF
BEAM

CALL
TRANS — — — CALCULATE TRANSMITTANCE
TO GROUND

CALCULATE
EQUIVALENT
IRRADIANCE
OF LINK

RETURN
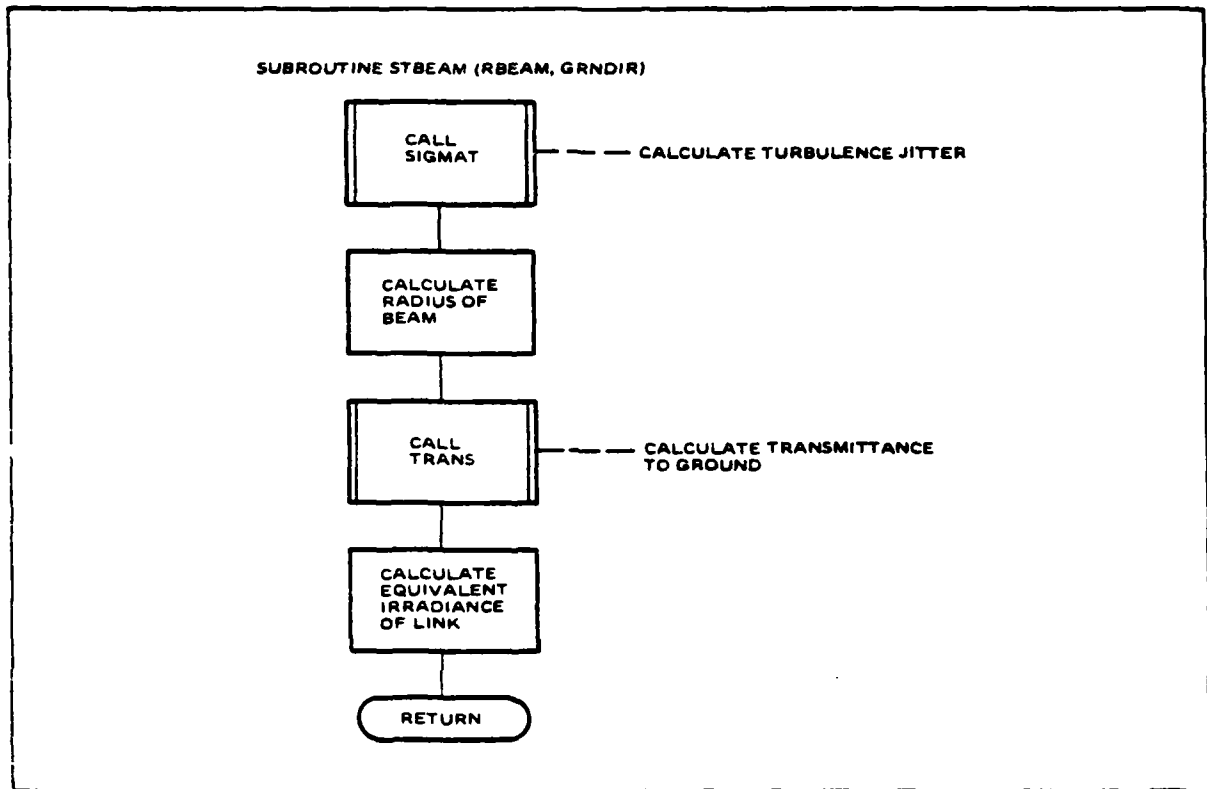
Figure B-27. Subroutine STBEAM. In the case the user prefers that the beam radius and intensity on the ground be calculated, this routine is called.

for on-axis intensity and beam radius discussed in Section 2. STBEAM is called only
if the user wants the beam radius and on-axis intensity calculated, for if he chooses
he may input those parameters.

Turbulence Routines

The subroutines SIGMAT and QGIO of Figures B-28 and B-29 respectively and
function CNSQ, shown in Figure B-30, are used to compute the half-angle beamspread
of the space-to-ground link beam. SIGMAT provides the geometry needed to describe
the path, calls QG10, which integrates CNSQ over the limits provided and the integra-
tion result is used to compute the beamspread. Function CNSQ returns the atmo-
spheric structure constant C_n^2 for a given altitude H. Subroutine QG10 is an
integrator that uses a 10-point guassian quadrature method.
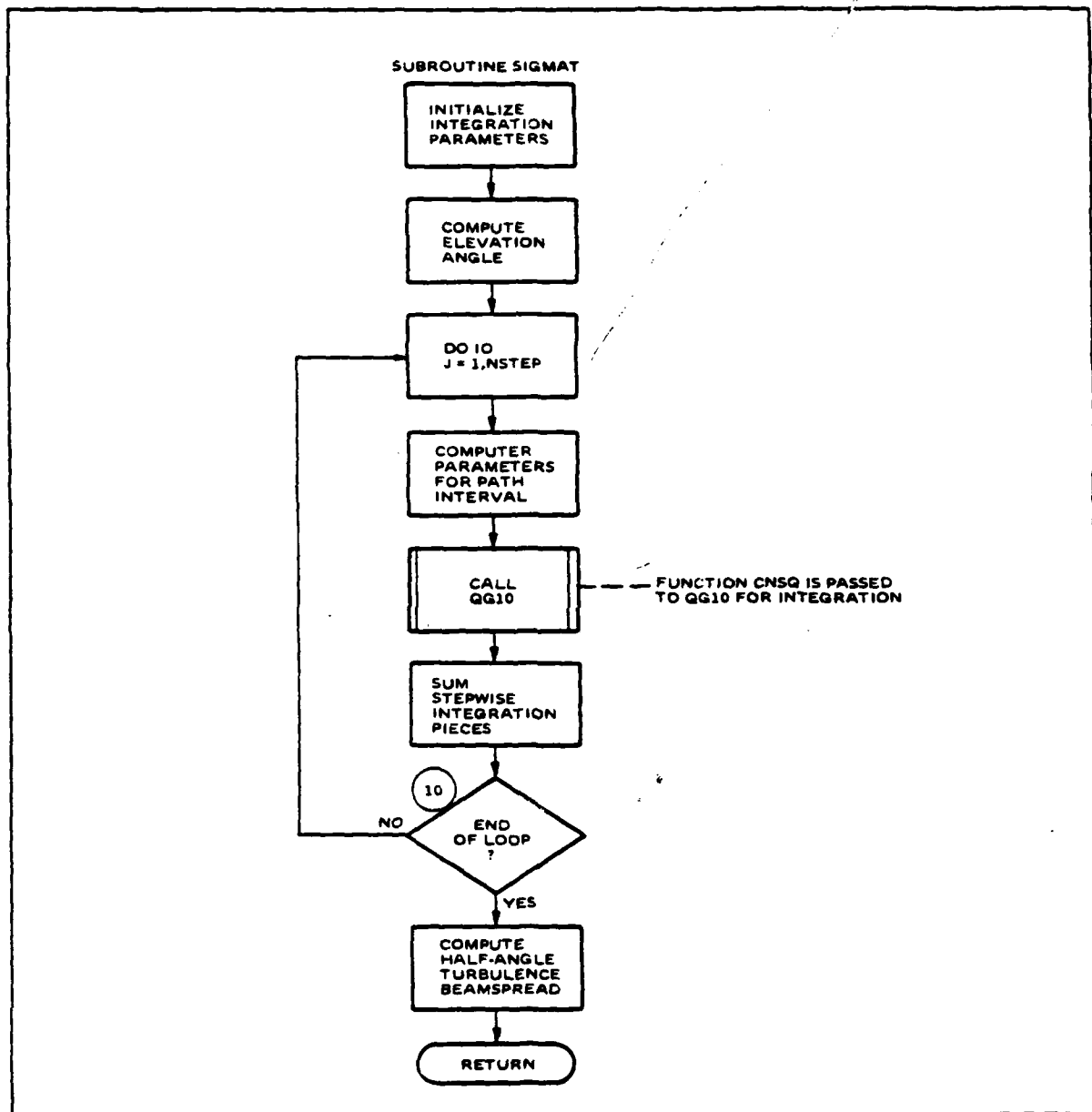
Figure B-28. Subroutine SIGMAT. This subroutine calculates the one-sigma jitter due to turbulence of the atmosphere.
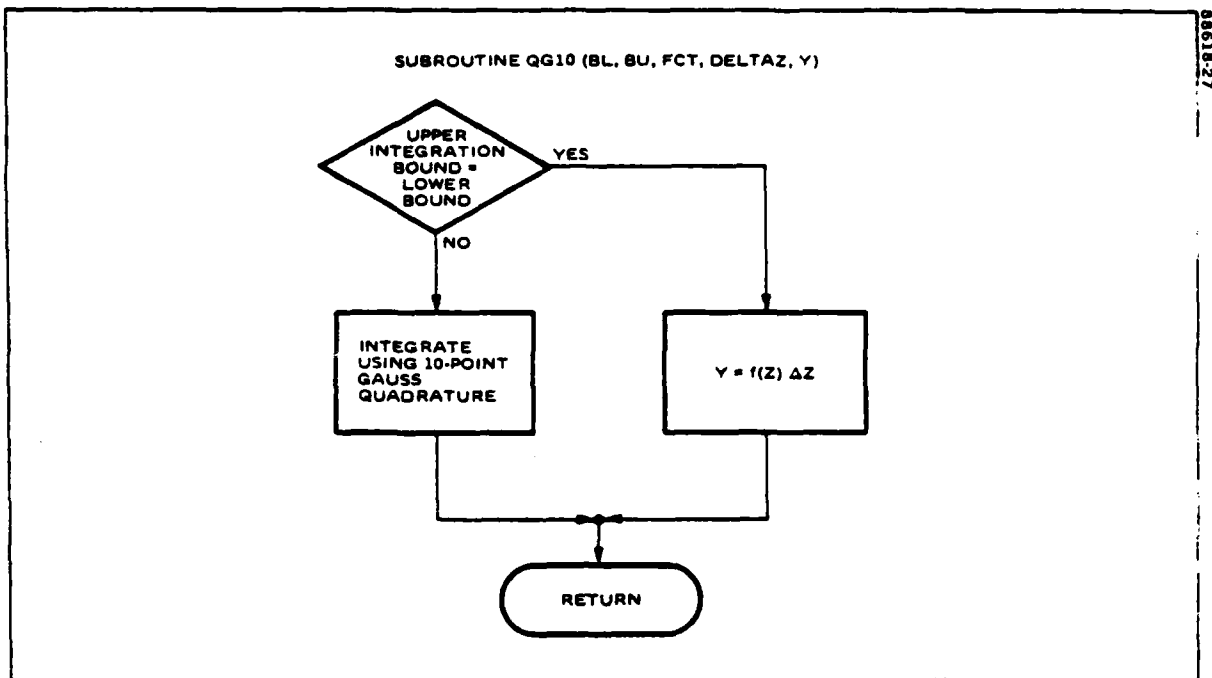
Figure B-29. Subroutine QG10. This is a ten-point gaussian quadrature integrator.
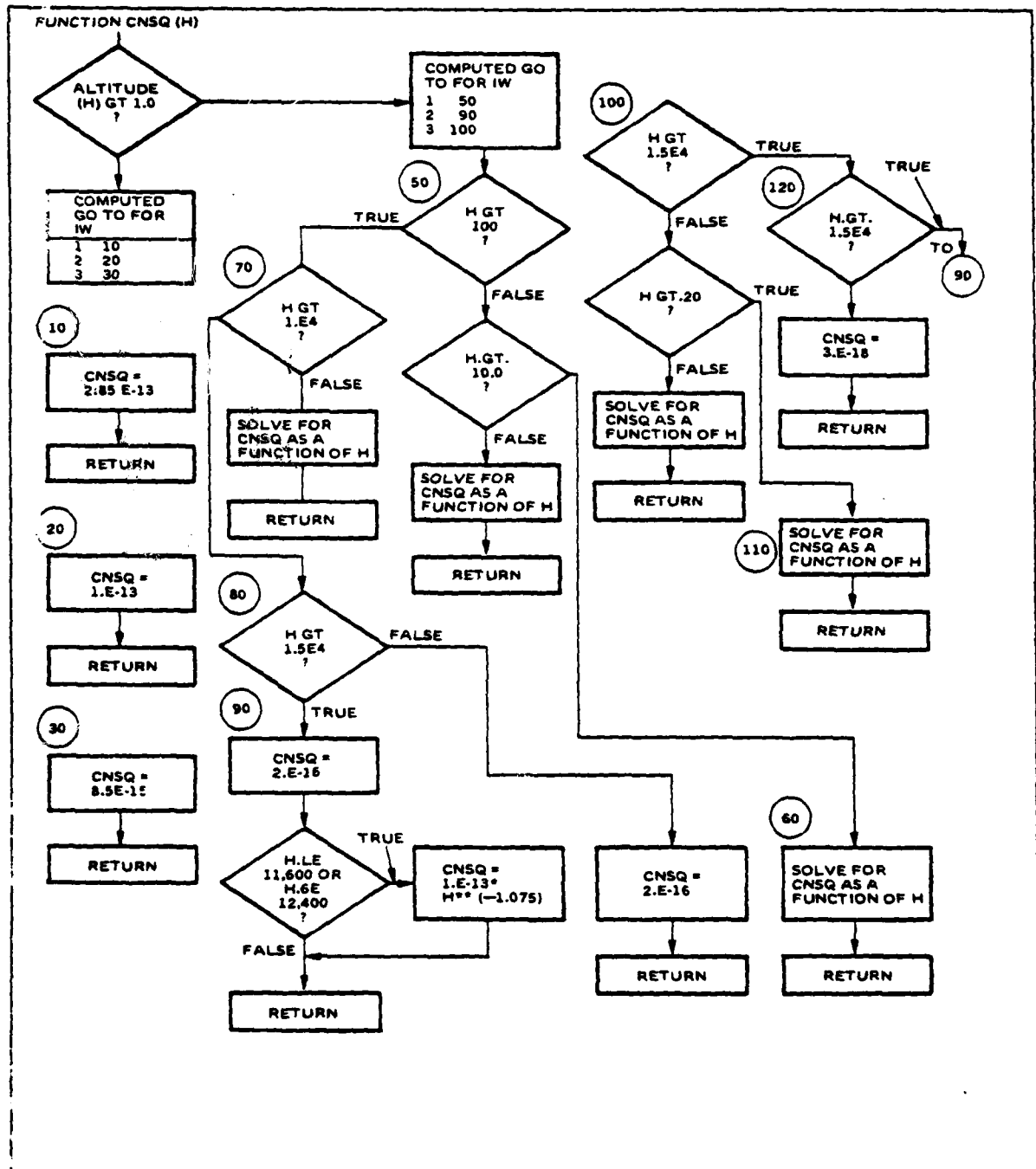
Figure B-30. Function CNSQ. This returns the atmospheric structure constant at a given altitude H for m.d, moderate, or strong turbulence.

Section II
Off-axis Sample Run

off-axis analysis program --
        enter 1 for interactive input - 0 for batch input

0

    input file?

99

    do you want an input summary?   0-no 1-yes

1

        ***   input summary   ***

scenario geometry

  link range, m ----   5.000E+03   tr alt, m --------   2.000E+01
  rc alt, m --------   2.000E+01   sr alt, m -------   1.000E+01
  background type --   sunny

link parameters

  wavelength, m ----   1.060E-06   tr power, w -----   1.000E+00
  rc aperture, m ---   0.10000   tr aperture, m --   0.10000
  rc hood length, m-   0.00   tr hood length, m   0.00
                                         tr beam width, rad 1.000E-04
                                         turbulence ------   mild

sr parameters

  linear fov, rad -   8.000E-02   aperture, sq.m. -   0.0500
  fov across beam, r   1.700E-02   detection type, -   dir
  gain ------------   1.00   excess noise ----   1.000E+00
  mod. depth ------   1.00
  bandwidth, hz ----   1.000E+06   quantum eff. ----   0.70
  dark current, a --   1.000E-09   thermal equ pwr -   1.000E-12
  opt bw, microns --   5.000E-02
  bit interval, s --   1.000E-06

Format for input file:

file99

```
$input lam=4, ia=2, mat=2, mvis=2, dt=.1, phit=.0001, rbsdf=2, wbsdf=200,
sbsdf=-2.5, ng=0, dr=.1, nbak=3, bdiff=.15, psiaz=0.0, psiel=0.0, npa=1,
pt=1.0, rl=5000, ht=20, hr=20, istog=0, iw=3, monma=2, ma=1, intvpa=2,
xm=1.0, eta=.7, g=1.0,  f=1.0, darki=0.0, ptherm=1.0e-12, bwr=1.0e6,
bwopt=.05, nfls=1, bw=1.0e6, asr=.05, phi=.080, phiaz=.017, blt=0.0,
blr=0.0, gamint=0.0, mode=6, rex=2.5e3, theta=150, x=1.0e5, t=1.0e-6,
npts=5, form1(1)=1.0, form1(2)=1.0, form1(3)=1.0, form0(1)=0.0,
form0(2)=0.0, form0(3)=0.0 $
```

3

```
          mat     -- atmospheric model                        2
                     1 - tropical
                     2 - midlatitude summer
                     3 - midlatitude winter
                     4 - subarctic summer
                     5 - subarctic winter
 2
          mvis    -- visibility (1-clear 2-hazy)              2
 2
     2    dt      -- transmitter optics diameter, m           0.100
 .1
     3    phit    -- transmitter beamwidth, radians           1.000E-04
1e-4
    31    ibsdf   -- bsdf (1-default, 2-user)                 2
 1
     4    dr      -- link receiver optics diameter, m         0.100
 .1
    32    nbak    -- backstop  (1-default, 2-user, 3-lambertian)    3
 3
          bdiff   -- diffuse reflectance (0 to 1)
                     (lambertian model, es. .1)
 .15
    44    psisz   -- az. orientation of backstop (des)        0.000
                     0 - normal to beam
 0
          psiel   -- el. orientation of backstop (des)        0.000
                     0 - normal to beam
 0
    33    nos     -- rcvr scatter (1-default, 2-user)         1
 1
     6    pt      -- transmit power, watts                    1.000E+00
 1
     8    rl      -- link range, meters                       5.000E+03
5e3
     9    ht      -- altitude of transmitter, meters          2.000E+01
20
    10    hr      -- altitude of link receiver, m             2.000E+01
20
    48    iw      -- turbulence                               3
                     1-severe 2-moderate 3-mild
 1
    25    mcomp   -- compute  1-power  2-s/n ratio            2
 2
     5    ms      -- source? 1-sum, 2-atm, 3-tr, 4-rc         1
 1
    13    irtype  -- sr type (1-default, 2-user input)        2
 2
    14    xm      -- modulation depth                         1.000
 1
    16    eta     -- quantum efficiency of detector           0.500
 .7
```

do you want an output table?   0-no 1-yes

1

which file? (must be allocated)

5

interceptibility mode 1

power contributed by each source, watts

theta, d	s/n, db	transmitter	receiver	atmosphere
2.4093E+01	-1.6929E+01	2.8738E-10	0.0000E+00	1.6620E-10
2.5093E+01	-2.6402E+01	0.0000E+00	0.0000E+00	1.5241E-10
2.6093E+01	-2.7146E+01	0.0000E+00	0.0000E+00	1.3989E-10
2.7093E+01	-2.7883E+01	0.0000E+00	0.0000E+00	1.2851E-10
2.8093E+01	-2.8612E+01	0.0000E+00	0.0000E+00	1.1817E-10
2.9093E+01	-2.9333E+01	0.0000E+00	0.0000E+00	1.0876E-10
3.0093E+01	-3.0045E+01	0.0000E+00	0.0000E+00	1.0020E-10
3.1093E+01	-3.0748E+01	0.0000E+00	0.0000E+00	9.2402E-11
3.2093E+01	-3.1443E+01	0.0000E+00	0.0000E+00	8.5298E-11
3.3093E+01	-3.2129E+01	0.0000E+00	0.0000E+00	7.8820E-11
4.0082E+01	-3.6671E+01	0.0000E+00	0.0000E+00	4.6726E-11
4.7070E+01	-4.0763E+01	0.0000E+00	0.0000E+00	2.9172E-11
5.4058E+01	-4.4422E+01	0.0000E+00	0.0000E+00	1.9142E-11
6.1047E+01	-4.7691E+01	0.0000E+00	0.0000E+00	1.3138E-11
6.8035E+01	-5.0619E+01	0.0000E+00	0.0000E+00	9.3787E-12
7.5023E+01	-5.3248E+01	0.0000E+00	0.0000E+00	6.9293E-12
8.2012E+01	-5.5605E+01	0.0000E+00	0.0000E+00	5.2823E-12
8.9000E+01	-5.7700E+01	0.0000E+00	0.0000E+00	4.1502E-12
9.5988E+01	-5.9526E+01	0.0000E+00	0.0000E+00	3.3434E-12
1.0298E+02	-6.1065E+01	0.0000E+00	0.0000E+00	2.8174E-12
1.0997E+02	-6.2299E+01	0.0000E+00	0.0000E+00	2.4441E-12
1.1695E+02	-6.3224E+01	0.0000E+00	0.0000E+00	2.1974E-12
1.2394E+02	-6.3857E+01	0.0000E+00	0.0000E+00	2.0428E-12
1.3093E+02	-6.4257E+01	0.0000E+00	0.0000E+00	1.9510E-12
1.3792E+02	-6.4544E+01	0.0000E+00	0.0000E+00	1.8874E-12
1.4491E+02	-6.4907E+01	0.0000E+00	0.0000E+00	1.8103E-12
1.4591E+02	-6.4982E+01	0.0000E+00	0.0000E+00	1.7947E-12
1.4691E+02	-6.5067E+01	0.0000E+00	0.0000E+00	1.7773E-12
1.4791E+02	-6.5162E+01	0.0000E+00	0.0000E+00	1.7579E-12
1.4891E+02	-6.5270E+01	0.0000E+00	0.0000E+00	1.7363E-12
1.4991E+02	-6.5392E+01	0.0000E+00	0.0000E+00	1.7121E-12
1.5091E+02	-6.5530E+01	0.0000E+00	0.0000E+00	1.6850E-12
1.5191E+02	-6.5686E+01	0.0000E+00	0.0000E+00	1.6549E-12
1.5291E+02	-6.5864E+01	0.0000E+00	0.0000E+00	1.6213E-12
1.5391E+02	-6.6066E+01	0.0000E+00	0.0000E+00	1.5841E-12
1.5491E+02	-6.6296E+01	0.0000E+00	0.0000E+00	1.5427E-12
1.5591E+02	-2.5531E+01	0.0000E+00	1.6699E-10	1.4971E-12

do you wish to do a sensitivity analysis? 0-no 1-yes

0

do you want another run? 1-yes 2-no

2

STOP

```
    52    s       -- predetection gain              1.000
1
    17    f       -- excess noise factor            1.000E+00
1
    18    bwr     -- bandwidth of sr, hz            1.000E+06
1e6
    19    ptherm  -- thermal noise equ. power of sr, w   7.000E-13
1e-12
    19    idark   -- dark current of sr             1.000E-09
0
    29    bwopt   -- sr optical bandwidth, microns  1.000E-03
1e-3
    30    nfls    -- 1-sunny 2-cloudy 3-nighttime    1
1
     7    bw      -- link bandwidth, hz             1.000E+06
1e6
    12    asr     -- area of sr aperture, sq. meters   5.000E-02
.05
    11    phi     -- sr field of view, radians      8.000E-02
80e-3
    40    phiaz   -- sr field of view (azimuth), rad   1.700E-02
17e-3
    20    blt     -- hood length of transmitter, m    0.000
0
    21    blr     -- hood length of receiver, m       0.000
.01
    43    bdlr    -- receiver hood diameter, m         0.100
.1
    41    gamint  -- angle of intercept plane, deg    0.000E+00
                      0 for horizontal plane
0
    26    mode    -- select output mode (7 for info)     6
1
    23    rpx     -- distance from xmtr to bisector, m   2.500E+03
2500
    24    x       -- perpendicular dist to beam axis, m  1.000E+03
1000


end of inputs
do you wish to change anything? 1-yes  2-no  3-all
2
do you want an input summary?     0-no  1-yes
1
```

***   input summary   ***

scenario geometry

link range, m -----	5.000E+03	tr alt, m -------	2.000E+01
rc alt, m --------	2.000E+01	sr alt, m -------	2.057E+01
background type --	sunny		

link parameters

wavelength, m ----	1.060E-06	tr power, w -----	1.000E+00
rc aperture, m ---	0.10000	tr aperture, m --	0.10000
rc hood length, m-	0.01	tr hood length, m	0.00
rc hood dia., m --	0.10	tr hood dia., m -	0.10
		tr beam width, rad	1.000E-04
		turbulence ------	severe

sr parameters

linear fov, rad -	8.000E-02	aperture, sq.m. -	0.0500
fov across beam, r	1.700E-02	detection type, -	dir
gain -----------	1.00	excess noise ----	1.000E+00
mod. depth -------	1.00		
bandwidth, hz ----	1.000E+06	quantum eff. ----	0.70
dark current, a --	0.000E+00	thermal eqv pwr --	1.000E-12
opt bw, microns --	1.000E+03		

intercept mode parameters

mode type --------	1	output type -----	s/n, db
rpx, meters ------	2.500E+03	x, meters -------	1.000E+03
sr plane, deg ----	0.00	specular gamint -	0.00

atmospheric parameters

| data source ------ | af41 | | |
| midlatitude summer | | visibility is | hazy |

coefficients for 0 to 1000 meters altitude

| scat coef 1/m ---- | 2.008E-04 | abs coef, 1/m --- | 5.820E-05 |

scattering data for transmitter, receiver, and backstop

bsdf model type --	average	bsdf slope dh/db	-2.500
nonlinearities ---	0	bsdf intercept -	200.000
backstop type ----	lambertian	reflection coef -	0.1500
backstop az, deg	0.00	backstop el, deg	0.00
oa type ----------	unknown	diffuse level ---	0.000
specular max ---	0.000	specular width, .	0.300

SECTION III
OFF-AXIS PROGRAM LISTING

PROGRAM LISTING OF off-axis

```
c      OFF-AXIS ANALYSIS PROGRAM
c      D. JONES   714-871-3232  X 4579
c      T. YUNGHANS              X 4582
c      HUGHES AIRCRAFT COMPANY
c      FULLERTON, CA
c
c      MODIFIED TO DO PROBABILITY OF BIT ERROR ANALYSIS
c      BILL JAEGER
c      MIT  BLG. 36-477
c      CAMBRIDGE, MA
c
       common/ flags /mode,mcomp,mp,lam,modesw,lunit,nout,istog,iotype,
     & irtype,ihet,ibflag,iw
       common/rsct/oasmax,diffoa,oafwhm,bmaxs,bfwhms,bdiff(6),psiaz,psiel
     & ,gams
       common/ atmos /alfa(5,2),alfsct,alfab,ia,ab(33),as(33),at(33,14,6)
     & ,mat,mvis
       common/ tbsdf / ng,gstart(3),gend(3),gampl(3),ybsdf,sbsdf,nbak,noa
     & ,ibsdf
       common/ tdata / blt,dt,ht,phit,pt,rb,grndi,bdrt,sigj,sigt
       common/ rdata / blr,dr,hr,gl,bdlr
       common/ srdata / asr,hs,phi,phiaz,dphi
       common/ ldata / rl,alam,rpx,theta,x,angtr,angrec,gamint,bw
c  * darki & ptherm replace pnep, add g *
       common/ sndata / bwr,eta,f,em,pb,ps,darki,ptherm,snpndb,sndb,xm,
     & bwopt,nflg,g
       common/ stgout / nvel,svel,avel,ndown,ncros,numtot,hvnear,
     & hvfar,xdis,hdis,hdisdf,xclos,hclos,hclsdf,kount
c  * srdark & srther replace srpnep *
       common/block1/xmod(6),gainsr(6),qe(6),fnoise(6),srbw(6),
     & srdark(6),srther(6),alamda(6),obw(6),nhol(6)
       common /pltc  / xint(200),yint(200),h(200),dcomp(2),np,note
c  * dimension heady1 & heady2 (2by3) *
       common/ hrith / title(18),headx1(2,2),headx2(2,2),heady1(2,3),
     & heady2(2,3),brhol(2),bakhol(2),oahol(2),mattyp(5,5),mvtyp(2,2),
     & mathol(2),holdet(2),holiw(2,3)
       common/err/ier,ierab,iersc,ierbr,devab,devsc,devbr
c  * add labeled common wavefm *
       common/ wavefm /npts,t,form0(1000),form1(1000),power0(1000),
     & power1(1000)
       data onedeg,pi,r2d/.0174532925,3.141592654,57.29577951/
c
c      INPUT DESCRIPTIONS
c
c      THE MKS SYSTEM OF UNITS IS USED UNLESS OTHERWISE
c      SPECIFIED
c
c
```

2

```
c     LINK VARIABLES
c
c     LAM      - WAVELENGTH INDEX
c     RL       - LINK RANGE (M)
c     IA       - ATMOSPHERICS (1-USER, 2-AFGL)
c     ALFSCT   - ATMOS. SCAT. COEF. (1/M)
c     ALFAB    - ATMOS. ABS. COEF. (1/M)
c
c     TRANSMITTER VARIABLES
c
c     HT       - ALTITUDE OF TRANSMITTER (M)
c     PT       - LINK TRANSMIT POWER OUT OF OPTICS (W)
c     DT       - TRANSMITTER OPTICS DIAMETER (M)
c     PHIT     - TRANSMITTER BEAMWIDTH (RAD)
c     BLT      - TRANSMITTER HOOD LENGTH (M)
c     IBSDF    - PORT SCATTER FLAG (1-DEFAULT, 2-USER)
c     (VALUES BELOW ARE DEFAULTED)
c     YBSDF    - Y-INTERCEPT OF BSDF CURVE (AT 1 DEGREE)
c     SBSDF    - SLOPE OF BSDF CURVE (LOG-LOG)
c     NG       - NO. OF DISCONTINUITIES (GLITCHES) IN BSDF (MAX. OF 3)
c     GSTART   - START OF GLITCH ,ARRAY OF 3 (DEGREES)
c     GEND     - END OF GLITCH,ARRAY OF 3 (DEGREES)
c     GAMPL    - AMPLITUDE OF GLITCH, OVER RANGE SPECIFIED ABOVE,
c     ARRAY OF 3 (DEGREES)
c
c     RECEIVER VARIABLES
c
c     HR       - ALTITUDE OF RECEIVER (M)
c     DR       - RECEIVER OPTICS DIAMETER (M)
c     BLR      - RECEIVER HOOD LENGTH (M)
c     NBAK     - RECEIVER BACKSTOP (1-DEFAULT, 2-USER)
c     (VALUES BELOW ARE DEFAULTED)
c     BMAXS    - MAXIMUM REFLECTION COEFFICIENT
c     BFWHMS   - FULL WIDTH AT HALF MAXIMUM (DEGREES)
c     BDIFF    - DIFFUSE BACKGROUND REFLECTANCE
c     NOA      - RECEIVER OPTICAL REFLECTION(1-USER, 2-DEFAULT)
c     (VALUES BELOW ARE DEFAULTED)
c     OASMAX   - MAXIMUM RECEIVER OPTICAL SCATTER
c     OAFWHM   - FULL WIDTH AT HALF MAXIMUM (DEGREES)
c     DIFFOA   - DIFFUSE BACKGROUND
c
c     SR VARIABLES
c
c     HS       - ALTITUDE OF SR (M)
c     ASR      - SR  APERTURE AREA (M**2)
c     PHI      - SR FIELD OF VIEW (ELEV) (RAD)
c     PHIAZ    - SR FIELD OF VIEW (AZIMUTH) (RAD)
c     IRTYPE   - SR CHARACTERISTICS (1-DEFAULT, 2-USER)
c     (VALUES BELOW DEFAULTED, ONLY NEEDED FOR S/N CASES)
c     XM       - MODULATION DEPTH
```

```
c       G       - PREDETECTION GAIN IN SR
c       ETA     - QUATUM EFFICIENCY OF DETECTOR
c       F       - EXCESS NOISE FACTOR
c       BWR     - BANDWIDTH OF SR, (HZ)
c       PTHERM  - THERMAL NOISE EQV. POWER OF SR
c       DARKI   - DARK CURRENT OF SR
c       BWOPT   - SR OPTICAL BANDWIDTH (MICRONS)
c       NFLG    - DAY/NIGHT FLAG (1-DAY, 2-NIGHT)
c       BW      - LINK BANDWIDTH (HZ)
c
c       INTERCEPT VARIABLES
c
c       MCOMP   - COMPUTE (1-POWER, 2-S/N RATIO)
c       MP      - CONTRIBUTION FLAG (1-ALL,2-ATMOS, 3-TRANS, 4-RCVR)
c       MODE    - SELECTS MODE OF OPERATION (1-5)
c       RPX     - DISTANCE FROM XMTR TO BISECTOR (M)
c       X       - DISTANCE ALONG BISECTOR TO BEAM (M)
c       DCOMP   - VALUE OF CONTOUR (DBW OR DB S/N) (MODES 4 AND 5)
c
c       SPACE TO GROUND VARIABLES
c       ISTOG   - SPACE TO GROUND FLAG (0-NO, 1-YES)
c       RB      - RADIUS OF LINK BEAM (M)
c       THETA   - ZENITH ANGLE OF SR (DEG)
c       GRNDI   - EQUIVALENT POWER (WATTS/SQ. M)
c       GL      - ALTITUDE OF GROUND LEVEL (M)
c
        nout=1
        inpsum=1
c
c       FIRST READ DETERMINES WHETHER THE SYSTEM IS INTERACTIVE
c       OR IN THE BATCH MODE.
c
c       IOTYPE=0   IS BATCH MODE
c
        write (6,300)
        read (5,310) iotype
        if (iotype.eq.0) go to 20
c
c       INTERACTIVE MODE
c
c       THE VALUE OF N TELLS TSHARE IF THIS IS THE FIRST CALL.
c       IF TSHARE RETURNS N=10, EXECUTION IS TERMINATED
        n=0
c
10      call tshare (n)
        if (n.eq.10) go to 280
        go to 70
c
c       BATCH INPUTS
c
```

```
c  * add batch input capabilities *
20     call batch
c      SET FALGS TO RETURN TO TSHARE FOR CHANGES
       n=1
       iotype=1
c
c      ***** WRITE THE INPUTS OUT *****
c
70     mfl=1
       if (mode.ge.4) mfl=2
c  * Pr(e) heading for mode 6 *
       if (mode.eq.6) mfl=3
       if (iotype.eq.0) go to 80
       write (6,380)
       read (lunit,1040) inpsum
       if (inpsum.eq.0) go to 170
c
80     write (6,480)
       if (istog.eq.1) write (6,930)
       write (6,490)
       write (6,500) rl,ht
       write (6,510) hr,hs
       theta=theta*r2d
       if (istog.eq.1) write (6,530) x,theta
       theta=theta/r2d
       if (istog.eq.1.and.ibflag.eq.2) write (6,540) gl,rb
       if (istog.eq.1.and.ibflag.eq.1) write (6,550) gl
       nf1=2*nflg-1
       nf2=nf1+1
       if (mcomp.eq.2.and.ihet.eq.1) write (6,520) nhol(nf1),nhol(nf2)
       write (6,560)
       if (istog.eq.0.or.ibflag.eq.1) write (6,570) alam,pt
       if (istog.eq.1.and.ibflag.eq.2) write (6,580) alam,grndi
       write (6,590) dr,dt
       write (6,600) blr,blt
       if (blr.ne.0..or.blt.ne.0.) write (6,610) bdlr,bdrt
       if (istog.eq.1.and.ibflag.eq.1) write (6,620) sigj,(holiw(i,iw),
&      i=1,2)
       write (6,630) phit
c  * add turbulence to narrow beam inputs *
       if (istog.eq.0) write (6,625) (holiw(i,iw),i=1,2)
       write (6,640)
       if (istog.eq.1) go to 90
       write (6,650) phi,asr
       go to 100
90     write (6,660) phi,phiaz,asr
100    if (mcomp.eq.2) write (6,670) phiaz,holdet(ihet)
c
       if (mcomp.eq.1) go to 110
c
```

```
      write (6,690) g,f
      write (6,695) xm
      write (6,700) bwr,eta
c  * darki & ptherm replace pnep *
      if (ihet.eq.1) write (6,681) darki,ptherm
      if (ihet.eq.1) write (6,680) bwopt
      if (ihet.eq.2) write (6,685) bwopt,em
c  * add bit interval time *
      if (mode.eq.6) write (6,686) t
c      MODE PARAMETERS
110   if (istog.eq.1) go to 120
      write (6,720)
      write (6,730) mode,heady1(mcomp,mfl),heady2(mcomp,mfl)
c  * skip SR location if mode 6 *
      if (mode.eq.6) go to 115
      if (mode.lt.4) write (6,760) rpx,x
      if (mode.ge.4) write (6,770) dcomp(mcomp)
115   gams=0.
      cs=cos(psiel)*sin(psiaz)
      if (cs.ne.0.) gams=atan2(sin(psiel),cs)
      gamsd=gams*r2d
      gamd=gamint*r2d
      write (6,740) gamd,gamsd
120   write (6,780)
      write (6,800) mathol(ia)
      if (ia.eq.2) go to 130
      write (6,810)
      write (6,790) alfsct,alfab
      go to 140
130   write (6,820) (mattyp(i,mat),i=1,5),(mvtyp(i,mvis),i=1,2)
      write (6,790) as(2),ab(2)
140   write (6,830)
      write (6,840) brhol(1),brhol(2),sbsdf
      write (6,850) ng,ybsdf
      if (ng.gt.0) write (6,860) (i,gstart(i),gend(i),gampl(i),i=1,ng)
c      LAMBERTIAN MODEL
      if (nbak.lt.3) go to 150
      write (6,870) bdiff(lam)
      go to 160
150   write (6,880) bakhol(1),bakhol(2),bdiff(lam)
      write (6,890) bmaxs,bfwhms
160   psiazd=psiaz*r2d
      psield=psiel*r2d
      write (6,750) psiazd,psield
      write (6,900) oahol(1),oahol(2),diffoa
      write (6,890) oasmax,oafwhm
170   if (istog.eq.1) go to 260
c
c      WRITE SENSITIVITY ANALYSIS SUMMARY IF DOING A SENSITIVITY .
c      ANALYSIS
```

```
c
180     if(ier.eq.0.or.iotype.eq.0) go to 190
        write (6,1000)
        if (ierab.eq.1) write (6,1010) devab
        if (iersc.eq.1) write (6,1020) devsc
        if (ierbr.eq.1) write (6,1030) devbr
c
c       ***** WRITE HEADING FOR OUTPUT *****
c
190     if (iotype.eq.0) go to 200
        write (6,390)
        read (lunit,1040) nout
        if (nout.eq.0) go to 210
        write (6,400)
        read (lunit,1040) nout
200     write (6,360) mode
c
c       NOUT=1 FOR EXPANDED OUTPUT FORMAT
c
c   * skip output heading if mode 6 *
        if (mode.eq.6) go to 210
        if (nout.ge.1) write (nout,910) headx1(mcomp,mfl),headx2(mcomp,
&       mfl),heady1(mcomp,mfl),heady2(mcomp,mfl)
c
c       ***** CALL THE COMPUTATIONAL ROUTINES *****
c
c       SETUP IS CALLED FOR NARROW BEAM ANALYSIS
c
210     call setup
c
c
c       WARNING MESSAGE FOR CONVERGENCE
        if (note.ge.1) write (6,370) note
        note=0
c
c       ***** CALL GRAPHING ROUTINE *****
c
c       GRAFIX IS A SYSTEM-DEPENDENT GRAPHICS ROUTINE.  IT MAY BE WRITTEN
c       BY A USER TO PROVIDE INTERACTIVE GRAPHICS, OR WHATEVER
c       HE HAS AT HIS DISPOSAL.  THE HUGHES ROUTINE INCLUDES A PRINTER
c       PLOT FOR USE ON TELETYPE TERMINALS.
c
c       call grafix
c
        if (iotype.eq.0) go to 270
c
c       SENSITIVITY ANALYSIS INPUTS
        write (6,410)
        read (lunit,1040) ier
        if (ier.ne.0) go to 220
```

```
c
c       NO SENSITIVITY ANALYSIS; SET FLAGS TO ZERO
c
        ier=0
        ierbr=0
        iersc=0
        ierab=0
        go to 270
c
c       SENSITIVITY ANALYSIS INPUTS
c
c       ABSORPTION DEV.
220     write (6,420)
        read (lunit,1040) ierab
        if (ierab.eq.0) go to 230
        write (6,430)
        read (lunit,1040) devab
c
c       SCATTERING DEV.
230     write (6,440)
        read (lunit,1040) iersc
        if (iersc.eq.0) go to 240
        write (6,430)
        read (lunit,1040) devsc
c
c       BSDF DEV.
240     write (6,460)
        read (lunit,1040) ierbr
        if (ierbr.eq.0) go to 250
        write (6,430)
        read (lunit,1040) devbr
c
250     go to 180
c
c       STOG COMPUTES SPACE TO GROUND INTERCEPTIBILITY
c
260     call stog (comp,ptstog,prstog,pastog,nret)
c
c       WRITE OUTPUT FOR SPACE TO GROUND CASE
c
        write (6,920)
        write (6,930)
        if (ibflag.eq.1) write (6,940) sigj,grndi
        write (6,950) rb,nvel,svel,svel,avel
        ndy=2*ncros-1
        ndown=ndown-1
        write (6,960) kount,ndown,ndy,numtot
        write (6,970) xdis,hdis,hdisdf
        write (6,980) xclos,hclos,hclsdf
        write (6,990) pastog,ptstog,prstog,comp
```

```
c
270    n=1+iotype
       go to (280,10), n
       if (nout.ne.6) close (nout)
280    stop
c
c
290    format ("1")
300    format (9x,"off-axis analysis program -- ",/,
&      15x,"enter 1 for interactive input - 0 for batch input")
310    format (i1)
320    format (22x,18a4,//)
330    format (4x,18a4)
340    format (i4,6e10.4)
350    format (4x,6e10.4)
360    format (//,5x,"interceptibility mode ",i2)
370    format (5x,"* iteration did not converge at ",i3," points")
380    format (10x,"do you want an input summary?     0-no  1-yes")
390    format (//,10x,"do you want an output table?   0-no 1-yes")
400    format (10x,"which file?  (must be allocated)")
410    format (//10x,"do you wish to do a sensitivity analysis? ",
&      "0-no 1-yes")
420    format (/10x,"do you wish to vary the absorption coef? ",
&      "0-no 1-yes")
430    format (/10x,"fractional change (eg .1 for 10%)",/,15x,
&      "default =.1")
440    format (/10x,"do you wish to vary the scattering coef? ",
&      "0-no 1-yes")
460    format (/10x,"do you wish to vary the bsdf? 0-no 1-yes")
480    format (///,20x,"***      input summary      ***")
490    format (///5x,"scenario geometry"/)
500    format (6x,"link range, m ----",2x,1pe10.3,5x,"tr alt, m --------",
&      2x,1pe10.3)
510    format (6x,"rc alt, m --------",2x,1pe10.3,5x,"sr alt, m --------",
&      2x,1pe10.3)
520    format (6x,"background type --",4x,2a4)
530    format (6x,"sr dist to beam,m-",2x,1pe10.3,5x,"sr zenith ang, d-",
&      6x,0pf6.2)
540    format (6x,"ground alt, m-----",7x,f5.2,5x,"linkbeam rad. m--",2x,
&      1pe10.3)
550    format (6x,"ground alt,m-----",7x,f5.2)
560    format (/5x,"link parameters"/)
570    format (6x,"wavelength, m ----",2x,1pe10.3,5x,"tr power, w -----",
&      2x,1pe10.3)
580    format (6x,"wavelength, m ----",2x,1pe10.3,5x,"eqv. irr., w/sq.m",
&      2x,1pe10.3)
590    format (6x,"rc aperture, m ---",4x,f8.5,5x,"tr aperture, m --",4x,
&      f8.5)
600    format (6x,"rc hood length, m-",7x,f5.2,5x,"tr hood length, m",7x,
&      f5.2)
```

```
610     format (6x,"rc hood dia., m --",7x,f5.2,5x,"tr hood dia., m -",7x,
&       f5.2)
620     format (6x,"total jitter,r ---",2x,1pe10.3,5x,"turbulence ------",
&       4x,2a4)
625     format (41x,"turbulence ------",4x,2a4)
630     format (41x,"tr beam width,rad",2x,1pe10.3)
640     format (/,5x,"sr parameters"/)
650     format (6x,"linear fov, rad  -",2x,1pe10.3,5x,"aperture, sq.m. -",
&       6x,0pf6.4)
660     format (6x,"fov (elev), rad  -",2x,1pe10.3,5x,"fov (az), rad ---",
&       2x,1pe10.3,/,6x,"aperture, sq.m ---",6x,0pf6.4)
670     format (6x,"fov across beam, r",2x,1pe10.3,5x,"detection type, -",
&       8x,a4)
680     format (6x,"opt bw, microns --",2x,1pe10.3)
681     format (6x,"dark current, a --",2x,1pe10.3,5x,"thermal eqv pwr -",
&       2x,1pe10.3)
685     format (6x,"opt bw, microns --",2x,1pe10.3,5x,"mixing efficiency",
&       6x,0pf6.4)
686     format (6x,"bit interval, s --",2x,1pe10.3)
690     format (6x,"gain ------------",7x,f5.2,5x,"excess noise ----",2x,
&       1pe10.3)
695     format (6x,"mod. depth -------",7x,f5.2)
700     format (6x,"bandwidth, hz ----",2x,1pe10.3,5x,"quantum eff. ----",
&       7x,0pf5.2)
720     format (/,5x,"intercept mode parameters"/)
730     format (6x,"mode type --------",10x,i2,5x,"output type -----",4x,
&       2a4)
740     format (6x,"sr plane, deg ----",5x,f7.2,5x,"specular gamint -",5x,
&       f7.2)
750     format (6x,"backstop az, deg  ",5x,f7.2,5x,"backstop el, deg ",5x,
&       f7.2)
760     format (6x,"rpx, meters ------",2x,1pe10.3,5x,"x, meters -------",
&       2x,1pe10.3)
770     format (6x,"iso-con value, db-",2x,1pe10.3)
780     format (/,5x,"atmospheric parameters"/)
790     format (6x,"scat coef 1/m ----",2x,1pe10.3,5x,"abs coef, 1/m ---",
&       2x,1pe10.3)
800     format (6x,"data source ------",8x,a4)
810     format (6x,"results are valid only for cases with near ",
&       "coaltitude geometry")
820     format (6x,5a4,15x,"visibility is",9x,2a4,/,17x,"coefficients ",
&       "for 0 to 1000 meters altitude")
830     format (//,5x,"scattering data for transmitter, receiver, and ",
&       "backstop")
840     format (/,6x,"bsdf model type --",4x,2a4,5x,"bsdf slope db/db ",
&       5x,f7.3)
850     format (6x,"nonlinearities ---",11x,i1,5x,"bsdf intercept - ",5x,
&       f7.3)
860     format (11x,"from",5x,"to",7x,"level",3(/,6x,0pi3,0pf7.2,0pf8.2,
&       1pe12.4))
```

```
 870   format (/,6x,"backstop type ----",2x,"lambertian",5x,
&      "reflection coef -",5x,f7.4)
 880   format (/,6x,"backstop type ----",4x,2a4,5x,"diffuse level ---",
&      5x,f7.3)
 890   format (6x,"specular max    --",5x,f7.3,5x,"specular width, d",5x,
&      f7.3)
 900   format (/,6x,"oa type ----------",4x,2a4,5x,"diffuse level ---",
&      5x,f7.3)
 910   format (//,40x,"power contributed by each source, watts",/,7x,2a4,
&      6x,2a4,11x,"transmitter    receiver    atmosphere")
 920   format (///)
 930   format (20x,"***    space to ground   ***")
 940   format (//5x,"turbulence beam spread (rad) -------------",1pe10.3,
&      /5x,"equivalent irradiance (w/sq.m) -----------",1pe10.3)
 950   format (//5x,"radius of transmitter beam (m) -----------",f8.2,/,
&      5x,"no. of elements in beam -------------------",i8,/8x,
&      "configuration of element --------------",2x,"square",/11x,
&      "length of element (m)  --------------",f8.2,/11x,"width of ",
&      "element (m)  --------------",f8.2,/11x,"area of element (sq.m) ",
&      "--------------",f8.2)
 960   format (//5x,"no.of vert. elements subtended by rcvr----",i8,/8x,
&      "no. of elements down beam (x-dir) -----",i8,/8x,"no. of ",
&      "elements across beam (y-dir) ---",i8,/8x,"total no. of ",
&      "elemental volumes --------",i8)
 970   format (//8x,"dist. to the farthest element ----------",1pe10.3,/,
&      8x,"altitude of the farthest element ------",1pe10.3,/8x,"alt. ",
&      "difference of subtended element --",1pe10.3)
 980   format (//8x,"dist. to the closest element ----------",1pe10.3,/,
&      8x,"altitude of the closest element -------",1pe10.3,/8x,"alt. ",
&      "difference of subtended element --",1pe10.3)
 990   format (///5x,"power contributions",/,8x,"atmospheric power ",
&      "contribution (watts)-",1pe10.3,/,8x,"transmitter power ",
&      "contribution (watts)-",1pe10.3,/,8x,"receiver power ",
&      "contribution (watts)----",1pe10.3,//,5x,"total power (watts)",
&      "----------------------",1pe10.3)
1000   format (//,13x,"***  sensitivity analysis summary  ***",//,10x,
&      "contributor",8x,"fractional deviation")
1010   format (/,11x,"scattering",15x,f8.3)
1020   format (/,11x,"absorption",15x,f8.3)
1030   format (/,11x,"bsdf",21x,f8.3)
1040   format(v)
       end
c.
       block data
c
       common/ flags /mode,mcomp,mp,lam,modesw,lunit,nout,istog,iotype,
&      irtype,ihet,ibflag,iw
       common/rsct/oasmax,diffoa,oafwhm,bmaxs,bfwhms,bdiff(6),psiaz,psiel
&      ,gams
       common/atmos/ alfa(5,2),alfsct,alfab,ia,ab(33),as(33),at(33,14,6)
```

```
     &      ,mat,mvis
            common/ tdata / blt,dt,ht,phit,pt,rb,grndi,bdrt,sigj,sigt
            common/ rdata / blr,dr,hr,gl,bdlr
            common/ srdata / asr,hs,phi,phiaz,dphi
            common/ ldata / rl,alam,rpx,theta,x,angtr,angrec,gamint,bw
     c  * darki & ptherm replace pnep, add g *
            common/ sndata / bwr,eta,f,em,pb,ps,darki,ptherm,snpndb,sndb,xm,
     &      bwopt,nflg,g
            common/ tbsdf / ng,gstart(3),gend(3),gampl(3),ybsdf,sbsdf,nbak,noa
     &      ,ibsdf
            common /pltc  / xint(200),yint(200),h(200),dcomp(2),np,note
     c  * srdark & srther replace srpnep *
            common/ block1 / xmod(6),gainsr(6),qe(6),fnoise(6),srbw(6),
     &      srdark(6),srther(6),alamda(6),obw(6),nhol(6)
     c  * dimension heady1 & heady2 (2by3)
            common/ hrith / title(18),headx1(2,2),headx2(2,2),heady1(2,3),
     &      heady2(2,3),brhol(2),bakhol(2),oahol(2),mattyp(5,5),mvtyp(2,2),
     &      mathol(2),holdet(2),holiw(2,3)
            common/err/ier,ierab,iersc,ierbr,devab,devsc,devbr
     c  * add labeled common wavefm *
            common/ wavefm /npts,t,form0(1000),form1(1000),power0(1000),
     &      power1(1000)
     c
            dimension at11(33),at12(33),at13(33),at14(33),at15(33),
     &             at16(33),at17(33),at18(33),at19(33),at10(33),
     &             at1a(33),at1b(33),at1c(33),at1d(33)
            dimension at21(33),at22(33),at23(33),at24(33),at25(33),
     &             at26(33),at27(33),at28(33),at29(33),at20(33),
     &             at2a(33),at2b(33),at2c(33),at2d(33)
            dimension at31(33),at32(33),at33(33),at34(33),at35(33),
     &             at36(33),at37(33),at38(33),at39(33),at30(33),
     &             at3a(33),at3b(33),at3c(33),at3d(33)
            dimension at41(33),at42(33),at43(33),at44(33),at45(33),
     &             at46(33),at47(33),at48(33),at49(33),at40(33),
     &             at4a(33),at4b(33),at4c(33),at4d(33)
            dimension at51(33),at52(33),at53(33),at54(33),at55(33),
     &             at56(33),at57(33),at58(33),at59(33),at50(33),
     &             at5a(33),at5b(33),at5c(33),at5d(33)
            dimension at61(33),at62(33),at63(33),at64(33),at65(33),
     &             at66(33),at67(33),at68(33),at69(33),at60(33),
     &             at6a(33),at6b(33),at6c(33),at6d(33)
            equivalence (at(1,1,1),at11(1)),(at(1,2,1),at12(1)),
     &             (at(1,3,1),at13(1)),(at(1,4,1),at14(1)),
     &             (at(1,5,1),at15(1)),(at(1,6,1),at16(1)),
     &             (at(1,7,1),at17(1)),(at(1,8,1),at18(1)),
     &             (at(1,9,1),at19(1)),(at(1,10,1),at10(1)),
     &             (at(1,11,1),at1a(1)),(at(1,12,1),at1b(1)),
     &             (at(1,13,1),at1c(1)),(at(1,14,1),at1d(1))
            equivalence (at(1,1,2),at21(1)),(at(1,2,2),at22(1)),
     &             (at(1,3,2),at23(1)),(at(1,4,2),at24(1)),
```

```
      &                    (at(1,5,2),at25(1)),(at(1,6,2),at26(1)),
      &                    (at(1,7,2),at27(1)),(at(1,8,2),at28(1)),
      &                    (at(1,9,2),at29(1)),(at(1,10,2),at20(1)),
      &                    (at(1,11,2),at2a(1)),(at(1,12,2),at2b(1)),
      &                    (at(1,13,2),at2c(1)),(at(1,14,2),at2d(1))
            equivalence (at(1,1,3),at31(1)),(at(1,2,3),at32(1)),
      &                    (at(1,3,3),at33(1)),(at(1,4,3),at34(1)),
      &                    (at(1,5,3),at35(1)),(at(1,6,3),at36(1)),
      &                    (at(1,7,3),at37(1)),(at(1,8,3),at38(1)),
      &                    (at(1,9,3),at39(1)),(at(1,10,3),at30(1)),
      &                    (at(1,11,3),at3a(1)),(at(1,12,3),at3b(1)),
      &                    (at(1,13,3),at3c(1)),(at(1,14,3),at3d(1))
            equivalence (at(1,1,4),at41(1)),(at(1,2,4),at42(1)),
      &                    (at(1,3,4),at43(1)),(at(1,4,4),at44(1)),
      &                    (at(1,5,4),at45(1)),(at(1,6,4),at46(1)),
      &                    (at(1,7,4),at47(1)),(at(1,8,4),at48(1)),
      &                    (at(1,9,4),at49(1)),(at(1,10,4),at40(1)),
      &                    (at(1,11,4),at4a(1)),(at(1,12,4),at4b(1)),
      &                    (at(1,13,4),at4c(1)),(at(1,14,4),at4d(1))
            equivalence (at(1,1,5),at51(1)),(at(1,2,5),at52(1)),
      &                    (at(1,3,5),at53(1)),(at(1,4,5),at54(1)),
      &                    (at(1,5,5),at55(1)),(at(1,6,5),at56(1)),
      &                    (at(1,7,5),at57(1)),(at(1,8,5),at58(1)),
      &                    (at(1,9,5),at59(1)),(at(1,10,5),at50(1)),
      &                    (at(1,11,5),at5a(1)),(at(1,12,5),at5b(1)),
      &                    (at(1,13,5),at5c(1)),(at(1,14,5),at5d(1))
            equivalence (at(1,1,6),at61(1)),(at(1,2,6),at62(1)),
      &                    (at(1,3,6),at63(1)),(at(1,4,6),at64(1)),
      &                    (at(1,5,6),at65(1)),(at(1,6,6),at66(1)),
      &                    (at(1,7,6),at67(1)),(at(1,8,6),at68(1)),
      &                    (at(1,9,6),at69(1)),(at(1,10,6),at60(1)),
      &                    (at(1,11,6),at6a(1)),(at(1,12,6),at6b(1)),
      &                    (at(1,13,6),at6c(1)),(at(1,14,6),at6d(1))
      c     **********************************************************
            data mode,mcomp,mp,lam,modesw,lunit,nout,istog/4,1,1,4,1,5,1,0/
      c * add Pr(e) heading for mode 6 *
            data heady1,heady2/"pwr ","s/n ","rpx ","rpx ","   p","   p",
      &     " dbw"," db ","  m ","  m ","r(e)","r(e)"/
            data headx1,headx2/"thet","thet","x,me","x,me","a, d","a, d",
      &     "ters","ters"/
            data brhol,bakhol,oahol/" ave","rage"," dif","fuse"," unk","nown"/
            data mattyp/"trop","ical","    ","    ","    ","    ",
      &     "midl","atit","ude ","summ","er  ",
      &     "midl","atit","ude ","wint","er  ",
      &     "suba","rcti","c   ","summ","er  ",
      &     "suba","rcti","c   ","wint","er  "/
            data mvtyp/"clea","r   ","hazy","    "/
            data mathol/"user","afgl"/
            data holdet/" dir"," het"/
            data holiw/"  se","vere","mode","rate","    ","mild"/
```

```
      data blt,dbrt,dt,ht,pt/0.0,0.0,.1,10.,1./
      data blr,dblr,dr,hr/0.0,0.0,.1,10./
      data asr,hs,phi,phiaz/.05,10.,.01,.01/
      data alam,rl,rpx,x/1.0e-6,5000.,2500.,1000./
c   * add default values for darki & ptherm *
      data bwr,eta,f,em,pb,darki,ptherm,xm,bwopt,g/0.0,0.0,0.0,0.7,
   &  0.0,0.0,0.0,0.0,0.0,0.0/
      data rb,grndi,gl,theta/200.,1.e-4,0.,.174533/
c     MODULATION DEPTH AND SR ELECTICAL BANDWIDTH
      data xmod,bw/1.,1.,1.,1.,1.,1.,1.e6/
      data gstart/0.,0.,0./
      data gend/0.,0.,0./
      data gampl/0.,0.,0./
      data bmaxs,bfwhms,bdiff,oasmax,diffoa,oafwhm/0.,3.,.3,.3,.3,.3,.1,
   &  .3,0.,0.,.3/
      data gainsr/1.,1.,1.,1.,1.,1./
      data qe/.5,.5,.75,.5,.6,0.7/
      data fnoise/1.,1.,1.,1.,1.,1./
      data srbw/1.0e6,1.0e6,1.0e6,1.0e6,1.0e6,1.0e6/
c   * add data for srdark & srther *
      data srdark/6*1.e-9/
      data srther/8.e-15,8.e-15,5.e-15,7.e-15,5.e-17,1.e-12/
      data alamda/.5145e-6,.6328e-6,.860e-6,1.06e-6,10.6e-6,0/
      data obw/.001,.001,.001,.001,.01,.05/
      data alfa/5.e-5,5.e-5,5.e-5,5.e-5,5.e-5,5.e-5,5.e-5,5.e-5,5.e-5,
   &  5.e-5/
      data ng,ybsdf,sbsdf/0,200.,-2.5/
      data nflg,irtype/1,2/
      data nhol/"   s","unny"," cl","oudy","   n","ight"/
      data ibsdf,nbak,noa/1,1,1/
      data gamint/0./
      data note/0/
      data ia,mat,mvis/1,2,1/
      data dcomp/-80.,0./
      data phit/.0001/
      data ier,ierab,iersc,ierbr/0,0,0,0/
      data devab,devsc,devbr/.1,.1,.1/
      data psiaz,psiel,gams/0.,0.,0./
      data ihet/o/
      data ibflag,iw,sigj/1,2,5.e-6/
c   * aadd data for labeled common wavefm *
      data npts,t,form0,form1/101,1.e-6,51*1.0,949*0.0,50*0.0,51*1.0,
   &  899*0.0/
c     ********************************************************
c        NOTE - UNITS ARE 1/KM., BUT ARE CONVERTED TO 1/M IN PROGRAM
c
c
c        WAVELENGTH IS .5145 MICRONS
c
c        TROPICAL MOLECULAR ABSORPTION
```

```
c
      data at11/
&     0.0     , 0.0    , 0.0    , 0.0    , 0.0    , 0.0      ,
&     0.0     , 0.0    , 0.0    , 0.0    , 0.0    , 0.0      ,
&     0.0     , 0.0    , 0.0    , 0.0    , 0.0    , 0.0      ,
&     0.0     , 0.0    , 0.0    , 0.0    , 0.0    , 0.0      ,
&     0.0     , 0.0    , 0.0    , 0.0    , 0.0    , 0.0      ,
&     0.0     , 0.0    , 0.0    /
c
c     TROPICAL MOLECULAR SCATTERING
c
      data at12/
&     1.47e-02, 1.40e-02, 1.28e-02, 1.15e-02, 1.04e-02, 9.46e-03,
&     8.55e-03, 7.70e-03, 6.94e-03, 6.22e-03, 5.55e-03, 4.96e-03,
&     4.40e-03, 3.89e-03, 3.44e-03, 3.02e-03, 2.63e-03, 2.27e-03,
&     1.91e-03, 1.57e-03, 1.31e-03, 1.09e-03, 9.08e-04, 7.64e-04,
&     6.48e-04, 5.50e-04, 3.67e-04, 1.68e-04, 7.97e-05, 3.91e-05,
&     1.99e-05, 7.45e-06, 0.0     /
c
c     MIDLATITUDE SUMMER MOLECULAR ABSORPTION
c
      data at13/
&     0.0     , 0.0    , 0.0    , 0.0    , 0.0    , 0.0      ,
&     0.0     , 0.0    , 0.0    , 0.0    , 0.0    , 0.0      ,
&     0.0     , 0.0    , 0.0    , 0.0    , 0.0    , 0.0      ,
&     0.0     , 0.0    , 0.0    , 0.0    , 0.0    , 0.0      ,
&     0.0     , 0.0    , 0.0    , 0.0    , 0.0    , 0.0      ,
&     0.0     , 0.0    , 0.0    /
c
c     MIDLATITUDE SUMMER MOLECULAR SCATTERING
c
      data at14/
&     1.50e-02, 1.43e-02, 1.29e-02, 1.16e-02, 1.05e-02, 9.51e-02,
&     8.56e-02, 7.68e-02, 6.89e-02, 6.16e-03, 6.50e-03, 4.90e-03,
&     4.36e-03, 3.85e-03, 3.34e-03, 2.85e-03, 2.42e-03, 2.07e-03,
&     1.77e-03, 1.51e-03, 1.29e-03, 1.10e-03, 9.38e-04, 8.00e-04,
&     6.82e-04, 5.83e-04, 3.91e-04, 1.80e-04, 8.59e-05, 4.22e-05,
&     2.17e-05, 8.16e-06, 0.0     /
c
c     MIDLATITUDE WINTER MOLECULAR ABSORPTION
c
      data at15/
&     0.0     , 0.0    , 0.0    , 0.0    , 0.0    , 0.0      ,
&     0.0     , 0.0    , 0.0    , 0.0    , 0.0    , 0.0      ,
&     0.0     , 0.0    , 0.0    , 0.0    , 0.0    , 0.0      ,
&     0.0     , 0.0    , 0.0    , 0.0    , 0.0    , 0.0      ,
&     0.0     , 0.0    , 0.0    , 0.0    , 0.0    , 0.0      ,
&     0.0     , 0.0    , 0.0    /
c
c     MIDLATITUDE WINTER MOLECULAR SCATTERING
```

```
c
         data at16/
&        1.63e-02, 1.54e-02, 1.37e-02, 1.22e-02, 1.09e-02, 9.79e-03,
&        8.75e-03, 7.80e-03, 6.93e-03, 6.14e-03, 5.42e-03, 4.72e-03,
&        4.05e-03, 3.47e-03, 2.98e-03, 2.55e-03, 2.19e-03, 1.88e-03,
&        1.61e-03, 1.38e-03, 1.18e-03, 1.01e-03, 8.57e-04, 7.32e-04,
&        6.26e-04, 5.34e-04, 3.56e-04, 1.60e-04, 7.20e-05, 3.35e-05,
&        1.64e-05, 6.01e-06, 0.0      /
c
c        SUBARCTIC SUMMER MOLECULAR ABSORPTION
c
         data at17/
&        0.0      , 0.0      , 0.0      , 0.0      , 0.0      , 0.0      ,
&        0.0      , 0.0      , 0.0      , 0.0      , 0.0      , 0.0      ,
&        0.0      , 0.0      , 0.0      , 0.0      , 0.0      , 0.0      ,
&        0.0      , 0.0      , 0.0      , 0.0      , 0.0      , 0.0      ,
&        0.0      , 0.0      , 0.0      , 0.0      , 0.0      , 0.0      ,
&        0.0      , 0.0      , 0.0      /
c
c        SUBARCTIC SUMMER MOLECULAR SCATTERING
c
         data at18/
&        1.53e-02, 1.46e-02, 1.32e-02, 1.19e-02, 1.06e-02, 9.55e-03,
&        8.58e-03, 7.71e-03, 6.91e-03, 6.17e-03, 5.50e-03, 4.81e-03,
&        4.13e-03, 3.55e-03, 3.05e-03, 2.62e-03, 2.25e-03, 1.94e-03,
&        1.67e-03, 1.43e-03, 1.23e-03, 1.06e-03, 9.11e-04, 7.83e-04,
&        6.72e-04, 5.75e-04, 3.89e-04, 1.82e-04, 8.64e-05, 4.26e-05,
&        2.21e-05, 8.45e-06, 0.0      /
c
c        SUBARCTIC WINTER MOLECULAR ABSORPTION
c
         data at19/
&        0.0      , 0.0      , 0.0      , 0.0      , 0.0      , 0.0      ,
&        0.0      , 0.0      , 0.0      , 0.0      , 0.0      , 0.0      ,
&        0.0      , 0.0      , 0.0      , 0.0      , 0.0      , 0.0      ,
&        0.0      , 0.0      , 0.0      , 0.0      , 0.0      , 0.0      ,
&        0.0      , 0.0      , 0.0      , 0.0      , 0.0      , 0.0      ,
&        0.0      , 0.0      , 0.0      /
c
c        SUBARCTIC WINTER MOLECULAR SCATTERING
c
         data at10/
&        1.71e-02, 1.60e-02, 1.41e-02, 1.25e-02, 1.10e-02, 9.86e-03,
&        8.80e-03, 7.83e-03, 6.94e-03, 6.09e-03, 5.25e-03, 4.49e-03,
&        3.84e-03, 3.28e-03, 2.80e-03, 2.40e-03, 2.05e-03, 1.76e-03,
&        1.51e-03, 1.29e-03, 1.10e-03, 9.44e-04, 8.07e-04, 6.90e-04,
&        5.90e-04, 5.04e-04, 3.36e-04, 1.49e-04, 6.67e-05, 3.06e-05,
&        1.46e-05, 5.15e-06, 0.0      /
c
c        AEROSOL ABSORPTION - CLEAR
```

```
c
        data at1a/
&       0.0     , 0.0     , 0.0     , 0.0     , 0.0     , 0.0     ,
&       0.0     , 0.0     , 0.0     , 0.0     , 0.0     , 0.0     ,
&       0.0     , 0.0     , 0.0     , 0.0     , 0.0     , 0.0     ,
&       0.0     , 0.0     , 0.0     , 0.0     , 0.0     , 0.0     ,
&       0.0     , 0.0     , 0.0     , 0.0     , 0.0     , 0.0     ,
&       0.0     , 0.0     , 0.0     /
c
c       AEROSOL SCATTERING - CLEAR
c
        data at1b/
&       1.68e-01, 1.12e-01, 4.86e-02, 2.07e-02, 9.76e-03, 6.16e-03,
&       4.49e-03, 3.64e-03, 3.56e-03, 3.54e-03, 3.42e-03, 3.27e-03,
&       3.24e-03, 3.19e-03, 3.04e-03, 2.91e-03, 2.75e-03, 2.67e-03,
&       2.61e-03, 2.36e-03, 1.85e-03, 1.35e-03, 9.98e-04, 7.58e-04,
&       5.90e-04, 4.82e-04, 2.43e-04, 6.83e-05, 1.80e-05, 4.73e-06,
&       1.25e-06, 0.0     , 0.0     /
c
c       AEROSOL ABSORPTION - HAZY
c
        data at1c/
&       0.0     , 0.0     , 0.0     , 0.0     , 0.0     , 0.0     ,
&       0.0     , 0.0     , 0.0     , 0.0     , 0.0     , 0.0     ,
&       0.0     , 0.0     , 0.0     , 0.0     , 0.0     , 0.0     ,
&       0.0     , 0.0     , 0.0     , 0.0     , 0.0     , 0.0     ,
&       0.0     , 0.0     , 0.0     , 0.0     , 0.0     , 0.0     ,
&       0.0     , 0.0     , 0.0     /
c
c       AEROSOL SCATTERING - HAZY
c
        data at1d/
&       8.20e-01, 4.96e-01, 1.81e-01, 6.63e-02, 2.42e-02, 8.84e-03,
&       4.49e-03, 3.64e-03, 3.56e-03, 3.54e-03, 3.42e-03, 3.27e-03,
&       3.24e-03, 3.19e-03, 3.04e-03, 2.91e-03, 2.75e-03, 2.67e-03,
&       2.61e-03, 2.36e-03, 1.85e-03, 1.35e-03, 9.98e-04, 7.58e-04,
&       5.90e-04, 4.82e-04, 2.43e-04, 6.83e-05, 1.80e-05, 4.73e-06,
&       1.25e-06, 0.0     , 0.0     /
c**********************************************************
c
c       WAVELENGTH IS .6328 MICRONS
c
c       TROPICAL MOLECULAR ABSORPTION
c
        data at21/
&       0.0     , 0.0     , 0.0     , 0.0     , 0.0     , 0.0     ,
&       0.0     , 0.0     , 0.0     , 0.0     , 0.0     , 0.0     ,
&       0.0     , 0.0     , 0.0     , 0.0     , 0.0     , 0.0     ,
&       0.0     , 0.0     , 0.0     , 0.0     , 0.0     , 0.0     ,
&       0.0     , 0.0     , 0.0     , 0.0     , 0.0     , 0.0     ,
```

```
&        0.0      , 0.0      , 0.0      /
c
c        TROPICAL MOLECULAR SCATTERING
c
         data at22/
&        6.31e-03, 6.03e-03, 5.48e-03, 4.97e-03, 4.49e-03, 4.07e-03,
&        3.68e-03, 3.31e-03, 2.99e-03, 2.67e-03, 2.39e-03, 2.13e-03,
&        1.89e-03, 1.67e-03, 1.48e-03, 1.30e-03, 1.13e-03, 9.76e-04,
&        8.20e-04, 6.77e-04, 5.62e-04, 4.68e-04, 3.91e-04, 3.29e-04,
&        2.79e-04, 2.37e-04, 1.58e-04, 7.22e-05, 3.43e-05, 1.68e-05,
&        3.57e-06, 3.20e-06, 0.0      /
c
c        MIDLATITUDE SUMMER MOLECULAR ABSORPTION
c
         data at23/
&        0.0      , 0.0      , 0.0      , 0.0      , 0.0      , 0.0      ,
&        0.0      , 0.0      , 0.0      , 0.0      , 0.0      , 0.0      ,
&        0.0      , 0.0      , 0.0      , 0.0      , 0.0      , 0.0      ,
&        0.0      , 0.0      , 0.0      , 0.0      , 0.0      , 0.0      ,
&        0.0      , 0.0      , 0.0      , 0.0      , 0.0      , 0.0      ,
&        0.0      , 0.0      , 0.0      /
c
c        MIDLATITUDE SUMMER MOLECULAR SCATTERING
c
         data at24/
&        6.44e-03, 6.13e-03, 5.54e-03, 5.01e-03, 4.53e-03, 4.09e-03,
&        3.68e-03, 3.31e-03, 2.96e-03, 2.66e-03, 2.37e-03, 2.11e-03,
&        1.87e-03, 1.66e-03, 1.44e-03, 1.23e-03, 1.04e-03, 8.92e-04,
&        7.63e-04, 6.51e-04, 5.55e-04, 4.73e-04, 4.03e-04, 3.44e-04,
&        2.93e-04, 2.51e-04, 1.68e-04, 7.76e-05, 3.69e-05, 1.82e-05,
&        9.31e-06, 3.51e-06, 0.0      /
c
c        MIDLATITUDE WINTER MOLECULAR ABSORPTION
c
         data at25/
&        0.0      , 0.0      , 0.0      , 0.0      , 0.0      , 0.0      ,
&        0.0      , 0.0      , 0.0      , 0.0      , 0.0      , 0.0      ,
&        0.0      , 0.0      , 0.0      , 0.0      , 0.0      , 0.0      ,
&        0.0      , 0.0      , 0.0      , 0.0      , 0.0      , 0.0      ,
&        0.0      , 0.0      , 0.0      , 0.0      , 0.0      , 0.0      ,
&        0.0      , 0.0      , 0.0      /
c
c        MIDLATITUDE WINTER MOLECULAR SCATTERING
c
         data at26/
&        6.79e-03, 6.62e-03, 5.91e-03, 5.26e-03, 4.70e-03, 4.21e-03,
&        3.76e-03, 3.35e-03, 2.98e-03, 2.64e-03, 2.33e-03, 2.03e-03,
&        1.74e-03, 1.49e-03, 1.28e-03, 1.10e-03, 9.41e-04, 8.07e-04,
&        6.91e-04, 5.91e-04, 5.06e-04, 4.32e-04, 3.69e-04, 3.15e-04,
&        2.69e-04, 2.30e-04, 1.53e-04, 6.90e-05, 3.10e-05, 1.44e-05,
```

```
&       7.06e-06, 2.59e-06, 0.0      /
c
c       SUBARCTIC SUMMER MOLECULAR ABSORPTION
c
        data at27/
&       0.0      , 0.0     , 0.0      , 0.0      , 0.0      , 0.0       ,
&       0.0      , 0.0     , 0.0      , 0.0      , 0.0      , 0.0       ,
&       0.0      , 0.0     , 0.0      , 0.0      , 0.0      , 0.0       ,
&       0.0      , 0.0     , 0.0      , 0.0      , 0.0      , 0.0       ,
&       0.0      , 0.0     , 0.0      , 0.0      , 0.0      , 0.0       ,
&       0.0      , 0.0     , 0.0      /
c
c       SUBARCTIC SUMMER MOLECULAR SCATTERING
c
        data at28/
&       6.58e-03, 6.26e-03, 5.66e-03, 5.10e-03, 4.58e-03, 4.11e-03,
&       3.69e-03, 3.32e-03, 2.97e-03, 2.66e-03, 2.36e-03, 2.07e-03,
&       1.78e-03, 1.53e-03, 1.31e-03, 1.13e-03, 9.68e-04, 8.34e-04,
&       7.17e-04, 6.17e-04, 5.30e-04, 4.55e-04, 3.92e-04, 3.37e-04,
&       2.89e-04, 2.48e-04, 1.67e-04, 7.83e-05, 3.72e-05, 1.83e-05,
&       9.51e-06, 3.64e-06, 0.0      /
c
c       SUBARCTIC WINTER MOLECULAR ABSORPTION
c
        data at29/
&       0.0      , 0.0     , 0.0      , 0.0      , 0.0      , 0.0       ,
&       0.0      , 0.0     , 0.0      , 0.0      , 0.0      , 0.0       ,
&       0.0      , 0.0     , 0.0      , 0.0      , 0.0      , 0.0       ,
&       0.0      , 0.0     , 0.0      , 0.0      , 0.0      , 0.0       ,
&       0.0      , 0.0     , 0.0      , 0.0      , 0.0      , 0.0       ,
&       0.0      , 0.0     , 0.0      /
c
c       SUBARCTIC WINTER MOLECULAR SCATTERING
c
        data at20/
&       7.37e-03, 6.88e-03, 6.04e-03, 5.36e-03, 4.75e-03, 4.24e-03,
&       3.79e-03, 3.37e-03, 2.99e-03, 2.62e-03, 2.26e-03, 1.93e-03,
&       1.65e-03, 1.41e-03, 1.21e-03, 1.03e-03, 8.82e-04, 7.56e-04,
&       6.47e-04, 5.54e-04, 4.75e-04, 4.06e-04, 3.47e-04, 2.97e-04,
&       2.54e-04, 2.17e-04, 1.44e-04, 6.39e-05, 2.87e-05, 1.32e-05,
&       6.27e-06, 2.22e-06, 0.0      /
c
c       AEROSOL ABSORPTION - CLEAR
c
        data at2a/
&       3.14e-03, 2.09e-03, 9.09e-04, 3.87e-04, 1.82e-04, 1.15e-04,
&       8.39e-05, 6.78e-05, 6.65e-05, 6.61e-05, 6.39e-05, 6.11e-05,
&       6.06e-05, 5.97e-05, 5.67e-05, 5.44e-05, 5.14e-05, 4.99e-05,
&       4.88e-05, 4.40e-05, 3.46e-05, 2.52e-05, 1.87e-05, 1.42e-05,
&       1.10e-05, 9.00e-06, 4.53e-06, 1.28e-06, 0.0      , 0.0       ,
```

```
&         0.0     , 0.0     , 0.0      /
c
c         AEROSOL SCATTERING - CLEAR
c
      data at2b/
&       1.36e-01, 9.03e-02, 3.93e-02, 1.67e-02, 7.89e-03, 4.98e-03,
&       3.63e-03, 2.94e-03, 2.88e-03, 2.86e-03, 2.77e-03, 2.64e-03,
&       2.62e-03, 2.58e-03, 2.45e-03, 2.35e-03, 2.23e-03, 2.16e-03,
&       2.11e-03, 1.91e-03, 1.50e-03, 1.09e-03, 8.07e-04, 6.13e-04,
&       4.77e-04, 3.90e-04, 1.96e-04, 5.52e-05, 1.45e-05, 3.83e-06,
&       1.01e-06, 0.0     , 0.0      /
c
c         AEROSOL ABSORPTION - HAZY
c
      data at2c/
&       1.53e-02, 9.26e-03, 3.39e-03, 1.24e-03, 4.52e-04, 1.65e-04,
&       8.39e-05, 6.79e-05, 6.65e-05, 6.61e-05, 6.39e-05, 6.11e-05,
&       6.06e-05, 5.97e-05, 5.67e-05, 5.44e-05, 5.14e-05, 4.99e-05,
&       4.88e-05, 4.40e-05, 3.46e-05, 2.52e-05, 1.87e-05, 1.42e-05,
&       1.10e-05, 9.00e-06, 4.53e-06, 1.28e-06, 0.0     , 0.0     ,
&       0.0     , 0.0     , 0.0      /
c
c         AEROSOL SCATTERING - HAZY
c
      data at2d/
&       6.63e-01, 4.01e-01, 1.47e-01, 5.36e-02, 1.96e-02, 7.14e-03,
&       3.63e-03, 2.94e-03, 2.88e-03, 2.86e-03, 2.77e-03, 2.64e-03,
&       2.62e-03, 2.58e-03, 2.45e-03, 2.35e-03, 2.23e-03, 2.16e-03,
&       2.11e-03, 1.91e-03, 1.50e-03, 1.09e-03, 8.07e-04, 6.13e-04,
&       4.77e-04, 3.90e-04, 1.96e-04, 5.52e-05, 1.45e-05, 3.83e-06,
&       1.01e-06, 0.0     , 0.0      /
c     ************************************************************
c
c         WAVELENGTH IS .860 MICRONS
c
c         TROPICAL MOLECULAR ABSORPTION
c
      data at31/
&       0.0     , 0.0     , 0.0     , 0.0     , 0.0     , 0.0      ,
&       0.0     , 0.0     , 0.0     , 0.0     , 0.0     , 0.0      ,
&       0.0     , 0.0     , 0.0     , 0.0     , 0.0     , 0.0      ,
&       0.0     , 0.0     , 0.0     , 0.0     , 0.0     , 0.0      ,
&       0.0     , 0.0     , 0.0     , 0.0     , 0.0     , 0.0      ,
&       0.0     , 0.0     , 0.0      /
c
c         TROPICAL MOLECULAR SCATTERING
c
      data at32/
&       1.89e-03, 1.81e-03, 1.64e-03, 1.49e-03, 1.34e-03, 1.22e-03,
&       1.10e-03, 9.92e-04, 8.94e-04, 8.00e-04, 7.16e-04, 6.38e-04,
```

```
      &       5.67e-04, 5.01e-04, 4.43e-04, 3.89e-04, 3.39e-04, 2.92e-04,
      &       2.45e-04, 2.03e-04, 1.68e-04, 1.40e-04, 1.17e-04, 9.84e-05,
      &       8.35e-05, 7.09e-05, 4.73e-05, 2.16e-05, 1.03e-05, 5.04e-06,
      &       2.56e-06, 0.0     , 0.0     /
      c
      c     MIDLATITUDE SUMMER MOLECULAR ABSORPTION
      c
            data at33/
      &       0.0      , 0.0     , 0.0      , 0.0     , 0.0     , 0.0     ,
      &       0.0      , 0.0     , 0.0      , 0.0     , 0.0     , 0.0     ,
      &       0.0      , 0.0     , 0.0      , 0.0     , 0.0     , 0.0     ,
      &       0.0      , 0.0     , 0.0      , 0.0     , 0.0     , 0.0     ,
      &       0.0      , 0.0     , 0.0      , 0.0     , 0.0     , 0.0     ,
      &       0.0      , 0.0     , 0.0      /
      c
      c     MIDLATITUDE SUMMER MOLECULAR SCATTERING
      c
            data at34/
      &       1.93e-03, 1.84e-03, 1.66e-03, 1.60e-03, 1.36e-03, 1.22e-03,
      &       1.10e-03, 9.90e-04, 8.87e-04, 7.96e-04, 7.11e-04, 6.32e-04,
      &       5.60e-04, 4.95e-04, 4.30e-04, 3.67e-04, 3.12e-04, 2.67e-04,
      &       2.28e-04, 1.95e-04, 1.66e-04, 1.42e-04, 1.21e-04, 1.03e-04,
      &       8.78e-05, 7.50e-06, 5.64e-05, 2.32e-05, 1.11e-05, 5.44e-06,
      &       2.79e-06, 1.05e-06, 0.0     /
      c
      c     MIDLATITUDE WINTER MOLECULAR ABSORPTION
      c
            data at35/
      &       0.0      , 0.0     , 0.0      , 0.0     , 0.0     , 0.0     ,
      &       0.0      , 0.0     , 0.0      , 0.0     , 0.0     , 0.0     ,
      &       0.0      , 0.0     , 0.0      , 0.0     , 0.0     , 0.0     ,
      &       0.0      , 0.0     , 0.0      , 0.0     , 0.0     , 0.0     ,
      &       0.0      , 0.0     , 0.0      , 0.0     , 0.0     , 0.0     ,
      &       0.0      , 0.0     , 0.0      /
      c
      c     MIDLATITUDE WINTER MOLECULAR SCATTERING
      c
            data at36/
      &       2.09e-03, 1.98e-03, 1.77e-03, 1.58e-03, 1.41e-03, 1.26e-03,
      &       1.13e-03, 1.00e-03, 8.92e-04, 7.90e-04, 6.98e-04, 6.08e-04,
      &       5.22e-04, 4.47e-04, 3.84e-04, 3.29e-04, 2.82e-04, 2.42e-04,
      &       2.07e-04, 1.77e-04, 1.52e-04, 1.29e-04, 1.10e-04, 9.43e-05,
      &       8.06e-05, 6.88e-05, 4.59e-05, 2.07e-06, 9.27e-06, 4.31e-06,
      &       2.12e-06, 0.0     , 0.0     /
      c
      c     SUBARCTIC SUMMER MOLECULAR ABSORPTION
      c
            data at37/
      &       0.0      , 0.0     , 0.0      , 0.0     , 0.0     , 0.0     ,
      &       0.0      , 0.0     , 0.0      , 0.0     , 0.0     , 0.0     ,
```

```
      &     0.0     , 0.0     , 0.0     , 0.0     , 0.0     , 0.0     ,
      &     0.0     , 0.0     , 0.0     , 0.0     , 0.0     , 0.0     ,
      &     0.0     , 0.0     , 0.0     , 0.0     , 0.0     , 0.0     ,
      &     0.0     , 0.0     , 0.0     /
      c
      c     SUBARCTIC SUMMER MOLECULAR SCATTERING
      c
            data at38/
      &     1.97e-03, 1.87e-03, 1.69e-03, 1.53e-03, 1.37e-03, 1.23e-03,
      &     1.11e-03, 9.93e-04, 8.90e-04, 7.95e-04, 7.08e-04, 6.19e-04,
      &     5.32e-04, 4.57e-04, 3.93e-04, 3.37e-04, 2.90e-04, 2.50e-04,
      &     2.15e-04, 1.85e-04, 1.59e-04, 1.36e-04, 1.17e-04, 1.01e-04,
      &     8.66e-05, 7.41e-05, 5.01e-05, 2.35e-05, 1.11e-05, 5.48e-06,
      &     2.85e-06, 1.09e-06, 0.0     /
      c
      c     SUBARCTIC WINTER MOLECULAR ABSORPTION
      c
            data at39/
      &     0.0     , 0.0     , 0.0     , 0.0     , 0.0     , 0.0     ,
      &     0.0     , 0.0     , 0.0     , 0.0     , 0.0     , 0.0     ,
      &     0.0     , 0.0     , 0.0     , 0.0     , 0.0     , 0.0     ,
      &     0.0     , 0.0     , 0.0     , 0.0     , 0.0     , 0.0     ,
      &     0.0     , 0.0     , 0.0     , 0.0     , 0.0     , 0.0     ,
      &     0.0     , 0.0     , 0.0     /
      c
      c     SUBARCTIC WINTER MOLECULAR SCATTERING
      c
            data at30/
      &     2.21e-03, 2.06e-03, 1.81e-04, 1.60e-04, 1.42e-04, 1.27e-04,
      &     1.13e-04, 1.01e-04, 8.94e-04, 7.84e-04, 6.76e-04, 5.78e-04,
      &     4.94e-04, 4.22e-04, 3.61e-04, 3.08e-04, 2.64e-04, 2.26e-04,
      &     1.94e-04, 1.66e-04, 1.42e-04, 1.22e-04, 1.04e-04, 8.89e-05,
      &     7.60e-05, 6.49e-05, 4.31e-05, 1.91e-05, 8.60e-06, 3.94e-06,
      &     1.88e-06, 0.0     , 0.0     /
      c
      c     AEROSOL ABSORPTION - CLEAR
      c
            data at3a/
      &     1.52e-02, 1.01e-02, 4.41e-03, 1.88e-03, 8.84e-04, 5.58e-04,
      &     4.07e-04, 3.29e-04, 3.22e-04, 3.20e-04, 3.10e-04, 2.96e-04,
      &     2.94e-04, 2.89e-04, 2.75e-04, 2.64e-04, 2.49e-04, 2.42e-04,
      &     2.36e-04, 2.13e-04, 1.68e-04, 1.22e-04, 9.04e-05, 6.86e-05,
      &     5.34e-05, 4.36e-05, 2.20e-05, 6.19e-06, 1.63e-06, 0.0     ,
      &     0.0     , 0.0     , 0.0     /
      c
      c     AEROSOL SCATTERING - CLEAR
      c
            data at3b/
      &     9.03e-02, 5.90e-02, 2.61e-02, 1.11e-02, 5.24e-03, 3.30e-03,
      &     2.41e-03, 1.9  -03, 1.91e-03, 1.90e-03, 1.83e-03, 1.75e-03,
```

```
&      1.74e-03, 1.71e-03, 1.63e-03, 1.56e-03, 1.48e-03, 1.43e-03,
&      1.40e-03, 1.26e-03, 9.94e-04, 7.25e-04, 5.36e-04, 4.06e-04,
c      3.16e-04, 2.59e-04, 1.30e-04, 3.67e-05, 9.65e-06, 2.54e-06,
&      0.0     , 0.0     , 0.0       /
c
c      AEROSOL ABSORPTION - HAZY
c
       data at3c/
&      7.43e-02, 4.49e-02, 1.64e-03, 6.00e-03, 2.19e-03, 8.00e-04,
&      4.07e-04, 3.29e-04, 3.22e-04, 3.20e-04, 3.10e-04, 2.96e-04,
&      2.94e-04, 2.89e-04, 2.75e-04, 2.64e-04, 2.49e-04, 2.42e-04,
&      2.36e-04, 2.13e-04, 1.68e-04, 1.22e-04, 9.04e-05, 6.86e-05,
&      5.34e-05, 4.36e-05, 2.20e-05, 6.19e-06, 1.63e-06, 0.0     ,
&      0.0     , 0.0     , 0.0       /
c
c      AEROSOL SCATTERING - HAZY
c
       data at3d/
&      4.40e-01, 2.66e-01, 9.72e-02, 3.56e-02, 1.30e-02, 4.74e-03,
&      2.41e-03, 1.95e-03, 1.91e-03, 1.90e-03, 1.83e-03, 1.75e-03,
&      1.74e-03, 1.71e-03, 1.63e-03, 1.56e-03, 1.48e-03, 1.43e-03,
&      1.40e-03, 1.26e-03, 9.94e-04, 7.25e-04, 5.36e-04, 4.06e-04,
&      3.16e-04, 2.59e-04, 1.30e-04, 3.67e-05, 9.65e-06, 2.54e-06,
&      0.0     , 0.0     , 0.0       /
c      ********************************************************
c
c
c      WAVELENGTH IS 1.06 MICRONS
c
c      TROPICAL MOLECULAR ABSORPTION
c
       data at41/
&      0.0     , 0.0     , 0.0     , 0.0     , 0.0     , 0.0     ,
&      0.0     , 0.0     , 0.0     , 0.0     , 0.0     , 0.0     ,
&      0.0     , 0.0     , 0.0     , 0.0     , 0.0     , 0.0     ,
&      0.0     , 0.0     , 0.0     , 0.0     , 0.0     , 0.0     ,
&      0.0     , 0.0     , 0.0     , 0.0     , 0.0     , 0.0     ,
&      0.0     , 0.0     , 0.0       /
c
c      TROPICAL MOLECULAR SCATTERING
c
       data at42/
&      8.04e-04, 7.68e-04, 6.99e-04, 6.33e-04, 5.72e-04, 5.19e-04,
&      4.69e-04, 4.22e-04, 3.80e-04, 3.41e-04, 3.04e-04, 2.72e-04,
&      2.41e-04, 2.13e-04, 1.88e-04, 1.66e-04, 1.44e-04, 1.24e-04,
&      1.05e-04, 8.63e-05, 7.16e-05, 5.96e-05, 4.98e-05, 4.19e-05,
&      3.55e-05, 3.02e-05, 2.01e-05, 9.20e-06, 4.37e-06, 2.15e-06,
&      1.09e-06, 0.0     , 0.0       /
c
c      MIDLATITUDE SUMMER MOLECULAR ABSORPTION
c
```

```
      data at43/
     &   0.0      , 0.0      , 0.0      , 0.0      , 0.0      , 0.0       ,
     &   0.0      , 0.0      , 0.0      , 0.0      , 0.0      , 0.0       ,
     &   0.0      , 0.0      , 0.0      , 0.0      , 0.0      , 0.0       ,
     &   0.0      , 0.0      , 0.0      , 0.0      , 0.0      , 0.0       ,
     &   0.0      , 0.0      , 0.0      , 0.0      , 0.0      , 0.0       ,
     &   0.0      , 0.0      , 0.0      /
      c
      c     MIDLATITUDE SUMMER MOLECULAR SCATTERING
      c
      data at44/
     &   8.20e-04, 7.81e-04, 7.06e-04, 5.38e-04, 5.77e-04, 5.21e-04,
     &   4.69e-04, 4.21e-04, 3.78e-04, 3.38e-04, 3.02e-04, 2.69e-04,
     &   2.39e-04, 2.11e-04, 1.83e-04, 1.56e-04, 1.33e-04, 1.14e-04,
     &   9.72e-05, 8.29e-05, 7.07e-05, 6.02e-05, 5.14e-05, 4.38e-05,
     &   3.74e-05, 3.19e-05, 2.15e-05, 9.89e-06, 4.71e-06, 2.31e-06,
     &   1.19e-06, 0.0     , 0.0      /
      c
      c     MIDLATITUDE WINTER MOLECULAR ABSORPTION
      c
      data at45/
     &   0.0      , 0.0      , 0.0      , 0.0      , 0.0      , 0.0       ,
     &   0.0      , 0.0      , 0.0      , 0.0      , 0.0      , 0.0       ,
     &   0.0      , 0.0      , 0.0      , 0.0      , 0.0      , 0.0       ,
     &   0.0      , 0.0      , 0.0      , 0.0      , 0.0      , 0.0       ,
     &   0.0      , 0.0      , 0.0      , 0.0      , 0.0      , 0.0       ,
     &   0.0      , 0.0      , 0.0      /
      c
      c     MIDLATITUDE WINTER MOLECULAR SCATTERING
      c
      data at46/
     &   8.91e-04, 8.43e-04, 7.52e-04, 6.70e-04, 5.99e-04, 5.37e-04,
     &   4.80e-04, 4.27e-04, 3.80e-04, 3.36e-04, 2.97e-04, 2.59e-04,
     &   2.22e-04, 1.90e-04, 1.63e-04, 1.40e-04, 1.20e-04, 1.03e-04,
     &   8.80e-05, 7.53e-05, 6.45e-05, 5.51e-05, 4.70e-05, 4.01e-05,
     &   3.43e-05, 2.83e-05, 1.95e-05, 8.79e-06, 3.95e-06, 1.83e-06,
     &   0.0      , 0.0      , 0.0      /
      c
      c     SUBARCTIC SUMMER MOLECULAR ABSORPTION
      c
      data at47/
     &   0.0      , 0.0      , 0.0      , 0.0      , 0.0      , 0.0       ,
     &   0.0      , 0.0      , 0.0      , 0.0      , 0.0      , 0.0       ,
     &   0.0      , 0.0      , 0.0      , 0.0      , 0.0      , 0.0       ,
     &   0.0      , 0.0      , 0.0      , 0.0      , 0.0      , 0.0       ,
     &   0.0      , 0.0      , 0.0      , 0.0      , 0.0      , 0.0       ,
     &   0.0      , 0.0      , 0.0      /
      c
      c     SUBARCTIC SUMMER MOLECULAR SCATTERING
      c
```

```
      data at48/
     &   8.38e-04, 7.98e-04, 7.21e-04, 6.50e-04, 5.84e-04, 5.24e-04,
     &   4.71e-04, 4.23e-04, 3.79e-04, 3.38e-04, 3.01e-04, 2.64e-04,
     &   2.26e-04, 1.95e-04, 1.67e-04, 1.44e-04, 1.23e-04, 1.06e-04,
     &   9.14e-05, 7.86e-05, 6.75e-05, 5.80e-05, 4.99e-05, 4.29e-05,
     &   3.69e-05, 3.15e-05, 2.13e-05, 9.98e-06, 4.73e-06, 2.33e-06,
     &   1.21e-06, 0.0     , 0.0      /
c
c     SUBARCTIC WINTER MOLECULAR ABSORPTION
c
      data at49/
     &   0.0     , 0.0     , 0.0      , 0.0      , 0.0      , 0.0      ,
     &   0.0     , 0.0     , 0.0      , 0.0      , 0.0      , 0.0      ,
     &   0.0     , 0.0     , 0.0      , 0.0      , 0.0      , 0.0      ,
     &   0.0     , 0.0     , 0.0      , 0.0      , 0.0      , 0.0      ,
     &   0.0     , 0.0     , 0.0      , 0.0      , 0.0      , 0.0      ,
     &   0.0     , 0.0     , 0.0      /
c
c     SUBARCTIC WINTER MOLECULAR SCATTERING
c
      data at40/
     &   9.39e-04, 8.77e-04, 7.70e-04, 6.82e-04, 6.06e-04, 5.40e-04,
     &   4.82e-04, 4.29e-04, 3.81e-04, 3.34e-04, 2.88e-04, 2.46e-04,
     &   2.10e-04, 1.80e-04, 1.54e-04, 1.31e-05, 1.12e-05, 9.63e-05,
     &   8.25e-05, 7.06e-05, 6.06e-05, 5.17e-05, 4.42e-05, 3.78e-05,
     &   3.23e-05, 2.76e-05, 1.84e-05, 8.14e-06, 3.66e-06, 1.68e-06,
     &   0.0     , 0.0     , 0.0      /
c
c     AEROSOL ABSORPTION - CLEAR
c
      data at4a/
     &   1.98e-02, 1.31e-02, 5.71e-03, 2.43e-03, 1.15e-03, 7.23e-04,
     &   5.27e-04, 4.27e-04, 4.18e-04, 4.15e-04, 4.01e-04, 3.84e-04,
     &   3.81e-04, 3.75e-04, 3.56e-04, 3.42e-04, 3.23e-04, 3.13e-04,
     &   3.06e-04, 2.77e-04, 2.18e-04, 1.59e-04, 1.17e-04, 8.89e-04,
     &   6.93e-05, 5.66e-05, 2.85e-05, 8.02e-06, 2.11e-06, 0.0     ,
     &   0.0     , 0.0     , 0.0      /
c
c     AEROSOL SCATTERING - CLEAR
c
      data at4b/
     &   6.79e-02, 4.50e-02, 1.96e-02, 8.36e-03, 3.94e-03, 2.49e-03,
     &   1.81e-03, 1.47e-03, 1.44e-03, 1.43e-03, 1.38e-03, 1.32e-03,
     &   1.31e-03, 1.29e-03, 1.22e-03, 1.18e-03, 1.11e-03, 1.08e-03,
     &   1.05e-03, 9.51e-04, 7.48e-04, 5.45e-04, 4.03e-04, 3.06e-04,
     &   2.38e-04, 1.94e-04, 9.79e-05, 2.76e-05, 7.28e-06, 1.91e-06,
     &   0.0     , 0.0     , 0.0      /
c
c     AEROSOL ABSORPTION - HAZY
c
```

```
      data at4c/
     &  9.63e-02, 5.82e-02, 2.13e-02, 7.78e-03, 2.84e-03, 1.04e-03,
     &  5.27e-04, 4.27e-04, 4.18e-04, 4.15e-04, 4.01e-04, 3.84e-04,
     &  3.81e-04, 3.75e-04, 3.56e-04, 3.42e-04, 3.23e-04, 3.13e-04,
     &  3.06e-04, 2.77e-04, 2.18e-04, 1.59e-04, 1.17e-04, 8.89e-04,
     &  6.93e-05, 5.66e-05, 2.85e-05, 8.02e-06, 2.11e-06, 0.0     ,
     &  0.0     , 0.0     , 0.0      /
      c
      c   AEROSOL SCATTERING - HAZY
      c
      data at4d/
     &  3.31e-01, 2.00e-01, 7.31e-02, 2.67e-02, 9.76e-03, 3.56e-03,
     &  1.81e-03, 1.47e-03, 1.44e-03, 1.43e-03, 1.38e-03, 1.32e-03,
     &  1.31e-03, 1.29e-03, 1.22e-03, 1.18e-03, 1.11e-03, 1.08e-03,
     &  1.05e-03, 9.51e-04, 7.48e-04, 5.45e-04, 4.03e-04, 3.06e-04,
     &  2.38e-04, 1.94e-04, 9.79e-05, 2.76e-05, 7.26e-06, 1.91e-06,
     &  0.0     , 0.0     , 0.0      /
      c  ************************************************************
      c
      c
      c   WAVELENGTH IS 10.591 MICRONS
      c
      c   TROPICAL MOLECULAR ABSORPTION
      c
      data at51/
     &  5.79e-01, 5.17e-01, 2.85e-01, 1.81e-01, 9.62e-02, 6.29e-02,
     &  5.02e-02, 3.99e-02, 3.20e-02, 2.63e-02, 2.07e-02, 1.65e-02,
     &  1.29e-02, 1.04e-02, 7.38e-03, 5.85e-03, 4.33e-03, 3.32e-03,
     &  3.56e-03, 4.35e-03, 5.19e-03, 6.27e-03, 7.47e-03, 8.35e-03,
     &  9.04e-03, 9.91e-03, 1.20e-02, 1.19e-02, 1.10e-02, 8.86e-03,
     &  6.04e-03, 9.01e-04, 1.54e-05/
      c
      c   TROPICAL MOLECULAR SCATTERING
      c
      data at52/
     &  0.0     , 0.0     , 0.0     , 0.0     , 0.0     , 0.0     ,
     &  0.0     , 0.0     , 0.0     , 0.0     , 0.0     , 0.0     ,
     &  0.0     , 0.0     , 0.0     , 0.0     , 0.0     , 0.0     ,
     &  0.0     , 0.0     , 0.0     , 0.0     , 0.0     , 0.0     ,
     &  0.0     , 0.0     , 0.0     , 0.0     , 0.0     , 0.0     ,
     &  0.0     , 0.0     , 0.0      /
      c
      c   MIDLATITUDE SUMMER MOLECULAR ABSORPTION
      c
      data at53/
     &  3.58e-01, 3.26e-01, 1.88e-01, 1.15e-01, 7.58e-02, 5.54e-02,
     &  4.47e-02, 3.76e-02, 3.02e-02, 2.38e-02, 1.95e-02, 1.57e-02,
     &  1.24e-02, 9.53e-03, 8.34e-03, 8.70e-03, 8.49e-03, 8.36e-03,
     &  8.47e-03, 8.56e-03, 8.93e-03, 9.19e-03, 9.72e-03, 1.01e-02,
     &  1.11e-02, 1.11e-02, 1.33e-02, 1.32e-02, 1.27e-02, 1.06e-02,
     &  7.52e-03, 1.08e-03, 1.74e-05/
```

```
c
c       MIDLATITUDE SUMMER MOLECULAR SCATTERING
c
        data at54/
&        0.0      , 0.0     , 0.0     , 0.0     , 0.0     , 0.0      ,
&        0.0      , 0.0     , 0.0     , 0.0     , 0.0     , 0.0      ,
&        0.0      , 0.0     , 0.0     , 0.0     , 0.0     , 0.0      ,
&        0.0      , 0.0     , 0.0     , 0.0     , 0.0     , 0.0      ,
&        0.0      , 0.0     , 0.0     , 0.0     , 0.0     , 0.0      ,
&        0.0      , 0.0     , 0.0     /
c
c       MIDLATITUDE WINTER MOLECULAR ABSORPTION
c
        data at55/
&        7.94e-02, 7.31e-02, 5.89e-02, 4.91e-02, 4.04e-02, 3.24e-02,
&        2.62e-02, 2.15e-02, 1.73e-02, 1.40e-02, 1.08e-02, 9.81e-03,
&        9.48e-03, 9.36e-03, 9.34e-03, 9.00e-03, 8.75e-03, 8.57e-03,
&        8.56e-03, 8.25e-03, 8.01e-03, 8.19e-03, 8.19e-03, 8.16e-03,
&        8.11e-03, 8.38e-03, 8.09e-03, 6.85e-03, 6.71e-03, 6.02e-03,
&        4.40e-03, 2.74e-04, 1.58e-04/
c
c       MIDLATITUDE WINTER MOLECULAR SCATTERING
c
        data at56/
&        0.0      , 0.0     , 0.0     , 0.0     , 0.0     , 0.0      ,
&        0.0      , 0.0     , 0.0     , 0.0     , 0.0     , 0.0      ,
&        0.0      , 0.0     , 0.0     , 0.0     , 0.0     , 0.0      ,
&        0.0      , 0.0     , 0.0     , 0.0     , 0.0     , 0.0      ,
&        0.0      , 0.0     , 0.0     , 0.0     , 0.0     , 0.0      ,
&        0.0      , 0.0     , 0.0     /
c
c       SUBARCTIC SUMMER MOLECULAR ABSORPTION
c
        data at57/
&        2.01e-01, 1.82e-01, 1.14e-01, 8.15e-02, 6.09e-02, 4.66e-02,
&        3.74e-02, 2.86e-02, 2.28e-02, 1.79e-02, 1.38e-02, 1.20e-02,
&        1.23e-02, 1.18e-02, 1.23e-02, 1.22e-02, 1.17e-02, 1.22e-02,
&        1.20e-02, 1.20e-02, 1.22e-02, 1.19e-02, 1.21e-02, 1.21e-02,
&        1.20e-02, 1.27e-02, 1.45e-02, 2.01e-02, 1.40e-02, 1.19e-02,
&        8.19e-03, 1.10e-03, 1.76e-05/
c
c       SUBARCTIC SUMMER MOLECULAR SCATTERING
c
        data at58/
&        0.0      , 0.0     , 0.0     , 0.0     , 0.0     , 0.0      ,
&        0.0      , 0.0     , 0.0     , 0.0     , 0.0     , 0.0      ,
&        0.0      , 0.0     , 0.0     , 0.0     , 0.0     , 0.0      ,
&        0.0      , 0.0     , 0.0     , 0.0     , 0.0     , 0.0      ,
&        0.0      , 0.0     , 0.0     , 0.0     , 0.0     , 0.0      ,
&        0.0      , 0.0     , 0.0     /
```

```
c
c       SUBARCTIC WINTER MOLECULAR ABSORPTION
c
        data at59/
&       4.12e-02, 4.15e-02, 4.00e-02, 3.52e-02, 3.05e-02, 2.45e-02,
&       1.93e-02, 1.51e-02, 1.17e-02, 9.59e-03, 8.93e-03, 8.92e-03,
&       8.91e-03, 8.73e-03, 9.11e-03, 8.89e-03, 8.77e-03, 8.56e-03,
&       8.32e-03, 8.21e-03, 7.88e-03, 7.78e-03, 7.52e-03, 7.21e-03,
&       7.33e-03, 6.84e-03, 7.24e-03, 5.78e-03, 5.10e-03, 4.10e-03,
&       3.08e-03, 7.76e-04, 1.79e-05/
c
c       SUBARCTIC WINTER MOLECULAR SCATTERING
c
        data at50/
&       0.0     , 0.0    , 0.0     , 0.0     , 0.0     , 0.0      ,
&       0.0     , 0.0    , 0.0     , 0.0     , 0.0     , 0.0      ,
&       0.0     , 0.0    , 0.0     , 0.0     , 0.0     , 0.0      ,
&       0.0     , 0.0    , 0.0     , 0.0     , 0.0     , 0.0      ,
&       0.0     , 0.0    , 0.0     , 0.0     , 0.0     , 0.0      ,
&       0.0     , 0.0    , 0.0     /
c
c       AEROSOL ABSORPTION - CLEAR
c
        data at5a/
&       5.48e-03, 3.64e-03, 1.58e-03, 6.75e-04, 3.18e-04, 2.01e-04,
&       1.46e-04, 1.18e-04, 1.16e-04, 1.15e-04, 1.11e-04, 1.06e-04,
&       1.06e-04, 1.04e-04, 9.89e-05, 9.49e-05, 8.97e-05, 8.69e-05,
&       8.50e-05, 7.68e-05, 6.04e-05, 4.40e-05, 3.25e-05, 2.47e-05,
&       1.92e-05, 1.57e-05, 7.90e-06, 2.23e-06, 0.0     , 0.0      ,
&       0.0     , 0.0    , 0.0     /
c
c      'AEROSOL SCATTERING - CLEAR
c
        data at5b/
&       4.65e-03, 3.09e-03, 1.34e-03, 5.73e-04, 2.70e-04, 1.70e-04,
&       1.24e-04, 1.00e-04, 9.83e-05, 9.77e-05, 9.45e-05, 9.04e-05,
&       8.96e-05, 8.83e-05, 8.39e-05, 8.05e-05, 7.61e-05, 7.38e-05,
&       7.21e-05, 6.51e-05, 5.12e-05, 3.74e-05, 2.76e-05, 2.09e-05,
&       1.63e-05, 1.33e-05, 6.71e-06, 1.89e-06, 0.0     , 0.0      ,
&       0.0     , 0.0    , 0.0     /
c
c       AEROSOL ABSORPTION - HAZY
c
        data at5c/
&       2.67e-02, 1.61e-02, 5.90e-03, 2.16e-03, 7.88e-04, 2.88e-04,
&       1.46e-04, 1.18e-04, 1.16e-04, 1.15e-04, 1.11e-04, 1.06e-04,
&       1.06e-04, 1.04e-04, 9.89e-05, 9.49e-05, 8.97e-05, 8.69e-05,
&       8.50e-05, 7.68e-05, 6.04e-05, 4.40e-05, 3.25e-05, 2.47e-05,
&       1.92e-05, 1.57e-05, 7.90e-06, 2.23e-06, 0.0     , 0.0      ,
&       0.0     , 0.0    , 0.0     /
```

```
c
c       AEROSOL SCATTERING - HAZY
c
      data at5d/
&     2.27e-02, 1.37e-02, 5.01e-03, 1.83e-03, 6.68e-04, 2.44e-04,
&     1.24e-04, 1.00e-04, 9.83e-05, 9.77e-05, 9.45e-05, 9.04e-05,
&     8.96e-05, 8.83e-05, 8.39e-05, 8.05e-05, 7.61e-05, 7.38e-05,
&     7.21e-05, 6.51e-05, 5.12e-05, 3.74e-05, 2.76e-05, 2.09e-05,
&     1.63e-05, 1.33e-05, 6.71e-06, 1.89e-06, 0.0     , 0.0     ,
&     0.0     , 0.0     , 0.0        /
c     ************************************************************
c
c
c     OPTIONAL STORAGE FOR INPUT DATA
c
c     TROPICAL MOLECULAR ABSORPTION
c
      data at61/
&     0.0     , 0.0     , 0.0     , 0.0     , 0.0     , 0.0     ,
&     0.0     , 0.0     , 0.0     , 0.0     , 0.0     , 0.0     ,
&     0.0     , 0.0     , 0.0     , 0.0     , 0.0     , 0.0     ,
&     0.0     , 0.0     , 0.0     , 0.0     , 0.0     , 0.0     ,
&     0.0     , 0.0     , 0.0     , 0.0     , 0.0     , 0.0     ,
&     0.0     , 0.0     , 0.0        /
c
c     TROPICAL MOLECULAR SCATTERING
c
      data at62/
&     0.0     , 0.0     , 0.0     , 0.0     , 0.0     , 0.0     ,
&     0.0     , 0.0     , 0.0     , 0.0     , 0.0     , 0.0     ,
&     0.0     , 0.0     , 0.0     , 0.0     , 0.0     , 0.0     ,
&     0.0     , 0.0     , 0.0     , 0.0     , 0.0     , 0.0     ,
&     0.0     , 0.0     , 0.0     , 0.0     , 0.0     , 0.0     ,
&     0.0     , 0.0     , 0.0        /
c
c     MIDLATITUDE SUMMER MOLECULAR ABSORPTION
c
      data at63/
&     0.0     , 0.0     , 0.0     , 0.0     , 0.0     , 0.0     ,
&     0.0     , 0.0     , 0.0     , 0.0     , 0.0     , 0.0     ,
&     0.0     , 0.0     , 0.0     , 0.0     , 0.0     , 0.0     ,
&     0.0     , 0.0     , 0.0     , 0.0     , 0.0     , 0.0     ,
&     0.0     , 0.0     , 0.0     , 0.0     , 0.0     , 0.0     ,
&     0.0     , 0.0     , 0.0        /
c
c     MIDLATITUDE SUMMER MOLECULAR SCATTERING
c
      data at64/
&     0.0     , 0.0     , 0.0     , 0.0     , 0.0     , 0.0     ,
&     0.0     , 0.0     , 0.0     , 0.0     , 0.0     , 0.0     ,
&     0.0     , 0.0     , 0.0     , 0.0     , 0.0     , 0.0     ,
```

```
     &      0.0      , 0.0     , 0.0      , 0.0     , 0.0     , 0.0      ,
     &      0.0      , 0.0     , 0.0      , 0.0     , 0.0     , 0.0      ,
     &      0.0      , 0.0     , 0.0      /
     c
     c      MIDLATITUDE WINTER MOLECULAR ABSORPTION
     c
            data at65/
     &      0.0      , 0.0     , 0.0      , 0.0     , 0.0     , 0.0      ,
     &      0.0      , 0.0     , 0.0      , 0.0     , 0.0     , 0.0      ,
     &      0.0      , 0.0     , 0.0      , 0.0     , 0.0     , 0.0      ,
     &      0.0      , 0.0     , 0.0      , 0.0     , 0.0     , 0.0      ,
     &      0.0      , 0.0     , 0.0      , 0.0     , 0.0     , 0.0      ,
     &      0.0      , 0.0     , 0.0      /
     c
     c      MIDLATITUDE WINTER MOLECULAR SCATTERING
     c
            data at66/
     &      0.0      , 0.0     , 0.0      , 0.0     , 0.0     , 0.0      ,
     &      0.0      , 0.0     , 0.0      , 0.0     , 0.0     , 0.0      ,
     &      0.0      , 0.0     , 0.0      , 0.0     , 0.0     , 0.0      ,
     &      0.0      , 0.0     , 0.0      , 0.0     , 0.0     , 0.0      ,
     &      0.0      , 0.0     , 0.0      , 0.0     , 0.0     , 0.0      ,
     &      0.0      , 0.0     , 0.0      /
     c
     c      SUBARCTIC SUMMER MOLECULAR ABSORPTION
     c
            data at67/
     &      0.0      , 0.0     , 0.0      , 0.0     , 0.0     , 0.0      ,
     &      0.0      , 0.0     , 0.0      , 0.0     , 0.0     , 0.0      ,
     &      0.0      , 0.0     , 0.0      , 0.0     , 0.0     , 0.0      ,
     &      0.0      , 0.0     , 0.0      , 0.0     , 0.0     , 0.0      ,
     &      0.0      , 0.0     , 0.0      , 0.0     , 0.0     , 0.0      ,
     &      0.0      , 0.0     , 0.0      /
     c
     c      SUBARCTIC SUMMER MOLECULAR SCATTERING
     c
            data at68/
     &      0.0      , 0.0     , 0.0      , 0.0     , 0.0     , 0.0      ,
     &      0.0      , 0.0     , 0.0      , 0.0     , 0.0     , 0.0      ,
     &      0.0      , 0.0     , 0.0      , 0.0     , 0.0     , 0.0      ,
     &      0.0      , 0.0     , 0.0      , 0.0     , 0.0     , 0.0      ,
     &      0.0      , 0.0     , 0.0      , 0.0     , 0.0     , 0.0      ,
     &      0.0      , 0.0     , 0.0      /
     c
     c      SUBARCTIC WINTER MOLECULAR ABSORPTION
     c
            data at69/
     &      0.0      , 0.0     , 0.0      , 0.0     , 0.0     , 0.0      ,
     &      0.0      , 0.0     , 0.0      , 0.0     , 0.0     , 0.0      ,
     &      0.0      , 0.0     , 0.0      , 0.0     , 0.0     , 0.0      ,
```

```
&      0.0      , 0.0     , 0.0     , 0.0      , 0.0       , 0.0       ,
&      0.0      , 0.0     , 0.0     , 0.0      , 0.0       , 0.0       ,
&      0.0      , 0.0     , 0.0     /
c
c
c      SUBARCTIC WINTER MOLECULAR SCATTERING
c
       data at60/
&      0.0      , 0.0     , 0.0     , 0.0      , 0.0       , 0.0       ,
&      0.0      , 0.0     , 0.0     , 0.0      , 0.0       , 0.0       ,
&      0.0      , 0.0     , 0.0     , 0.0      , 0.0       , 0.0       ,
&      0.0      , 0.0     , 0.0     , 0.0      , 0.0       , 0.0       ,
&      0.0      , 0.0     , 0.0     , 0.0      , 0.0       , 0.0       ,
&      0.0      , 0.0     , 0.0     /
c
c      AEROSOL ABSORPTION - CLEAR
c
       data at6a/
&      0.0      , 0.0     , 0.0     , 0.0      , 0.0       , 0.0       ,
&      0.0      , 0.0     , 0.0     , 0.0      , 0.0       , 0.0       ,
&      0.0      , 0.0     , 0.0     , 0.0      , 0.0       , 0.0       ,
&      0.0      , 0.0     , 0.0     , 0.0      , 0.0       , 0.0       ,
&      0.0      , 0.0     , 0.0     , 0.0      , 0.0       , 0.0       ,
&      0.0      , 0.0     , 0.0     /
c
c      AEROSOL SCATTERING - CLEAR
c
       data at6b/
&      0.0      , 0.0     , 0.0     , 0.0      , 0.0       , 0.0       ,
&      0.0      , 0.0     , 0.0     , 0.0      , 0.0       , 0.0       ,
&      0.0      , 0.0     , 0.0     , 0.0      , 0.0       , 0.0       ,
&      0.0      , 0.0     , 0.0     , 0.0      , 0.0       , 0.0       ,
&      0.0      , 0.0     , 0.0     , 0.0      , 0.0       , 0.0       ,
&      0.0      , 0.0     , 0.0     /
c
c      AEROSOL ABSORPTION - HAZY
c
       data at6c/
&      0.0      , 0.0     , 0.0     , 0.0      , 0.0       , 0.0       ,
&      0.0      , 0.0     , 0.0     , 0.0      , 0.0       , 0.0       ,
&      0.0      , 0.0     , 0.0     , 0.0      , 0.0       , 0.0       ,
&      0.0      , 0.0     , 0.0     , 0.0      , 0.0       , 0.0       ,
&      0.0      , 0.0     , 0.0     , 0.0      , 0.0       , 0.0       ,
&      0.0      , 0.0     , 0.0     /
c
c      AEROSOL SCATTERING - HAZY
c
       data at6d/
&      0.0      , 0.0     , 0.0     , 0.0      , 0.0       , 0.0       ,
&      0.0      , 0.0     , 0.0     , 0.0      , 0.0       , 0.0       ,
&      0.0      , 0.0     , 0.0     , 0.0      , 0.0       , 0.0       ,
```

```
     &      0.0      , 0.0      , 0.0      , 0.0      , 0.0      , 0.0       ,
     &      0.0      , 0.0      , 0.0      , 0.0      , 0.0      , 0.0       ,
     &      0.0      , 0.0      , 0.0      /
            end
c.
            subroutine tshare (nstop)
c
            common/atmos/ alfa(5,2),alfsct,alfab,ia,ab(33),as(33),at(33,14,6)
     &      ,mat,mvis
            common/flags/mode,mcomp,mp,lam,modesw,lunit,nout,istog,iotype,
     &      irtype,ihet,ibflag,iw
            common/ tdata / blt,dt,ht,phit,pt,rb,grndi,bdrt,sigj,sigt
            common/ rdata / blr,dr,hr,gl,bdlr
            common/ srdata / asr,hs,phi,phiaz,dphi
            common/ ldata / rl,alam,rpx,theta,x,angtr,angrec,gamint,bw
c  * darki & ptherm replace pnep, add g *
            common/ sndata / bwr,eta,f,em,pb,ps,darki,ptherm,snpndb,sndb,xm,
     &      bwopt,nflg,g
            common/ stgout / nvel,svel,avel,ndown,ncros,numtot,hvnear,
     &      hvfar,xdis,hdis,hdisdf,xclos,hclos,hclsdf,kount
            common /pltc  / xint(200),yint(200),h(200),dcomp(2),np,note
c  * srdark & srther replace srpnep *
            common/block1/xmod(6),gainsr(6),qe(6),fnoise(6),srbw(6),
     &      srdark(6),srther(6),alamda(6),obw(6),nhol(6)
            common/ tbsdf / ng,gstart(3),gend(3),gampl(3),ybsdf,sbsdf,nbak,noa
     &      ,ibsdf
            common/rsct/oasmax,diffoa,oafwhm,bmaxs,bfwhms,bdiff(6),psiaz,psiel
     &      ,gams
c  * add labeled common wavefm *
            common/ wavefm /npts,t,form0(1000),form1(1000),power0(1000),
     &      power1(1000)
            logical prompt,change
            data prompt,change/.true.,.false./
            data onedeg,pi,r2d/.0174532925,3.141592654,57.29577951/
            data hatm/100000./
c
c
c      SWITCH FLAG --  DEPENDS ON FILE STRUCTURE =MODESW
c      LOGICAL UNIT NUMBER FOR TERMINAL INPUT =LUNIT
c
c      IF FIRST CALL GO DIRECTLY TO INPUT LIST
            if (nstop.eq.0) go to 10
            nstop=1
c
c      IF LAST CALL TO TSHARE, TERMINATE RUNS
c
            write (6,1220)
            read (lunit,1890,end=650) nstop
            if (nstop.eq.1) go to 680
            nstop=10
```

```
                 go to 700
c
c        WAVELENGTH, LAM AND ALAMDA
10       nim=1
         if (.not.prompt) write (6,750) nim
         if (prompt) write (6,1230) nim,lam
         read (lunit,1890,end=650) lam
         if (lam.ne.6) go to 20
         write (6,1240)
         read (lunit,1890,end=650) alamda(6)
20       alam=alamda(lam)
         if (change) change=.not.change
c
c        ATMOSPHERIC COEFFICIENTS
30       nim=28
         if (.not.prompt) write (6,760) nim
         if (prompt) write (6,1250) nim,ia
         read (lunit,1890,end=650) ia
         if (ia.eq.2) go to 40
c        SET DEFAULT ATMOSPHERIC COEFFICIENTS
         alfsct=alfa(lam,1)
         alfab=alfa(lam,2)
c
c        ALLOWS USER TO OVERRIDE DEFAULT VALUES
c
         write (6,1310) alfsct
         read (lunit,1890,end=650) alfsct
         write (6,1320) alfab
         read (lunit,1890,end=650) alfab
         go to 70
40       if (lam.ne.6) go to 50
c
c        READ IN DATA FOR NEW WAVELENGTH
c
         write (6,1300)
         read (lunit,1890,end=650) natfil
         if (natfil.le.0) go to 10
         read (natfil,1210) ((at(i,j,6),j=1,14),i=1,33)
c
c        AFGL OPTIONS FOR ATMOSPHERIC MODEL AND VISIBILITY
c
50       write (6,1280) mat
         read (lunit,1890,end=650) mat
         write (6,1290) mvis
         read (lunit,1890,end=650) mvis
c
c        LOAD THE ABSORPTION AND SCATTERING ARRAYS  AB AND AS
c
         mat1=2*mat-1
         mat2=mat1+1
```

```
            mvis1=10+2*mvis-1
            mvis2=mvis1+1
            do 60 j=1,33
            ab(j)=(at(j,mat1,lam)+at(j,mvis1,lam))*1.e-3
60          as(j)=(at(j,mat2,lam)+at(j,mvis2,lam))*1.e-3
70          if (change) go to 670
c
c           TRANSMITTER OPTICS DIAMETER, DT
80          nim=2
            if (.not.prompt) write (6,770) nim
            if (prompt) write (6,1330) nim,dt
            read (lunit,1890,end=650) dt
            if (change) go to 670
c
c           TRANSMITTER BEAMWIDTH, PHIT
90          nim=3
            if (.not.prompt) write (6,780) nim
            if (prompt) write (6,1340) nim,phit
            read (lunit,1890,end=650) phit
c           CHECK TO SEE IF DIFFRACTION LIMIT IS EXCEEDED
            diffl=1.22*alamda(lam)/dt
            if (phit.gt.diffl) go to 100
            write (6,1270) diffl
            go to 90
100         if (change) go to 670
c
c           BSDF PARAMETERS
110         nim=31
            if (prompt) write (6,1350) nim,ibsdf
            read (lunit,1890,end=650) ibsdf
            if (ibsdf.eq.1) go to 130
            write (6,1360) ybsdf
            read (lunit,1890,end=650) ybsdf
            write (6,1370) sbsdf
            read (lunit,1890,end=650) sbsdf
            write (6,1380) ng
            read (lunit,1890,end=650) ng
            if (ng.eq.0) go to 130
            do 120 i=1,ng
            write (6,1390) i,gstart(i),i,gend(i),i,gampl(i)
            read (lunit,1890,end=650) gstart(i),gend(i),gampl(i)
120         continue
130         if (change) go to 670
c
c           LINK RECEIVER OPTICS DIAMETER, DR
140         nim=4
            if (.not.prompt) write (6,790) nim
            if (prompt) write (6,1400) nim,dr
            read (lunit,1890,end=650) dr
            if (change) go to 670
```

```
c
c       BACKSTOP PARAMETERS
150     nim=32
        write (6,1430) nim,nbak
        read (lunit,1890,end=650) nbak
        if (nbak.eq.1) go to 170
        if (nbak.eq.2) go to 160
        write (6,1450)
        read (lunit,1890,end=650) bdiff(lam)
        bmaxs=bdiff(lam)
        go to 170
160     write (6,1440) bmaxs,bfwhms,bdiff(lam)
        read (lunit,1890,end=650) bmaxs,bfwhms,bdiff(lam)
170     if (change) go to 670
c
c       ORIENTATION OF BACKSTOP
180     nim=44
        psiaz=psiaz*r2d
        if (.not.prompt) write (6,800) nim
        if (prompt) write (6,1410) nim,psiaz
        read (lunit,1890,end=650) psiaz
        psiaz=psiaz/r2d
c
        psiel=psiel*r2d
        if (.not.prompt) write (6,810)
        if (prompt) write (6,1420) psiel
        read (lunit,1890,end=650) psiel
        psiel=psiel/r2d
        if (change) go to 670
c
c       RECEIVER OPTICS REFLECTION PARAMETERS
190     nim=33
        if (prompt) write (6,1460) nim,noa
        read (lunit,1890,end=650) noa
        if (noa.eq.1) go to 200
        write (6,1470) oasmax,oafwhm,diffoa
        read (lunit,1890,end=650) oasmax,oafwhm,diffoa
200     if (change) go to 670
c
c       LINK TRANSMIT POWER (OUT OF OPTICS), PT
210     nim=6
        if (.not.prompt) write (6,820) nim
        if (prompt) write (6,1480) nim,pt
        read (lunit,1890,end=650) pt
        if (change) go to 670
c
c       LINK RANGE, RL
220     nim=8
        if (.not.prompt) write (6,840) nim
        if (prompt) write (6,1500) nim,rl
```
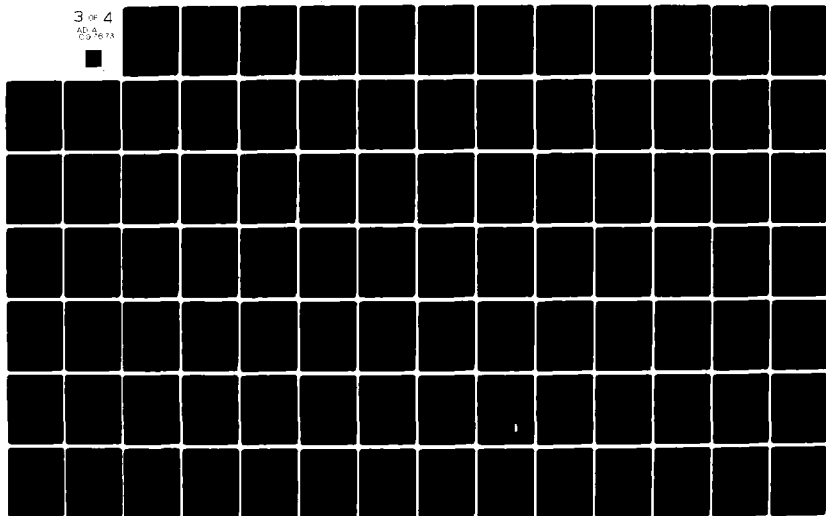
```
              read (lunit,1890,end=650) rl
              if (change) go to 670
c
c        LINK TRANSMITTER ALTITUDE, HT
230       nim=9
          if (.not.prompt) write (6,850) nim
          if (prompt) write (6,1510) nim,ht
          read (lunit,1890,end=650) ht
          if (change) go to 670
c
c        LINK RECEIVER ALTITUDE, HR
240       nim=10
          if (.not.prompt) write (6,860) nim
          if (prompt) write (6,1520) nim,hr
          read (lunit,1890,end=650) hr
          if (change) go to 670
c
c        SPACE TO GROUND FLAG
250       nim=34
          if (.not.change) go to 260
c        IF SWITCH TO STOG THEN MUST REDO REST OF INPUTS
          change=.not.change
          write (6,1260)
          go to 10
260       if(ht.lt.hatm) go to 275
          if (.not.prompt) write (6,870) nim
          if (prompt) write (6,1530) nim,istog
          read (lunit,1890,end=650) istog
c
c        REST OF SPACE TO GROUND INPUTS
c
c   *  jump to get turbulence for narrow beam analysis
275       if (istog.eq.0) go to 320
          mcomp=1
c
c        PERPENDICULAR DISTANCE TO CENTER OF BEAM
270       nim=35
          if (.not.prompt) write (6,880) nim
          if (prompt) write (6,1540) nim,x
          read (lunit,1890,end=650) x
          if (change) go to 670
c
c        ELEVATION ANGLE OF SR
280       nim=36
          if (.not.prompt) write (6,890) nim
          theta=theta*r2d
          if (prompt) write (6,1550) nim,theta
          read (lunit,1890,end=650) theta
          theta=theta/r2d
          if (change) go to 670
```

```
c
c       ALTITUDE AT GROUND LEVEL
290     nim=39
        if (.not.prompt) write (6,950) nim
        if (prompt) write (6,1610) nim,gl
        read (lunit,1890,end=650) gl
        if (change) go to 670
c
c       FLAG FOR STOG INPUTS, IBFLAG
300     nim=46
        if (.not.prompt) write (6,900) nim
        if (prompt) write (6,1560) nim,ibflag
        read (lunit,1890,end=650) ibflag
        if (ibflag.eq.2) go to 330
c
c       TOTAL JITTER,SIGJ
310     nim=47
        if (.not.prompt) write (6,910) nim
        if (prompt) write (6,1570) nim,sigj
        read (lunit,1890,end=650) sigj
c
c       TURBULENCE FLAG, IW
320     nim=48
        if (.not.prompt) write (6,920) nim
        if (prompt) write (6,1580) nim,iw
        read (lunit,1890,end=650) iw
        if (change) go to 670
c   *  jump out if narrow beam analysis *
        if (istog.eq.0) go to 350
        go to 490
c
c       RADIUS OF LINK BEAM
330     nim=37
        if (.not.prompt) write (6,930) nim
        if (prompt) write (6,1590) nim,rb
        read (lunit,1890,end=650) rb
c
c       EQUIVALENT POWER PER SQ.M
340     nim=38
        if (.not.prompt) write (6,940) nim
        if (prompt) write (6,1600) nim,grndi
        read (lunit,1890,end=650) grndi
        if (change) go to 670
c
        go to 490
c
c       COMPUTATION FLAG, MCOMP
c       MCOMP=1    COMPUTE POWER RECEIVED
c       MCOMP=2    COMPUTE S/N
c
```

```
350    nim=25
       if (.not.prompt) write (6,980) nim
       if (prompt) write (6,1640) nim,mcomp
       read (lunit,1890,end=650) mcomp
       if (change) change=.not.change
c
c      IF POWER IS THE DESIRED OUTPUT THE DETECTOR PARAMETERS ARE SKIPPED
c
c      MP  =  1   ALL SOURCES INCLUDED
c             2   ATMOSPHERIC CONTRIBUTION ONLY
c             3   TRANSMITTER CONTRIBUTION ONLY
c             4   RECEIVER AND BACKSTOP CONTRIBUTION
c
360    nim=5
       if (.not.prompt) write (6,990) nim
       if (prompt) write (6,1650) nim,mp
       read (lunit,1890,end=650) mp
       if (change) go to 670
c
       if (mcomp.eq.1) go to 490
c
370    nim=13
       if (.not.prompt) write (6,1200) nim
       if (prompt) write (6,1660) nim,irtype
       read (lunit,1890,end=650) irtype
c
c      DEFAULT SR PARAMETERS IF DESIRED
c
       xm=xmod(lam)
       g=gainsr(lam)
       eta=qe(lam)
       f=fnoise(lam)
       bwr=srbw(lam)
c  * set wavelength default values for darki & ptherm
       darki=srdark(lam)
       ptherm=srther(lam)
       bwopt=obw(lam)
c
       if (irtype.ne.1) go to 380
       if (change) go to 670
       go to 470
c
c      INPUT USER SUPPLIED PARAMETERS
c
c      MODULATION DEPTH, XM
380    nim=14
       if (.not.prompt) write (6,1000) nim
       if (prompt) write (6,1670) nim,xm
       read (lunit,1890,end=650) xm
       if (change) go to 670
```

```
c
c       DETECTION TYPE,IHET
390     nim=45
        ihet=1
        if (alam.lt.2.e-6) go to 400
        if (.not.prompt) write (6,1010) nim
        if (prompt) write (6,1680) nim,ihet
        read (lunit,1890,end=650) ihet
400     if (change) go to 670
c
c
c       HETERODYNE MIXING EFFICIENCY, EM
410     nim=15
        if(ihet.eq.1) go to 415
        if (.not.prompt) write (6,1020) nim
        if (prompt) write (6,1690) nim,em
        read (lunit,1890,end=650) em
415     if (change) go to 670
c
c       QUANTUM EFFICIENCY, ETA
420     nim=16
        if (.not.prompt) write (6,1030) nim
        if (prompt) write (6,1700) nim,eta
        read (lunit,1890,end=650) eta
        if (change) go to 670
c
c  * add detector gain *
c       DETECTOR GAIN
435     nim=52
        if (ihet.eq.2) go to 440
        if (.not.prompt) write (6,1035) nim
        if (prompt) write (6,1705) nim,g
        read (lunit,1890,end=650) g
        if (change) go to 670
c
c       NOISE ASSOCIATED WITH GAIN, F
430     nim=17
        if (.not.prompt) write (6,1040) nim
        if (prompt) write (6,1710) nim,f
        read (lunit,1890,end=650) f
        if (change) go to 670
c
c       SR BANDWIDTH, BWR
440     nim=18
        if (.not.prompt) write (6,1050) nim
        if (prompt) write (6,1720) nim,bwr
        read (lunit,1890,end=650) bwr
        if (change) go to 670
c
c  * due to fundamental difference in resulting noise statistics
```

```
c      lumped noise parameter pnep must be separated into darki & ptherm *
c         THERMAL NOISE POWER, PTHERM, & DARK CURRENT, DARKI
450    nim=19
c
       if(ihet.eq.2) go to 451
       if (.not.prompt) write (6,1060) nim
       if (prompt) write (6,1730) nim,ptherm
       read (lunit,1890,end=650) ptherm
       if (.not.prompt) write (6,1065) nim
       if (prompt) write (6,1735) nim,darki
       read (lunit,1890,end=650) darki
451    if (change) go to 670
c
c         SR OPTICAL BANDWIDTH
460    nim=29
       if (.not.prompt) write (6,1070) nim
       if (prompt) write (6,1740) nim,bwopt
       read (lunit,1890,end=650) bwopt
       if (change) go to 670
c
c      DAY/NIGHT SWITCH FOR BACKGROUND NOISE COMPUTATION
470    nim=30
c
       if(ihet.eq.2) go to 471
       if (.not.prompt) write (6,1080) nim
       if (prompt) write (6,1750) nim,nflg
       read (lunit,1890,end=650) nflg
471    if (change) go to 670
c
c
c      LINK INFORMATION BANDWIDTH, BW
480    nim=7
       if (.not.prompt) write (6,830) nim
       if (prompt) write (6,1490) nim,bw
       read (lunit,1890,end=650) bw
       if (change) go to 670
c
c      SR  APERTURE AREA
490    nim=12
       if (.not.prompt) write (6,970) nim
       if (prompt) write (6,1630) nim,asr
       read (lunit,1890,end=650) asr
       if (change) go to 670
c
c      SR LINEAL FIELD OF VIEW, PHI
500    nim=11
       if (.not.prompt) write (6,960) nim
       if (prompt) write (6,1620) nim,phi
       read (lunit,1890,end=650) phi
       if (change) go to 670
```

```
c
c       SR LINEAL FIELD OF VIEW (AZIMUTH), PHIAZ
510     if (mcomp.ne.2.and.istog.eq.0) go to 520
        nim=40
        if (.not.prompt) write (6,1090) nim
        if (prompt) write (6,1760) nim,phiaz
        read (lunit,1890,end=650) phiaz
        if (change) go to 670
c
c       TRANSMITTER HOOD LENGTH, BLT
520     nim=20
        if (.not.prompt) write (6,1100) nim
        if (prompt) write (6,1770) nim,blt
        read (lunit,1890,end=650) blt
c
c       TRANSMITTER HOOD DIAMETER, BDRT
530     nim=42
c       SET DEFAULT VALUE = TO OPTICS DIAMETER
        bdrt=dt
        if (blt.eq.0.) go to 540
        if (.not.prompt) write (6,1110) nim
        if (prompt) write (6,1780) nim,bdrt
        read (lunit,1890,end=650) bdrt
        if (change) go to 670
c
c       RECEIVER HOOD LENGTH, BLR
540     nim=21
        if (.not.prompt) write (6,1130) nim
        if (prompt) write (6,1790) nim,blr
        read (lunit,1890,end=650) blr
c
c       RECEIVER HOOD DIAMETER, BDLR
550     nim=43
c       SET DEFAULT VALUE = TO OPTICS DIAMETER
        bdlr=dr
        if (blr.eq.C.) go to 560
        if (.not.prompt) write (6,1120) nim
        if (prompt) write (6,1800) nim,bdlr
        read (lunit,1890,end=650) bdlr
        if (change) go to 670
c
c       SR ALTITUDE, HS
560     nim=22
        if (istog.eq.0) go to 570
        if (.not.prompt) write (6,1140) nim
        if (prompt) write (6,1810) nim,hs
        read (lunit,1890,end=650) hs
570     if (change) go to 670
c
c       ANGLE OF INTERCEPT PLANE, GAMINT
```

```
580    nim=41
       if (istog.eq.1) go to 590
       if (.not.prompt) write (6,1160) nim
       gamd=gamint*r2d
       if (prompt) write (6,1830) nim,gamd
       read (lunit,1890,end=650) gamd
       gamint=gamd/r2d
590    if (change) go to 670
c
c      INTERCEPT MODE, MODE
600    if (istog.eq.1) go to 660
       nim=26
       if (.not.prompt) write (6,1150) nim
       if (prompt) write (6,1820) nim,mode
       read (5,1890,end=650) mode
c  * Pr(e) analysis not valid for heterodyne case *
c      PR(E) ANALYSIS NOT VALID FOR HETERODYNE RCVR
       if (mode.eq.6.and.ihet.eq.2) go to 605
c  * add additional branching for mode 6 *
       if (mode.eq.6) go to 610
       if (mode.ge.4.and.mode.lt.7) go to 630
       if (mode.ne.7) go to 610
       write (6,1870)
       write (6,1880)
       go to 600
c
c      GO BACK TO ALLOW FOR CHANGE OF DECTECTION TYPE
605    write (6,1868)
       go to 390
c
610    if (change) change=.not.change
c
c  * add branching for mode 6 *
620    if (mode.gt.3.and.mode.ne.6) go to 630
       nim=23
       if (.not.prompt) write (6,1170) nim
       if (prompt) write (6,1840) nim,rpx
       read (lunit,1890,end=650) rpx
       if (change) go to 670
c
c  * add branching for mode 6 *
630    if (mode.gt.3.and.mode.ne.6) go to 640
       nim=24
       if (.not.prompt) write (6,1180) nim
       if (prompt) write (6,1850) nim,x
       read (lunit,1890,end=650) x
       if (change) go to 670
c
c  * inputs for Pr(e0 analysis - theta,t,npts,form0,form1
635    if (mode.ne.6) go to 660
```

```
c       HAVE SR PARAMETERS NEEDED FOR MODE 6 BEEN INPUT?
        if (mcomp.eq.2) go to 636
        mcomp=2
        change=.not.change
        go to 350
c
636     nim=49
        if (.not.prompt) write (6,890) nim
        theta=theta*r2d
        if (prompt) write (6,1865) nim,theta
        read (lunit,1890,end=650) theta
        theta=theta/r2d
        if (change) go to 670
c
c       BIT INTERVAL TIME, T
637     nim=50
        if (.not.prompt) write (6,891) nim
        if (prompt) write (6,1866) nim,t
        read (lunit,1890,end=650) t
        if (change) go to 670
c
c       SAMPLED SIGNAL WAVEFORMS, NPTS, FORMO & FORM1
638     nim=51
        if (.not.prompt) write (6,892) nim
        if (prompt) write (6,1867) nim,npts
        read (lunit,1890,end=650) npts
        if (npts.eq.2*(npts/2)) go to 638
        write (6,893)
        read (lunit,1890,end=650) (form0(i),i=1,npts)
        write (6,894)
        read (lunit,1890,end=650) (form1(i),i=1,npts)
        if (change) go to 670
        go to 660
c
640     if (mode.lt.4) go to 660
        nim=27
        if (.not.prompt) write (6,1190)
        if (prompt) write (6,1860) nim,dcomp(mcomp)
        read (lunit,1890,end=650) dcomp(mcomp)
        if (change) go to 670
        go to 660
c
c       PROMPT SWITCH
c       TWO SCHEMES ARE POSSIBLE, ONE USING SEVERAL FILES
c       ON THE SAME LOGICAL UNIT, THE OTHER USING INCREMENTING
c       LOGICAL UNIT NUMBERS.  IN EACH CASE SEVERAL FILES MUST BE
c       ALLOCATED TO THE TERMINAL SINCE EACH TIME THE PROMPT SWITCH
c       IS USED THE CURRENT TERMINAL INPUT FILE IS TERMINATED.
c
650     prompt=.not.prompt
```

```
        if (modesw.eq.2) lunit=lunit+1
        go to 690
c
660     write (6,710)
        go to 680
c
670     write (6,720)
        read (lunit,1890) nim
        if (nim.eq.0) go to 680
        go to 690
c
680     change=.false.
        write (6,730)
        read (lunit,1890) ic
        if (ic.eq.3) go to 10
        if (ic.eq.2) go to 700
        change=.true.
        write (6,740)
        read (lunit,1890) nim
c  * add input code branch points *
690     go to (10,80,90,140,360,210,480,220,230,240,500,490,370,380,410,42
     &   0,430,440,450,520,540,560,620,630,350,600,640,30,460,470,110,150,1
     &   90,250,270,280,330,340,290,510,580,530,550,180,390,300,310,
     &   320,635,637,638,435), nim
-700    return
c
c       FORMAT STATEMENTS FOR PARTIAL PROMPT MODE
c
c
710     format (//,10x,"end of inputs")
720     format (10x,"next input? if none, enter 0")
730     format (10x,"do you wish to change anything? 1-yes  2-no  3-all")
740     format (10x,"which input?  enter input code.")
750     format (3x,i3,4x,"lamda ",2x,i3)
760     format (3x,i3,4x,"ia    ",2x,i3)
770     format (3x,i3,4x,"dt    ",2x,f7.3)
780     format (3x,i3,4x,"phit  ",2x,1pe11.3)
790     format (3x,i3,4x,"dr    ",2x,f7.3)
800     format (3x,i3,4x,"psiaz ",2x,f7.3)
810     format (10x,"psiel ",2x,f7.3)
820     format (3x,i3,4x,"pt    ",2x,1pe11.3)
830     format (3x,i3,4x,"bw    ",2x,1pe11.3)
840     format (3x,i3,4x,"rl    ",2x,1pe11.3)
850     format (3x,i3,4x,"ht    ",2x,1pe11.3)
86C     format (3x,i3,4x,"hr    ",2x,1pe11.3)
870     format (3x,i3,4x,"istog ",2x,i3)
880     format (3x,i3,4x,"x     ",2x,1pe11.3)
890     format (3x,i3,4x,"theta ",2x,1pe11.3)
891     format (3x,i3,4x,"t     ",2x,1pe11.3)
892     format (3x,i3,4x,"npts  ",2x,i3)
```

```
893    format (10x,"space waveform")
894    format (10x,"mark waveform")
900    format (3x,i3,4x,"ibflag",2x,i3)
910    format (3x,i3,4x,"sigj  ",2x,1pe11.3)
920    format (3x,i3,4x,"iw    ",2x,i3)
930    format (3x,i3,4x,"rb    ",2x,1pe11.3)
940    format (3x,i3,4x,"grndi ",2x,1pe11.3)
950    format (3x,i3,4x,"gl    ",2x,1pe11.3)
960    format (3x,i3,4x,"phi   ",2x,1pe11.3)
970    format (3x,i3,4x,"asr   ",2x,1pe11.3)
980    format (3x,i3,4x,"mcomp ",2x,i3)
990    format (3x,i3,4x,"mp    ",2x,i3)
1000   format (3x,i3,4x,"xm    ",2x,f7.3)
1010   format (3x,i3,4x,"ihet  ",2x,i3)
1020   format (3x,i3,4x,"em    ",2x,f7.3)
1030   format (3x,i3,4x,"eta   ",2x,f7.3)
1035   format (3x,i3,4x,"g     ",2x,f7.3)
1040   format (3x,i3,4x,"f     ",2x,f7.3)
1050   format (3x,i3,4x,"bwr   ",2x,1pe11.3)
1060   format (3x,i3,4x,"ptherm",2x,1pe11.3)
1065   format (3x,i3,4x,"darki ",2x,1pe11.3)
1070   format (3x,i3,4x,"bwopt ",2x,1pe11.3)
1080   format (3x,i3,4x,"nite  ",2x,i3)
1090   format (3x,i3,4x,"phiaz ",2x,1pe11.3)
1100   format (3x,i3,4x,"blt   ",2x,f7.3)
1110   format (3x,i3,4x,"bdrt  ",2x,f7.3)
1120   format (3x,i3,4x,"bdlr  ",2x,f7.3)
1130   format (3x,i3,4x,"blr   ",2x,f7.3)
1140   format (3x,i3,4x,"hs    ",2x,1pe11.3)
1150   format (3x,i3,4x,"mode  ",2x,i3)
1160   format (3x,i3,4x,"gamint",2x,i3)
1170   format (3x,i3,4x,"rpx   ",2x,1pe11.3)
1180   format (3x,i3,4x,"x     ",2x,1pe11.3)
1190   format (3x,i3,4x,"dcomp ",2x,i3)
1200   format (3x,i3,4x,"irtype",2x,i3)
1210   format (6x,7(1pe9.2))
1220   format (10x,"do you want another run?  1-yes   2-no")
c
c      FORMAT STATEMENTS FOR FULL PROMPT MODE
c
1230   format (3x,i3,4x,"lam    -- wavelength index                 ",2x,
&      i3,/10x,"(1-.5145   2-.6328  3-.85   4-1.06   5-10.591  6-other)")
1240   format (10x,"enter wavelength in meters")
1250   format (3x,i3,4x,"ia      -- atmospherics (1-user 2-afgl)  ",2x,i3)
1260   format (10x,"if changing to or from space to ground analysis, ",
&      "must input all values")
1270   format (10x,"diffraction limit is ",1pe11.3," radians")
1280   format (10x,"mat    -- atmospheric model              ",2x,i3,/,
&      20x,"1 - tropical",/,20x,"2 - midlatitude summer",/,20x,
&      "3 - midlatitude winter",/,20x,"4 - subarctic summer",/,20x,
```

```
&       "5 - subarctic winter")
1290    format (10x,"mvis  -- visibility (1-clear 2-hazy)      ",2x,i3)
1300    format (10x,"which input file?  must be allocated (eg.4)",/,10x,
&       "0 - skip back to top of inputs")
1310    format (10x,"alfsct -- atmospheric scattering coef, 1/m",2x,
&       1pe11.3)
1320    format (10x,"alfab  -- atmospheric absorption coef, 1/m",2x,
&       1pe11.3)
1330    format (3x,i3,4x,"dt      -- transmitter optics diameter, m  ",2x,
&       f7.3)
1340    format (3x,i3,4x,"phit   -- transmitter beamwidth, radians  ",2x,
&       1pe11.3)
1350    format (3x,i3,4x,"ibsdf  -- bsdf (1-default, 2-user)        ",2x,
&       i3)
1360    format (10x,"ybsdf  -- bsdf y-intercept at 1 degree    ",2x,
&       1pe11.3)
1370    format (10x,"sbsdf  -- bsdf slope (log-log)            ",2x,
&       1pe11.3)
1380    format (10x,"ng       -- number of glitches  (0 - 3)      ",2x,i3)
1390    format (10x,"enter  --",/,15x,"gstart(",i1,") - start of glitch ",
&       "(degrees)",4x,0pf7.2,/,15x,"gend(",i1,") - end of glitch ",
&       "(degrees)",8x,0pf7.2,/,15x,"gampl(",i1,") - amplitude of glitch",
&       11x,1pe12.4)
1400    format (3x,i3,4x,"dr      -- link receiver optics diameter, m",2x,
&       f7.3)
1410    format (3x,i3,4x,"psiaz -- az. orientation of backstop (deg) ",
&       2x,f7.3,/,21x," 0 - normal to beam")
1420    format (10x,"psiel  -- el. orientation of backstop (deg) ",2x,
&       f7.3,/,21x," 0 - normal to beam")
1430    format (3x,i3,4x,"nbak    -- backstop  (1-default, 2-user, ",
&       "3-lambertian) ",2x,i3)
1440    format (10x,"enter  -- bmaxs,  bfwhms,  bdiff "/21x,f8.4,2x,f8.4,
&       2x,f8.4)
1450    format (10x,"bdiff -- diffuse reflectance (0 to 1)        ",2x,/,
&       20x,"(lambertian model, eg. .1)",f7.3)
1460    format (3x,i3,4x,"noa     -- rcvr scatter (1-default, 2-user)",2x,
&       i3)
1470    format (10x,"enter  -- oasmax,  oafwhm, diffoa "/21x,f8.4,2x,f8.4,
&       2x,f8.4)
1480    format (3x,i3,4x,"pt      -- transmit power, watts          ",2x,
&       1pe11.3)
1490    format (3x,i3,4x,"bw      -- link bandwidth, hz             ",2x,
&       1pe11.3)
1500    format (3x,i3,4x,"rl      -- link range, meters             ",2x,
&       1pe11.3)
1510    format (3x,i3,4x,"ht      -- altitude of transmitter, meters ",2x,
&       1pe11.3)
1520    format (3x,i3,4x,"hr      -- altitude of link receiver, m    ",2x,
&       1pe11.3)
1530    format (3x,i3,4x,"istog -- space to ground (0-no, 1-yes)    ",2x,
```

```
&      i3)
1540   format (3x,i3,4x,"x       --  sr distance. to beam center, m ",2x,
&      1pe11.3)
1550   format (3x,i3,4x,"theta  --  zenith angle of sr, deg          ",2x,
&      1pe11.3)
1560   format (3x,i3,4x,"ibflag --  inputs using turbulence 1-yes 2-no",
&      2x,i3)
1570   format (3x,i3,4x,"sigj   --  total jitter, rad               ",2x,
&      1pe11.3)
1580   format (3x,i3,4x,"iw     --  turbulence                      ",2x,
&      i3,/,21x,"1-severe 2-moderate 3-mild")
1590   format (3x,i3,4x,"rb     --  radius of link beam, m          ",2x,
&      1pe11.3)
1600   format (3x,i3,4x,"grndi  --  equivalent irradiance, watts/sq.m",2x,
&      1pe11.3)
1610   format (3x,i3,4x,"gl     --  altitude at ground level, m     ",2x,
&      1pe11.3)
1620   format (3x,i3,4x,"phi    --  sr field of view, radians       ",2x,
&      1pe11.3)
1630   format (3x,i3,4x,"asr    --  area of sr aperture, sq. meters ",2x,
&      1pe11.3)
1640   format (3x,i3,4x,"mcomp  --  compute   1-power   2-s/n ratio ",2x,
&      i3)
1650   format (3x,i3,4x,"mp     --  source? 1-sum, 2-atm, 3-tr, 4-rc",2x,
&      i3)
1660   format (3x,i3,4x,"irtype --  sr type (1-default, 2-user input)",1x,
&      i3)
1670   format (3x,i3,4x,"xm     --  modulation depth               ",2x,
&      f7.3)
1680   format (3x,i3,4x,"ihet   --  detection type                 ",2x,
&      i3,/,21x,"1 - direct  2 - heterodyne")
1690   format (3x,i3,4x,"em     --  mixing efficiency              ",2x,
&      1pe11.3)
1700   format (3x,i3,4x,"eta    --  quantum efficiency of detector ",2x,
&      f7.3)
1705   format (3x,i3,4x,"g      --  predetection gain              ",2x,
&      f7.3)
1710   format (3x,i3,4x,"f      --  excess noise factor            ",2x,
&      1pe11.3)
1720   format (3x,i3,4x,"bwr    --  bandwidth of sr, hz            ",2x,
&      1pe11.3)
1730   format (3x,i3,4x,"ptherm --  thermal noise eqv. power of sr, w",1x,
&      1pe11.3)
1735   format (3x,i3,4x,"idark  --  dark current of sr             ",2x,
&      1pe11.3)
1740   format (3x,i3,4x,"bwopt  --  sr optical bandwidth, microns   ",2x,
&      1pe11.3)
1750   format (3x,i3,4x,"nflg   --  1-sunny 2-cloudy 3-nighttime    ",2x,
&      i3)
1760   format (3x,i3,4x,"phiaz  --  sr field of view (azimuth), rad ",2x,
```

```
     &      1pe11.3)
1770   format (3x,i3,4x,"blt     -- hood length of transmitter, m    ",2x,
     &      f7.3)
1780   format (3x,i3,4x,"bdrt    -- transmitter hood diameter, m      ",2x,
     &      f7.3)
1790   format (3x,i3,4x,"blr     -- hood length of receiver, m        ",2x,
     &      f7.3)
1800   format (3x,i3,4x,"bdlr    -- receiver hood diameter, m         ",2x,
     &      f7.3)
1810   format (3x,i3,4x,"hs      -- altitude of sr, meters            ",2x,
     &      1pe11.3)
1820   format (3x,i3,4x,"mode    -- select output mode (7 for info) ",2x,
     &      i3)
1830'  format (3x,i3,4x,"gamint -- angle of  intercept plane, deg   ",2x,
     &      1pe11.3,/,21x," 0 for horizontal plane")
1840   format (3x,i3,4x,"rpx     -- distance from xmtr to bisector, m",1x,
     &      1pe11.3)
1850   format (3x,i3,4x,"x       -- perpendicular dist to beam axis, m",
     &      1pe11.3)
1860   format (3x,i3,4x,"dcomp  -- value of contour, dbw or db s/n ",2x,
     &      1pe11.3)
1865   format (3x,i3,4x,"theta  -- angle link axis to sr axis, d    ",2x,
     &      1pe11.3)
1866   format (3x,i3,4x,"t       -- bit interval, s",19x,1pe11.3)
1867   format (3x,i3,4x,"npts    -- sample pts in signal waveform      ",
     &      2x,i3,/,22x,"(npts must be odd)")
1868   format (/,20x,"Pr(e) analysis not valid for heterodyne rcvr")
1870   format (/11x,"<-- rpx -->",//,10x,"t)-------------------","+",
     &      "--------(r",/,21x,"a",9x,"/",/,21x,"!",8x,"/",2x,"theta",/,21x,
     &      "!",7x,"/",/,21x,"!",6x,"/",/,27x,"/",/,21x,"x",4x,"/",/,25x,"/",
     &      /,21x,"!",2x,"/",/,21x,"!",1x,"/",/,21x,"v","/",/,21x,"sr)"//,10x,
     &      "rs = distance from sr to +",/,10x,"rv = distance from t to +",/)
1880   format (10x,"mode 1 - fix x, rpx, and vary theta",/,19x,"to scan ",
     &      "link with sr position fixed.",/,10x,"mode 2 - fix rs, rv, and ",
     &      "vary theta",/,19x,"to observe same point in link from different ",
     &      "angles.",/,10x,"mode 3 - fix x and vary theta and rpx",/,19x,
     &      "to observe beam along a line parallel to the link axis.",/,10x,
     &      "mode 4 - isophotes looking at the transmitter only."/,10x,
     &      "mode 5 - isophotes summing total power from sweeping the entire ",
     &      "link.",/,10x,"mode 6 - probability of bit error fixing rpx, x ",
     &      "and theta."/)
1890   format(v)
       end
c.

       subroutine setup
c
c      THIS ROUTINE CALLS THE SINGLE POINT ROUTINE
c      TO CALCULATE A SERIES OF POINTS GIVING A
c      PROFILE OF THE OFF-AXIS S/N IN SEVERAL
c      MANNERS DETERMINED BY THE MODE SELECTED.
```

```
c
c       SCENARIO DIAGRAM
c
c       <-- RPX -->
c       T)---------------------+------(R
c       A               /
c       !             /   THETA
c       !           /
c       !         /
c       /       /
c       X     /
c       /   /
c       ! /
c       ! /
c       V/
c       SR)
c
c       RV      - DIST. FROM XMTR TO BEAM(+)
c       RS      - DIST. FROM SR TO BEAM(+)
c       RT      - DIST. FROM XMTR TO SR
c       RL      - DIST. FROM XMTR TO RCVR
c       HS      - ALTITUDE OF SR
c       PHI     - FOV (ELEV) OF SR IN RAD
c       THETA   - ANGLE BETWEEN SR OPTICAL AXIS AND LINK BEAM SEGMENT
c       TO THE LINK RECEIVER
c       RPX     - DIST. FROM XMTR TO INTERSECTION OF ORTHOGONAL RAY
c       FROM SR
c       X       - DIST. ALONG ORTHOGONAL RAY TO BEAM
c       ANGTR   - THETA TO XMTR
c       ANGREC  - THETA TO RECEIVER
c       DP      - LINK PATH ZENITH ANGLE
c       ANGTOT  - TOTAL ANGLE SUBTENDED BY LINK AT SR
c
c       COMP    - CONTRIBUTION FROM LINK BEAM (POWER OR S/N)
c       TD      - THETA IN DEGREES
c       NRET    - SET TO 1 IF COMP=0 TO AVOID LOG(0)
c       DANG    - INCREMENT OF THETA
c       ANGMAX  - MAXIMUM THETA
c       GAMINT  - ANGLE OF INTERCEPT PLANE
c       GAMP    -  ZENITH ANGLE FROM TR TO SR
c
c       COMPB4  - LAST VALUE OF COMP
c       RSB4    - LAST VALUE OF RS
c       DCOMP   - DESIRED CONVERGENCE VALUE OF COMP
c       SLOPE   - SLOPE BETWEEN LAST TWO POINTS
c       RSNEW   - ESTIMATED VALUE FOR RS
c       H       - NO. OF ITERATIONS NEEDED TO CONVERGE (ARRAY)
c
c       XINT    - X ARRAY FOR STORING OUTPUT
c       YINT    - Y ARRAY FOR STORING OUTPUT
```

```
c
      common/ flags /mode,mcomp,mp,lam,modesw,lunit,nout,istog,iotype,
&     irtype,ihet,ibflag,iw
      common/ tdata / blt,dt,ht,phit,pt,rb,grndi,bdrt,sigj,sigt
      common/ rdata / blr,dr,hr,gl,bdlr
      common/ srdata / asr,hs,phi,phiaz,dphi
      common/ ldata / rl,alam,rpx,theta,x,angtr,angrec,gamint,bw
c  * darki & ptherm replace pnep add g *
      common/ sndata / bwr,eta,f,em,pb,ps,darki,ptherm,snpndb,sndb,xm,
&     bwopt,nflg,g
      common/ pltc  / xint(200),yint(200),h(200),dcomp(2),np,note
      common/ parts / pa,prtr,prec,pat,prt,pre
c  * add labeled common wavefm *
      common/ wavefm / npts,t,form0(1000),form1(1000),power0(1000),
&     power1(1000)
c
      double precision re,reht,rehr,gamp,disc
      data re/6.31131d6/
      data onedeg,pi,r2d/.0174532925,3.141592654,57.29577951/
      data blank,star/" ","*"/
c     BLANK OUT CONVERGENCE WARNING SYMBOL ARRAY
      do 10 i=1,100
 10   h(i)=blank
c
      nret=0
      np=0
      rehr=re+hr
      reht=re+ht
c     ANGTR  - THETA TO TRANSMITTER
c     ANGREC - THETA TO RECEIVER
c     LINK PATH ZENITH ANGLE DP
      dp=dacos((rehr**2-reht**2-rl**2)/(2.*reht*rl))
c     USE ATAN2 TO GET ANGLES IN THE RIGHT QUADRANT
      angtr=atan2(x,rpx)
      angrec=atan2(x,(rpx-rl))
c
c     CHECK TO SEE IF BOTTOM OF BEAM HITS A CURVED EARTH
c
      xi=dp+phit
      disc=re**2-(reht*sin(xi))**2
c
c     IF DISC IS NEGATIVE NO REAL ROOT EXISTS
c
      if (disc.le.0.) go to 20
c
c     CALCULATE RANGE TO GROUND, RG
c
      rg=-reht*cos(xi)-dsqrt(disc)
c
      if(rg.gt.0..and.rg.lt.rl) write (6,210) rg
```

```
c   * add mode 6 *
20    go to (30,50,80,130,130,125), mode
c
c
c     MODE=1  FIX X, RPX,  AND VARY THETA TO SCAN LINK WITH A FIXED
c     SURVEILLANCE RECEIVER LOCATION
c
c
c     ANGTOT IS THE TOTAL ANGLE SUBTENDED BY THE LINK AT THE
c     SURVEILLANCE RECEIVER
c
30    angtot=angrec-angtr-phi
c
      rt=sqrt(rpx**2+x**2)
      gamp=acos((rpx*cos(dp)+x*sin(gamint)*sin(dp))/rt)
      hs=dsqrt(reht**2+rt**2+2.*rt*reht*dcos(gamp))-re
      dang=(angtot-20.*onedeg)/16.
      if (dang.lt.onedeg) dang=onedeg
c
c     START FROM TRANSMITTER TOWARD RECEIVER
c
      theta=angtr+phi/2.
      do 40 i=1,50
      call comtot (comp,nret)
      td=theta*r2d
c
c     WRITE THE OUTPUT
      if (nout.ge.1) write (nout,190) td,comp,prtr,prec,pa
c
c     STORE THE RESULTS
      xint(i)=td
      yint(i)=comp
      delta=onedeg
c
c     PICK DELTA OF ONE DEGREE NEAR THE TRANSMITTER & RECEIVER
c
      if (i.gt.9.and.i.lt.26) delta=dang
      theta=theta+delta
      if (theta.gt.(angrec-phi/2.)) go to 180
40    continue
c
c
c     MODE=2  FIX RS, RV, VARY THETA TO OBSERVE ONE POINT ALONG THE
c     LINK AXIS FROM DIFFERENT ASPECT ANGLES. NOTE THAT
c     THE SCATTERING VOLUME CHANGES WITH ANGLE.
c
50    theta=onedeg
c     STORE RPX AND X TEMPORARILY IN RPX1 AND X1
      rpx1=rpx
      x1=x
```

```
        rs=x
c       MAXIMUM THETA
        angmax=pi-onedeg
c       THETA INCREMENT
        dang=(pi-phi-22*onedeg)/16.
c
c       START LOOKING TOWARD THE XMTR; LAST POINT HAS THE RCVR IN FOV.
c
        do 60 i=1,40
c       COMPUTE SR POSITION COORDINATES X,RPX
        x=rs*sin(theta)
        rpx=rs*cos(theta)+rpx1
c
        rt=sqrt(rpx**2+x**2)
        angtr=atan2(x,rpx)
        angrec=atan2(x,(rpx-rl))
        gamp=acos((rpx*cos(dp)+x*sin(gamint)*sin(dp))/rt)
        hs=dsqrt(reht**2+rt**2+2.*rt*reht*dcos(gamp))-re
        call comtot (comp,nret)
c       WRITE OUTPUT
        td=theta*r2d
        if (nout.ge.1) write (nout,190) td,comp,prtr,prec,pa
c
c       STORE THETA, COMP
c
        xint(i)=td
        yint(i)=comp
c       THETA INCREMENT IS ONE DEGREE NEAR XMTR AND RCVR
        delta=onedeg
c
c       SAME COMMENT APPLIES AS IN MODE 1
c
        if (i.gt.9.and.i.lt.26) delta=dang
        theta=theta+delta
        if (theta.gt.angmax) go to 70
60      continue
70      x=x1
        rpx=rpx1
        go to 180
c
c
c       MODE=3  FIX X, VARY THETA AND RPX TO OBSERVE BEAM FROM DIFFERENT
c       POINTS ALONG A LINE PARALLEL TO THE LINK OPTICAL AXIS.
c       NOTE THAT AS THETA IS NEAR ZERO OR PI, THE RANGE TO
c       THE SR BECOMES VERY LARGE.
c
80      theta=onedeg+phi/2.
        rpx1=rpx
c       COMPUTE INCREMENT OF THETA
        dang=(pi-phi-22*onedeg)/16.
```

```
c
c       ALWAYS LOOK AT PORTION OF BEAM AT RPX1 METERS AWAY FROM XMTR
c
        do 110 i=1,40
c       AVOID DIVIDE CHECK IN COMPUTING RPX
        if (abs(theta-pi/2.).lt.onedeg) go to 90
        rpx=x/tan(theta)+rpx1
        go to 100
90      rpx=rpx1
100     rs=sqrt(rpx1**2+x**2)
c
        rt=sqrt(rpx**2+x**2)
        angtr=atan2(x,rpx)
        angrec=atan2(x,(rpx-rl))
        gamp=acos((rpx*cos(dp)+x*sin(gamint)*sin(dp))/rt)
        hs=dsqrt(reht**2+rt**2+2.*rt*dcos(gamp))-re
        call comtot (comp,nret)
c
c       WRITE OUTPUT
        td=theta*r2d
        if (nout.ge.1) write (nout,190) td,comp,prtr,prec,pa
c
c       STORE THETA, SNDB
c
        xint(i)=td
        yint(i)=comp
c       INCREMENT BY ONE DEGREE
        delta=onedeg
        if (i.gt.9.and.i.lt.26) delta=dang
        theta=theta+delta
        if (theta.gt.3.1241) go to 120
110     continue
120     rpx=rpx1
        go to 180


c
c   * add mode 6 *
c     MODE=6   PROBABILITY OF BIT ERROR
c
125     rt=sqrt(rpx**2+x**2)
        angtr=atan2(x,rpx)
        angrec=atan2(x,(rpx-rl))
        gamp=acos((rpx*cos(dp)+x*sin(gamint)*sin(dp))/rt)
        hs=dsqrt(reht**2+rt**2+2.*rt*dcos(gamp))-re
        write (nout,230) rpx,x,theta
c       CALCULATE SIGNAL POWER
        call comtot(comp,nret)
        do 126 i=1,npts
        power0(i)=ps*form0(i)
        power1(i)=ps*form1(i)
```

```
126     continue
        call back
        call apertr
        call error(nflag,bound1,bound2,bound3,bound4)
        if (nflag.eq.3) write (6,240)
        if (nflag.eq.1.or.nflag.eq.3) write (nout,250) bound1,bound2
        if (nflag.eq.2.or.nflag.eq.3) write (nout,260) bound3,bound4
        go to 180
c
c       *** ITERATIVE ALGORITHM TO FIND CONTOURS ***
c
c       THIS IS BASICALLY A NEWTON-RAPHSON SECANT METHOD MODIFIED TO
c       ALLOW FOR AN EXTREMELY SENSITIVE FUNCTION.  IT ONLY ALLOWS
c       CONVERGENCE FOR ROOTS WHERE THE SLOPE IS NEGATIVE
c       (SEE DOCUMENTATION)
c
c       MODE=4    ISOPHOTES LOOKING AT THE TRANSMITTER
c
c       MODE=5    TOTAL POWER AVAILABLE AT SR LOCATION
c
130     dang=2*onedeg
c
        tdang=2.96*onedeg
        angtr=-onedeg
        kk=0
        do 170 i=1,124
c
135     nret=0
        angtr=angtr+dang
c
c       COMPUTE THETA INCREMENT TO SPACE DATA POINTS APPROPRIATELY IN X,
c       RPX COORDINATES
        dang=.03158826*(angtr)**.71533599
        if (angtr.gt.1.56) dang=tdang
c
c
c       MAKE A CALCULATED FIRST GUESS AT THE RIGHT RS
c          NOTE HERE RS=RT SINCE WE ARE LOOKING AT THE TRANSMITTER
c
        rs=rl*(.2+cos(angtr/2.))
c
c       COMPUTE SR LOCATION COORDINATES X,RPX
        x=rs*sin(angtr)
        rpx=rs*cos(angtr)
        angrec=atan2(x,(rpx-rl))
        gamp=dp-acos(sqrt(rpx**2+(x*sin(gamint))**2)/rs)
        hs=dsqrt(reht**2+rs**2+2.*rs*reht*dcos(gamp))-re
c
c       COMPUTE INITIAL VALUE FOR ITERATION
        theta=angtr+phi/2.
```

```
              if (mode.eq.4) call comtot (compb4,nret)
              if (mode.eq.5) call mode5 (compb4,nret)
c
c       IF POWER IS ZERO, SKIP TO NEXT ANGLE
c
              if (nret.eq.1) go to 135
              rsb4=rs
              rs=rsb4*1.10
c
c       ALLOW NLOOP TRIES FOR CONVERGENCE
              nloop=20
              do 140 ii=1,nloop
              x=rs*sin(angtr)
              rpx=rs*cos(angtr)
              angrec=atan2(x,(rpx-rl))
              gamp=acos((rpx*cos(dp)+x*sin(gamint)*sin(dp))/rs)
              hs=dsqrt(reht**2+rs**2+2.*rs*reht*dcos(gamp))-re
              theta=angtr+phi/2.
              if (mode.eq.4) call comtot (comp,nret)
              if (mode.eq.5) call mode5 (comp,nret)
c
c       IF POWER IS ZERO, SKIP TO NEXT ANGLE
c
              if (nret.eq.1) go to 135
c
c       CONVERGENCE TEST
              if (abs(comp-dcomp(mcomp)).lt..2) go to 150
              slope=(rs-rsb4)/(comp-compb4)
              rsnew=(rs-(comp-dcomp(mcomp))*slope)
c       SET TO ONE HALF PREVIOUS GUESS IF THE GUESS IS NEGATIVE
              if (rsnew.le.0.) rsnew=rs/2.
              rsb4=rs
              rs=rsnew
              compb4=comp
140           continue
c       DID NOT CONVERGE IN NLOOP TRIES
c       SET FLAG FOR CONVERGENCE WARNING
              note=note+1
              go to 160
c       CHECK FOR SLOPE AT ROOT
c
150           if (slope.gt.0.) go to 135
160           xint(i)=rpx
              yint(i)=x
              h(i)=ii
              if (nout.ge.1.and.mode.eq.4) write (nout,200) x,rpx,h(i),prtr,prec
     &        ,pa
              if (nout.ge.1.and.mode.eq.5) write (nout,200) x,rpx,h(i),prt,pre,p
     &        at
              if(hs.lt.0) kk=1
```

```
170     continue
        if(kk.eq.1) write (6,220)
c
180     np=1
        return
c
190     format (2x,2(3x,1pe11.4),7x,4(3x,1pe11.4))
200     format (2x,2(3x,1pe11.4),2x,0pf3.0,2x,4(3x,1pe11.4))
210     format (5x,"link beam hit ground at a range of ",1pe11.3,"meters")
220     format (2x,"warning -- part of the contour is below sea level ",
     &        "altitude.",/,13x,"keep this in mind when you interpret the ",
     &        "output.")
230     format (/,6x,"SR location:",/,6x,"rpx =",1pe10.1,"  x =",1pe10.3,
     &        "  theta =",1pe10.3,/)
240     format (6x,"receiver noise is a  combination of shot and thermal ",
     &        "or excess noise - ",/,6x,"bounds are not absolute",/)
250     format (6x,"shot noise limited performance -    ",1pe8.2,
     &        " < Pr(e) < ",1pe8.2)
260     format (6x,"thermal noise limited performance - ",1pe8.2,
     &        " < Pr(e) < ",1pe8.2)
        end
c.
        subroutine mode5 (comp,nret)
c
c       INTEGRATES TO FIND TOTAL POWER AVAILABLE FROM LINK AT A POINT
c       DEFINED BY X,RPX
c
c       ANGTOT - TOTAL ANGLE SUBTENDED BY LINK
c       NTHETA - NUMBER OF STEPS OF INTEGRATION
c       DTHETA - INCREMENT OF THETA
c       ANGTR  - THETA TO XMTR
c
c       COMP   - POWER OR S/N CONTRIBUTION FROM LINK
c       SUM    - SUM OF COMP CONTRIBUTIONS FROM EACH THETA
c       NRET   - FLAG TO INDICATE THAT COMP=0
c
        common / ldata / rl,alam,rpx,theta,x,angtr,angrec,gamint,bw
        common / srdata / asr,hs,phi,phiaz,dphi
        common/parts/pa,prtr,prec,pat,prt,pre
c
c       COMPUTE TOTAL ANGLE SUBTENDED AT SR
        angtot=angrec-angtr
c
c       COMPUTE NUMBER OF STEPS USED IN INTEGRATION
        ntheta=amax1((angtot/3.4+1.),2.)
        ntheta=ntheta*2+1
        dtheta=angtot/ntheta
c
c       USE SIMPSON*S RULE FOR INTEGRATION
c       NTHETA MUST BE ODD
```

```
c
        sum=0.
        theta=angtr
c       COMPUTE BEAM POWER ONLY; ADD XMTR AND RCVR LATER
        mp=2
        do 10 n=1,ntheta
c
c       COMPUTE POWER
        call comtot (comp,nret)
c       NORMALIZE CONTRIBUTION TO 1/RAD
        comp=pa/phi
        coef=2*(2-mod(n,2))
        if (n.eq.1.or.n.eq.ntheta) coef=1.
        sum=comp*coef+sum
        theta=theta+dtheta
10      continue
        sum=dtheta/3.*sum
        pat=sum
c
c       FINAL INTEGRAL VALUE IS RETURNED AS COMP TO FIND ISO-CONTOUR
c       USING MODE 4 ITERATION ALGORITHM
c
c
c       TRANSMITTER CONTRIBUTION
c
        mp=3
        theta=angtr
        call comtot (comp,nret)
        sum=sum+prtr
        prt=prtr
c
c       RECEIVER CONTRIBUTION
c
        mp=4
        theta=angrec
        call comtot (comp,nret)
        sum=sum+prec
        pre=prec
        mp=1
c
        if (sum.eq.0) go to 20
        nret=0
c
c       CONVERT TO DB
c
        comp=10*alog10(sum)
        go to 30
c
c       NRET IS FLAG FOR NO POWER
20      nret=1
```

```
c
      comp=-200.
30    return
      end
c.
      subroutine comtot (comp,nret)
c
c     COMTOT COMPUTES THE POWER FROM THE LINK BY CALLING THE
c     ROUTINES WHICH COMPUTE THE POWER FROM ATMOSPHERIC
c     SCATTERING, THE RECEIVER, AND THE TRANSMITTER.  IT RETURNS
c     VARIABLE COMP WHICH IS EITHER POWER (DBW) OR S/N (DB), AS
c     SELECTED. IF COMP IS ZERO, NRET IS RETURNED WITH A VALUE
c     OF 1.
c
c     THTMAX - MAXIMUM THETA FOR FIELD OF VIEW (FOV)
c     THTMIN - MINIMUM THETA FOR FIELD OF VIEW (FOV)
c     PR      - SUM OF POWER FROM DESIRED SOURCES
c     PA      - POWER CONTRIBUTION FROM ATMOSPHERE
c     PRTR    - POWER CONTRIBUTION FROM TRANSMITTER
c     PREC    - POWER CONTRIBUTION FROM RECEIVER
c     PS      - SIGNAL POWER USED FOR S/N CALCULATION
c
      common/ flags / mode,mcomp,mp,lam,modesw,lunit,nout,istog,iotype,
&     irtype,ihet,ibflag,iw
      common/ ldata / rl,alam,rpx,theta,x,angtr,angrec,gamint,bw
      common/ srdata / asr,hs,phi,phiaz,dphi
      common/parts/pa,prtr,prec,pat,prt,pre
c  *  darki & ptherm replace pnep add g *
      common/ sndata / bwr,eta,f,em,pb,ps,darki,ptherm,snpndb,sndb,xm,
&     bwopt,nflg,g
      data epsi/1.e-4/
      phio2=phi/2.
c
      thtmax=theta+phio2+epsi
      thtmin=theta-phio2-epsi
      pr=0.
      pa=0.
      prtr=0.
      prec=0.
c
c     MP  --   COMPUTE FLAG USED TO DETERMINE WHICH SOURCES TO INCLUDE
c     1 -- SUM OF ALL SURCES
c     2 -- ATMOSPHERIC CONTRIBUTION ONLY
c     3 -- TRANSMITTER CONTRIBUTION ONLY
c     4 -- RECEIVER CONTRIBUTION ONLY
c
      if (mp.gt.2) go to 10
      call beam (pa)
      pr=pa+pr
10    if (mp.eq.2.or.mp.eq.4) go to 20
```

```
c
c       CHECK TO SEE IF TRANSMITTER IS IN FOV, IF SO, CALL TSCAT
c
        if (angtr.ge.thtmin.and.angtr.le.thtmax) call tscat (prtr)
        pr=pr+prtr
20      if (mp.eq.2.or.mp.eq.3) go to 30
c
c       CHECK TO SEE IF RECEIVER IS IN FOV, IF SO, CALL RSCAT
c
        if (thtmax.ge.angrec.and.thtmin.le.angrec) call rscat (prec)
c
        pr=pr+prec
30      if (pr.le.0) go to 40
        comp=10.*alog10(pr)
c
        if (mcomp.eq.1) go to 50
c
c       COMPUTE S/N IF DESIRED
c
        ps=pr
        call ston
        comp=sndb
        go to 50
c       POWER WAS ZERO; SET FLAG AND RETURN
40      nret=1
c
        comp=-200.
50      return
        end
c.
        subroutine stog (comp,ptstog,prstog,pastog,nret)
c
c       COMPUTES POWER FOR THE CASE OF A VERTICAL SPACE-TO-GROUND LINK.
c
c       *** SEE DOCUMENTATION FOR LIMITATIONS ***
c
c       WARNING:  THE EFFORT EXPENDED ON THIS PORTION OF THE PROGRAM WAS
c       MINIMAL COMPARED TO THE NARROWBEAM PORTIONS, SO THAT
c       THE RESULTS OF SPACE TO GROUND CASES SHOULD BE
c       CAREFULLY SCRUTINIZED.
c
c       VARIABLES (UNITS ARE MKS SYSTEM)
c
c       NVEL    - NO. OF VERT ELEMENTS IN BEAM
c       AVEL    - AREA OF A VERT. ELEMENT
c       SVEL    - WIDTH OF A VERT. ELEMENT
c       NDOWN   - NO. OF VERT. ELEMENTS IN X-DIR.
c       NCROS   - NO. OF VERT . ELEMENTS FROM CENTER IN Y-DIR.
c       XB      - X COORDINATE IN LINK BEAM CENTERED COORDINATES
c       YB      - Y CORRDINATE IN LINK BEAM CENTERED COORDINATES
```

```
c      RVEL   - DIST. OF VERT. ELEMENT FROM CENTER OF BEAM
c
c      RB     - RADIUS OF LINK BEAM TO 1/E**2 POINT
c      XTEMP  - PERP. DISTANCE FROM SR TO CENTER OF BEAM
c      X      - DIST. FROM SR TO VERTICAL ELEMENT
c      RPX    - DIST. FROM BISECTOR OF BEAM TO XMTR
c      PHIAZ  - FOV(AZIMUTH)
c      RL     - LINK RANGE
c      HS     - ALTITUDE OF SR
c      HR     - ALTITUDE OF RCVR
c      HEFF   - EFFECTIVE ALTITUDE OF XMTR
c      PT     - EFFECTIVE POWER OF SOURCE
c      GRNDI  - FACTOR FOR DETERMING EFFECTIVE POWER (W/M**2)
c      WEIGHT - WEIGHTING FACTOR FOR POSITON IN BEAM (FUNCTION)
c
c      ANGTR  - ANGLE TO XMTR
c      ANGREC - ANGLE TO RCVR
c      NUMTOT - TOTAL NUMBER OF INCREMENTAL VOLUMES
c      KOUNT  - NO. OF VERT. ELEMENTS IN INTERCEPTED VOLUME
c
c      XCLOS  - DISTANCE TO CLOSEST INTERCEPTED VERT. ELEMENT
c      HCLOS  - ALTITUDE OF TOP OF CLOSEST INTERCEPTED ELEMENT
c      HCLSDF - SUBTENDED LENGTH OF CLOSEST VERT ELEMENT
c      XDIS   - DISTANCE TO MOST DISTANT INTERCEPTED VERT. ELEMENT
c      HDIS   - ALTITUDE OF TOP OF MOST DISTANT INTERCEPTED ELEMENT
c      HDISDF - SUBTENDED LENGTH OF MOST DISTANT VERT. ELEMENT
c
c      FACTOR - SYMMETRY FACTOR
c      SUMP   - RUNNING SUM OF POWER CONTRIBUTIONS
c      COMP   - POWER CONTRIBUTION
c
c
       common/ flags / mode,mcomp,mp,lam,modesw,lunit,nout,istog,iotype,
     & irtype,ihet,ibflag,iw
       common/ tdata / blt,dt,ht,phit,pt,rb,grndi,bdrt,sigj,sigt
       common/ rdata / blr,dr,hr,gl,bdlr
       common/ srdata / asr,hs,phi,phiaz,dphi
       common/ ldata / rl,alam,rpx,theta,x,angtr,angrec,gamint,bw
       common/ stgout / nvel,svel,avel,ndown,ncros,numtot,hvnear,hvfar,
     & xdis,hdis,hdisdf,xclos,hclos,hclsdf,kount
       data epsi/1.e-4/
c
c      RB IS 1/E**2 POINT OF BEAM. WEIGHT(A) IS THE POWER DISTRIBUTION
c      OFF THE AXIS OF THE BEAM. A GAUSSIAN PROFILE IS ASSUMED.
c
       weight(a)=exp(-2.*(a/rb)**2)
c
c      STORE X
       kount=0
       xtemp=x
```

```
        rltemp=rl
        hstemp=hs
        httemp=ht
        ptemp=pt
        thtemp=theta
c
c       CHECK TO SEE IF THETA<PHI/2
c
        if (theta.lt.phi/2.) theta=phi/2. + epsi
c
c       COMPUTE GRNDI AND RB IF IBFLAG=1
c
        if (ibflag.eq.2) go to 10
        call stbeam (rbeam,grndir)
        rb=rbeam
        grndi=grndir
c
c
c       COMPUTE TANGENT OF AZ FOV HALF-ANGLE-TP2
c
10      tp2=tan(phiaz/2.)
c
c       NUMBER OF VERTICAL ELEMENTS IN LINK BEAM
c
        nvel=100
c
c       AREA OF VERTICAL ELEMENT
c
        avel=4.*rb*xtemp*tp2/nvel
c
c       WIDTH OF VERTICAL ELEMENT
c
        svel=sqrt(avel)
c
c       NUMBER OF VERTICAL ELEMENTS ACROSS BEAM
        ndown=2.*rb/svel+1
c       NUMBER FROM CENTER IN YB DIRECTION
c
        ncros=(xtemp+rb)*tp2/svel+1
c
c       INITIALIZE INTEGRAL
        sump=0.
c       SET SYMMETRY FACTOR FOR CENTER ROW OF VERTICAL ELEMENTS
        factor=1.
c
c       LOOP TO COMPUTE FOR EACH VERTICAL ELEMENT
c
        do 50 ny=1,ncros
        do 30 nx=1,ndown
c
```

```
c       POSITION IN LINK BEAM CENTER COORDINATES
c
        xb=(nx-ndown/2)*svel
        yb=(ny-1)*svel
        rvel=sqrt(xb**2+yb**2)
c
c       TEST IF THE ELEMENT IS INSIDE THE 1/E**2 PTS.
c
        if (rvel.gt.rb) go to 30
c
c       COMPUTE SR FOV BOUNDS FOR TEST
c
        x=sqrt((xtemp-xb)**2+yb**2)
        testp=atan(yb/x)*2.
        if (testp.gt.phiaz) go to 40
c
c       VERTICAL ELEMENT IS IN FOV, SO COMPUTE POWER
c
        heff=hs+x/tan(theta-phi/2.)
        rl=heff-hr
        call trans (hr,heff,rl,tb)
c
c       CALCULATE POWER OF EFFECTIVE SOURCE
c
        pt=grndi*weight(rvel)*avel/tb
        ht=heff
        rpx=heff-hs
c
c       CALCULATE ANGTR AND ANGREC FOR BEAM, ANGTR IS ANGLE TO
c       EFFECTIVE SOURCE
c
        angtr=theta-phi/2.
        angrec=3.14159-atan(x/hs)
c
c       CALL BEAM FOR POWER CONTRIBUTION OF VERTICAL ELEMENT
c
        call beam (comp)
        sump=sump+comp*factor
        kount=kount+factor
c
c       COMPUTE TOTAL NUMBER OF INCREMENTAL VOLUMES
c
        numtot=kount*phi/dphi
c
c       CALCULATE PARAMETERS TO MOST DISTANT ELEMENT
        if (nx.ne.1.or.ny.ne.1) go to 20
        xdis=x/sin(theta)
        hdis=heff
        hdisdf=hvnear-hvfar
c
```

```
c       CALCULATE PARAMETERS TO CLOSEST ELEMENT
20      if (nx.ne.(ndown-2).or.ny.ne.1) go to 30
        xclos=x/sin(theta)
        hclos=heff
        hclsdf=hvnear-hvfar
c
30      continue
c       SET SYMMETRY FACTOR FOR ROWS OFF SR OPTICAL AXIS
c
40      factor=2.
50      continue
        pastog=sump
c
        x=xtemp
        rl=rltemp
        hs=hstemp
        ht=httemp
        pt=ptemp
        theta=thtemp
c
c       TRANSMITTER CONTRIBUTION
c
c       INITIALIZE PARAMETERS FOR CALL TO TSCAT
c
        ptstog=0.
        angtr=atan2(x,rl-hs)
c
c       CALL TSCAT IF TRANSMITTER IS IN FOV
c
        if (theta.ge.angtr-phi/2.and.theta.le.angtr+phi/2.)
&       call tscat (ptstog)
c
c       RECEIVER CONTRIBUTION
c
c       INITIALIZE PARAMETERS FOR CALL TO RSCAT
c
        prstog=0.
        if (gl.eq.hs) go to 60
        angrec=atan2(x,gl-hs)
        go to 70
60      angrec=1.570796
c
c       CALL RSCAT IF RECEIVER IS IN FOV
c
70      if (theta.ge.angrec-phi/2.and.theta.le.angtr+phi/2.)
&       call rscat (prstog)
c
c       SUM FOR TOTAL POWER
c
        comp=prstog+ptstog+pastog
```

```
c
      return
      end
c.
      subroutine stbeam (rbeam,grndir)
c
c     THIS SUBROUTINE CALCULATES THE RADIUS OF THE BEAM
c     AT THE GROUND AND THE PEAK INTENSITY.
c
      common/tdata/blt,dt,ht,phit,pt,rb,grndi,bdrt,sigj,sigt
      common/ldata/rl,alam,rpx,theta,x,angtr,angrec,gamint,bw
      common/rdata/blr,dr,hr,gl,bdlr
      data onedeg,pi,r2d/.0174532925,3.141592654,57.29577951/
c
c     CALCULATE TURBULENCE OF ATMOSPHERE
c
      call sigmat (ht,hr,rl,alam,gl,sigt)
c
c     CALCULATE RADIUS OF BEAM
c
      r2=4.*rl**2*((phit/2.)**2+sigj**2+sigt**2)
      rbeam=sqrt(r2)
c
      call trans (gl,100000.,100000.-gl,tstog)
c
c     CALCULATE EQUIVALENT IRRADIANCE
c
      grndir=.865*pt*tstog/(.4325*pi*r2)
      return
      end
c.
      subroutine sigmat (ht,hr,rl,alam,gl,sigt)
      external cnsq
      common/flags/mode,mcomp,mp,lam,modesw,lunit,nout,istog,iotype,
     &  irtype,ihet,ibflag,iw
      data hatm/100000./
c
c     THIS ROUTINE COMPUTES THE HALF ANGLE BEAMSPREAD(SIGT)
c     DUE TO TURBULENCE.  IW IS A TURBULENCE PARAMETERUSED AS FOLLOWS:
c     1  --  SEVERE TURBULENCE
c     2  --  NOMINAL TURBULENCE
c     3  --  MILD TURBULENCE
c
c     FOR REFERENCE SEE *A SIMPLIFIED PROPAGATION MODEL FOR LASER
c     SYSTEM STUDIES*.  AFWL-TR-72-95(REV),  APRIL 1973
c
c     USE NSTEP NUMBER OF STEPS TO INTEGRATE ALONG PATH LENGTH
      nstep=50
      sig=0.
      deltaz=(hatm-gl)/nstep
```

```
c       MODIFIED FOR VERTICAL USE
        sinphi=-1.
        do 10 j=1,nstep
        aj=j
c
c       WEIGHT CLOSEST PORTIONS TO APERTURE HIGHEST
c
        rnaj=1.-aj*deltaz/rl
        z=deltaz*j+(rl-hatm)
        z1=deltaz*(j-1)+(rl-hatm)
c       HL AND HU ARE THE HEIGHT ABOVE TERRAIN AT THE BEGINNING AND
c       END OF EACH INCREMENT ALONG THE PROPAGATION PATH.
        hl=z*sinphi+ht
        hu=z1*sinphi+ht
        call qg10 (hl-gl,hu-gl,cnsq,deltaz,y)
        sig=rnaj**1.666*y+sig
10      continue
        sigt=(((2.06/alam)**.333)*sig)**.6
        return
        end
c.
        subroutine qg10 (bl,bu,fct,deltaz,y)
c       SUBROUTINE QG10 COMPUTES INTEGRALS OF THE FORM
c       (FCT(X), SUMMED OVER X FROM BL TO BU)
c
c       USAGE
c
c       CALL QG10(BL,BU,FCT,DELTAZ,Y)
c       PARAMETER FCT REQUIRES AN EXTERNAL STATEMENT
c
c       DESCRIPTION OF PARAMETERS
c       BL - THE LOWER BOUND OF THE INTERVAL
c       BU - THE UPPER BOUND OF THE INTERVAL
c       FCT - THE NAME OF AN EXTERNAL FUNCTION SUBPROGRAM USED
c       Y - THE RESULTING INTEGRAL VALUE
c
c       SUBROUTINES AND FUNCTION SUBPROGRAMS REQUIRED
c       THE EXTERNAL FUNCTION SUBPROGRAM FCT(X) MUST BE FURNISHED
c       BY THE USER.
c
c       METHOD
c
c       THE EVALUATION IS DONE BY 10-POINT GAUSS QUADRATURE
c       FORMULA WHICH INTEGRATES POLYNOMIALS UP TO DEGREE 19
c       EXACTLY
c
c       FOR REFERENCE SEE
c       V.1.KRYLOV,APPROXIMATE CALCULATION OF INTEGRALS
c
c
```

```
          if ((bu.eq.bl)) go to 10
          go to 20
10        y=fct(bl)*deltaz
          return
20        a=.5*(bu+bl)
          b=bu-bl
          c=.4869533*b
          y=.03333567*(fct(a+c)+fct(a-c))
          c=.4325317*b
          y=y+.07472567*(fct(a+c)+fct(a-c))
          c=.3397048*b
          y=y+.1095432*(fct(a+c)+fct(a-c))
          c=.2166977*b
          y=y+.1346334*(fct(a+c)+fct(a-c))
          c=.07443717*b
          y=deltaz*(y+.1477621*(fct(a+c)+fct(a-c)))
          return
          end
c.
          function cnsq (h)
c
c         ATMOSPHERIC STRUCTURE CONSTANT IN M**(2/3)
c
          common/flags/mode,mcomp,mp,lam,modesw,lunit,nout,istog,iotype,
&         irtype,ihet,ibflag,iw
c
          if (h.gt.1.0) go to 40
c         SET CNSQ FOR HEIGHT ABOVE TERRAIN LESS THAN ONE METER
c
          go to (10,20,30), iw
c
c         BAD WEATHER CONDITIONS
10        cnsq=2.85e-13
          return
c
c         NOMINAL WEATHER CONDITIONS
20        cnsq=1.e-13
          return
c
c         GOOD WEATHER CONDITIONS
30        cnsq=8.5e-15
          return
c
c         SET CNSQ FOR ALTITUDES LESS THAN ONE METER
c
40        go to (50,90,100), iw
c
c         BAD WEATHER CONDITIONS
50        if (h.gt.100.0) go to 70
          if (h.gt.10.0) go to 60
```

```
            cnsq=2.9e-13*h**(-.6993)
            return
    c
    60      cnsq=9.496e-13*h**(-1.214)
            return
    c
    70      if (h.gt.1.0e04) go to 80
            cnsq=2.56e-12*h**(-1.4386)
            return
    c
    80      if (h.gt.1.5e4) go to 90
            cnsq=2.0e-16
            return
    c
    c       NOMINAL WEATHER CONDITIONS
    90      cnsq=2.0e-16
            if (h.le.11600..or.h.ge.12400.) cnsq=1e-13*h**(-1.07535)
            return
    c
    c       GOOD WEATHER CONDITIONS
    100     if (h.gt.2.5e3) go to 120
            if (h.gt.20.0) go to 110
            cnsq=8.586e-15*h**(-0.4444)
            return
    c
    110     cnsq=1.51e-13*h**(-1.396)
            return
    c
    120     if (h.gt.1.5e4) go to 90
            cnsq=3.0e-18
            return
            end
    c.
            subroutine beam (pa)
    c
    c       BEAM COMPUTES THE POWER FROM THE LINK BEAM DUE TO ATMOSPHERIC
    c       SCATTERING
    c
    c       RL      LINK RANGE
    c       RS      RANGE FROM SCATTERING VOLUME TO S
    c       RV      RANGE FROM XMTR TO SCATTERING VOLUME
    c
    c       HT      XMTR HEIGHT
    c       HR      RCVR HEIGHT
    c       HS      SURVEILLANGE RCVR HEIGHT
    c       HV      SCATTERING VOLUME HEIGHT
    c
    c       THETA   SCATTERING ANGLE (OFF-AXIS ANGLE)
    c       PHI     TOTAL FOV
    c       DPHI    INCREMENTAL FOV
```

```
c       NRET        FLAG TO INDICATE THAT COMP=0
c
        common/flags/mode,mcomp,mp,lam,modesw,lunit,nout,istog,iotype,
     &  irtype,ihet,ibflag,iw
        common/ tdata / blt,dt,ht,phit,pt,rb,grndi,bdrt,sigj,sigt
        common/ rdata / blr,dr,hr,gl,bdlr
        common/ srdata / asr,hs,phi,phiaz,dphi
        common/ ldata / rl,alam,rpx,theta,x,angtr,angrec,gamint,bw
c   * darki & ptherm replace pnep add g *
        common/ sndata / bwr,eta,f,em,pb,ps,darki,ptherm,snpndb,sndb,xm,
     &  bwopt,nflg,g
        common/ stgout / nvel,svel,avel,ndown,ncros,numtot,hvnear,
     &  hvfar,xdis,hdis,hdisdf,xclos,hclos,hclsdf,kount
        double precision re,reht,rehr
c
        data re/6.31131d6/
        data epsi/1.e-6/
c
        pa=0.
        phio2=phi/2.
        reht=re+ht
        rehr=re+hr
c
c       CALCULATE RVNEAR,RVFAR
c
        rvnear=rpx-x/tan(theta-phio2)
        rvfar=rpx-x/tan(theta+phio2)
c
c       RSNEAR,RSFAR ARE RANGES TO RVNEAR,RVFAR   FROM SR
c
        rsnear=x/sin(theta-phio2)
        rsfar=x/sin(theta+phio2)
c
c       CALCULATE ALTITUDES, HVNEAR, HVFAR
c
        hvnear=dsqrt(reht**2+(dble(rvnear))**2+dble(rvnear)*(rehr**2-reht*
     &  *2-(dble(rl))**2)/dble(rl))-re
        hvfar=dsqrt(reht**2+(dble(rvfar))**2+dble(rvfar)*(rehr**2-reht**2-
     &  (dble(rl))**2)/dble(rl))-re
c
c       CALCULATE T1,T2 TO SEE IF PATH DIFFERENCE IN TRANSMITTANCE IS
c       IMPORTANT
c
        call trans (ht,hvnear,rvnear,t1n)
        call trans (hvnear,hs,rsnear,t2n)
        call trans (ht,hvfar,rvfar,t1f)
        call trans (hvfar,hs,rsfar,t2f)
c
c       COMPARE TRANSMITTANCE VARIATION DUE TO SCATTERING VOLUME PATH
c       DIFFERENCE :        TN= NEAR PATH TRANSMITTANCE
```

```
c       TF= FAR PATH TRANSMITTANCE
c
        tn=t1n*t2n
        tf=t1f*t2f
        tp=(tn+tf)/2.
        hv=(hvnear+hvfar)/2.
        tps=tp*alfasc(hv)
        itflag=1
c       CHECK FOR TRANSMITTANCE DIFFERENCE
        if (abs(1.-tn/tp).lt..025) itflag=0
c
c       ITFLAG=0  MEANS TRANSMITTANCE NEED NOT BE COMPUTED FOR EVERY DPHI
c
c       COMPUTE DPHI TO ACHIEVE DESIRED ACCURACY OUT OF FTHETA
c
        call delphi (theta,phi,dphi)
c
c       NDPHI = NUMBER OF ELEMENTAL FOV. ROUND DOWN
c
        ndphi=phi/dphi
        dphi=phi/ndphi
c
c       LOOP TO COMPUTE ELEMENTAL CONTRIBUTIONS FROM DPHI ELEMENTS
c
        do 20 i=1,ndphi
        theta1=theta-phio2+dphi*(i-.5)
c
c       CHECK TO SEE IF PAST LINK RECEIVER
c
        if (theta1.gt.angrec) go to 30
        rs1=x/sin(theta1)
        if (itflag.eq.0) go to 10
c       COMPUTE TRANSMITTANCE IF REQUIRED FOR EACH DPHI
c
c       COMPUTE RANGE TO ELEMENTAL VOLUME
        rv1=rpx-x/tan(theta1)
c       COMPUTE ALTITUDE OF ELEMENTAL VOLUME
        hv1=dsqrt(reht**2+(dble(rv1))**2+dble(rv1)*(rehr**2-reht**2-
     &  (dble(rl))**2)/dble(rl))-re
        call trans (ht,hv1,rv1,t1)
        call trans (hv1,hs,rs1,t2)
        tps=t1*t2*alfasc(hv1)
c
10      continue
c
c
c       COMPUTE THE SUM FOR POWER CALCULATION
c
        fth=fth ta(theta1)
        pa=tps*fth/sin(theta1)/rs1+pa
```

```
20        continue
c         COMPUTE POWER AT SR FROM BEAM SCATTER
30        pa=pa*pt*asr*dphi
          return
          end
c.
          subroutine trans (h1,h2,r,t)
c
c         THIS ROUTINE CALCULATES THE TRANSMITTANCE DUE TO ATMOSPHERIC
c         EFFECTS BY INTEGRATING ALONG THE BEAMPATH
c
c         R          RANGE
c         H1         ALTITUDE OF ONE ENDPOINT OF BEAM PATH
c         H2         ALTITUDE OF OPPOSITE ENDPOINT
c         T          TRANSMITTANCE
c         NSTEP      NUMBER OF INTEGRATION STEPS
c         RE         EARTH RADIUS, M
c         ALFAEX(H)  EXTERNAL FUNCTION WHICH RETURNS EXTINCTION
c         COEFFICIENT FOR ALTITUDE H.
c
c
          common/atmos/ alfa(5,2),alfsct,alfab,ia,ab(33),as(33),at(33,14,6)
     &    ,mat,mvis
          double precision reh2s,reh1,reh1s,re,dcosp,zd2
          data re/6.31131d6/
c
c         COMPUTE NUMBER OF STEPS ALONG PATH
c
          nstep=1+r/500.
          nstep=max0(nstep,60)
c
c         COMPUTE COSINE OF ZENITH ANGLE
c
c
          if (r.lt.200..or.ia.eq.1) go to 20
          reh1=re+h1
          reh2s=(re+h2)**2
          reh1s=reh1**2
c
          dcosp=(reh2s-reh1s-(dble(r))**2)/(2*reh1*dble(r))
c
c         SET UP FOR INTEGRATION LOOP
c
c         STEPSIZE ALONG PATH IS DZ
c
          dz=r/nstep
c
c         HU,HL ARE UPPER AND LOWER INTEGRATION BOUNDS
c
          hu=h1
```

```
      alfl=0.
c
c         INTEGRATE BY SUMMING
          do 10 k=1,nstep
          z=dz*k
          zd2=dble(z**2)
c
          hl=hu
          hu=dsqrt(reh1s+zd2+2*z*reh1*dcosp)-re
c
c         AVERAGE EXTINCTION
c
          alf=.5*(alfaex(hl)+alfaex(hu))
c
c         ALFL IS INTEGRATION RESULT - EXTINCTION * RANGE
c
          alfl=alfl+alf*dz
10        continue
c
c         COMPUTE TRANSMITTANCE
c
          t=exp(-alfl)
          return
c
c         RANGE IS LESS THAN 200 METERS OR CO-ALTITUDE CASE
20        t=exp(-alfaex(hl)*r)
          return
          end
c.
          function ftheta(theta)
c         THIS ROUTINE CALCULATES THE SCATTERING COEFFICIENT AS A FUNCTION
c         OF THETA.
c
          common/ ldata / rl,alam,rpx,dummy,x,angtr,angrec,gamint,bw
c
          dimension fact(2),slope(2),thtmn(2),amp1(2),tcon1(2),amp2(2),
     &    tcon2(2),shft(2)
          data fact,slope,thtmn,shft/.0008,.0012,1.4,1.0,2.1,2.4,3.6,3.25/
          data amp1,amp2,tcon1,tcon2/3.5,2.5,.1,.01,-6.,-7.5,-4.5,-4./
          l=2
c
          if (alam.le.5.e-6) l=1
c
c         SOLVE FOR FTHETA
          ftheta=fact(l)*10.**(sqrt(slope(l)*(theta-thtmn(l))**2+1.))+amp1(l
     &    )*exp(tcon1(l)*theta)-amp2(l)*exp(tcon2(l)*(shft(l)-theta))
c
          return
          end
c.
```

```
            subroutine delphi (theta,phi,dphi)
c     THIS ROUTINE CALCULATES THE DPHI REQUIRED TO MINIMIZE THE
c     ERROR IN CALCULATING FTHETA.
c
      data onedeg/.017/
c
c     STATEMENT FUNCTION TO COMPUTE DPHI
c
      dphix(ac,thet)=abs(ac*sqrt(2.*(thet-2.)**2+1.)/(.08*10.**(sqrt(2.*
     &(thet-2.)**2+1.))*(thet-2.)))
c
c     GIVE ACCURACY VALUE
      acc=.01
c
c     CALCULATE THE ELEMENTAL FOV AT THE EDGES OF THE WHOLE FOV
      thtner=theta-phi/2.
      thtfar=theta+phi/2.
      dphi1=dphix(acc,thtner)
      dphi2=dphix(acc,thtfar)
c
c     FIND OUT WHICH ANGLE IS SMALLER AND SET EQUAL TO DPHI
      dphi=amin1(dphi1,dphi2,phi,onedeg)
      return
      end
c.
      function alfaex(h)
      alfaex=alfaab(h)+alfasc(h)
      return
      end
c.
      function alfaab(h)
c
c     THIS ROUTINE COMPUTES THE ATMOSPHERIC ABSORPTION COEFFICIENT
c
      common/atmos/alfa(5,2),alfsct,alfab,ia,ab(33),as(33),at(33,14,6)
     &,mat,mvis
      common/err/ier,ierab,iersc,ierbr,devab,devsc,devbr
c
c     CHECK TO SEE IF USER HAS SPECIFIED THE AFGL MODEL
c
      if (ia.eq.2) go to 10
      alfaab=alfab*(1.+devab)**ierab
      go to 80
c
10    if (h.gt.25000.) go to 20
      i=h/1000.+2.
      go to 60
c
20    if (h.gt.50000.) go to 30
      i=h/5000+22.
```

```
         go to 60
c
30       if (h.gt.70000.) go to 40
         i=32
         go to 60
c
40       if (h.gt.100000.) go to 50
         i=33
         go to 60
c
50       alfaab=0.
         go to 80
c
60       if (i.gt.0) go to 70
c        USE COEF. AT GROUND LEVEL IF BELOW GROUND ALTITUDE
         i=1
c
70       alfaab=ab(i)
         alfaab=alfaab*(1.+devab)**ierab
80       return
c
         end
c.
         function alfasc(h)
c
c        THIS ROUTINE COMPUTES THE ATMOSPHERIC SCATTERING COEFFICIENT
c        .
         common/atmos/alfa(5,2),alfsct,alfab,ia,ab(33),as(33),at(33,14,6)
&        ,mat,mvis
         common/err/ier,ierab,iersc,ierbr,devab,devsc,devbr
c
c        CHECK TO SEE IF USER HAS SPECIFIED THE AFGL MODEL
c
         if (ia.eq.2) go to 10
         alfasc=alfsct*(1.+devsc)**iersc
         go to 80
c
10       if (h.gt.25000.) go to 20
         i=h/1000.+2.
         go to 60
c
20       if (h.gt.50000.) go to 30
         i=h/5000+22.
         go to 60
c
30       if (h.gt.70000.) go to 40
         i=32
         go to 60
c
40       if (h.gt.100000.) go to 50
```

```
          i=33
          go to 60
c
50        alfasc=0.
          go to 80
c
60        if (i.gt.0) go to 70
c         USE COEF. AT GROUND LEVEL IF BELOW GROUND ALTITUDE
          i=1
c
70        alfasc=as(i)
          alfasc=alfasc*(1.+devab)**ierab
80        return
c
          end
c.
          subroutine tscat (prtr)
c
c         TSCAT COMPUTES THE SCATTERED POWER AT THE SR DUE TO SCATTERING
c         FROM THE TRANSMITTER.  INCLUDED IN THE CALCULATIONS
c         ARE SIDELOBES AND SCATTER FROM THE OPTICS.
c
c         ALAM   - LINK WAVELENGTH
c         DT     - DIAMETER OF XMTR OPTICS
c         PT     - XMTR POWER
c         ASR    - AREA OF SR OPTICS
c         ANG    - THETA TO TRANSMITTER
c         BSDFX  - FACTOR USED IN COMPUTING WINDOW SCATTER
c         BAFEFF - EFFECTIVE SUPPRESSION OF BAFFLE FACTOR
c         BAFRAT - FUNCTION WHICH CALCULATES BAFEFF
c
c         PTS    - TOTAL POWER FROM WINDOW SCATTER
c         PSL    - TOTAL POWER FROM SIDE LOBES
c         PRTR   - TOTAL POWER CONTRIBUTION FROM XMTR
c
          common/ flags /mode,mcomp,mp,lam,modesw,lunit,nout,istog,iotype,
     &    irtype,ihet,ibflag,iw
          common/ tdata /blt,dt,ht,phit,pt,rb,grndi,bdrt,sigj,sigt
          common/ srdata /asr,hs,phi,phiaz,dphi
          common/ ldata / rl,alam,rpx,theta,x,angtr,angrec,gamint,bw
          data hatm/100000./
c
          pi=3.1415927
          pts=0.
          psl=0.
          prtr=0.
          bafeff=0.
          ang=angtr
          if (ang.gt.1.57) go to 30
c
```

```
c       CALCULATE EFFECTIVNESS OF BAFFLE
c
        bafeff=bafrat(bdrt,dt,ang,blt)
c
c       COMPUTE WINDOW SCATTER
c
c       COMPUTE DISTANCE TO TRANSMITTER
        rs=sqrt(x**2+rpx**2)
c
c       COMPUTE TRANSMITTANCE
c
        if (istog.eq.0) go to 10
c
c       SPACE TO GROUND EXCEPTION
c
        call trans (hatm,hs,hatm-hs,t)
        go to 20
c
10      call trans (ht,hs,rs,t)
c
c       COMPUTE TOTAL POWER DUE TO WINDOW SCATTER
20      bsdfx=bsdf(ang)
        pts=asr*bsdfx*pt*t/rs**2*bafeff*cos(ang)
c
c
c       CALCULATE SIDELOBE LEVEL FOR XMTR
        xj=8.*alam*pt*cos(ang)/(97.40909*dt*ang**3)
c
        psl=xj*asr*t*bafeff/rs**2
c
c       COMPUTE TOTAL POWER FOR WINDOW SCATTERING AND SIDELOBE LEVEL
30      prtr=pts+psl
        return
        end
c.
        function bsdf(ang)
c
c       THIS ROUTINE CALCULATES THE SCATTERING OFF OF THE TRANSMITTER
c       OPTICS.  THEORY PREDICTS A LOG-LOG LINEAR CURVE WITH A SLOPE OF
c       -2.0. THE USER CAN SELECT ANY SLOPE HE WISHES.  GROSS ANOMALIES
c       MAY BE ACCOUNTED FOR BY USING NG *GLITCHES* OF AMPLITUDE
c       GAMPL(NG), FROM THETA=GSTART(NG) DEGREES TO THETA= GEND(NG)
c       DEGREES.
c
c       YBSDF   - Y-INTERCEPT OF BSDF (AT 1 DEGREE)
c       SBSDF   - LOG-LOG SLOPE OF BSDF
c       GSTRA   - START OF DISCONTINUITY (GLITCH)
c       GENRA   - END OF DISCONTINUITY (GLITCH)
c       GAMPL   - AMPLITUDE OF DISCONTINUITY IN SPECIFIED RANGE
c
```

```
          common/ tbsdf / ng,gstart(3),gend(3),gampl(3),ybsdf,sbsdf,nbak,noa
    &     ,ibsdf
          common/err/ier,ierab,iersc,ierbr,devab,devsc,devbr
c
c         BSDF CURVE USING LOG-LOG STRAIGHT LINE APPROXIMATION
          bsdf=ybsdf*(ang*57.2958)**sbsdf
c
          if (ng.eq.0) go to 20
c
c         ADD IN GLITCHES IF SPECIFIED
c
          do 10 i=1,ng
          gstra=gstart(i)/57.2958
          genra=gend(i)/57.2958
          if (ang.ge.gstra.and.ang.le.genra) bsdf=gampl(i)
10        continue
c
c         ADD ERROR ANALYSIS DEVIATION
c
20        bsdf=bsdf*(1.+devbr)**ierbr
          return
          end
c.
          subroutine rscat (prec)
c
c         RSCAT COMPUTES THE CONTRIBUTIONS FROM REFLECTIONS OFF THE
c         BACKSTOP AND RECEIVER
c
c         DR     - DIAMETER OF RCVR OPTICS
c         ASR    - AREA OF SR OPTICS
c         PHIT   - XMTR BEAMWIDTH
c         TL     - TRANSMITTANCE BETWEEN XMTR AND RCVR
c         TS     - TRANSMITTANCE BETWEEN RCVR AND SR
c         PBACKS - POWER REFLECTEDFROM BACKSTOP
c         POA    - POWER REFLECTED FROM RECEIVER OPTICS
c         BAFEFF - FACTOR REPRESENTING EFFECTIVENESS OF BAFFLE
c         BAFRAT - FUNCTION TO CALCULATE BAFEFF
c
          common/ flags /mode,mcomp,mp,lam,modesw,lunit,nout,istog,iotype,
    &     irtype,ihet,ibflag,iw
          common/ tdata / blt,dt,ht,phit,pt,rb,grndi,bdrt,sigj,sigt
          common/ rdata / blr,dr,hr,gl,bdlr
          common/ srdata / asr,hs,phi,phiaz,dphi
          common/ ldata / rl,alam,rpx,theta,x,angtr,angrec,gamint,bw
          data pi / 3.1415927 /
          data hatm/100000./
c
          thetap=pi-angrec
          rbacks=0.
          poa=0.
```

```
          bafeff=0.
c
c         CALCULATE EFFECTIVENESS OF BAFFLE
c
          bafeff=bafrat(bdlr,dr,thetap,blr)
c
          if (istog.eq.0) go to 10
c
c         SPACE TO GROUND EXCEPTION
c
          call trans (hatm,hr,hatm-hr,tl)
          go to 20
c
10        call trans (ht,hr,rl,tl)
20        rs=sqrt((rl-rpx)**2+x**2)
          call trans (hr,hs,rs,ts)
c         COMPUTE POWER AT RECEIVER
          prec=pt*tl
c
c         COMPUTE POWER REFLECTED FROM BACKSTOP - ASSUMES BACKSTOP
c         IS AT LEAST AS LARGE AS THE BEAM DIAMETER
c
          pbacks=prec*ts*rhobak(thetap)*asr/(rs)**2
c
c         COMPUTE POWER REFLECTED FROM RECEIVER
c
          if (thetap.gt.1.57) go to 30
          poa=prec*ts*asr*(dr/(rs*rl*phit))**2*bafeff*rhooa(thetap)
c
c         SUM CONTRIBUTIONS
c
30        prec=pbacks+poa
          return
          end
c.
          function rhobak(thetap)
c
c
c         RHOBAK COMPUTES REFLECTANCE OF BACKSTOP
c
c         BMAXS  - MAXIMUM OF SPECULAR COMPONENT
c         BFWHMS - FULL WIDTH AT HALF-MAXIMUM OF SPECULAR COMPONENT
c         PSIEFF - ANGLE BETWEEN NORMAL OF BACKSTOP AND LINK OPT. AXIS
c         THETS  - ANGLE BETWEEN SPECULAR COMPONENT AND SR OPT. AXIS
c         RHOBAK - REFLECTANCE OF BACKSTOP
c
          common/rsct/oasmax,diffoa,oafwhm,bmaxs,bfwhms,bdiff(6),psiaz,psiel
     &    ,gams
          common/ flags /mode,mcomp,mp,lam,modesw,lunit,nout,istog,iotype,
     &    irtype,ihet,ibflag,iw
```

```
      common/ ldata / rl,alam,rpx,theta,x,angtr,angrec,gamint,bw
c
c     COMPUTE BACKSTOP ORIENTATION FACTORS
c
      rhobak=0.
      cs1=x*(sin(psiaz)*cos(gamint)+sin(psiel)*sin(gamint))+(rl-rpx)*cos
     & (psiel)*cos(psiaz)
c
c     ANGLE BETWEEN BACKSTOP NORMAL AND SR
c
      psieff=acos(cs1/sqrt(x**2+(rl-rpx)**2))
c
c     CHECK TO SEE IF SR IS BEHIND BACKSTOP
c
      if (psieff.gt.1.57) go to 10
      cs2=2.*asin((sin(psiaz))**2+(sin(psiel))**2)
      thets=acos((x*sin(cs2)+(rl-rpx)*cos(cs2))/sqrt(x**2+(rl-rpx)**2))
c
      backst=bmaxs*exp(-2.773*(thets/bfwhms)**2)
c
c     ADD DIFFUSE AND SPECULAR COMPONENTS
c
      rhobak=(bdiff(lam)/3.14159+backst)*cos(psieff)
c
c
10    return
      end
c.
      function rhooa(thetap)
c
c     RHOOA COMPUTES THE DIRECTIONAL REFLECTANCE OF THE RECEIVER
c     NORMALIZED TO 1 WATT/SR.  A SPECULAR COMPONENT IS DEFINED BY
c     A GAUSSIAN, AND A DIFFUSE COMPONENT IS A CONSTANT REFLECTION COEF
c
c     OASMAX - MAXIMUM OF SPECULAR COMPONENT
c     OAFWHM - FULL WIDTH AT HALF MAXIMUM OF SPECULAR COMPONENT
c     DIFFOA - DIFFUSE REFLECTANCE
c     RHOOA  - REFLECTANCE OF RECEIVER OPTICS
c
      common/rsct/oasmax,diffoa,oafwhm,bmaxs,bfwhms,bdiff(6),psiaz,psiel
     & ,gams
      common/ ldata / rl,alam,rpx,theta,x,angtr,angrec,gamint,bw
      data onedeg,pi,r2d/.0174532925,3.141592654,57.29577951/
c
      thetap=pi-angrec
c
c     SPECULAR COMPONENT
      oa=(oasmax-diffoa)*exp(-2.773*(thetap/oafwhm)**2)
c
c     ADD DIFFUSE COMPONENT
```

```fortran
c
      rhooa=(diffoa/pi+oa)*cos(thetap)
c
      return
      end
c.
      function bafrat(d1,d2,theta,bl)
c
c     THIS FUNCTION CALCULATES THE EFFECTIVENESS OF THE RECEIVER
c     AND TRANSMITTER HOODS. D1 MUST BE >= D2.
c
      if (bl.le.0.) go to 20
      pi=3.1415927
      r1=d1/2.
      r2=d2/2.
c
      thetap=theta
      if (thetap.ge.1.57) thetap=pi-theta
c
c     C2 IS THE PERP. DISTANCE BETWEEN THE CENTER OF THE CIRCLES
c
      c2=tan(thetap)*bl
      if (c2.ge.(r1+r2)) go to 10
      if (c2.le.(r1-r2)) go to 20
c
c     X AND Y ARE COORDINANTS OF INTERSECTION OF THE TWO CIRCLES
c
      x=(r1**2-r2**2+c2**2)/(2.*c2)
      y=sqrt(r1**2-x**2)
c
      theta1=atan2(y,x)
      theta2=atan2(y,(c2-x))
c
c     SOLVE FOR OVERLAPPING AREA OF CIRCLES
c
      area=r1**2*theta1-x*y+r2**2*theta2-(c2-x)*y
c
      bafrat=area/(pi*r2**2)
      go to 30
c
10    bafrat=0.
      go to 30
c
20    bafrat=1.
30    return
      end
c.
      subroutine ston
c
c     INPUTS
```

```
c      XM   =   MODULATION INDEX =1
c      ETA  =   QUANTUM EFFICIENCY
c      ALAM =   WAVELENGTH
c      F    =   NOISE ASSOCIATED WITH GAIN
c      BWR  =   RECEIVER BANDWIDTH
c      PTHERM=  THERMAL NOISE EQV POWER
c      DARKI=   DARK CURRENT
c      G    =   PREDETECTION GAIN
c      PS   =   SIGNAL POWER
c      PB   =   BACKGROUND (ROUTINE)
c
c      OUTPUTS
c      SN= SIGNAL TO NOISE,DB
c
c      ROUTINES CALLED - BACK COMPUTES BACKGROUND SIGNAL POWER
c
       common/ flags /mode,mcomp,mp,lam,modesw,lunit,nout,istog,iotype,
&      irtype,ihet,ibflag,iw
       common/ tdata / blt,dt,ht,phit,pt,rb,grndi,bdrt,sigj,sigt
       common/ rdata / blr,dr,hr,gl,bdlr
       common/ srdata / asr,hs,phi,phiaz,dphi
       common/ ldata / rl,alam,rpx,theta,x,angtr,angrec,gamint,bw
c   * darki & ptherm replace pnep add g *
       common/ sndata / bwr,eta,f,em,pb,ps,darki,ptherm,snpndb,sndb,xm,
&      bwopt,nflg,g
       data hc/1.986305188e-25/
c
       if (ihet.eq.1) go to 10
c
c      HETERODYNE S/N EXPRESSION
c      WARNING :  THE VALIDITY OF THIS EXPRESSION WAS UNDER
c      QUESTION AT TIME OF WRITING(SEE DOCUMENTATION)
c
       sn=em*eta*alam*xm**2*ps/(bwr*hc)
       go to 20
c
c
c   * modify s/n expression to account for separation of
c     dark current and thermal noise *
c      DIRECT DETECTION S/N
10     xn1=xm**2*ps**2
       xn2=2.*hc/(eta*alam)*f
c      EQV. POWER THAT GIVES RISE TO DARK CURRENT
       pd=hc/(eta*alam*1.6e-19*g)*darki
       call back
       sn=xn1/((xn2*(ps+pb+pd)+ptherm**2)*bwr)
20     sndb=10.*alog10(sn)
       return
       end
c.
```

```
      subroutine back
c
c     THIS SUBROUTINE CALCULATES THE BACKGROUND POWER
c
c     EMM    - EMMISTIVITY OF SOURCE
c     OMGREC - SOLID ANGLE FOV OF RECEIVER
c     NFLG   - DAY/NIGHT FLAG (1 IF NIGHT)
c     RHO    - REFLECTANCE OF SURFACE
c     BWOPT  - OPTICAL BANDWIDTH, MICRONS
c     OMGSUM - SOLID ANGLE SUBTENDED BY SUN(SR)
c     PSOLAR - BACKGROUND POWER FROM RADIATION OF SUN
c     PBLK   - BACKGROUND POWER FROM BLACKBODY RADIATION OF EARTH
c     PBACK  - TOTAL BACKGROUND POWER
c
c
c     * darki & ptherm replace pnep add g *
      common/sndata/bwr,eta,f,em,pb,ps,darki,ptherm,snpndb,sndb,xm,
     &      bwopt,nflg,g
      common/srdata/ asr,hs,phi,phiaz,dphi
      common/ldata/rl,alam,rpx,theta,x,angtr,angrec,gamint,bw
      data rho/3./,emm/1./,temblk/293./
      data cfudge/.01/
      dimension solvir(183),soluv(20)
c     THE DATA IN ARRAYS SOLVIR AND SOLUV ARE HLAMDA IN UNITS
c     OF WATTS PER SQUARE METER PER MICRON AND ARE FROM
c     THE HANDBOOK OF GEOPHYSICS AND SPACE ENVIRONMENTS
c     FOR AN AIR MASS OF 2.
c
      data solvir/
     &     54.0, 101., 151., 188., 233., 279., 336., 379., 470., 672.,
     &     733., 787., 911.,1006.,1080.,1138.,1183.,1210.,1215.,1206.,
     &    1199.,1188.,1198.,1190.,1182.,1178.,1168.,1161.,1167.,1168.,
     &    1165.,1176.,1175.,1173.,1166.,1160.,1149., 978.,1108.,1070.,
     &     832., 965.,1041., 867., 566., 968., 907., 923., 857., 698.,
     &     801., 863., 858., 839., 813., 798., 614., 517., 480., 375.,
     &     258., 169., 278., 487., 584., 633., 645., 643., 630., 620.,
     &     610., 601., 592., 551., 526., 519., 512., 514., 252., 126.,
     &     69.9, 98.3, 164., 216., 271., 328., 346., 344., 373., 402.,
     &     431., 420., 387., 328., 311., 381., 382., 346., 264., 208.,
     &     168., 115., 58.1, 18.1, .660, 0.00, 0.00, 0.00, 0.00, 1.91,
     &     3.72, 7.53, 13.7, 23.8, 30.5, 45.1, 83.7, 128., 157., 187.,
     &     209., 217., 226., 221., 217., 213., 209., 205., 202., 198.,
     &     194., 189., 184., 173., 163., 159., 145., 139., 132., 124.,
     &     115., 105., 97.1, 80.2, 58.9, 38.8, 18.4, 5.70, .920, 0.00,
     &     0.00, 0.00, 0.00, 0.00, 0.00, 0.00, 0.00, 0.00, 0.00, .705,
     &     2.34, 3.68, 5.30, 17.7, 31.7, 37.7, 22.6, 1.58, 2.66, 19.5,
     &     47.6, 55.4, 54.7, 38.3, 56.2, 77.0, 88.0, 86.8, 85.0, 84.4,
     &     83.2, 20.7, 0.00/
      data soluv/
     &     .177, .342, .647, 1.16, 1.91, 2.89, 4.15, 6.11, 8.38, 11.0,
```

```
      &      13.9, 17.2, 21.0, 25.4, 30.0, 34.8, 39.8, 44.9, 49.5, 54.0/
      c
      c      PLANCK*S EQUATION FOR SPECTRAL DISTRIBUTION
             c1(alamda,temp)=emm*1.19096e-22/(alamda**5*(exp(1.43879e-2/(alamda
      &      *temp))-1.))
      c
      c      SOLVE FOR HLAM USING INTERPOLATION ROUTINES
      c
             hlam=0.
             pblk=0.
             psolar=0.
      c      CALCULATE RECEIVER*S SOLID ANGLE FOV, STER
             omgrec=phi*phiaz
      c
      c      CHECK TO SEE IF DAY OR NIGHT
             if (nflg.eq.3) go to 40
      c
             if (alam.ge.3.01e-7.and.alam.lt.3.20e-7) go to 10
             if (alam.ge.3.20e-7.and.alam.lt.2.14e-6) go to 20
             go to 30
      c
      10     hlam=odlie(alam,soluv,.001e-6,.301e-6,20)
             go to 30
      c
      20     hlam=odlie(alam,solvir,.01e-6,.32e-6,183)
      c
      c
      c      COMPUTE CONTRIBUTION FROM SOLAR RADIATION
      30     psolar=rho*bwopt*asr*omgrec*hlam/(3.14159*2)
      c
      c
      c      CLOUDY DAY FUDGE FACTOR
      c
             if (nflg.eq.2) psolar=psolar*cfudge
      c
      c      COMPUTE CONTRIBUTION FROM BLACKBODY RADIATION OF EARTH
      40     if (alam.gt.1.5e-6) pblk=asr*omgrec*bwopt*c1(alam,temblk)
      c
      c      SUM CONTRIBUTIONS
      c
             pb=psolar+pblk
             return
             end
      c.
             function odlie(x0,f,dx,xs,n)
      c
      c      one-dimensional linear interpolation routine for
      c      equally-spaced data
      c
      c      x0=value for which f(x0) is desired
```

82

```fortran
c     f=array containing values of dependent variable
c     dx=increment for independent variable
c     xs=starting value of independent variable
c     n=number of points in f
c
      dimension f(n)
      q=(x0-xs)/dx+1.0
      k=int(q)
      if (k.lt.1) i=1
      if (k.gt.n-1) i=n-1
      if (k.ge.1.and.k.le.n-1) i=k
      odlie=(f(i)+(f(i+1)-f(i))*(q-i))
      return
      end
c.
c  * add subroutine batch *
      subroutine batch
c
c     READS INPUTS FROM A USER SPECIFIED FILE, N, IN NAMELIST
c     FORMAT.  THE NAMELIST NAME IS INPUT.
c
      common / flags / mode,mcomp,mp,lam,modesw,lunit,nout,istog,iotype,
     &  irtype,ihet,ibflag,iw
      common / block1 / xmod(6),gainsr(6),qe(6),fnoise(6),srbw(6),
     &  srdark(6),srther(6),
     &  alamda(6),obw(6),nhol(6)
      common / tdata / blt,dt,ht,phit,pt,rb,grndi,bdrt,sigj,sigt
      common / rdata / blr,dr,hr,gl,bdlr
      common / srdata / asr,hs,phi,phiaz,dphi
      common / ldata / rl,alam,rpx,theta,x,angtr,angrec,gamint,bw
      common / sndata / bwr,eta,f,em,pb,ps,darki,ptherm,snpndb,sn db,xm,
     &  bwopt,nflg,g
      common / atmos / alfa(5,2),alfsct,alfab,ia,ab(33),as(33),at(33,14,6),
     &  mat,mvis
      common / tbsdf / ng,gstart(3),gend(3),gampl(3),ybsdf,sbsdf,nbak,noa,
     &  ibsdf
      common / rsct / oasmax,diffoa,oafwhm,bmaxs,bfwhms,diff(6),psiaz,
     &  psiel,gams
      common / pltc / xint(200),yint(200),h(200),contr(2),np,note
      common / wavefm  /npts,t,form0(1000),form1(1000),power0(1000),
     &  power1(1000)
      data dcomp,r2d /0.0,57.295779 /
      namelist /input / lam,alamda,ia,alfsct,alfab,at,mat,mvis,ab,as,
     &  dt,phit,ibsdf,ybsdf,sbsdf,ng,gstart,gend,gampl,dr,nbak,bmaxs,bfwhms,
     &  bdiff,psiaz,psiel,noa,oasmax,oafwhm,diffoa,pt,rl,ht,hr,istog,x,
     &  theta,gl,ibflag,sigj,iw,rd,grndi,mcomp,mp,irtype,xm,ihet,em,eta,f,
     &  bwr,darki,ptherm,bwopt,nflg,bw,asr,phi,phiaz,blt,bdrt,blr,bdlr,hs,
     &  gamint,mode,rpx,dcomp,t,npts,form0,form1,g
c     READ INPUTS
      write(6,200)
```

```fortran
200     format(/,10x,"input file?")
        read(5,100) n
100     format(v)
        read(n,input)
        close (n)
c       SELECT WAVELENGTH
        if (lam.ne.6.and.lam.ne.0) alam=alamda(lam)
c       LOAD THE ABSORPTION AND SCATTERING ARRAYS  AB AND AS
        mat1=2*mat-1
        mat2=mat1+1
        mvis1=10+2*mvis-1
        mvis2=mvis1+1
        do 10 j=1,33
        ab(j)=(at(j,mat1,lam)+at(j,mvis1,lam))*1.0e-3
10      as(j)=(at(j,mat2,lam)+at(j,mvis2,lam))*1.0e-3
c       CHECK FOR DIFFRACTION LIMIT
        diffl=1.22*alam/dt
        if (phit.lt.diffl) go to 20
c       CHECK FOR HETERODYNE RCVR IN MODE 6
        if (mode.eq.6.and.ihet.eq.2) go to 30
c       CHECK NPTS ODD
        if (npts.eq.2*(npts/2)) go to 40
c       CONVERT TO RADIANS
        psiaz=psiaz/r2d
        psiel=psiel/r2d
        theta=theta/r2d
        gamint=gamint/r2d
c       SET DEFAULT VALUES
        if (bdiff.gt.0.0) diff(lam)=bdiff
        if (nbak.eq.3) bmaxs=bdiff
        if (istog.eq.1) mcomp=1
        if (xm.eq.0.0) xm=xmod(lam)
        if (ihet.eq.0) ihet=1
        if (eta.eq.0.0) eta=qe(lam)
        if (f.eq.0.0) f=fnoise(lam)
        if (bwr.eq.0.0) bwr=srbw(lam)
        if (darki.eq.0.0) darki=srdark(lam)
        if (ptherm.eq.0.0) ptherm=srther(lam)
        if (g.eq.0.0) g=gainsr(lam).
        if (bwopt.eq.0.0) bwopt=obw(lam)
        if (bdrt.eq.0.0) bdrt=dt
        if (bdlr.eq.0.0) bdlr=dr
        if (dcomp.ne.0.and.mode.eq.4) contr(1)=dcomp
        if (dcomp.ne.0.and.mode.eq.5) contr(2)=dcomp
        return
c
20      write(6,210) phit,diffl
210     format(/,10x,"transmitter beamwidth, ",1pe11.3,
     &  "radians, is less than diffraction limit, ",1pe11.3," radians")
        stop
```

```
c
30     write(6,220)
220    format(/,10x,"Pr(e) analysis not valid for heterodyne receivers")
       stop
c
40     write(6,230)
230    format(/,10x,"npts must be odd")
       stop
       end
```

SECTION IV

PROBABILITY OF ERROR SUBROUTINE

PROBABILITY OF ERROR SUBROUTINE

The subroutine ERROR is a FORTRAN program to calculate upper and lower bounds on the probability of bit error for any direct detection optical communication receiver for which the power waveform incident on the detector may be considered non-stochastic. The probability of error bounds are implemented by means of the Bhattacharyya distance measure.

The performance bounds are based on the received power waveforms given mark and space. Thus, the lower bound is the absolute best performance one might possibly achieve given the received signal set. The upper bound is the worst one will do *assuming* the receiver implements the optimal decison rule on the detector output.

The inputs are passed to the program in labeled common. The sampled received power waveform given mark and the received waveform given space as well as the number of sample points and the bit duration appear in the common WAVEFM. The number of sample points must be odd. The pertinent receiver parameters are passed in the common RCVR. Or it may be more convenient to insert the common blocks from the main program that contain the necessary information. The labeled common INTER passes data to the external Bhattacharyya distance functions.

The program returns as arguments the upper and lower bounds on the probability of bit error and a flag indicating whether the

performance is (1) shot noise limited, (2) thermal noise limited, or
(3) a combination of shot and thermal noise. If the receiver noise is
a combination of shot and thermal or excess noise, both the performance
assuming a Poisson model and the performance assuming a Gaussian
model are returned for user comparison.

The Bhattacharyya distance integrals are evaluated using Simpson's
rule for integration. To the extent that the sample points adequately
represent the waveform in a piece-wise sense, Simpson's rule is
accurate enough.

The OFF-AXIS program supplies the dark current, i_D, and the
thermal noise equivilent power, P_{therm}, rather than the dark power, P_D,
and the spectral density of the thermal noise, $N_0/2$. To avoid unnecessary
computations the subroutine as it appears in my thesis was modified
slightly. The relationship between the parameters is

$$P_D = i_D/\alpha eG \qquad\qquad N_0/2 = 1/2(eG_\alpha P_{therm})^2$$

The modification is straightforward substitution and cancelation of
terms.

Following is a flow chart and listing of the subroutine
ERROR.

Program listing of subroutine ERROR
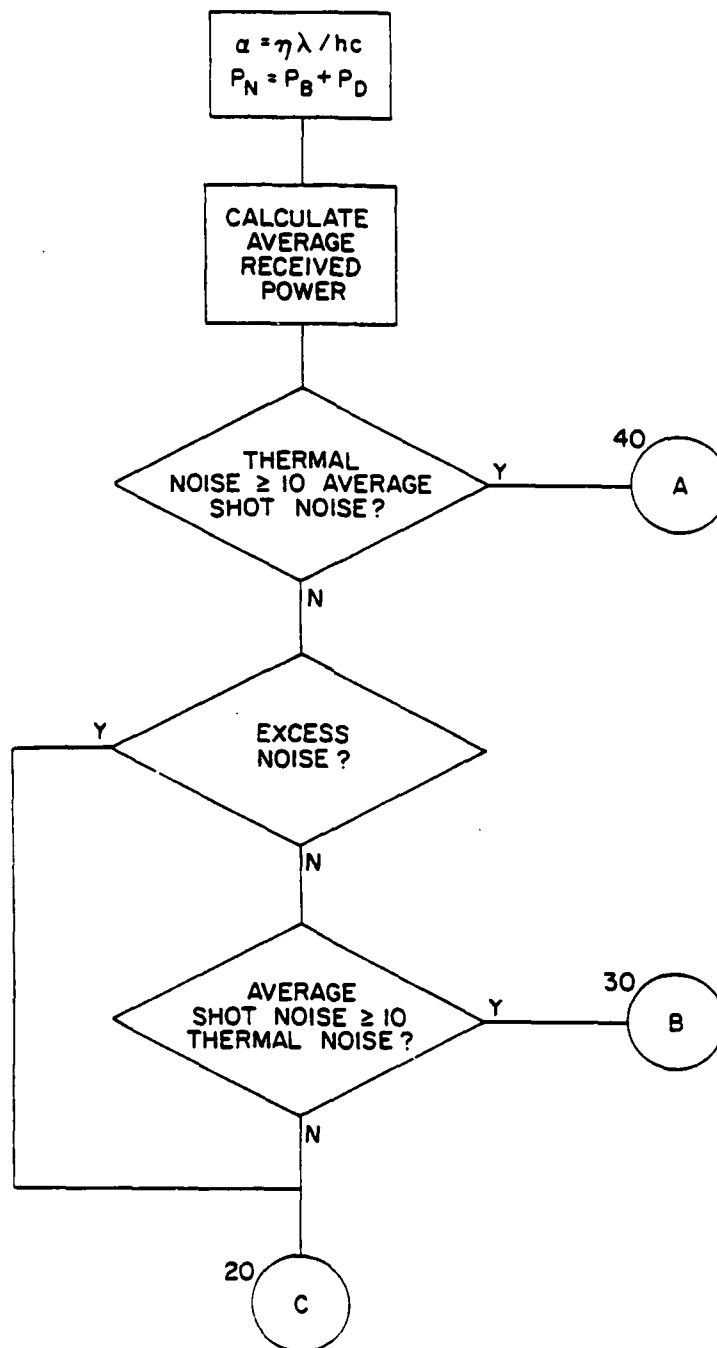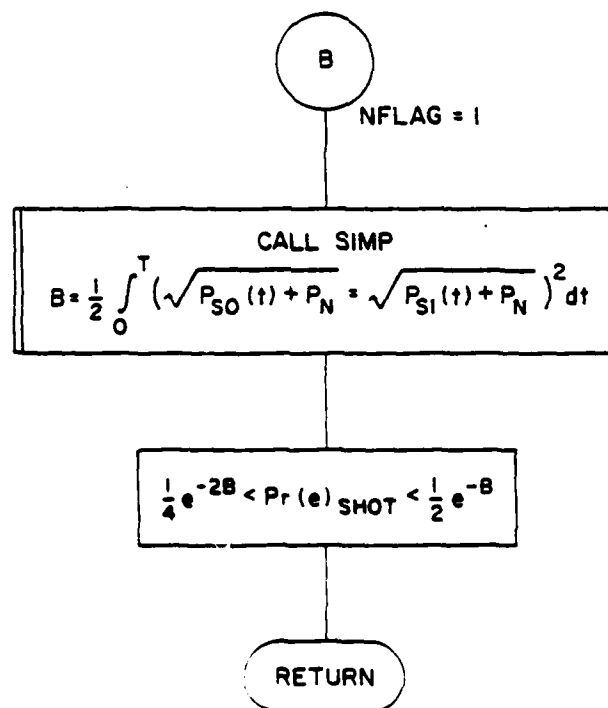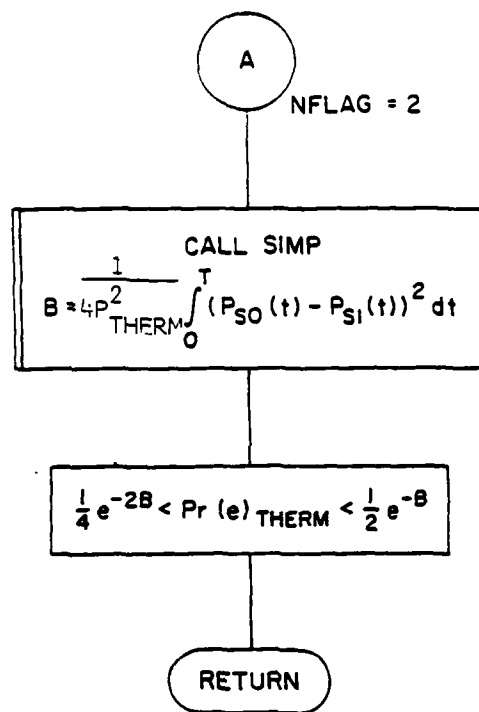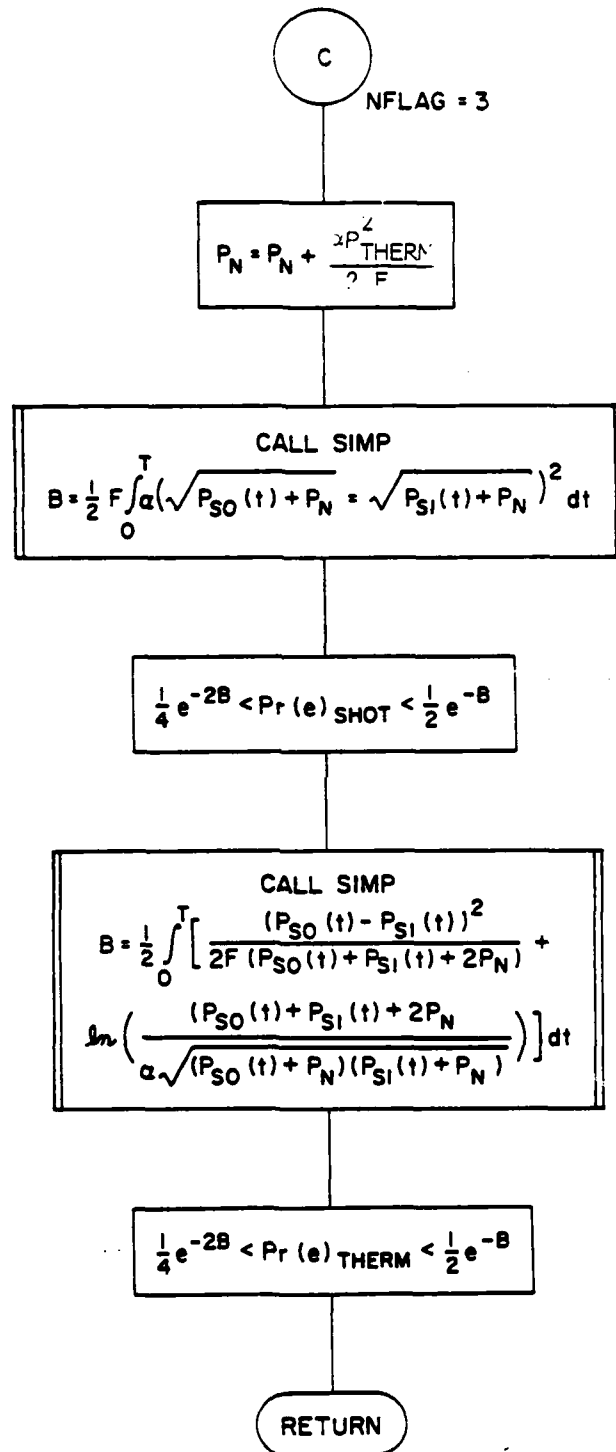
4

SUBROUTINE ERROR

$$\alpha = \eta \lambda / hc$$
$$P_N = P_B + P_D$$

CALCULATE
AVERAGE
RECEIVED
POWER

THERMAL
NOISE ≥ 10 AVERAGE
SHOT NOISE ?

Y → 40 A

N

EXCESS
NOISE ?

Y

N

AVERAGE
SHOT NOISE ≥ 10
THERMAL NOISE ?

Y → 30 B

N

20 C

5

A

NFLAG = 2

CALL SIMP

$$B = \frac{1}{4P^2_{THERM}} \int_0^T (P_{SO}(t) - P_{SI}(t))^2 \, dt$$

$$\frac{1}{4} e^{-2B} < Pr(e)_{THERM} < \frac{1}{2} e^{-B}$$

RETURN

B

NFLAG = 1

CALL SIMP

$$B = \frac{1}{2} \int_0^T \left(\sqrt{P_{SO}(t) + P_N} - \sqrt{P_{SI}(t) + P_N} \right)^2 \, dt$$

$$\frac{1}{4} e^{-2B} < Pr(e)_{SHOT} < \frac{1}{2} e^{-B}$$

RETURN

6

$$C$$

NFLAG = 3

$$P_N = P_N + \frac{\alpha P_{THERM}^2}{2 F}$$

CALL SIMP

$$B = \frac{1}{2} F \int_0^T \alpha \left(\sqrt{P_{SO}(t) + P_N} = \sqrt{P_{SI}(t) + P_N} \right)^2 dt$$

$$\frac{1}{4} e^{-2B} < Pr(e)_{SHOT} < \frac{1}{2} e^{-B}$$

CALL SIMP

$$B = \frac{1}{2} \int_0^T \left[\frac{(P_{SO}(t) - P_{SI}(t))^2}{2F (P_{SO}(t) + P_{SI}(t) + 2P_N)} + \ln \left(\frac{(P_{SO}(t) + P_{SI}(t) + 2P_N)}{\alpha \sqrt{(P_{SO}(t) + P_N)(P_{SI}(t) + P_N)}} \right) \right] dt$$

$$\frac{1}{4} e^{-2B} < Pr(e)_{THERM} < \frac{1}{2} e^{-B}$$

RETURN

Flow chart of subroutine ERROR

```
c.
        subroutine error(nflag,lobnd1,upbnd1,
     &  lobnd2,upbnd2)
c
c       CALCULATE PROBABILITY OF BIT ERROR
c
c       INPUTS:
c           ps0(i)      - SAMPLED RCVD SIGNAL POWER
c                           WAVEFORM GIVEN SPACE (W)
c           ps1(i)      - SAMPLED RCVD SIGNAL POWER
c                           WAVEFORM GIVEN MARK (W)
c           npts        - NUMBER OF SAMPLED WAVEFORM
c                           POINTS.  NPTS MUST BE ODD.
c           t           - BIT TIME INTERVAL (S)
c           eta         - DETECTOR QUANTUM EFFICIENCY
c           g           - DETECTOR GAIN
c           f           - EXCESS NOISE
c           alam        - OPTICAL WAVELENGTH (M)
c           ptherm      - NOISE EQUIVALENT POWER OF
c                           THERMAL NOISE (W)
c           pback       - BACKGROUND POWER (W)
c           darki       - DETECTOR DARK CURRENT (A)
c
c       RETURN:
c           upbnd1      - SHOT NOISE LIMITED UPPER
c                           BOUND ON PROBABILITY OF ERROR
c           lobnd1      - SHOT NOISE LIMITED LOWER
c                           BOUND ON PROBABILITY OF ERROR
c           upbnd2      - THERMAL NOISE LIMITED UPPER
c                           BOUND ON PROBABILITY OF ERROR
c           lobnd2      - THERMAL NOISE LIMITED LOWER
c                           BOUND ON PROBABILITY OF ERROR
c           nflag       - PERFORMANCE FLAG
c                           1 - SHOT NOISE LIMITED
c                           2 - THERMAL NOISE LIMITED
c                           3 - COMBINATION OF SHOT AND
c                               THERMAL OR EXCESS NOISE
c
c       INTERNAL VARIABLES:
c           b           - BHATTACHARAYYA DISTANCE
c           pnoise      - EFFECTIVE NOISE POWER (W)
c           pave        - AVERAGE RECEIVED POWER
c           alpha       - OPTICAL POWER TO AVERAGE
c                           PHOTON COUNTS
c           eg          - PHOTON COUNTS TO CURRENT
c
        common / wavefm / npts,t,form0(1000),
     &  form1(1000),ps0(1000),ps1(1000)
        common / ldata / rl,alam,rpx,theta,x,
     &  angtr,angrec,gamint,bw
```

```fortran
      common / sndata / bwr,eta,f,em,pback,ps,darki,
     &  ptherm,snpndb,sndb,xm,bwopt,nflg,g
      common / inter / pnoise,alpha,eg,fnoise
c
      external func1,func2,func3
      real lobnd1,lobnd2
c
      alpha=eta*alam/(2.998e8*6.626e-34)
      eg=g*1.6e-19
      fnoise=f
c
      pnoise=pback+darki/(alpha*eg)
c
c     CALCULATE AVERAGE POWER
      pave=0.0
      do 10 i=1,npts
      pave=pave+ps0(i)+ps1(i)
10    continue
      pave=0.5*pave/npts+pnoise
c
c     THERMAL NOISE LIMITED?
      if (alpha*0.5*ptherm**2.gt.10.0*f*pave)
     &  go to 40
c     EXCESS NOISE?
      if (f.gt.1.0) go to 20
c     SHOT NOISE LIMITED?
      if (pave.gt.10.0*alpha*0.5*ptherm**2)
     &  go to 30
c
20    nflag=3
      pnoise=pnoise+alpha*0.5*ptherm**2/f
      b=0.5*f*simp(func1)
      upbnd1=0.5*exp(-b)
      lobnd1=0.25*exp(-2.0*b)
      b=0.5*simp(func3)
      upbnd2=0.5*exp(-b)
      lobnd2=0.25*exp(-2.0*b)
      return
c
30    nflag=1
      b=0.5*simp(func1)
      upbnd1=0.5*exp(-b)
      lobnd1=0.25*exp(-2.0*b)
      return
c
40    nflag=2
      b=0.25*simp(func2)/ptherm**2
      upbnd2=0.5*exp(-b)
      lobnd2=0.25*exp(-2.0*b)
      return
      end
```

```
c.
          function simp(func)
c
c         SIMPSONS RULE INTEGRATION OF
c         FUNCTION FUNC
c
          common / wavefm / npts,t,form0(1000),
&         form1(1000),ps0(1000),ps1(1000)
          double precision sum
c
          sum=0.0
          do 10 i=1,npts-2,2
          term=func(i)+4*func(i+1)+func(i+2)
          sum=sum+term
10        continue
          simp=t*sum/(3*(npts-1))
          return
          end
c.
          function func(i)
c
c         BHATACHARAYYA DISTANCE FUNCTIONS
c
          common / wavefm / npts,t,f0(1000),
&         f1(1000),p0(1000),p1(1000)
          common / inter / pn,a,e,f
c
c         POISSON PROCESS
          entry func1(i)
          func=a*(sqrt(p1(i)+pn)-sqrt(p0(i)+pn))**2
          return
c
c         GAUSSIAN PROCESS
          entry func2(i)
          func=(p1(i)-p0(i))**2
          return
c
c         GAUSSIAN PROCESS - TIME VARYING VARIANCE
          entry func3(i)
          func=a*(p1(i)-p0(i))**2/
&         (2.0*f*(p1(i)+p0(i)+2.0*pn))+
&         alog((p1(i)+p0(i)+2.0*pn)/
&         (2.0*sqrt((p1(i)+pn)*(p0(i)+pn))))
          return
          end
```

SECTION V

APERTURE AVERAGING CHECK ROUTINE

APERTURE AVERAGING CHECK SUBROUTINE

The subroutine APERTR is a FORTRAN subprogram to calculate if there is enough aperture averaging to ignore the effects of atmospheric turbulence in the clear atmosphere between the scattering volume and the off-axis receiver.

As shown in Figure 1, the scattering volume may be viewed as an extended incoherent source localized to a plane parallel to the receiver aperture. This *effective* transmitter aperture is located a distance L from the receiver. If we assume that the scattering volume fills the receiver field of view, the area of the effective transmitter aperture may be calculated from the rectangular field of view of the receiver

$$A_t = 2L \sin(\phi/2) \cdot 2L \sin(\phi_p/2) \tag{1}$$

where ϕ is the receiver field of view in the intercept plane and ϕ_p is the field of view perpendicular to the plane.

The effective transmitter aperture may be thought of as a collection of coherence cells, from each of which the light will arrive at the receiver with statistically independent fading. The area of each coherence cell is $\pi \rho_o^2/4$ where ρ_o is the coherence distance. If the effective transmitter contains many, one hundred or more, coherence cells the random fading will be 'averaged out' over the statistically independent channels. For receivers collecting power from a scattering volume, the field of view will most likely be large enough that this condition is met.
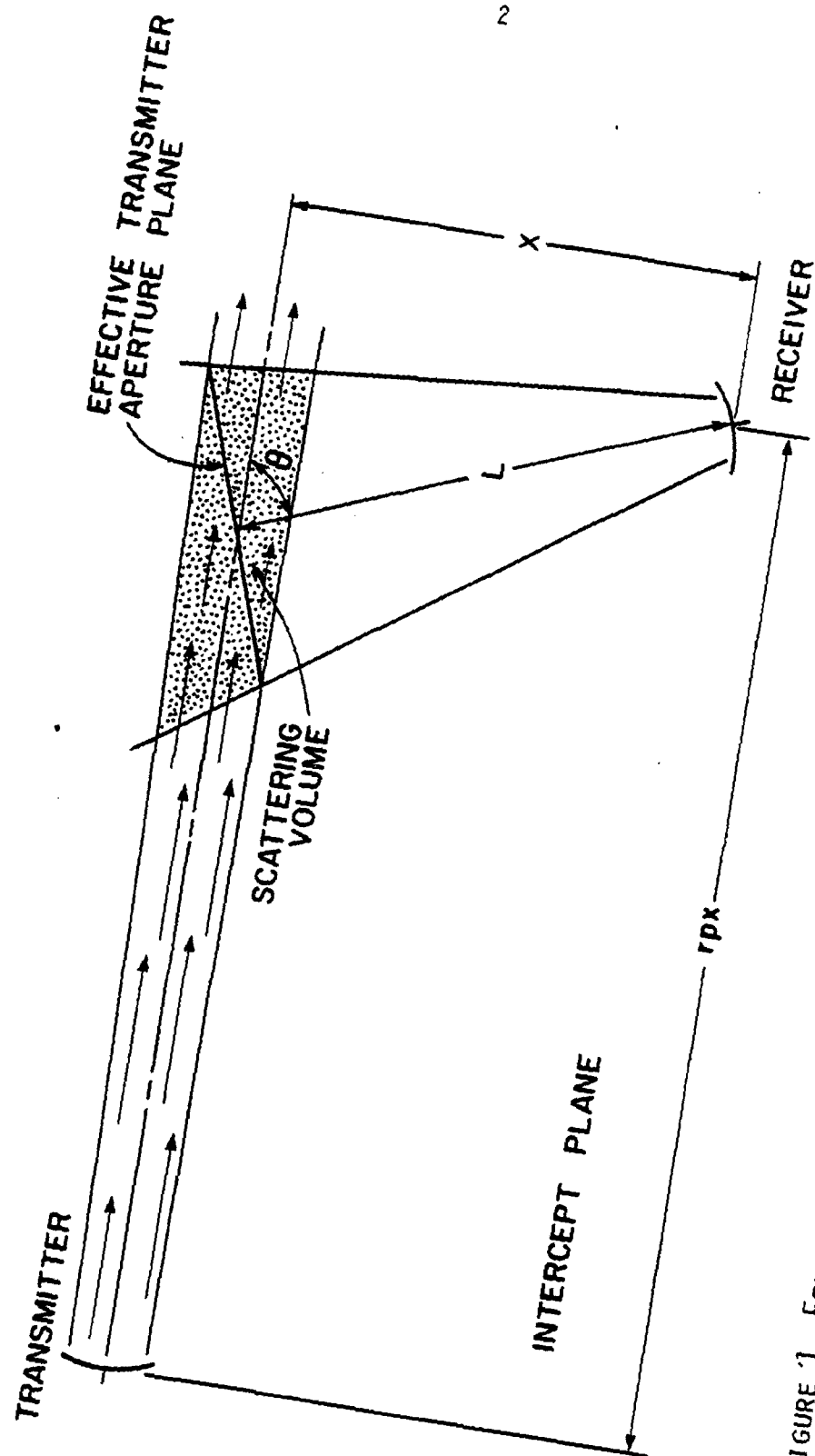
FIGURE 1 EFFECTIVE TRANSMITTER APERTURE GEOMETRY

For paths with uniform turbulence

$$\rho_o = [1.09 \ (2\pi/\lambda)^2 \ Cn^2 \ L]^{-3/5} \tag{2}$$

where λ is the wavelength and Cn^2 the atmospheric structure constant. The program selects from three values of Cn^2, corresponding to mild, moderate or severe turbulence.

If the above condition is not met, the program assumes that the off-axis receiver is narrowing in on a signal from a reflecting surface. The effective path length is now the total path from the transmitter to the reflecting surface to the receiver.

$$L = [rpx - x/\tan(\theta)] + x/\sin(\theta) \tag{3}$$

In a similar manner the receiver aperture can be broken up into coherence cells each of area $\pi\rho_o^2/4$. The coherence distance, ρ_o, is calculated as above using the value of L calculated in Eq.(3). Again, if there are one hundred or more coherence cells in the receiver aperture, each experiencing random fading, the effects of fading will be averaged out.

If neither of the above conditions is met, the program prints out a warning that performance may be degraded due to turbulence induced fading.

Following is a listing of the subroutine APERTR.

4

Program Listing of Subroutine APERTR

```fortran
c.
          subroutine apertr
c
c     CALCULATES IF THERE IS ENOUGH APERTURE
c     AVERAGING TO IGNORE THE EFFECTS OF
c     FADING DUE TO TURBULENCE
c
c     VARIABLES:
c         iw          - TURBULENCE FLAG
c                         1-SEVERE 2-MODERATE 3-WEAK
c         cnsq        - ATMOSPHERIC STRUCTURE
c                         CONSTANT (M**2/3)
c         arho        - TURBULENCE COHERENCE
c                         CELL AREA (M**2)
c         x           - PERPENDICULAR DISTANCE
c                         SR TO BEAM (M)
c         rpx         - DISTANCE TRANSMITTER TO SR
c                         OPTICAL AXIS (M)
c         theta       - ANGLE LINK AXIS TO SR
c                         OPTICAL AXIS (RAD)
c         phi         - SR FOV IN INTERCEPT
c                         PLANE (RAD)
c         phiaz       - SR FOV OUT OF PLANE (RAD)
c         l           - EFFECTIVE PATH LENGTH (M)
c         asr         - SR APERTURE AREA (M**2)
c         atr         - SCATTERING VOLUME EFFECTIVE
c                         APERTURE AREA (M**2)
c         alam        - WAVELENGTH (M)
c
          common / flags / mode,mcomp,mp,lam,modesw,
     &    lunit,nout,istog,iotype,irtype,ihet,ibflag,
     &    iw
          common / ldata / rl,alam,rpx,theta,x,
     &    angtr,angrec,gamint,bw
          common / srdata / asr,hs,phi,phiaz,dphi
          dimension cnsq(3)
          data cnsq / 2.85e-13,1.0e-13,8.5e-15 /
          data pi / 3.142 /
c
          l=x/sin(theta)
          atr=4.0*l**2*tan(0.5*phi)*tan(0.5*phiaz)
          arho=pi*(43.03*cnsq(iw)*l/alam**2)**-0.6/4
          if (atr.gt.100*arho) return
c
          write (6,200)
200       format (6x,"program assumes SR is ",
     &    "narrowing in on a reflecting target",/)
          l=rpx-x/tan(theta)+x/sin(theta)
          arho=pi*(43.03*cnsq(iw)*l/alam**2)**-0.6/4
          if (asr.gt.100*arho) return
```

```
c
      temp=100*arho
      write (6,210) temp
210   format (6x,"performance may be degraded by",
&     " fading due to turbulence",/,6x,"minimum ",
&     "SR aperture for complete averaging is ",
&     1pe11.3," meters**2",/)
      return
      end
```

PERFORMANCE OF
OFF-AXIS OPTICAL COMMUNICATION RECEIVERS
IN SCATTERING ATMOSPHERES

BY

WILLIAM PAUL JAEGER

B.S., University of Wisconsin - Parkside
(1978)

SUBMITTED IN PARTIAL FULFILLMENT
OF THE REQUIREMENTS FOR THE
DEGREE OF

MASTER OF SCIENCE

at the

MASSACHUSETTS INSTITUTE OF TECHNOLOGY

September 1980

Signature of Author_____
Department of Electrical Engineering and
Computer Science, July 30, 1980

Certified by_____
Robert S. Kennedy
Thesis Supervisor

Accepted by_____
Chairman
Departmental Committee on Theses

PERFORMANCE OF
OFF-AXIS OPTICAL COMMUNICATION RECEIVERS
IN SCATTERING ATMOSPHERES

by

WILLIAM PAUL JAEGER

Submitted to the Department of Electrical Engineering and
Computer Science on July 30, 1980 in partial fulfillment
of the requirements for the degree of Master of Science.

ABSTRACT

The performance of off-axis optical communication receivers
is considered. A statistical model of the photodetection process is
presented and the influence of the received field statistics on the
photodetection process is discussed. Upper and lower bounds on the
probability of bit error for binary, one-shot, digital communication
systems utilizing direct detection are developed. These bounds are
based on the Bhattacharyya distance measure. A computer program is
developed, which when interfaced with existing programs that model the
propagation of optical radiation through the atmosphere, predicts the
probability of bit error performance for off-axis optical communication
systems.

Thesis Supervisor: Robert S. Kennedy

Title: Professor of Electrical Engineering

ACKNOWLEDGEMENTS

I would like to thank my thesis advisor, Dr. Robert S. Kennedy, for his insight and guidance during this work. His knowledge and experience proved an invaluable resource to me. I would also like to thank Mr. Warren Ross. Our discussions, both technical and otherwise, helped me get through this maze that is M.I.T.

4

TABLE OF CONTENTS

LIST OF FIGURES

GLOSSARY

α - Proportionality constant, $\eta P(t)/h\nu$.

B - Bhattacharyya distance

B_0 - Bandwidth of optical filter

C_n^2 - Atmospheric structure constant

F - Excess noise factor

G - Mean detector gain

η - Detector quantum efficiency

h - Planck's constant

$h(t)$ - Impulse response of the post-detection electronics

I - Identity matrix

L - Optical path length

$L(\underline{x})$ - Likelihood ratio

$\lambda(t)$ - Rate function of an Inhomogeneous Poisson process

Λ - Covariance matrix of a Gaussian random vector

m - Mean of a Gaussian random process or variable

ν - Nominal optical frequency

N - Number of samples of a random process

N_B - Power density of background noise

$N_0/2$ - Bilateral spectral density of thermal noise

$N(t)$ - Poisson process

$P_S(t)$ - Received signal power waveform

P_S - Average received signal power

P_B - Collected background power

P_D - Equivalent power that gives rise to the dark current

7

P_N — Effective noise power

$Pr(e)$ — Probability of bit error

$P_{\underline{x}|H}(\underline{x}|H)$ — Probability distribution of $\underline{x}$ conditioned on hypothesis H

ρ_o — Atmospheric coherence distance

σ^2 — Variance of a Gaussian random process or variable

T — Bit duration time

τ_i — Event times of carrier generation

Ω — Field of view

Ω_d — Diffraction limited field of view

w — Bandwidth of post-detection processing

x — A random process or variable

y — A random process of variable

CHAPTER ONE

INTRODUCTION

In recent years there has been a tremendous interest and growth
in communication systems utilizing light transmitted over optical fibers.
Opitcal fibers provide a more benign propagation medium than is
available in the open atmosphere. The atmospheric channel suffers from
scattering due to suspended particles, random refractive index fluctuations
and limitations due to bad weather. However, the increasing congestion
of the electro-magnetic spectrum has increased interest in the use of
optical frequencies for situations in which mobility, geographical
constraints or the desire to broadcast to a number of users precludes
the use of cabled connections.

Off-axis Optical Communication

This study will concentrate on systems that *rely* on the atmospheric
scattering to establish over-the-horizon communications or non-line-of-
sight broadcast capabilities. A number of authors have considered such
systems [1-4]. Typical geometries for off-axis communication systems are
shown in Figure 1. The complex geometry of the off-axis link atmospheric
scattering dictates that the propagation of radiation from transmitter
to receiver will usually be modeled in a computer program. In this
paper a computer code to analyze the performance of off-axis communica-
tion receivers will be developed. This code will interface with existing
propagation programs. Analog communication will be discussed briefly,
but the major emphasis will be on analyzing the performance of digital

9

FIGURE 1 TYPICAL OFF-AXIS COMMUNICATION GEOMETRIES

systems.

A block diagram of an off-axis optical communication system is shown in Figure 2. The information is used to modulate an optical source. The transmitter antenna couples the source power into the atmospheric channel. Optical antennas are basically telescopes. Similarly, the receiver antenna couples the atmospheric channel to the receiver detector. The characteristics of the optical antennas, particularly the transmitter beam divergence and receiver field of view, will greatly influence the nature of the atmospheric propagation by determining the size of the scattering volume.

The receiver predetection processing may include an optical filter to limit the out-of-band background radiation or optical processing to separate different polarization or frequency components of the received field into different detectors. (Heterodyne receivers, the predetection mixing of the received field with a local oscillator laser, will not be considered for reasons discussed in Chapter Two.) The detector converts the optical signals into electrical signals. Finally, the post-detection processing demodulates or decodes the electrical signal to extract the desired information.

The off-axis optical receiver problem can be separated into a propagation problem and a performance problem. The dividing line will be the detector surface. The optical power incident on the receiver detector will be a function of the receiver collecting optics area and field of view, as well as the transmitter power, beam divergence, modula-
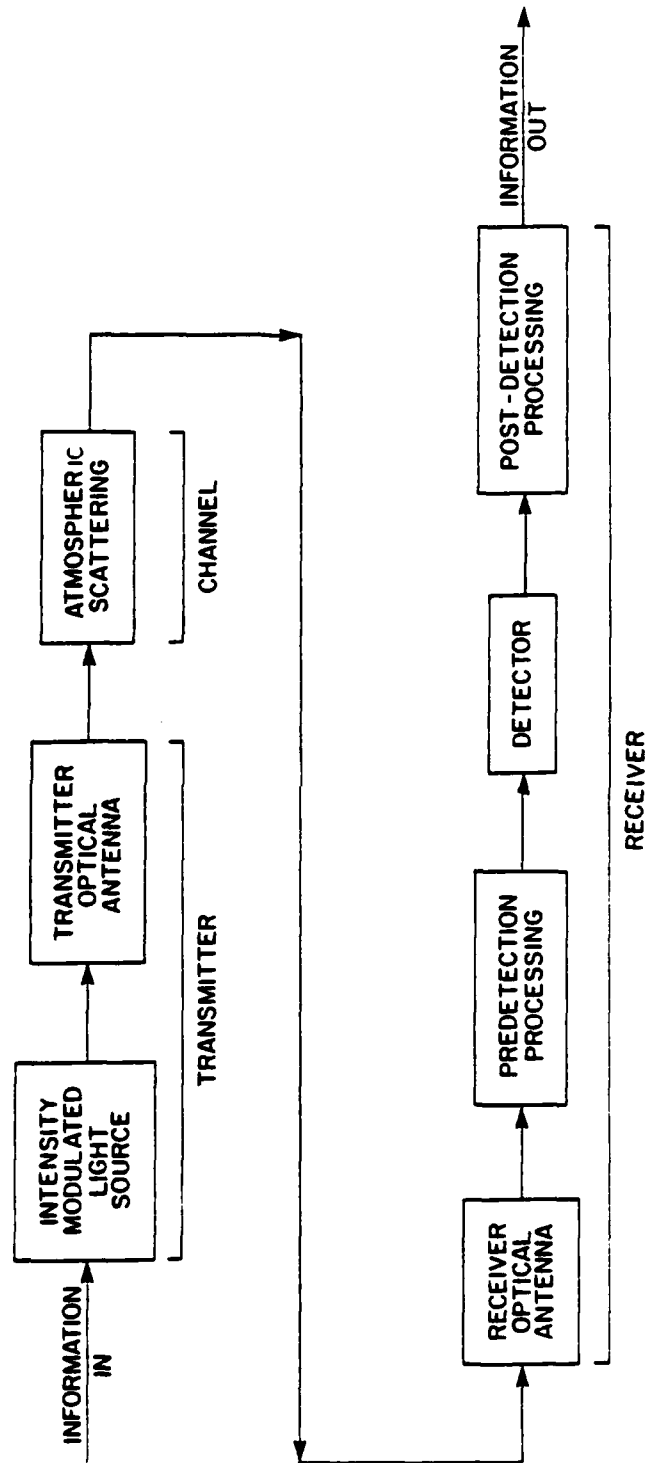
FIGURE 2 OFF-AXIS OPTICAL COMMUNICATION SYSTEM

tion, the link geometry and the atmospheric scattering. In general, this waveform will suffer both attenuation and time dispersion during propagation. Receiver performance will be limited by the optical power waveform incident on the detector, the collected background radiation and the receiver parameters that specify the quantity and nature of the detector noise. Optical receivers exhibit fundamentally different noise character from radio receivers due to quantum effects. Quantum effects are important at optical frequencies because the photon energy greatly exceeds the thermal agitation.

Preview

The formulation of the performance analysis problem will be developed in Chapter Two. A statistical model of the detection process will be presented and assumptions about the nature of the signal incident on the detector will be explored. In Chapter Three a bound on the performance of digital receivers based on the Bhattacharyya distance will be developed. It will be shown that the bound provided by the Bhattacharyya distance is a general, yet relatively simple to calculate, bound that is amenable to computer implementation. The algorithm for such a computer implementation will be outlined. A FORTRAN computer routine based on the results of Chapter Three appears in the Appendix.

CHAPTER TWO

PROBLEM FORMULATION

In this chapter the background and restrictions of the problem formulation will be developed. These can be roughly divided into two areas: the detector noise model and assumptions about the interface between the propagation and performance analysis.

Detector Noise Mechanisms

All current devices for converting optical signals into electric signals involve energy measurement. A quantum of optical energy, the photon, is absorbed and a charge carrier generated. Thus, photodetectors respond only to the power, or intensity, of the optical signal rather than to the electromagnetic field itself. The power is proportional to the rate of photo-absorption.

The principle detectors for use in optical communication receivers are photomultiplier tubes, semiconductor photodiodes and avalanche photodiodes. While there are important physical differences between these devices, it is possible to develop a single statistical model which can, by appropriate selection of parameters, describe the behavior of any of the above detectors. The output current of the photodetector may be modeled as

$$i(t) = [\sum_i eg_i \delta(t-\tau_i) + i_T(t)] * h(t)$$

where τ_i are the event times of carrier generation, e the charge on the electron, g_i the detector gain for each photon detection, i_T a noise

current of thermal origin and $h(t)$ the impulse response of the post-detection amplifier or load resistor network. It is assumed that the impulse response of the detector is faster than that of the following electronics. A block diagram of a photodetector is shown in Figure 3.

The generation of carriers can be modeled as a Conditional Inhomogeneous Poisson process, $N(t)$, with rate parameter proportional to the instantaneous signal plus background power incident on the detector, $P_S(t)$ and P_B respectively. The proportionality constant α is $\eta/h\nu$, where $h\nu$ is the photon energy at optical frequency ν and η is the quantum efficiency of the detector -- essentially the probability a photon will generate a carrier. The discrete nature of carrier generation gives rise to shot noise in low light levels. Additional shot noise results from spontaneously generated charge carriers referred to as the dark current. These emissions occur at random with average rate αP_D, where P_D is a fictitious power called the dark power. Though they arise from physically different sources, it is convenient to lump P_B and P_D together into an equivalent noise power, P_N.

In photomultipliers and avalanche photodiodes, the charge carriers generated by photo-absorption undergo a current multiplication within the device. The initial charge carriers are accelerated by an electric field creating additional carriers as they collide with the photodetector material. These new carriers in turn create more carriers in a similar fashion. The gain for each carrier created by photo-absorption is random. These random gains may be modeled as independent, identically distributed random variables of mean value G and second moment G^{2+x}.

FIGURE 3 OPTICAL RECEIVER NOISE GENERATION MECHANISMS
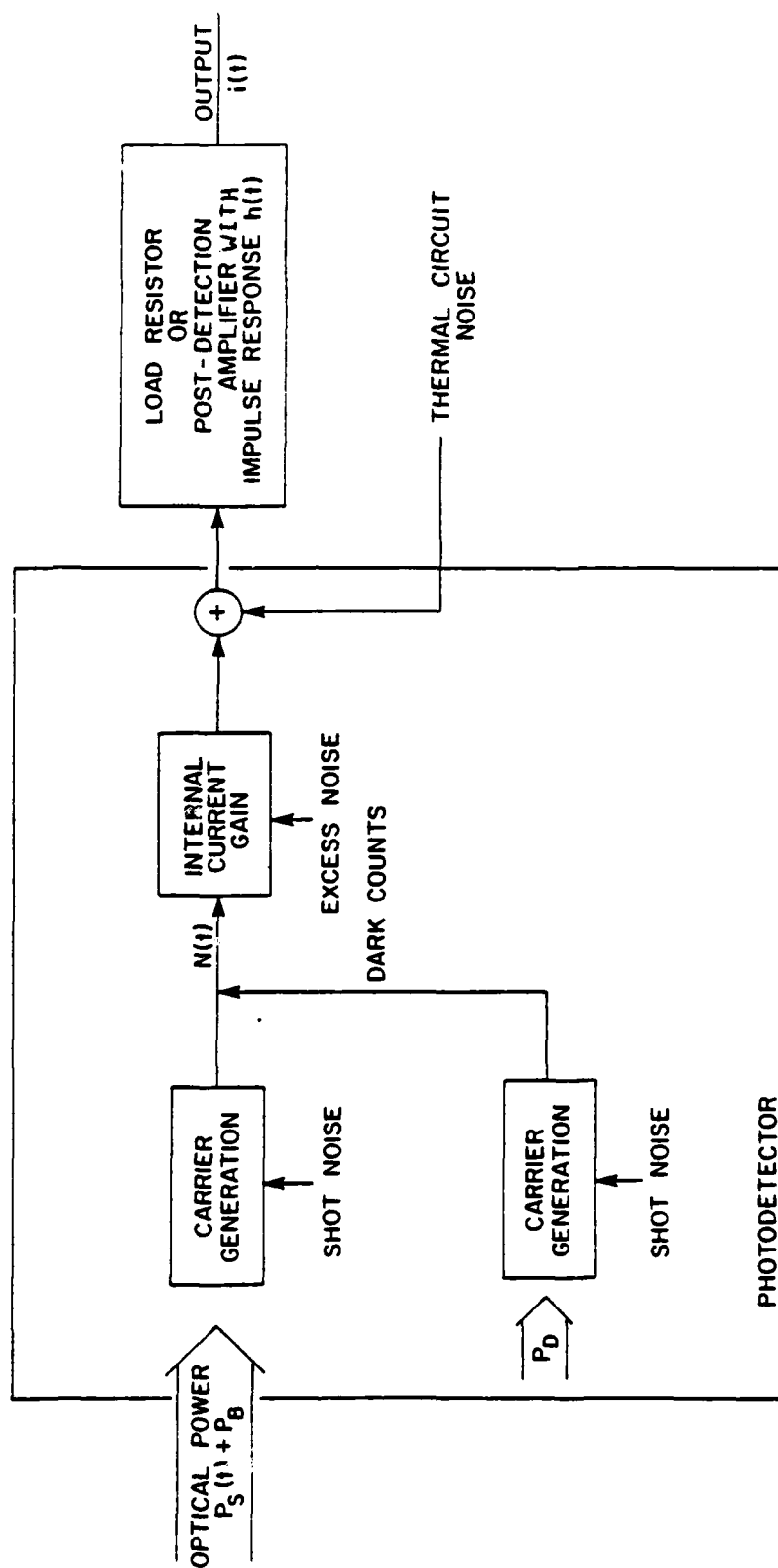
The quantity G^x is referred to as the excess noise factor, F. The value of x is dependent on the particular device. For photomultipliers the value of x is small and the gain may be considered constant. The excess noise in avalanche photodiodes is significant enough that it must be modeled. In contrast to photomultipliers and avalanche photodiodes, photodiodes have unity gain.

To these current pulses is added a thermal noise $i_T(t)$. This current is a wide-band noise associated with any internal detector resistance, the load resistor, or the front-end noise of any following electronics. It is reasonably modelled as a white Gaussian random process with zero mean and bilateral spectral density, $N_0/2$, of $2kT_k/R_e$. Here k is Boltzmann's constant, T_k the absolute temperature and R_e the effective load resistance. The thermal noise will be especially significant for detectors that do not have internal gain.

One may define a signal-to-noise ratio, SNR, as the squared average expected value of the signal component of i(t) divided by the variance of i(t). It can be shown [5] that

$$SNR = \frac{E[i(t)_{sig}]^2}{VAR[i(t)]} = \frac{(\alpha P_S)^2}{[F\alpha(P_S+P_N) + N_0/2(eG)^2]2W}$$

where W is the bandwidth of the following electronics. The first term of the denominator is the variance due to shot noise while the second term is due to the thermal noise. Notice that if the gain is large and constant the effects of thermal noise can be neglected. This is the

shot noise limit. However, if gain fluctuations exist, F will be a function of G. Thus, some optimal mean gain value will exist which maximizes the signal-to-noise ratio by balancing the shot noise variance and the thermal noise variance. Without internal gain or cryogenic cooling the thermal noise will usually swamp out the shot noise. This is the thermal noise limit. The choice of photodetector -- photomultiplier, photodiode or avalanche photodiode -- will often depend on what type is available at the optical frequency at which one is working.

Photodetector Output Statistics

While signal-to-noise ratio expressions are appropriate for analyzing the performance of analog communication systems, the performance analysis for digital communication receivers requires a more complete knowledge of the detector output statistics. The digital receiver will apply a decision rule to the received signal to determine which of a finite number of signals, or characters, was most likely sent. The performance measure of interest is the probability of making an error in decoding. Determining the probability of error, $Pr(e)$, requires knowledge of the probability distribution of the detector output given one knows which character was sent.

If there is no excess noise and the average shot noise variance, $\alpha(P_S+P_N)$, greatly exceeds (by a factor of ten or more) the thermal noise variance, $N_0/2(eG)^2$, the Poisson counting statistics will dominate. The detector output current pulses can be modeled as a Conditional Inhomoge-

neous Poisson process with rate parameter $\alpha[P_S(t)+P_N]$.

If the thermal noise variance greatly exceeds (again by a factor of ten) the average shot and excess noise variance, $\alpha F(P_S+P_N)$, the Gaussian statistics of the thermal noise will dominate. The detector output current may then be modeled as a Gaussian random process with mean value $eG\alpha[P_S(t)+P_N]$ and variance $N_0/2$.

If the receiver noise is a combination of shot and thermal noise, finding the underlying statistics of the detector output becomes quite complicated, if not intractable. The approach used in this study has been to model the shot noise as a Gaussian process of the same variance and then alternatively to model the thermal noise as a Poisson process, again on a second moment basis. If the performance predicted by both analyses are numerically close, it can reasonably be assumed that the true performance is also numerically close. There are no guarantees on how close however!

Finding the underlying statistics for the compound Poisson process resulting from random gain fluctuations is a more tractable problem [6]. However, receivers with gain fluctuations will most likely utilize an optimal mean gain to maximize the signal-to-noise ratio by balancing the shot and thermal noise variance terms. Thus, the approach used here is to again model the shot and excess noise as a Gaussian process and then the thermal and excess noise as a Poisson process to achieve a 'handle' on the performance.

Deterministic Power Assumption

The preceding discussion has assumed that the optical power incident on the detector is known. In reality the power waveform will be the output of a random atmospheric channel and thus a stochastic process. It will be shown in this section that for most off-axis optical communication systems the receiver statistics will behave as if the detector were illuminated by a deterministic signal equal to the mean value of the stochastic power waveform actually illuminating it.

The signal from an off-axis scatter channel can be thought of as a distributed incoherent source, much the same way as background light is modeled. The off-axis receiver will, within constraints, open the field of view to take in as much of the extended source as possible.

It is possible to think of the receiver as the sum of an array of diffraction limited field of view receivers, arranged to make up the entire field of view. Due to the short wavelength of optical frequencies, even modest fields of view will contain on the order of 10^6 to 10^8 diffraction limited fields of view. Each diffraction limited field of view is looking at a different part of the scattering atmosphere and the stochastic intensity fields incident on each can be assumed to be statistically independent.

If the extended source approximately fills the receiver field of view, to first approximation, the total average received signal power may be thought of as equally divided among the diffraction limited fields of view. (If the extended signal source does not fill the field of

view, the field of view could be made smaller thereby decreasing the collected background at no loss of signal.) Because of the large number of diffraction limited fields of view, the signal plus background power per diffraction limited field of view will be small. In fact, for most off-axis receivers an average of less than one photon count will be generated per diffraction limited field of view over the counting interval of the receiver. Kennedy has called channels which satisfy this supposition *weakly coherent quantum channels* [7].

The representation theorem for doubly stochastic Poisson processes (that is a Poisson process in which the rate parameter is also stochastic) states that the statistics of a doubly stochastic Poisson process will behave as a conditional Poisson process with rate parameter equal to the minimum mean square error estimate of the stochastic rate parameter [8]. The minimum mean square estimate is based on all previous events and any conditioning. If the probability of getting one or more counts or events is small, the minimum mean square estimate is simply the expected value of the rate parameter given any conditioning. Since each of the diffraction limited fields of view is independent, the output of the entire detector is a Poisson process with rate parameter equal to the sum of the individual rate parameters. Thus, to the extent that the off-axis scattering channel is weakly coherent, performance analysis will require only the expected value of the received power waveform from the propagation analysis.

To see that this is all reasonable, consider a not atypical off-axis receiver with 10 cm diameter optics, 5° circular field of

view (about 90 mR), and optical filter bandwidth of 10^{-3} µ (B_o), a
counting interval of 1 µ sec, and operating at a wavelength of 1 micron.
The diffraction limited field of view is

$$\Omega_d = \frac{\lambda^2}{\pi d^2/4} = 10^{-10} \text{ SR}$$

While the total field of view is

$$\Omega = \pi(.09)^2 = .02 \text{ SR}$$

or about 10^8 diffraction limited fields of view. The background power
per diffraction limited field of view is $N_B B_0$ where N_B is the power
density of the background noise. Since N_B is typically on the order
of 10^{-25} W µ for atmospheric operation [9], the average number of
background counts per diffraction limited field of view over the
counting internal ($\alpha N_B B_0 T$) is on the order of 10^{-12}. Thus, this
receiver can operate with about 10^8 signal photon counts and still be
in the low photon coherence regime. For this receiver this corresponds
to about 10 µ watts of signal power!

Fading Due to Turbulence

If the atmospheric scattering is primarily single scatter or
the off-axis receiver is not immersed in the scattering medium, one
must also consider the effects of atmospheric turbulence in the clear
atmosphere between the scattering volume and the receiver. Atmospheric
turbulence refers to the slight atmospheric refractive index fluctua-
tions due to uneven heating. Such refractive index fluctuations act

as a random lens. When random lensing results in destructive inter-
ference in the receiver aperture, the random signal losses are known
as fading.

As shown in Figure 4, the scattering volume can be viewed as
a distributed incoherent source localized to a plane parallel to the
receiver aperture. This effective transmitter is located a distance L
from the receiver. Light emitted from points in this plane separated
by a distance greater than the transmitter coherence distance, ρ'_o ,
will pass through substantially different atmosphere and arrive at
the receiver with statistically independent random fading. One may
thus define a transmitter coherence cell with area $(\rho'_o)^2/4$. As long
as the effective transmitter contains many (one hundred or more)
coherence cells, the effects of fading will tend to 'average out' over
the statistically independent channels.

In a similar manner, light arriving at points in the receiver
aperture separated by greater than the receiver coherence distance, ρ_o ,
will have statistically independent fading. Thus, if there are many
receiver coherence cells each of area $(\rho_o)^2/4$ in the receiver aperture,
the effects of fading will again be averaged out.

For a path with uniform turbulence

$$\rho'_o = \rho_o = [1.09 \ (2\pi/\lambda)^2 \ Cn^2 \ L]^{-3/5}$$

where Cn^2 is the atmospheric structure constant [10].

In addition to either of the above effects, the receiver field
of view must be large enough to compensate for random angle of arrival
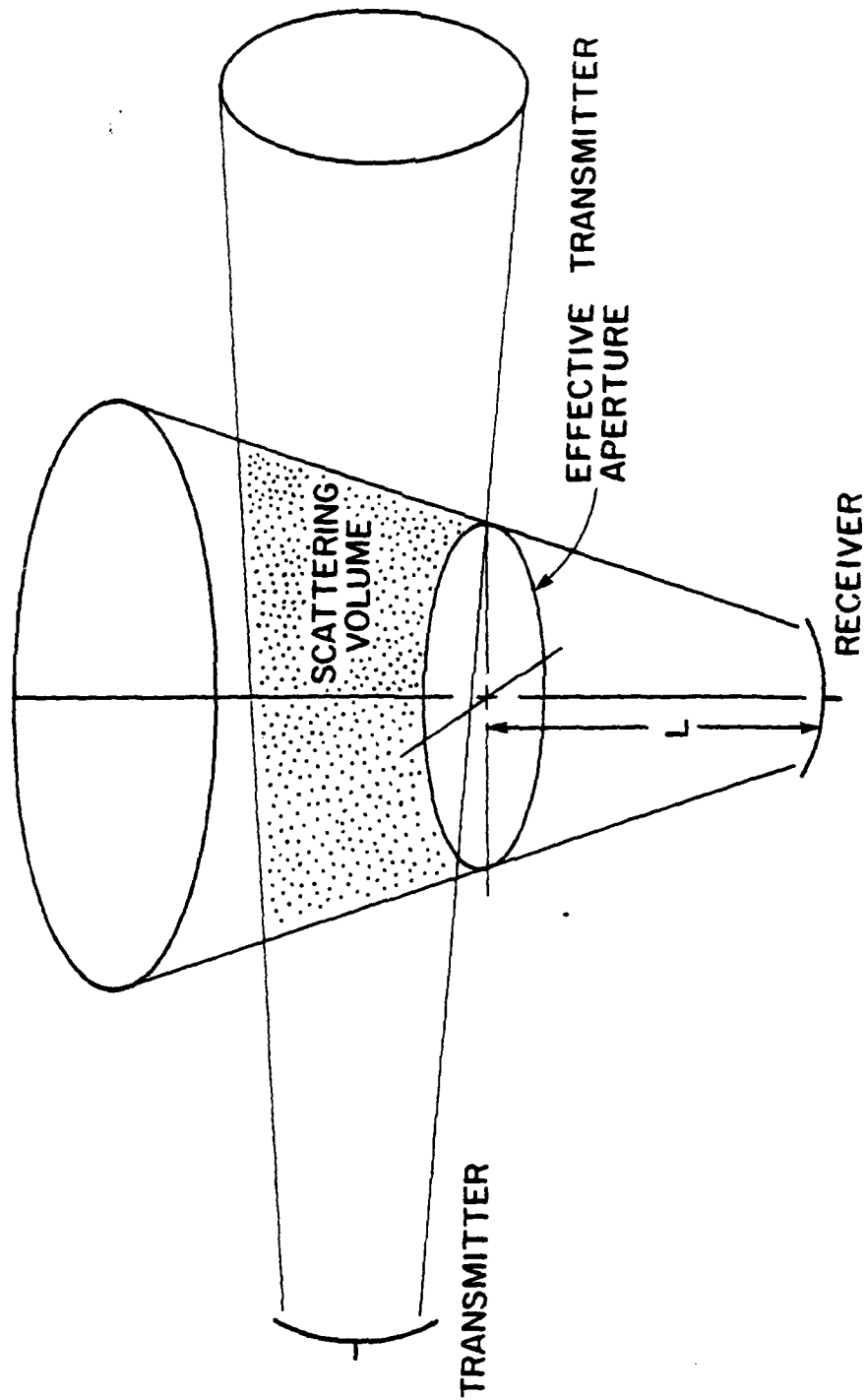
FIGURE 4 SCATTERING VOLUME VIEWED AS EFFECTIVE SOURCE

variations caused by turbulence. Typically the angular spectrum of turbulence is on the order of tenths of milliradians so this condition will always be met for a receiver in a scattering environment.

Again assuming that the scattering volume approximately fills the receiver field of view, the area of the effective transmitter may be calculated from the receiver field of view and the distance to the scattering volume. As ρ_o is typically on the order of centimeters to meters, the complete transmitter aperture averaging condition will almost always be met.

Heterodyne Receivers

Transmitter aperture averaging to ignore the effects of turbulence relies on the receiver having a large field of view and the weakly coherent channel assumption implies that a diffraction limited field of view will not collect much power. Yet, heterodyne receivers are restricted to extracting information from a diffraction limited field of view by local oscillator laser mixing requirements. Heterodyne reception thus seems impractical for off-axis receivers.

One could consider an array of heterodyne receivers each with diffraction limited field of view arranged to make up a large field of view. This has the added complication of deciding how to optimally combine and process the individual detector outputs which is essentially decided for us in a direct detection receiver. Seeking to avoid this added complication as well as considering the practical difficulties of building such an array, (on the order of 10^6 diffraction limited

fields of view), this study was limited to direct detection receivers.

Having laid the groundwork for communication in off-axis scattering channels, the next chapter will turn toward quantifying the off-axis receiver performance for digital signaling.

CHAPTER THREE

THE BHATTACHARYYA DISTANCE

The digital communication receiver will implement a decision rule on the detector output to determine which of a finite number of waveforms was most likely sent. In the real world there is always a probability that the signal will be so noisy that the receiver will make a mistake in decoding. The probability of error, Pr(e), may be obtained by integrating the probability distribution of the received signal, given one knows what was sent, over the region on the 'wrong' side of the decision rule. In general exact expressions for Pr(e) are difficult to obtain. Often it will be necessary to settle for bounds on the probability of error. In this chapter the bound provided by the Bhattacharyya distance will be explored. Binary one-shot communication will be considered. The waveform for a single bit (binary one or zero) is sent and the receiver makes a decision on a bit-by-bit basis.

Bound Provided by the Bhattacharyaa Distance

The Bhattacharyya distance is defined:

$$B = -\ln \int_{-\infty}^{\infty} \sqrt{p_{\underline{x}|H_0}(\underline{x}|H_0)\, p_{\underline{x}|H_1}(\underline{x}|H_1)}\; d\underline{x} \tag{3.1}$$

The underbar denotes a vector and $p_{\underline{x}|H_i}(\underline{x}|H_i)$ is the probability distribution of the vector $\underline{x}$ conditioned on hypothesis H_i.

Kailath [11] has shown that for equally likely hypotheses the

Bhattacharyya distance may be used to provide upper and lower bounds on the probability of error (independent of the underlying statistics).

$$\frac{1}{4} e^{-2B} \le Pr(e) \le \frac{1}{2} e^{-B} \qquad (3.2)$$

Notice that the bound provided by the Bhattacharyya distance does not involve the decision rule. Implicit in Kailath's derivation is the use of a decision rule that minimizes the probability of error. Thus, the bound based on the Bhattacharyya distance provides a bench mark performance based on the shape and amplitude of the received signal. The lower bound is the absolute best performance one might achieve given the received power signal set. The upper bound is the worst one can do *assuming* the receiver optimally processes the detector output.

The bound provided by the Bhattacharyya distance is closely related to the Chernoff bound and the Maximum Aposteriori decision rule (MAP rule). The MAP rule is the minimum probability of error rule. It can be shown that the Chernoff bound is the exponentially tightest bound on the probability of error [12]. For equally likely hypotheses the MAP rule reduces to the Maximum Likelihood decision rule. The likelihood ratio

$$L(\underline{x}) = \frac{p_{\underline{x}|H_1}(\underline{x}|H_1)}{p_{\underline{x}|H_0}(\underline{x}|H_0)} \qquad (3.3)$$

is evaluated at the received value of $\underline{x}$. If $L(\underline{x})$ is greater than one, decide one was sent; if $L(\underline{x})$ is less than one, decide zero was sent.

Let $\underline{y} = \ln L(\underline{x})$. Assuming that both types of errors occur with equal probability, the probability of error is the probability $\underline{y}$ is greater than $\underline{0}$ given one knows zero was sent. The Chernoff bound on this probability is given by

$$Pr(e) = Pr(\underline{y} > 0 | H_0) \leq \frac{1}{2} E [e^{s\underline{y}} | H_0] \qquad (3.4)$$

There is an optimal value of s for which the bound is minimized, though the bound is valid for non-optimal values of s.

An alternative form of the Bhattacharyya distance is

$$B = -\ln \int_{-\infty}^{\infty} \sqrt{p_{\underline{x}|H_0}(\underline{x}|H_0) \, p_{\underline{x}|H_1}(\underline{x}|H_1)} \, d\underline{x} = -\ln E[L(\underline{x})^{1/2} | H_0] \quad (3.5)$$

The upper bound provided by the Bhattacharyya distance may be written

$$\frac{1}{2} e^{-B} = \frac{1}{2} E[L(\underline{x}) | H_0] = \frac{1}{2} [e^{1/2\ln L(\underline{x})} | H_0] \qquad (3.6)$$

Thus, the upper bound provided by the Bhattacharyya distance is the Chernoff bound for the MAP decision rule evaluated at the possibly sub-optimal value of s=1/2.

The Chernoff bound provides a tighter upper bound on the probability of error than that provided by the Bhattacharyya distance. However, the general and simple nature of the bound provided by the Bhattacharyya distance (no need to explicitly find the decision rule or optimize on s) as well as the fact that it provides a lower bound make the Bhattacharyya distance measure attractive for bench mark analysis.

In the remainder of this chapter the Bhattacharyya distance for the cases of Poisson processes, Gaussian processes, and Gaussian processes with time varying variance will be developed. The latter will be important when modeling the time varying shot noise as a Gaussian process. It will be shown how the Bhattacharyya distance results may be applied to a computer algorithm to calculate the probability of bit error rate for optical communication systems. Finally, the Bhattacharyya distance for twin channel processes will be developed. Such receivers might be used in frequency shift keying systems, polarization modulation systems or any system where predetection processing separates the received field between two detectors.

Inhomogeneous Poisson Processes

For a Poisson process the probability distribution for the unordered event times on an interval T is

$$P_{\tau_1 \cdots \tau_N, N|H}(\tau_1 \cdots \tau_N, N|H) = \sum_{n=0}^{\infty} \frac{1}{n!} \prod_{j=1}^{n} \lambda_i(\tau_j) \mathrm{Exp}[-\int_0^T \lambda_i(t)dt]\delta(N-n)$$

$$(3.7)$$

where $\lambda_i(t)$ is the rate function under the hypothesis that i is sent.

The Bhattacharyya distance between two Poisson processes may be found by substituting in the definition for the Bhattacharyya distance [Eq.(3.1)].

$$B = -\ln \int_{-\infty}^{\infty} \int_{0}^{T} \cdots \int_{0}^{T} \left| \sum_{n=0}^{\infty} \frac{1}{n!} \prod_{j=1}^{n} \lambda_0(\tau_i) \text{Exp}[-\int_{0}^{T} \lambda_0(t)dt]\delta(N-n) \right.$$

$$\left. \sum_{m=0}^{\infty} \frac{1}{m!} \prod_{j=1}^{m} \lambda_1(\tau_j) \text{Exp}[-\int_{0}^{T} \lambda_1(t)dt]\delta(N-n) \right|^{1/2} d\tau_1 \ldots d\tau_N dN$$

$$= \frac{1}{2}\left[\int_{0}^{T} \lambda_0(t)dt + \int_{0}^{T} \lambda_1(t)dt \right] - \ln \sum_{n=0}^{\infty} \frac{1}{n!}$$

$$\int_{0}^{T} \cdots \int_{0}^{T} \prod_{j=1}^{n} [\lambda_0(\tau_i)\lambda_1(\tau_i)]^{1/2} d\tau_1 \ldots d\tau_N$$

$$= \frac{1}{2} \int_{0}^{T} [\lambda_0(t)+\lambda_1(t)]dt - \ln \sum_{n=0}^{\infty} \frac{1}{n!}\left[\int_{0}^{T} \sqrt{\lambda_0(t)\lambda_1(t)}\ dt \right]^{n}$$

$$= \frac{1}{2} \int_{0}^{T} [\lambda_0(t)+\lambda_1(t)]dt - \ln \text{Exp}\left[\int_{0}^{T} \sqrt{\lambda_0(t)\lambda_1(t)}\ dt \right]$$

$$= \frac{1}{2} \int_{0}^{T} [\lambda_0(t)-2\sqrt{\lambda_0(t)\lambda_1(t)} + \lambda_1(t)]dt$$

$$B = \frac{1}{2} \int_{0}^{T} [\sqrt{\lambda_0(t)} - \sqrt{\lambda_1(t)}]^2\ dt \tag{3.8}$$

Gaussian Random Processes

The concept of the Bhattacharyya distance may be extended to continuous time processes, of duration T, by considering ˅ vector of time samples of the process and then taking the limit as the number of samples approaches infinity. Defining $\underline{x}$ as a vector of time samples of the process $x(t)$.

$$\underline{x} = \begin{bmatrix} x(t_1) \\ \vdots \\ x(t_N) \end{bmatrix} \text{ and } \quad x(t_j) = \frac{1}{\delta} \int_{(j-1)\delta}^{j\delta} x(t)dt$$

$$\delta = T/N$$

The probability density for multivar te Gaussian random variable is

$$P_{\underline{x}|H_i}(\underline{x}|H_i) = \frac{\text{Exp}[-(\underline{x}-\underline{m}_i)^T \Lambda_i^{-1}(\underline{x}-\underline{m}_i)/2]}{(2\pi)^{N/2}\det^{1/2}(\Lambda_i)} \tag{3.9}$$

where Λ_i is the covariance matrix of $\underline{x}$ under hypothesis i and $\underline{m}_i$ is the mean of $\underline{x}$ under hypothesis i. Notice that

$$E[\underline{x}|H_i] = \begin{bmatrix} m_i(t_1) \\ \vdots \\ m_i(t_N) \end{bmatrix} \quad m_i(t_j) = \frac{1}{\delta} \int_{(j-1)\delta}^{j\delta} m_i(t)dt$$

where $m_i(t)$ is the mean of the process under hypothesis i.

The Bhattacharyya distance between two continuous time Gaussian processes is then

$$B = -\ell n \lim_{N\to\infty} \int_{-\infty}^{\infty} \left[\frac{\text{Exp}[-(\underline{x}-\underline{m}_0)^T \Lambda_0^{-1}(\underline{x}-\underline{m}_0)/2]}{(2\pi)^{N/2}\det^{1/2}(\Lambda_0)} \cdot \right.$$
$$\left. \frac{\text{Exp}[-(\underline{x}-m_1)^T \Lambda_1^{-1}(\underline{x}-\underline{m}_1)/2]}{(2\pi)^{N/2}\det^{1/2}(\Lambda_1)} \right]^{1/2} d\underline{x}$$

$$= -\ell n \lim_{N \to \infty} \int_{-\infty}^{\infty} \frac{Exp[-(\underline{x}-\underline{m}_0)^T \Lambda_0^{-1}(\underline{x}-\underline{m}_0)/4]}{(2\pi)^{N/2} det^{1/4}(\Lambda_0)} \cdot$$

$$\frac{Exp[-(\underline{x}-\underline{m}_1)^T \Lambda_1^{-1}(\underline{x}-\underline{m}_1)/4]}{det^{1/4}(\Lambda_1)} \ d\underline{x}$$

This may be rewitten as the convolution of Gaussian distributions

$$= -\ell n \lim_{N \to \infty} \frac{(2\pi)^N \ 2^N \ det^{1/2}(\Lambda_0) det^{1/2}(\Lambda_1)}{(2\pi)^{N/2} det^{1/4}(\Lambda_0) \ det^{1/4}(\Lambda_1)} \cdot$$

$$\int_{-\infty}^{\infty} \frac{Exp[-(\underline{x}-\underline{m}_0)^T (2\Lambda_0)^{-1}(\underline{x}-\underline{m}_0)/2] \ Exp[-(\underline{x}-\underline{m}_1)^T (2\Lambda_1)^{-1}(\underline{x}-\underline{m}_1)/2]}{(2\pi)^{N/2} det^{1/2}(2\Lambda_0)(2\pi)^{N/2} det^{1/2}(2\Lambda_1)} \ d\underline{x}$$

$$(3.10)$$

$$B = -\ell n \lim_{N \to \infty} \frac{2^{N/2} det^{1/4}(\Lambda_0) det^{1/4}(\Lambda_1)}{det^{1/2}(\Lambda_0+\Lambda_1)} \cdot$$

$$Exp[-(\underline{m}_0-\underline{m}_1)^T(\Lambda_0+\Lambda_1)^{-1}(\underline{m}_0-\underline{m}_1)/4]$$

If the time samples are statistically independent (white) and of uniform variance $\Lambda_0 = \Lambda_1 = \sigma^2 I$, where I is the identity matrix. Eq.(3.9) may be simplified as follows:

$$B = -\ell n \lim_{N \to \infty} \frac{2^{N/2} det^{1/2}(\sigma^2 I)}{2^{N/2} det^{1/2}(\sigma^2 I)} \ Exp[-\sum_{j=1}^{N} [m_0(t_j)-m_1(t_j)]^2/8\sigma^2]$$

$$B = \frac{1}{8\sigma^2} \int_0^T [m_0(t)-m_1(t)]^2 dt \qquad (3.11)$$

Gaussian Processes with Time Varying Variance

Consider now a Gaussian process that is still white but with a variance that changes from time sample to time sample and under the hypothesis. That is

$$\Lambda_i = \begin{bmatrix} \sigma_i^2(t_1) & & 0 \\ & \cdot & \\ & & \cdot \\ 0 & & \sigma_i^2(t_N) \end{bmatrix} \qquad \sigma_i^2(t_j) = \frac{1}{\delta} \int_{(j-1)\delta}^{j\delta} \sigma_i^2(t)\, dt$$

The Bhattacharyya distance expression may be found by substituting in Eq.(3.9)

$$B = -\ln \lim_{N\to\infty} \left[\frac{2^N \prod\limits_{j=1}^N \sigma_0(t_j) \prod\limits_{j=1}^N \sigma_1(t_j)}{\prod\limits_{j=1}^N [\sigma_0^2(t_j) + \sigma_1^2(t_j)]} \right]^{1/2}$$

$$\mathrm{Exp}\left[-\sum_{j=1}^N \frac{[m_0(t_j)-m_1(t_j)]^2}{4[\sigma_0^2(t_j)+\sigma_1^2(t_j)]} \right]$$

$$= \frac{1}{2} \lim_{N\to\infty} \sum_{j=1}^N \left[\frac{[m_0(t_j)-m_1(t_j)]^2}{2[(\sigma_0^2(t_j) + \sigma_1^2(t_j)]} + \ln\left[\frac{\sigma_0^2(t_j)+\sigma_1^2(t_j)}{2\sigma_0(t_j)\sigma_1(t_j)} \right] \right]$$

$$B = \frac{1}{2} \int_0^T \left[\frac{[m_0(t)-m_1(t)]^2}{2[\sigma_0^2(t)+\sigma_1^2(t)]} + \ln\left[\frac{\sigma_0^2(t)+\sigma_1^2(t)}{2\sigma_0(t)\sigma_1(t)} \right] \right] dt \qquad (3.12)$$

Application to Optical Communication

The application to optical communication is now clear. The

detector output for direct detection optical receivers in which shot noise dominates is modeled as an Inhomogeneous Poisson process with rate function $\lambda_i(t) = \alpha(P_{Si}(t) + P_N)$ given i was sent. The received signal power waveform given i was sent is $P_{Si}(t)$. Substituting in Eq.(3.7) to evaluate the Bhattacharyya distance

$$B = \frac{1}{2} \int_0^T \alpha(\sqrt{P_{S0}(t) + P_N} - \sqrt{P_{S1}(t) + P_N})^2 \, dt \qquad (3.13)$$

The detector output of thermal noise limited receivers is modeled as a Gaussian random process with mean $m_i(t) = eG\alpha[P_{Si}(t) + P_N]$ and variance $N_0/2$. The Bhattacharyya distance is evaluated using Eq.(3.10).

$$B = \frac{(eG\alpha)^2}{8N_0/2} \int_0^T [P_{S0}(t) - P_{S1}(t)]^2 \, dt \qquad (3.14)$$

If the receiver noise is a combination of shot, thermal or excess noise the detector output will be modeled as a Poisson process, then as a Gaussian process and the performance compared.

Modeling the excess noise and thermal noise as multiplicative and additive increases, respectively, in the variance of the Poisson process, the rate function is

$$\lambda_i(t) = F\alpha(P_{Si}(t) + P_N) + \frac{N_0/2}{(eG)^2} \qquad (3.15)$$

Notice that the thermal noise must be divided by the square of the multiplicative gain to refer it back to the shot noise generation.

Defining

$$\hat{P}_N = P_N + \frac{N_0/2}{F\alpha(eG)^2} \qquad (3.16)$$

The rate function may be rewritten

$$\lambda_i(t) = F\alpha[P_{Si}(t) + \hat{P}_N] \qquad (3.17)$$

and the estimate of the Bhattacharyya distance evaluated using Eq.(3.7).

$$B = \frac{F}{2} \int_0^T \alpha\left(\sqrt{P_{So}(t)+\hat{P}_N} - \sqrt{P_{S1}(t)+\hat{P}_N}\right)^2 dt \qquad (3.18)$$

Modeling the shot and excess noise as an increase in the variance of the thermal Gaussian process

$$m_i(t) = eG\alpha(P_{Si}(t) + P_N) \qquad (3.19)$$

$$\sigma_i^2(t) = F(eG)^2 \alpha(P_{Si}(t) + P_N) + N_0/2$$

Again defining $\hat{P}_N$ as in Eq.(3.15)

$$\sigma_i^2(t) = F(eG)^2 \alpha(P_{Si}(t) + \hat{P}_N) \qquad (3.20)$$

The Bhattacharyya distance is approximated using Eq.(3.11), the Bhattacharyya distance for Gaussian processes with time varying variance.

$$B = \frac{1}{2} \int_0^T \left[\frac{\alpha[P_{So}(t)-P_{S1}(t)]^2}{2F[P_{So}(t)+P_{S1}(t)+2\hat{P}_N]} + \ell n \left[\frac{P_{So}(t)+P_{S1}(t)+2\hat{P}_N}{2\sqrt{(P_{So}(t)+\hat{P}_N)[P_{S1}(t)+\hat{P}_N]}} \right] \right] dt \qquad (3.21)$$

Once the Bhattacharyya distance between the received signal given one was sent and the signal given zero was sent has been calculated, the performance may be evaluated using the bounds provided by Eq.(3.2).

The received power waveforms given mark and space will usually be supplied by a propagation computer program as sampled waveforms. It is natural then to evaluate the integrals involving the received power in Eqs. (3.12), (3.13), (3.17), and (3.20) using a numerical integration technique. Since the received waveforms will usually be supplied as sample points rather than functional representations, one is limited to numerical integration techniques such as Simpson's rule or the trapazoid rule. The Appendix describes a FORTRAN computer program subroutine that calculates bounds on the probability of bit error based on the Bhattacharyya distance measure.

Twin Channel Receivers

Finally consider an optical communication receiver that employs two detectors, each monitoring a different frequency, polarization or spatial component of the received signal. Such a receiver will have two random processes available to it in making a decision. The processes, $x(t)$ and $y(t)$, will be statistically independent since the noise mechanisms between the detectors can be assumed to be independent.

$$p_{\underline{x},\underline{y}|H_i}(\underline{x},\underline{y}|H_i) = p_{\underline{x}|H_i}(\underline{x}|H_i)\, p_{\underline{y}|H_i}(\underline{y}|H_i) \tag{3.22}$$

The Bhattacharyya distance is then

$$B = -\ln \int_{-\infty}^{\infty} \int_{-\infty}^{\infty} \sqrt{P_{\underline{x},\underline{y}|H_0}(\underline{x},\underline{y}|H_0) \, P_{\underline{x},\underline{y}|H_1}(\underline{x},\underline{y}|H_1)} \; d\underline{x}d\underline{y}$$

$$= -\ln \int_{-\infty}^{\infty} \int_{-\infty}^{\infty} [P_{\underline{x}|H_0}(\underline{x}|H_0) \, P_{\underline{y}|H_0}(\underline{y}|H_0) \cdot$$

$$P_{\underline{x}|H_1}(\underline{x}|H_1) \, P_{\underline{y}|H_1}(\underline{y}|H_1)]^{1/2} \; d\underline{x}d\underline{y}$$

$$B = -\ln \int_{-\infty}^{\infty} \sqrt{P_{\underline{x}|H_0}(\underline{x}|H_0) \, P_{\underline{x}|H_1}(\underline{x}|H_1)} \; d\underline{x} \; +$$

$$-\ln \int_{-\infty}^{\infty} \sqrt{P_{\underline{y}|H_0}(\underline{y}|H_0) \, P_{\underline{y}|H_1}(\underline{y}|H_1)} \; d\underline{y}$$

$$(3.23)$$

Each term of the above expression may be evaluated using the single channel results. One is even able to consider the case where one detector is shot noise limited and the other thermal noise limited. The performance analysis for twin channel receivers will require four waveforms -- the power waveforms incident on each detector under both hypotheses of what was sent.

CHAPTER FOUR

SUMMARY

The bound on the probability of error provided by the Bhattacharyya distance is a general, yet relatively simple to evaluate, measure of the performance of optical communication systems. The Bhattacharyya distance is applicable to any intensity modulated digital signaling format: On-off, pulse position modulation or phase or frequency shifting of a sinusoidal intensity subcarrier. To the extent that the propagation analysis models the distortion of the wave-forms during propagation, the Bhattacharyya distance measure will reflect performance degradation due to this. However, it should be noted that as developed here the Bhattacharyya distance is only applicable to the one shot communication problem. Thus, if the time dispersion becomes significant enough that intersymbol interference results, the Bhattacharyya distance will not account for the performance degradation.

The bench mark type performance measure that the bound provided by the Bhattacharyya distance supplies is appropriate for interfacing with a propagation analysis. By calculating upper and lower bounds on the probability of error assuming optimal processing, the Bhattacharyya distance provides a quick check on the performance that could be achieved as the receiver location, link geometry or atmospheric scattering parameters are changed. The receiver parameters are not that crictical, and will often be used to specify the general *type* of receiver one wishes to consider.

Finally, though the Bhattacharyya distance results for twin channel receivers were not explicitly implemented in computer code, at such time as propagation programs that adequately model the propagation of the various polarization or frequency components of the field become available, the extension of the computer code to twin channel receivers is straightforward.

APPENDIX

PROBABILITY OF ERROR SUBROUTINE

The subroutine ERROR is a FORTRAN program to calculate upper
and lower bounds on the probability of bit error for any direct
detection optical communication receiver for which the power waveform
incident on the detector may be considered non-stochastic. The probabil-
ity of error bounds are implemented by means of the Bhattacharyya
distance measure.

The performance bounds are based on the received power wave-
forms given mark and space. Thus, the lower bound is the absolute best
performance one might possibly achieve given the received signal set.
The upper bound is the worst one will do *assuming* the receiver implements
the optimal decison rule on the detector output.

The inputs are passed to the program in labeled common. The
sampled received power waveform given mark and the received waveform
given space as well as the number of sample points and the bit duration
appear in the common WAVEFM. The number of sample points must be odd.
The pertinent receiver parameters are passed in the common RCVR. Or
it may be more convenient to insert the common blocks from the main
program that contain the necessary information. The labeled common
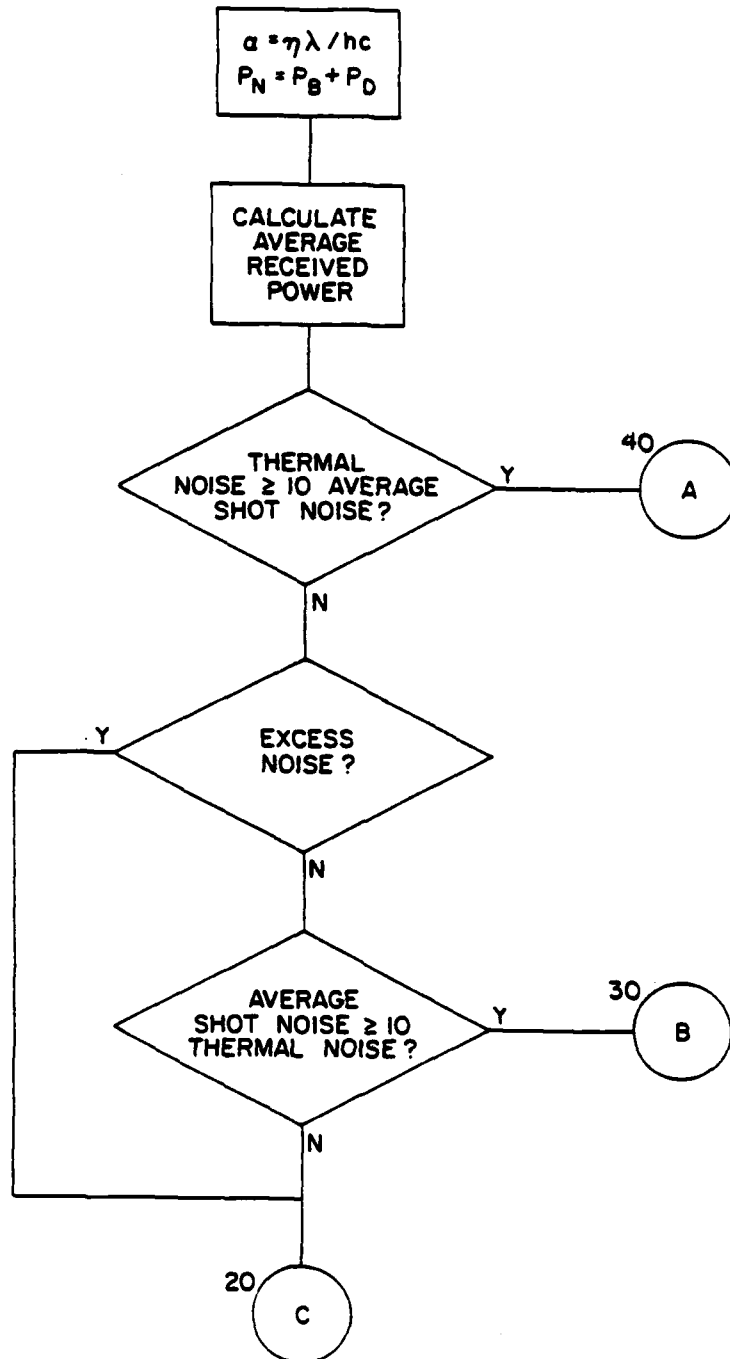INTER passes data to the external Bhattacharyya distance functions.

The program returns as arguments the upper and lower bounds
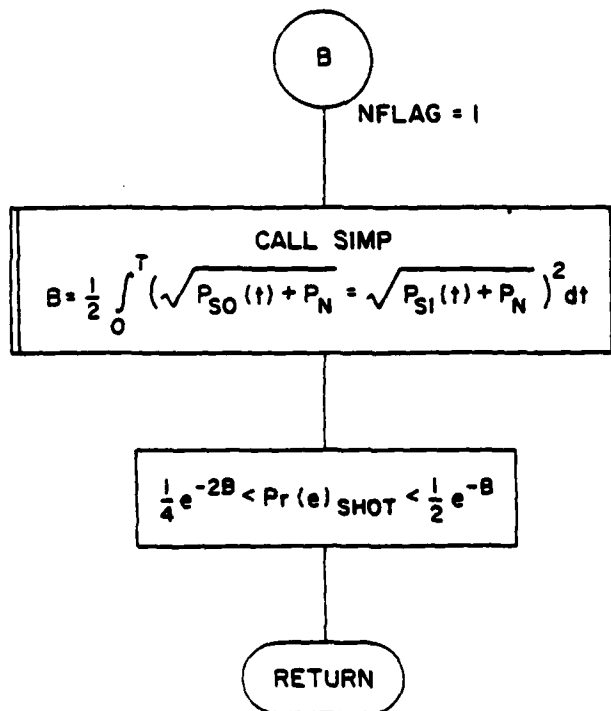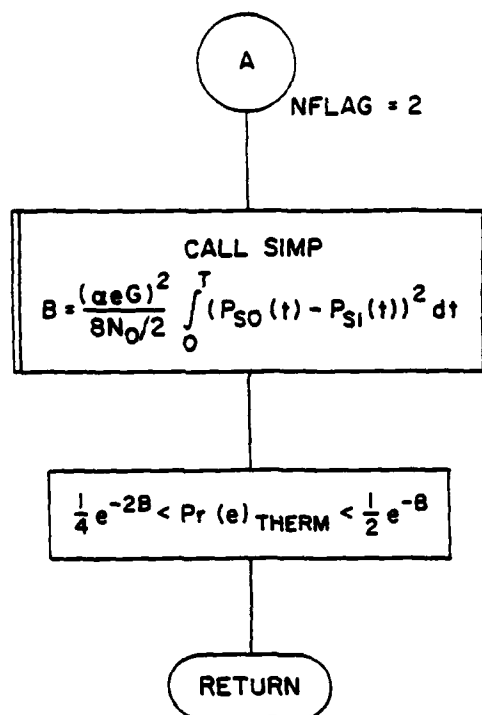on the probability of bit error and a flag indicating whether the

performance is (1) shot noise limited, (2) thermal noise limited, or (3) a combination of shot and thermal noise. If the receiver noise is a combination of shot and thermal or excess noise, both the performance assuming a Poisson model and the performance assuming a Gaussian model are returned for user comparison.
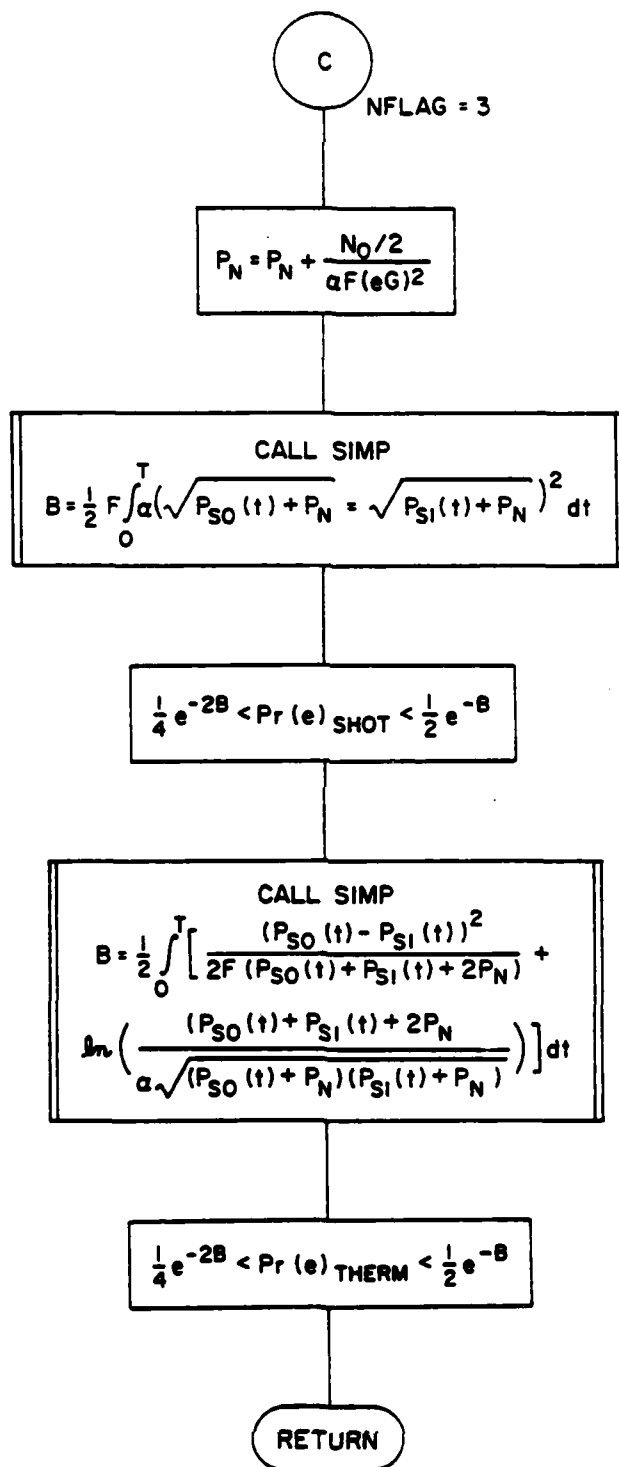
The Bhattacharyya distance integrals are evaluated using Simpson's rule for integration. To the extent that the sample points adequately represent the waveform in a piece-wise sense, Simpson's rule is accurate enough.

Following is a flow chart and program listing of the subroutine ERROR.

Flow chart of subroutine ERROR

SUBROUTINE ERROR

44

A

NFLAG = 2

CALL SIMP

$$B = \frac{(\alpha eG)^2}{8N_0/2} \int_0^T (P_{SO}(t) - P_{SI}(t))^2 \, dt$$

$$\frac{1}{4} e^{-2B} < Pr(e)_{THERM} < \frac{1}{2} e^{-B}$$

RETURN

B

NFLAG = 1

CALL SIMP

$$B = \frac{1}{2} \int_0^T \left(\sqrt{P_{SO}(t) + P_N} = \sqrt{P_{SI}(t) + P_N} \right)^2 \, dt$$

$$\frac{1}{4} e^{-2B} < Pr(e)_{SHOT} < \frac{1}{2} e^{-B}$$

RETURN

$$C$$

NFLAG = 3

$$P_N = P_N + \frac{N_0/2}{\alpha F(eG)^2}$$

CALL SIMP
$$B = \frac{1}{2} F \int_0^T \alpha \left(\sqrt{P_{SO}(t) + P_N} = \sqrt{P_{SI}(t) + P_N} \right)^2 dt$$

$$\frac{1}{4} e^{-2B} < Pr(e)_{SHOT} < \frac{1}{2} e^{-B}$$

CALL SIMP
$$B = \frac{1}{2} \int_0^T \left[\frac{(P_{SO}(t) - P_{SI}(t))^2}{2F(P_{SO}(t) + P_{SI}(t) + 2P_N)} + \right.$$
$$\left. \ln \left(\frac{P_{SO}(t) + P_{SI}(t) + 2P_N}{\alpha \sqrt{(P_{SO}(t) + P_N)(P_{SI}(t) + P_N)}} \right) \right] dt$$

$$\frac{1}{4} e^{-2B} < Pr(e)_{THERM} < \frac{1}{2} e^{-B}$$

RETURN

46

Program listing of subroutine ERROR

```
c.
            subroutine error(nflag,lobnd1,upbnd1,
    &       lobnd2,upbnd2)
c
c       CALCULATE PROBABILITY OF BIT ERROR
c
c       INPUTS:
c           ps0(i)      - SAMPLED RCVD SIGNAL POWER
c                         WAVEFORM GIVEN SPACE (W)
c           ps1(i)      - SAMPLED RCVD SIGNAL POWER
c                         WAVEFORM GIVEN MARK (W)
c           npts        - NUMBER OF SAMPLED WAVEFORM
c                         POINTS.  NPTS MUST BE ODD.
c           t           - BIT TIME INTERVAL (S)
c           eta         - DETECTOR QUANTUM EFFICIENCY
c           g           - DETECTOR GAIN
c           f           - EXCESS NOISE
c           lambda      - OPTICAL WAVELENGTH (M)
c           enzero      - BILATERAL SPECTRAL DENSITY
c                         OF THERMAL NOISE (J)
c           pback       - BACKGROUND POWER (W)
c           pdark       - EQV POWER THAT GIVES RISE
c                         TO DARK CURRENT (W)
c
c       RETURN:
c           upbnd1      - SHOT NOISE LIMITED UPPER
c                         BOUND ON PROBABILITY OF ERROR
c           lobnd1      - SHOT NOISE LIMITED LOWER
c                         BOUND ON PROBABILITY OF ERROR
c           upbnd2      - THERMAL NOISE LIMITED UPPER
c                         BOUND ON PROBABILITY OF ERROR
c           lobnd2      - THERMAL NOISE LIMITED LOWER
c                         BOUND ON PROBABILITY OF ERROR
c           nflag       - PERFORMANCE FLAG
c                         1 - SHOT NOISE LIMITED
c                         2 - THERMAL NOISE LIMITED
c                         3 - COMBINATION OF SHOT AND
c                             THERMAL OR EXCESS NOISE
c
c       INTERNAL VARIABLES:
c           b           - BHATTACHARAYYA DISTANCE
c           pnoise      - EFFECTIVE NOISE POWER (W)
c           pave        - AVERAGE RECEIVED POWER (W)
c           alpha       - OPTICAL POWER TO AVERAGE
c                         PHOTON COUNTS
c           eg          - PHOTON COUNTS TO CURRENT
c
        common / wavefm / npts,t,ps0(1000),ps1(1000)
        common / rcvr / eta,g,f,enzero,pback,pdark,
    &   lambda
        common / inter / pnoise,alpha,eg,fnoise
```

48

```
c
        external func1,func2,func3
        real lambda,lobnd1,lobnd2
c
        alpha=eta*lambda/(2.998e8*6.626e-34)
        eg=1.6e-19*g
        fnoise=f
c
        pnoise=pback+pdark
c
c       CALCULATE AVERAGE POWER
        pave=0.0
        do 10 i=1,npts
        pave=pave+ps1(i)+ps0(i)
10      continue
        pave=0.5*pave/npts+pnoise
c
c       THERMAL NOISE LIMITED?
        if (enzero/eg**2.gt.10.0*f*alpha*pave)
&       go to 40
c       EXCESS NOISE?
        if (f.gt.1.0) go to 20
c       SHOT NOISE LIMITED?
        if (alpha*pave.gt.10.0*enzero/eg**2)
&       go to 30
c
20      nflag=3
        pnoise=pnoise+enzero/(alpha*eg**2*f)
        b=0.5*f*simp(func1)
        upbnd1=0.5*exp(-b)
        lobnd1=0.25*exp(-2.0*b)
        b=0.5*simp(func3)
        upbnd2=0.5*exp(-b)
        lobnd2=0.25*exp(-2.0*b)
        return
c
30      nflag=1
        b=0.5*simp(func1)
        upbnd1=0.5*exp(-b)
        lobnd1=0.25*exp(-2.0*b)
        return
c
40      nflag=2
        b=0.125*(alpha*eg)**2*simp(func2)/enzero
        upbnd2=0.5*exp(-b)
        lobnd2=0.25*exp(-2.0*b)
        return
        end
```

```fortran
c.
      function simp(func)
c
c     SIMPSONS RULE INTEGRATION OF
c     FUNCTION FUNC
c
      common / wavefm / npts,t,ps0(1000),ps1(1000)
      double precision sum
c
      sum=0.0
      do 10 i=1,npts-2,2
      term=func(i)+4*func(i+1)+func(i+2)
      sum=sum+term
10    continue
      simp=t*sum/(3*(npts-1))
      return
      end
c.
      function func(i)
c
c     BHATACHARAYYA DISTANCE FUNCTIONS
c
      common / wavefm / npts,t,p0(1000),p1(1000)
      common / inter / pn,a,e,f
c
c     POISSON PROCESS
      entry func1(i)
      func=a*(sqrt(p1(i)+pn)-sqrt(p0(i)+pn))**2
      return
c
c     GAUSSIAN PROCESS
      entry func2(i)
      func=(p1(i)-p0(i))**2
      return
c
c     GAUSSIAN PROCESS - TIME VARYING VARIANCE
      entry func3(i)
      func=a*(p1(i)-p0(i))**2/
     &    (2.0*f*(p1(i)+p0(i)+2.0*pn))+
     &    alog((p1(i)+p0(i)+2.0*pn)/
     &    (2.0*sqrt((p1(i)+pn)*(p0(i)+pn))))
      return
      end
```

REFERENCES

1. M. King and S. Kainer, "Some Parameters of a Lasertype Beyond-the-horizon Communication Link," *Proceedings IEEE*, Vol. 53, No. 2, February 1965, pp. 137-141.

2. G. T. Ruck, "Feasibility of Non-line-of-sight Laser Communications," Battelle Memorial Institute, Report BAT-171-4, December 15, 1964.

3. E. S. Fishburne, M. E. Neer, and G. Sandri, "Voice Communication Via Scattered Ultraviolet Radiation," Aeronautical Research Associates of Princeton, Report No. 274, March 1976.

4. W. S. Ross, "An Investigation of Atmospheric Optical Scattered Non-line-of-sight Communication Links." Final Report US ARO contract DAAG29-77-c-0048, September 26, 1978.

5. R. M. Gagliardi and S. Karp, *Optical Communication*. New York: John Wiley and Sons, 1976.

6. S. D. Personik, "Statistics of a General Class of Avalanche Detectors with Application to Optical Communication," *Bell System Technical Journal*, Vol. 50, No. 10, December 1971, pp. 3075-3094.

7. R. S. Kennedy, "Communication through Optical Scattering Channels: An Introduction," *Proc IEEE*, Vol. 58, No. 10, October 1970, pp. 1651-1665.

8, I. Rubin, "Regular Point Processes and Their Detection," *IEEE Transactions on Information Theory*, Vol. 18, No. 5, September 1972, pp. 547-557.

9. N. S. Kopeika and J. Bordogna, "Background Noise in Optical Communication Systems," *Proc. IEEE*, Vol. 58, No. 10, October 1970, pp. 1571-1577.

10. J. H. Shapiro, "Imaging and Optical Communication Through Atmospheric Turbulence," in *Laser Beam Propagation Through the Atmosphere*. Berlin: Springer-Verlag, 1978.

11. T. Kailath, "The Divergence and Bhattacharyya Distance Measures in Signal Selection," *IEEE Transactions on Communication Technology*, Vol. 15, No. 1, February 1967, pp. 52-60.

12. J. Wozencraft and I. Jacobs, *Principles of Communication Engineering*. New York: John Wiley and Sons, 1965.

DATE
ILMED

—8